

Zika virus negatively impacts rhesus macaque placentas, embryos, and trophoblasts

By:

Lindsey Block

A dissertation submitted in partial fulfillment

of the degree requirements for the degree of

Doctor of Philosophy

(Cellular and Molecular Pathology)

at the

University of Wisconsin-Madison

2021

Date of final oral examination: 6/16/2021

The dissertation is approved by the following members of the Final Oral Committee:

Thaddeus Golos, Professor and Chair, Comparative Biosciences

Thomas Friedrich, Professor, Pathobiological Sciences

Kristen Bernard, Professor, Pathobiological Sciences

Margaret Petroff, Associate Professor, Pathobiology and Diagnostic Investigation

Aleksandar Stanic-Kostic, Assistant Professor, Obstetrics & Gynecology

Donna Peters, Professor, Pathology and Laboratory Medicine

Contents

List of Tables	iv
List of Figures	v
Acknowledgements	vii
Abstract	viii
Chapter 1: Introduction	1
1.1 Infection during pregnancy can have severe consequences	1
1.2 The impact of ZIKV and other Flaviviruses on pregnancy	2
1.3 Sexually transmitted viruses can infect and impact embryos.....	4
1.4 The early placenta.....	5
1.5 Viral infection of the placenta	7
1.6 The Flavivirus life cycle.....	9
1.7 The impact of ZIKV on trophoblast cells: how ZIKV overcomes intrinsic host defense mechanisms	11
1.8 The innate immune defense and its interaction with ZIKV.....	14
1.9 Extracellular vesicles may modulate viral infection.....	18
1.10 Thesis Overview	19
1.11 Significance	22
1.12 References	23
Chapter 2: Ocular and uteroplacental pathology in macaque congenital Zika virus infection	36
2.1 Abstract.....	39
2.2 Introduction.....	40
2.3 Materials and Methods.....	43
2.4 Results.....	53
2.5 Discussion.....	73
2.6 References.....	79

Chapter 3: Embryotoxic impact of Zika virus in a rhesus macaque in vitro implantation model.....	86
3.1 Abstract.....	86
3.2 Introduction.....	87
3.3 Materials and Methods	90
3.4 Results	96
3.5 Discussion	106
3.6 Conclusions.....	111
3.7 References.....	112
Chapter 4: Rhesus macaque early-gestation trophoblast cells are permissive to Zika virus infection and extracellular vesicle cargo is altered with virus exposure	119
4.1 Abstract.....	120
4.2 Introduction.....	121
4.3 Materials and Methods.....	123
4.4 Results	144
4.5 Discussion.....	173
4.6 References.....	184
Chapter 5: Concluding Remarks	191
5.1 Concluding remarks.....	191
5.2 References.....	202
Appendix A: The promise of placental extracellular vesicles: models and challenges for diagnosing placental dysfunction in utero	204
A.1 Abstract.....	205
A.2 Introduction.....	206
A.3 What are extracellular vesicles (EVs)?	211
A.4 EV formation, cargo packaging, and function	213
A.5 PEVs: sample sources, interactions with immune cells, and clinical potential	215
A.6 Current in vivo and in vitro sources for isolating PEVs	221

A.7 PEVs isolated from adverse human pregnancies.	223
A.8 PEVs interact with immune cells during pregnancy.	224
A.9 Surveying PEV markers and cargo to identify pregnancy complications.	225
A.10 Animal models of human pregnancy complications	228
A.11 Spontaneous versus induced animal models of adverse pregnancies	233
A.12 Animal models of experimental infections during pregnancy	238
A.13 Current knowledge of PEVs in animal pregnancy models	239
A.14 Future perspectives: expansion of PEV research in animal pregnancy models.....	242
A.15 Next steps in establishing animal pregnancy models for PEV research.	244
A.16 Current questions and future opportunities in the PEV field	245
A.17 References	247

List of Tables

Table 2.1 Tissues with detectable ZIKV RNA from mother and fetus.....	62
Supplementary Table 2.1. Tissues evaluated by qRT-PCR that were negative.	63
Supplementary Table 2.2. Histology description of fetal and maternal tissues.	65
Table 2.2 Tissue vRNA burden, ISH and mFISH results.....	72
Table 3.1. In vitro embryo development rates following ZIKV exposure at fertilization.....	97
Table 3.2. The percent of embryos attached to the Matrigel and alive on each day post-plating is shown.....	98
Supplemental Table 4.1 Immunocytochemistry, fluorescent conjugates, and Western Blot antibodies	132
Supplemental Table 4.2 Primer sequences for qRT-PCR.....	139
Supplemental Table 4.3 qRT-PCR, DESeq2, and edgeR log fold change (log ₂ FC) and significance (p-value/adjusted p-value) comparisons.....	155
Table A.1. Human pregnancy complications.....	209
Supplemental Table A.1: Citations based on the pregnancy complication and animal model studied.....	210
Table A.2. Summary of known EV markers and placenta-specific markers across species.....	215
Table A.3. PEV studies in humans, rodents, cows, pigs, and sheep.....	217
Table A.4. Comparison of placentation across different research models.....	231
Table A.5. Induced animal models of human pregnancy complications.....	235
Table A.6. Pathogens in animal models that cause adverse pregnancy outcomes (APOs)....	239

List of Figures

Figure 1.1 Cells of the human placenta proper placenta proper	7
Figure 1.2 The ZIKV life cycle	11
Figure 1.3 Cellular immune response to ZIKV infection and Zika viral strategies to inhibit that response	15
Figure 2.1 Timeline depicting body fluid sampling and procedures throughout pregnancy	52
Figure 2.2 ZIKV vRNA levels in maternal body fluids	53
Figure 2.3 Neutralizing antibody titers following ZIKV infection.	54
Figure 2.4 Amniotic fluid (AF) markers confirm rupture of membranes	56
Figure 2.5 Fetal growth measured by ultrasonography.....	58
Figure 2.6 Maternal and fetal necropsy images	60
Supplemental Figure 2.1 Histology and gram stain of fetal esophagus	60
Figure 2.7 Uteroplacental histopathology.....	66
Figure 2.8 Fetal ocular pathology.....	69
Figure 2.9 Tissue histology and viral localization of maternal spleen, maternal uterus, amniotic/chorionic membrane, and fetal lung.....	71
Supplementary Figure 2.2. Multiplex fluorescent in situ hybridization of positive and negative strand vRNA in fetal lung.....	72
Figure 3.1. Schematic depiction of ZIKV exposure to gametes (A) and hatched blastocysts.....	94
Figure 3.2. Peri-implantation in vitro embryo outgrowths exposed to ZIKV reduces growth..	100
Supplemental Figure 3.1. Trophoblast cell morphology.....	101
Figure 3.3. Secretion of hormones and immunomodulators by embryo outgrowths.....	103
Supplemental Figure 3.2. Secretion of progesterone and mCG by embryo outgrowths.....	104
Figure 3.4. Infectious virus was detected in culture media following ZIKV exposure.....	106
Supplemental Figure 4.1. Methods overview.....	125
Figure 4.1. Early gestation trophoblast cells are permissive to ZIKV infection.....	147
Supplemental Figure 4.2. Rabbit IgG controls and ZIKV uninfected control images.....	148
Supplemental Figure 4.3. Full Western Blots and control immunocytochemistry images.....	149
Figure 4.2. The impact of ZIKV on the cellular transcriptome.....	153
Figure 4.3. The impact of ZIKV exposure on the cellular miRNAome.....	158
Supplemental Figure 4.4. miRNA comparison across cell types.....	166

Supplemental Figure 4.5. Hormone, cytokine, and growth factor secretion by cell type and infection group.....	162
Figure 4.4. EV characterization from trophoblast-conditioned media.....	165
Figure 4.5. EV verification analyses and protein information analyses.....	168
Figure 4.6. EV proteomics analysis.....	172
Figure 4.7. mRNA and miRNA transcripts vary between EVs from ZIKV exposed cells and uninfected controls.....	176
Figure A.1. Schematic diagram of human placental villous structure and PEV biogenesis.....	212
Figure A.2 Experimental models of human pregnancy.....	229

Acknowledgements

I would like to thank all Team Placenta lab members (past and current) for their mentorship, support, and guidance – especially Greg Wiepz. A special thanks to my mentor Ted Golos for his unwavering support and helping me to explore a very new area of science. A special thanks to Jenna Schmidt for her patience and persistence in ensuring I leave my Ph.D. well rounded. Together, you two taught me how to look past the failed experiments and long hours of pipetting and taught me how to plan for bigger, better studies. My goal was to leave my graduate program with a full toolbox, and I can definitely say I am. Thank you.

I would also like to express thanks to each of my committee members, Kristen Bernard, Donna Peters, Peggy Petroff, Aleks Stanic-Kostic, and Thomas Friedrich. Thank you each for your advice and thought-provoking questions. You have made me a better scientist.

Thank you to the FIR program and all the FIRbees. I have learned so much from you all and look forward to growing together in our careers.

A very warm thank you to my CMP cohort. I could not have gotten through these five years without all of you. Thank you for the good times and scientific support, emotional support, and guidance. Non-CMP friends: Thank you for putting up with my weird schedule over the years and listening to me drone on about whatever experiments I was currently working on. Thank you for believing in me and encouraging me to “just go for it!”

To my family: You are all amazing and intelligent people. Thank you for sharing your endless joy and energy. Thank you getting me interested in science (-especially dad!). Your successes motivate me to keep learning. Thank you for also being open about your failures – it helped me cope with mine. You also have taught me to not let anyone stop me or get in my way (especially mom). This life lesson kept me in grad school and will continue to carry me through my next careers.

Kyle, thank you for encouraging me and most especially for making me laugh. Your limitless positivity is admiring and has changed me for the better. You make the worst days better days and good days great days.

Watch out world!

Abstract

Zika virus (ZIKV) infection during pregnancy can result in pregnancy loss and fetal malformations. In addition, ZIKV was detected in human, nonhuman primate, and mouse placentas with associated placental pathology. Overall, this thesis addresses the impact of ZIKV on pregnancy and the placenta in nonhuman primate models. The first chapter describes a case study of a pregnant rhesus macaque who experienced a miscarriage ~50 days post-ZIKV exposure. Extreme placental and fetal ocular pathology were observed. The outcome from this case study raised questions as to how ZIKV impacted the placenta. The objective of this thesis was to evaluate the impact of ZIKV on early embryonic and placental development with *in vitro* rhesus macaque models.

Sexual transmission of ZIKV also has been demonstrated, yet the impact of infection during the initial stages of pregnancy remains unexplored. The second chapter aimed to determine the impact of ZIKV on *in vitro* oocyte fertilization and embryo development rates. ZIKV exposure at the time of conception did not impact subsequent *in vitro* embryo development rates. Exposure of embryos to ZIKV at the peri-implantation stage of development significantly impacted embryo development with decreased rates of embryo survival, attachment, and growth. Overall, the early stages of pregnancy may be profoundly sensitive to infection and pregnancy loss, and the negative impact of ZIKV infection on pregnancy outcomes in the human population may be underestimated.

The permissiveness of the trophoctoderm to ZIKV infection in the peri-implantation stage prompted the study of ZIKV infection on the early trophoblast cells of the fully formed placenta. Trophoblast cells present in the mature placenta include trophoblast stem cells (TSCs), syncytiotrophoblasts (STs), and extravillous trophoblasts (EVTs). Altogether, these trophoblast cell types work to ensure the fetus receives sufficient nutrients and oxygen from mom as well as protect the fetus from pathogens potentially present in maternal blood. Inoculation of trophoblast cell cultures revealed that TSCs and STs are susceptible to ZIKV infection

and that infection inhibits cell death. EVT_s maintained a level of resistance to infection; however, this was not due to lack of expression of putative ZIKV receptors.

Extracellular vesicles (EVs) are widely studied as a means to monitor cell function as a “liquid biopsy” since they are secreted by all cells into various bodily fluids. EV cargo, which includes nucleic acids and proteins, can be altered during diseased and infected states. Extensive alterations in EV cargo were observed following ZIKV exposure. EVs isolated from infected TSC and ST culture media were shown to be infectious. Although the presence of virions in the EV isolations could not be completely ruled out, data support the possibility that ZIKV proteins, and potentially ZIKV genomes, are packaged within EVs.

In summary, these experiments demonstrate that *in vitro* rhesus macaque embryos and trophoblasts representative of early pregnancy are permissive to ZIKV infection. In addition, EV cargo was altered by ZIKV exposure. These changes suggest that EVs have the potential to serve as biomarkers of placental ZIKV infection, and perhaps more broadly to provide a means to monitor placental changes that portend adverse pregnancy outcomes.

Chapter 1

Introduction

1.1 Infection during pregnancy can have severe consequences.

Immunological, hormonal, and physiological changes occur during pregnancy [1]. A successful pregnancy requires a degree of immune tolerance because the fetus and placenta are semi-allografts since half of the genetic material expressed comes from the sperm. Hormone changes are necessary to signal the presence of an embryo/fetus and to alter the immune response to be less inflammatory and more tolerant [2]. Due to these physiological changes, infections during pregnancy can have dire consequences. Transmission of maternal infection to the fetus is estimated to cause 2-3% of congenital anomalies [3] and the World Health Organization estimates that ~11% of maternal deaths are due to sepsis [1]. Nicely put, “The corollary of this capacity for immunological tolerance is an increased susceptibility to infection” [1].

Viral infection during pregnancy results in more severe outcomes for both the mother and fetus than seen in nonpregnant persons [1]. Pregnant persons infected with Lassa fever, SARS/MERS/SARS-COV-2 coronaviruses, dengue, hepatitis E, influenza, and herpes simplex viruses often experience increased severity of infection with worse outcomes in comparison to infected individuals that are not pregnant [1, 4-9]. For example, pregnant persons have 45% increased morbidity and mortality from an Influenza infection than nonpregnant persons [1].

Adverse pregnancy outcomes can arise if there is an infection from a pathogen in the TORCHZ group. It should be noted though that this acronym is not all encompassing. Pathogens included in this group are **T**oxoplasma gondii, **O**ther [Listeria monocytogenes, Treponema pallidum, varicella zoster virus (VZV), human immunodeficiency virus (HIV), enteroviruses and parvovirus B19], **R**ubella virus, **C**ytomegalovirus (CMV), **H**erpes simplex virus, and **Z**ika Virus (ZIKV) [10, 11]. ZIKV, the newest addition to the TORCHZ group, will be the main topic of this thesis, but information regarding the pathogenesis of related viruses and viruses with similar transmission routes can be enlightening and is discussed throughout.

1.2 The impact of ZIKV and other flaviviruses on pregnancy

Several viruses in the *Flaviviridae* family can infect the placenta and cause adverse pregnancy outcomes, including dengue virus (DENV), japanese encephalitis virus (JEV), yellow fever virus (YFV), West Nile virus (WNV), and ZIKV [12-21]. Maternal DENV infection early in pregnancy is associated with miscarriage and, in several cases, DENV has been detected in the placenta [22-24]. JEV can infect the placenta and cause adverse pregnancy outcomes in mice [25]. Vaccination of pregnant women against YFV with the live attenuated virus may be associated with increased pregnancy loss [26]; however, more recent studies reported no increased risk [27, 28]. To determine whether YFV vaccine could be associated with pregnancy loss, mice were vaccinated at gestation day (gd) 0.5, 5.5, or 11.5 (term = gd 20). Vaccination was shown to negatively impact embryo implantation, and in post-implantation pregnancies YFV was detected in placental and fetal tissues of infected mice [29].

There is limited information regarding the potential for WNV to be vertically transmitted or cause adverse pregnancy outcomes in humans [30, 31]. To determine if WNV could be vertically transmitted, 77 women infected with WNV during pregnancy were monitored [17]. At birth, blood and tissue biopsies were collected from the newborn and the placenta, respectively. WNV was only detected in one of 50 human term placentas analyzed and all other samples were negative [17]. However, evidence from mouse in vivo pregnancy and in vitro embryo culture studies suggests that WNV negatively impacts pregnancy and can infect the trophoblast cells of the placenta [32, 33].

Although ZIKV was first discovered in a sentinel rhesus macaque in the Zika Forest in Uganda in 1947, it was not until the 2015 outbreak in Brazil that ZIKV was identified as a teratogen, a substance that causes malformations in an embryo/fetus [14]. ZIKV infection during pregnancy is associated with abnormal fetal development in 5-10% of cases, some with lifelong complications [14]. Common effects of ZIKV infection on the fetus include brain and skull abnormalities (e.g. microcephaly and thinning of the cerebral cortices), eye malformations (e.g. colobomas), congenital contractures of the joints, and motor and cognitive impairments [14]. The impact of ZIKV on fetal development is termed “congenital ZIKV syndrome” (CZS) [12-14]. In addition to ZIKV, maternal infection of rubella, cytomegalovirus, chikungunya virus, and WNV have been associated with fetal microcephaly [34-36].

In addition to abnormal fetal development, ZIKV infection during pregnancy can also result in pregnancy loss [37-40]. ZIKV infection before 10 weeks of gestation has been directly correlated

with an elevated risk of developing fetal microcephaly [36]. Data collected across six national nonhuman primate research centers showed that nonhuman primates experimentally infected with ZIKV in early pregnancy resulted in 26% pregnancy loss [41]. However, it is unclear whether viral infection itself, or rather, the maternal immune response to infection is the primary cause of pregnancy loss. Regardless of what is causing the adverse effect(s), ZIKV can infect the placenta and cause placental damage [42, 43].

1.3 Sexually transmitted viruses can infect and impact embryos.

Sexual transmission of pathogens can be detrimental to pregnancy. Assisted reproductive technologies, including in vitro fertilization (IVF), are commonly used in human clinical, research, and livestock production settings. Devastating consequences of viral presence in semen during artificial insemination have been reported in livestock [44] as sexually transmitted viruses can infect both embryos and the dam [44-47]. Human case reports and studies utilizing animal models of infection have demonstrated that flaviviruses can infect the male reproductive tract and be sexually transmitted [48]. ZIKV has been detected in human semen for up to 181 days [49] and infectious virus has been detected [50]. ZIKV can be sexually transmitted in humans [51-53], and two cases of human sexual transmission during pregnancy have been reported [54, 55]. Importantly, significantly more ZIKV infection cases were observed in women of sexually reproductive age, despite accounting for increased surveillance [56]. This finding supports that sexual transmission of ZIKV was a significant contributor to increased cases. In endemic areas, it was estimated that 3% of ZIKV cases were due to sexual transmission [34]. Vaginal inoculation of ZIKV to mimic sexual transmission in mice also resulted in decreased pregnancy rates [57, 58].

Since ZIKV can be sexually transmitted and is known to impact pregnancy, part of the work presented in this thesis attempts to determine when viral exposure can impact oocyte fertilization and embryo development in a nonhuman primate model. It should be noted that several studies have detected Zika viral RNA (vRNA) in nonhuman primate semen and male reproductive tract tissues [59-61], which support the translatability of the model. To date, human, mouse, and nonhuman primate embryos have been shown to be permissive to ZIKV in vitro [57, 62]. In addition, vaginal inoculation of pregnant baboons resulted in maternal viremia and infection of reproductive and placental tissues [63, 64]. Altogether, these data indicate that ZIKV can be sexually transmitted, which can have devastating consequences on the pregnancy.

1.4 The early placenta

The placenta ensures that the developing fetus receives sufficient nutrients and oxygen for development throughout the pregnancy [65, 66]. The first placental progenitor cells, termed trophoctoderm, arise during embryogenesis. The trophoctoderm allows the embryo to attach to and implant into the uterus [66], where it then differentiates to give rise to the trophoblast cells that constitute the placenta proper [66]. The placenta comprises several trophoblast cell types including syncytiotrophoblasts (STs), extravillous trophoblasts (EVTs), villous cytotrophoblasts (vCTB), and trophoblast stem cells (TSCs). The placenta is also populated by placental macrophages (Hofbauer cells), other immune cells, fibroblasts, and fetal endothelial cells [67] (Figure 1). TSCs are postulated to reside in the human placenta at the base of the chorionic villi and within the proximal cell columns and serve as progenitor cells (Figure 1) [68, 69]. The vCTBs divide and

differentiate into STs and EVT_s [70]. ST_s provide a continuous barrier between maternal and fetal blood, which in part works to protect the fetus from any pathogens present in maternal blood [66, 70]. ST_s also exchange nutrients, waste, and oxygen as well as secrete hormones. Conversely, EVT_s migrate away from the placenta proper to invade and remodel maternal spiral arteries to increase blood flow to the placenta [70].

It should be acknowledged that the human placenta changes drastically over its nine-month lifespan. For the first few weeks, the placenta is in a hypoxic environment as trophoblast plugs prevent blood flow to the developing placenta [65, 71]. In addition, early placental development occurs within a pro-inflammatory environment that shifts to an anti-inflammatory state as pregnancy progresses [1, 72]. Placental miRNA expression [73], hormone secretion [74], and receptor expression [75] as well as nutritional sources [76] change over gestation as well. These factors could contribute to differences in infection outcome and are important to consider as the trimester in which infection occurs is often correlated to the severity of an adverse outcome [1, 11, 77]. Maternal ZIKV infection in the early stages of pregnancy has often resulted in worse outcomes [13, 14, 36, 40, 78-80], thus comprehensively evaluating the impact of ZIKV at this stage is warranted.

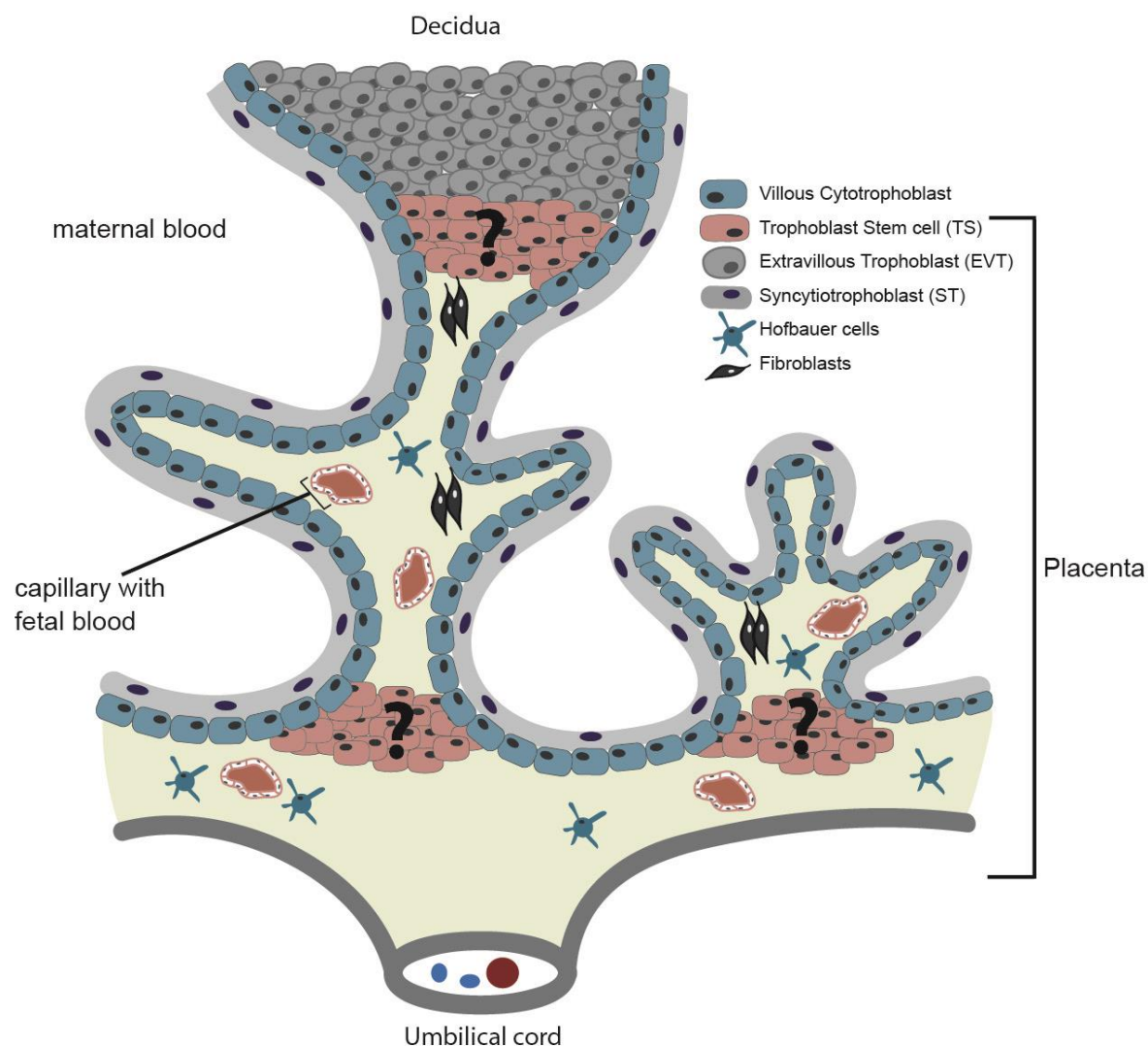


Figure 1.1. Cells of the human placenta proper placenta proper. A schematic of the trophoblast cell types, Hofbauer cells, fibroblasts, and capillaries that comprise the placenta proper. Question marks are placed on the TSC populations the location of these cells has not been confirmed with molecular or histological methods. Figure made by LNB.

1.5 Viral infection of the placenta

The trimester in which infection occurs is often correlated with the likelihood of a poor outcome. For Lassa, influenza, and hepatitis E viruses, infection in the third trimester has been associated with very high fetal loss rates [1, 11]. The rate of CMV transplacental transmission actually

increases with gestational age, while severity of outcome decreases, partly due to the fetus being more developed before infection occurs [11, 77]. However, transplacental transmission of rubella virus is greatest within the first 12 weeks of pregnancy [11]. The severity of ZIKV infection is also trimester dependent with worse outcomes occurring if infection occurs during the first or second trimesters [14, 36, 78-81]. These trends are important to keep in mind when considering the translatability and appropriateness of the model used. The studies presented in this thesis focus on the impact of ZIKV infection early in pregnancy, spanning oocyte fertilization through the first/early second trimester. For that reason and for brevity, only studies on early pregnancy will be discussed, although the impact of in utero infection on postnatal life is well-recognized [36, 82].

Placental ZIKV infection in humans has been documented [42, 81, 83-86]. Severe placental pathologies have been observed including infarcts, hemorrhage, and atypical quantities of calcifications [42, 81, 83-86]. Following in vivo maternal infection, ZIKV has been detected in the placenta of experimentally infected mice [87-90] and nonhuman primates [64, 91]. In vitro ZIKV inoculation has shown that first trimester placental explants [92-95], first trimester primary cells [92, 95], embryonic-stem cell derived trophoblasts [75], and various immortalized placental cell lines [75, 93, 96-98] are permissive to ZIKV. The placenta is essential for proper fetal development and impaired function is associated with adverse pregnancy outcomes. It is therefore important to determine which trophoblast cells are permissive to ZIKV, when these cells are most vulnerable, and how infection impacts cell function.

1.6 The flavivirus life cycle

First, to understand how ZIKV infection could impact the placental cell, the flavivirus life cycle is briefly described and illustrated in Figure 2. Flaviviruses consist of 40-60 nm virions in the *Flaviviridae* family. Their genomes are ~11 kilobases and consist of a positive sense single strand of RNA (+ssRNA), which is translated into a polyprotein once inside a host cell [19]. Viral and host enzymes cleave the polyprotein into three structural proteins (capsid (C), pre-membrane (preM), and envelope (E)), and seven nonstructural proteins (NS1, NS2A, NS2B, NS3, NS4A, NS4B, and NS5). Together, these proteins work to ensure viral progeny are properly assembled and released from infected cells [19, 99].

ZIKV E protein attaches to specific receptors on the host cell and then virions enter the cell via clathrin-mediated endocytosis [100]. Although the specific receptors are not known, candidate receptors include AXL, MERTK, DC-SIGN, TYRO3, and TIM1 [75, 101]. Once inside the host cell, fusion with the lysosome results in a decrease in the pH of the environment containing the virus. This decrease alters the conformation of the virion, and leads to release of the capsid shell, which contains the genome, into the cell's cytoplasm [19, 100]. Viral protein translation and viral genome replication then ensues via usage of the host cell's machinery. To deceive host RNA degradation mechanisms and evade host immune response elements, the viral genome, like other endogenous mRNAs in the cell, has a 5' methyl-cap. However, the viral genome lacks a poly-A tail, which is unlike that of endogenous mRNAs. For genome replication, first a negative sense (-ssRNA) copy is transcribed and then positive sense strands (+ssRNA) are transcribed from the negative sense template. For efficient propagation, viral protein translation occurs prior to genome

transcription as the virus encodes its replication machinery. Since eukaryotic cells do not transcribe RNA from RNA, the virus must provide an enzyme capable of doing so and NS5 is the RNA-dependent RNA-polymerase that facilitates genome transcription [99].

Immature virions are pre-infectious viral particles that assemble in the endoplasmic reticulum, and then travel through the Golgi network[19]. Viral protein maturation occurs in the Golgi where furin cleaves the structural pre-membrane protein (prM) into two segments: pr and M [100]. Mature virions continue through the secretory pathway and are then secreted by the cell into the extracellular environment. The final virion consists of 180 copies of E, 180 copies of prM/M, and one complete +ssRNA genome that resides within the C protein shell.

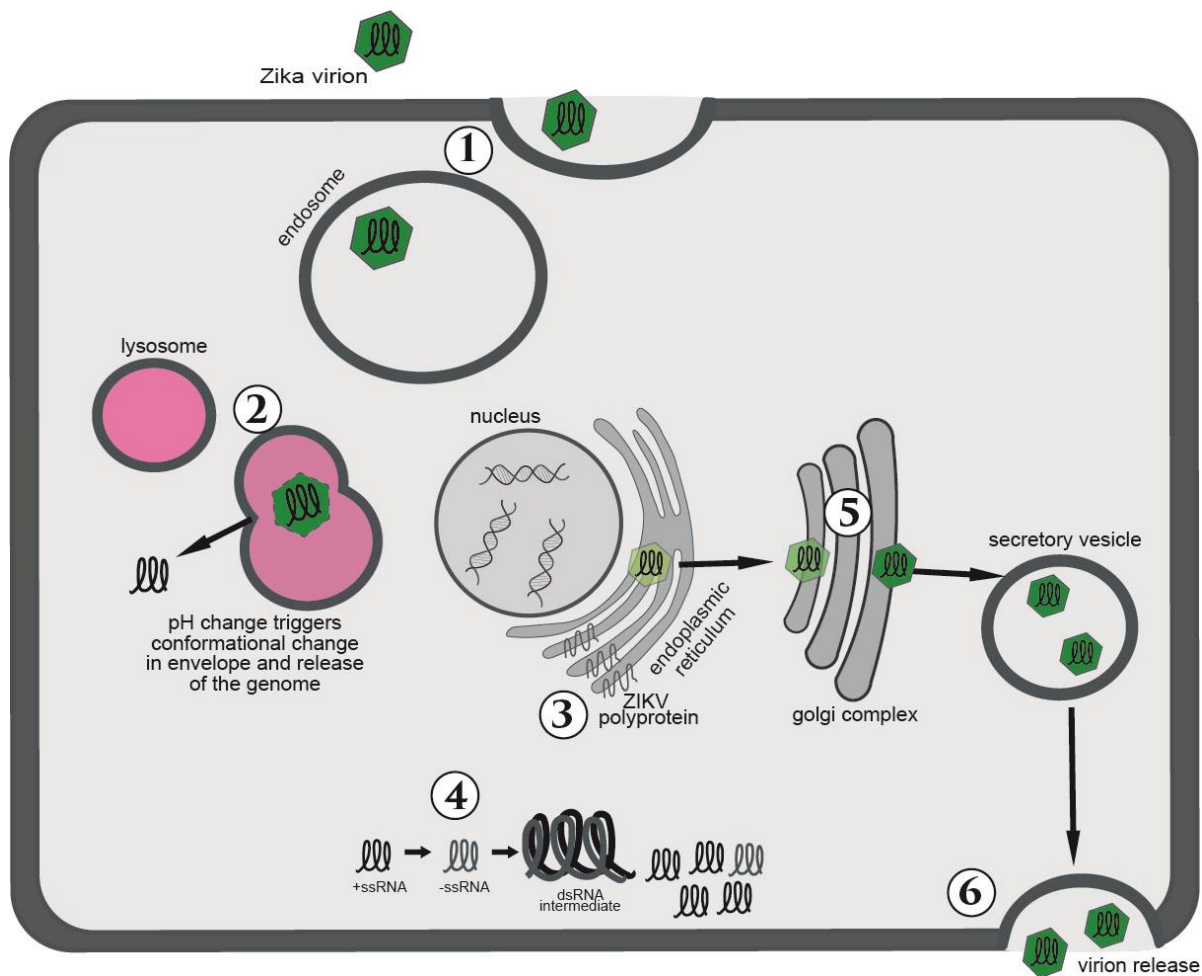


Figure 1.2. The ZIKV life cycle. *1)* A Zika virion (with the genome encased) binds to a receptor on the cell surface, which triggers clathrin-mediated endocytosis. Once the endosome containing the virion is internalized, *2)* endosomal fusion with a lysosome and exposure to the lysosomal pH triggers a conformational change in the virion (as depicted by the change from a solid to a dashed line). This results in genome release into the cytoplasm. *3-4)* Once in the cytoplasm, translation and genome replication occur. *3)* Viral proteins are translated in the endoplasmic reticulum. *4)* For vRNA replication a negative sense single RNA (-ssRNA) is first synthesized and then more positive sense single RNA (+ssRNA) strands are made. *5)* The viral proteins and genome come together in the ER and mature in the Golgi apparatus (as depicted with a change in virion color from yellow to dark green). Viral maturation requires prM cleavage into pr and M. *6)* Mature infectious virions are then released at the plasma membrane. Figure made by LNB.

1.7 The impact of ZIKV on trophoblast cells: how ZIKV overcomes intrinsic host defense mechanisms

The mechanism(s) of ZIKV entry and its subsequent impact on trophoblasts is a key aspect of placental infection that remains poorly understood. As mentioned previously, two types of trophoblast cells are in direct contact with maternal blood, EVTs and STs. STs serve as a barrier to infection; however, ZIKV-mediated changes to cellular permeability may compromise its barrier function. Inoculation of JEG3 cells, an EVT-like trophoblast choriocarcinoma cell line, with ZIKV resulted in increased cell permeability due to decreased expression of tight junction proteins, tight junction protein ZO-1 and occludin [96]. Exposure of JAr cells, an EVT-like trophoblast choriocarcinoma cell line and first trimester placental explants to Zika NS1 protein increased cell permeability and reduced cellular expression, and increased secretion, of hyaluronic acid, heparan sulfate, and sialic acid, which are all important for extracellular matrix integrity and signaling [93]. Importantly, flaviviruses interact with glycosaminoglycans, such as hyaluronic acid and heparan sulfate, for cell entry [102], and increased secretion of these may enhance viral infection. Another means by which ZIKV can overcome the cell barrier is via transcytosis, passage across and through a cell [96]. The increased permeability, alterations in extracellular matrix, and transcytosis are possible mechanisms by which ZIKV could breach the ST barrier and reach the fetus. In summary, STs are a barrier to protect the other trophoblast cells and fetus from pathogens; however, if ZIKV can breach this barrier without directly infecting these cells then other trophoblast cells, such as TSCs, could become infected.

Apoptosis, programmed cell death, is one way a cell can prevent viral spread [103]. However, it remains unclear under what circumstances apoptosis may advance or suppress ZIKV infection. ZIKV infection was reported to induce apoptosis via caspase-3 activation [98], however, another

study reported that infection was not cytotoxic [96]. ZIKV infection was more widespread in the immortalized human trophoblast cell line Sw.71 in the log phase of growth [98], which further supports the idea that maintenance of cell proliferation, as opposed to induction of cell death, contributes to viral dissemination. Interferon (IFN)-induced transmembrane protein (IFITM) expression is regulated by type I and II IFNs; however IFITMs are constitutively expressed in many cells [104]. IFITM-1 and -3 work to inhibit viral entry by preventing virion fusion to the cell membrane, viral replication, and cell death induced by ZIKV in human cervical carcinoma (HeLa) cells [105, 106]. IFITM expression also impairs syncytiotrophoblast formation, which occurs via cell-cell fusion, and is an essential aspect of placental formation [107]. Flaviviral proteins may be more pro-apoptotic than anti-apoptotic as increased apoptosis has been associated with less infection and decreased severity [102]. Additional research is needed to clarify when ZIKV may induce apoptosis and what advantages to the virus this may provide.

Autophagy is another important antiviral pathway cells use in response to infection that many flaviviruses actually induce as part of their life cycle [108-110]. Autophagy-related 16-like 1 (ATG16L1) protein is important for autophagosome maturation, and ZIKV infection in ATG16L1^{-/-} mice results in limited placental infection and vertical transmission [111]. Chemical inhibitors of autophagy also result in decreased viral replication in JEG3 trophoblast cells and in mouse placentas and fetuses [111]. This finding suggests that ZIKV replication and infection is largely mediated by the induction of autophagy in trophoblasts [108, 111]. In human fetal neural stem cell cultures, it was shown that ZIKV proteins NS4A and NS4B work to increase autophagy by

interfering with the Akt-mTOR pathway [110]. Altogether, these data show that ZIKV can surpass barriers and manipulate cell function to produce progeny and disseminate.

1.8 The innate immune defense and its interaction with ZIKV

In addition to the intrinsic host defenses (cell barriers, apoptosis, and autophagy) [112] previously discussed, cells have additional mechanisms to identify infection called the innate immune system [112]. The intrinsic and innate immune responses activate the adaptive immune response, which will not be discussed. This includes a range of proteins that identify various aspects of the pathogen life cycle to then alert the adaptive immune system. IFNs, interferon stimulatory genes (ISGs), and Toll Like Receptors (TLRs) are important elements of the innate immune response and are discussed in terms of data collected during ZIKV infection. Low levels of TLRs and ISGs are present within cells to screen for the presence of viral genomes and proteins. While the figure below depicts TLR or RIG-I/MDA5 activation as the first step in the host innate immune response, it should be noted that there are already low levels of these proteins and others (such as IFNAR and STAT1/2) present in the cell but that their activation triggers enhanced production of innate immune proteins in a paracrine and autocrine manner [113].

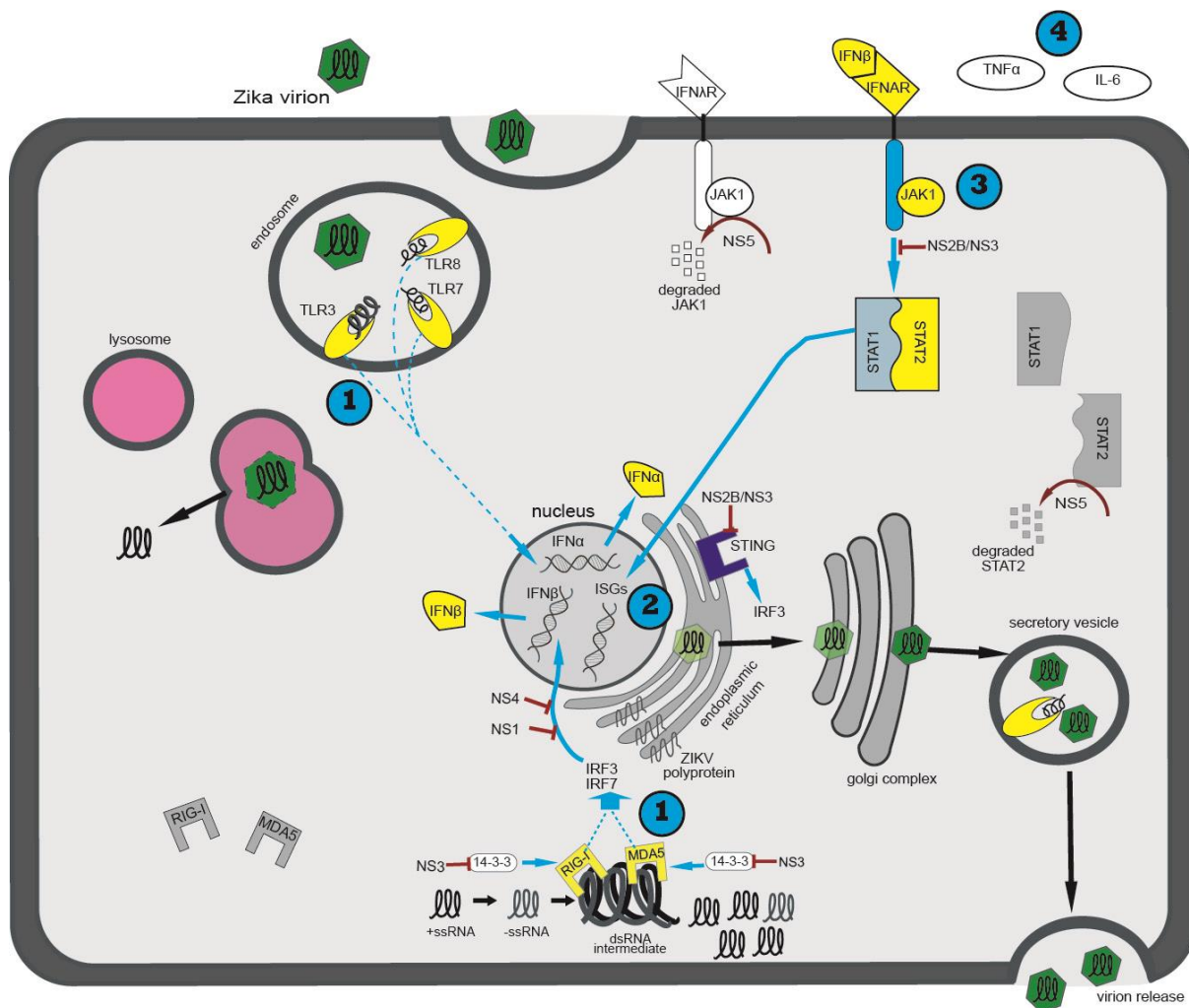


Figure 1.3. Cellular immune response to ZIKV infection and Zika viral strategies to inhibit that response. The innate immune response elements discussed herein are depicted alongside the ZIKV life cycle with numerical indicators based on how the innate immune response is activated. Once the Zika vRNA is released into the cytoplasm, it can be detected by TLR7 and TLR8 (step 1). The replication intermediate, dsRNA, can be recognized by TLR3, RIG-I, or MDA-5 (step 1). Both steps are considered step 1 because once the RNA is replicated, it could be recognized by either set of innate immune proteins. This recognition triggers production of IFN α and IFN β (step 2). IFN α and IFN β are secreted products that then signal to that cell and neighboring cells through IFNAR. Activation of this receptor results in STAT1 and STAT2 activation (step 3), which then leads to the production and release of IFN stimulated genes (ISGs) (step 4). Zika viral proteins work to impair these recognition elements and prevent ISG production. Black arrows indicate the ZIKV life cycle. Inhibition by ZIKV proteins is depicted by the red inhibition signs. Blue arrows indicate activation. Yellow indicates activation and gray indicates inactive. Solid lines mean direct activation. Dashed lines mean indirect activation. Figure made by LNB.

Mammalian cells express proteins that monitor various aspects of the viral life cycle to thwart infection. For instance, retinoic acid-inducible gene I (RIG-I/DDX58) and melanoma differentiation-associated protein 5 (MDA5) recognize dsRNA, which occurs as a transient stage during viral genome replication. These proteins are important in flavivirus genome recognition and activation of the innate immune system [58]. TLRs identify pathogens via specific patterns (pathogen-associated microbial patterns; PAMPs). The presence of vRNA triggers TLR3 and TLR7. The activation of these receptors leads to cellular production of IFN β and IFN γ [101] followed by downstream activation of ISGs including ISG15, OAS2, MX1, and IFIT [101]. The presence of Zika vRNA-activated TLR3 and TLR8 in HTR-8 trophoblasts, an EVT-like immortalized trophoblast cell line, resulted in significantly increased production of tumor necrosis factor (TNF)- α and IL-6 [97]. TNF- α and IL-6 are pro-inflammatory cytokines that trigger an adaptive immune response [114, 115].

IFNs play an important role in the trophoblast antiviral response. IFNs work to activate genes involved in mRNA degradation and protein translation inhibition to control viral replication, as well as inhibit cell proliferation [116]. There are three main classes of IFNs: type I (INF α , IFN β), type II (IFN γ), and type III (IFN λ). IFN λ 1 is constitutively released by primary human term trophoblast cells and protects them from ZIKV infection [117]. Early gestation trophoblast cells may not constitutively express these IFNs [75], which may explain in part increased susceptibility to infection at this stage. However, further investigation of trophoblast defense mechanisms within the earliest stages of gestation is needed to resolve why first trimester trophoblasts have increased susceptibility to ZIKV infection.

Mice are not naturally susceptible to ZIKV infection and must be immune compromised to model ZIKV infection in part because ZIKV cannot interfere with the immune response [118]. For instance, the ZIKV NS5 protein can interfere with IFN signaling in humans by promoting signal transducers and activators of transcription 2 (STAT2) degradation and preventing ISG expression [119]. However, the ZIKV NS5 protein cannot recognize mouse STAT2, which allows expression of ISGs and then IFNs [119, 120]. RIG-I deficient, IFN deficient, IFNAR deficient, and humanized STAT2-deficient mouse models are used to study the impact of ZIKV in vivo [58, 118, 120, 121]. The importance of IFNs in ZIKV infection was further established by in vivo mouse experiments. For instance, mice with a fully functioning type I IFN response had minor symptoms with ZIKV infection, whereas IFN^{-/-} increased severity. Also, vaginal inoculation of pregnant wild type mice resulted in modest fetal growth restriction (FGR), whereas inoculation of immunocompromised (IFNAR deficient) pregnant mice resulted in severe FGR and a significant elevation in fetal death [58]. Stimulator of IFN genes (STING) activates IFN regulatory factors (IRF) 3, which results in type I IFN production [122]. An IRF 3 and IRF7 knockout mouse study further supports the importance of these ISGs in controlling ZIKV replication in the placenta since these IRFs trigger the type I IFN response [58]. These studies show the importance of IFN in controlling and ablating ZIKV infection.

To overcome the cell's immune response, several ZIKV proteins function to block the antiviral IFN pathway. For example, the host cell's STING protein is targeted by the NS2B-NS3 protein complex to impair IFN β production, which also is impeded by NS1 and NS4B [101]. NS3 interferes with the 14-3-3 pathway, which prevents RIG-I and MDA5 from activating their

downstream antiviral pathways [123]. The NS2B-NS3 complex and NS5 block STAT1 and STAT2 activation, and STAT2 triggers degradation of Janus kinase 1 (JAK1) and STAT2 [101, 124, 125]. These actions limit a productive IFN response by preventing transcription of ISGs [101, 124, 125], thereby allowing increased ZIKV replication.

In summary, cells possess numerous means of detecting and truncating a viral infection. The presence of ZIKV initially triggers an innate immune response [101] and the release of ISGs and proinflammatory cytokines, which alert the adaptive immune system. An immune response can also trigger a cell to undergo apoptosis or autophagy with the goal being to prevent further viral replication and spread. In order to ensure viral propagation, ZIKV possesses several mechanisms to overcome these barriers. Overall, it is the ability of ZIKV to impede the immune response that allows dissemination and continued infection.

1.9 Extracellular vesicles may modulate viral infection.

Another way viruses can evade the immune response and host defenses is by using extracellular vesicles (EVs). EVs are cell-derived particles that are released into the extracellular environment and contain cargo such as proteins, nucleic acids, and lipids [126]. EV cargo is altered under various disease and infection conditions [126-133], and viral proteins and genomes have been found within EVs [128-130, 134, 135]. Viruses may use EVs to alter cell permissiveness. Non-permissive cells (cells lacking CCR5 and CXCR4) exposed to EVs that contained CCR5 and CXCR4 became permissive to HIV infection [136, 137].

EVs can disseminate viruses in the *Flaviviridae* family as demonstrated by studies of hepatitis C virus, DENV and WNV. For example, EVs were shown to carry and deliver hepatitis C vRNA to other cells. The hepatitis C virus used was modified such that the genome could be replicated but infectious virions could not be produced or released. A subsequent study in which exosome secretion was inhibited with a chemical resulted in decreased vRNA genome transfer to susceptible target cells; therefore supporting EVs as a means of viral dissemination [129]. EVs released by DENV-infected cells also were shown to be infectious, and chemical inhibition of exosome release resulted in decreased dengue vRNA quantities [134]. Furthermore, Langat virus and WNV, two arboviruses, have been shown to utilize EVs to enhance transmission [135]. These data suggest that viruses may utilize EVs as a Trojan horse to promote infection by hijacking these extracellular shuttles.

1.10 Thesis Overview

ZIKV infection remains an important research focus given the severe effects of infection on fetal and neonatal development, and the historical threat of sporadic outbreaks. The motivating objectives of this thesis are 1) to determine how early ZIKV can impact the placenta, 2) to assess which trophoblast cell types are permissive to infection, and 3) to evaluate the use of EVs as a readout of cellular infection.

The rhesus macaque is a highly translational model for human pregnancy as it has similar placental structure, prolonged gestation, and gives birth to precocious offspring [126, 138]. Numerous studies with pregnant rhesus macaques support their use to understand the impact of ZIKV on human pregnancy as infection has a similar outcome [139-141]. In the case study discussed in the Chapter 2, a dam was infected towards the end of the first trimester with ZIKV. This resulted in prolonged maternal viremia and pregnancy loss during the second trimester. Although ZIKV was not detected in the placenta, there was extreme placental pathology including infarcts, hemorrhages, and extensive calcifications. This study, as well as other studies across different National Primate Research Centers [41], further supports that infection early in pregnancy can result in an adverse pregnancy outcome in the macaque. The outcome from this case study raised questions as to how ZIKV may impact the placenta and at what time points of gestation placental infection could occur.

Due to practical limitations of early pregnancy detection in humans, the inability to typically detect infection onset in symptomatic and asymptomatic individuals, and limitations of knowing when pregnancy first begins in human patients as well as limited access to sampling opportunities, an animal model is imperative to understanding how early ZIKV can impact pregnancy. Since ZIKV can be sexually transmitted, it is critical to know how early infection can disrupt pregnancy. We hypothesized that zona-enclosed oocytes are not permissive to infection, whereas trophoblast cells of the implanting blastocyst that are exposed to the maternal uterine environment are permissive. Using in vitro fertilization in a rhesus macaque model, we determined that ZIKV was embryotoxic at high doses and impeded cellular growth at lower doses. These findings are presented in Chapter

3 and supported our hypothesis, in agreement with previous and subsequently published studies [13, 36, 40, 78-80], that early gestation trophoblast cells were more permissive to infection than those from later stages of gestation.

We next transitioned to an in vitro macaque trophoblast cell culture system to determine which trophoblast cell types were permissive to infection, and to determine how infection impacted cell function. This model adds tremendous value to this study as these cells are more representative of in vivo trophoblast cells than currently established cell lines and provides more clarity than placental tissue explants, which contain numerous cell types in a platform of limited lifespan. We hypothesized that all trophoblast cell types would be permissive to infection and that EVs could serve as a readout of cellular infection. The results from this study are presented in Chapter 4 and demonstrate that TSCs and STs are permissive to infection, whereas EVT_s were not readily infected.

As mentioned above, ZIKV uses the secretory pathway for viral propagation. Exosomes, a type of EV, are also derived in the secretory pathway and therefore, we hypothesized that ZIKV proteins or whole virions are likely to be packaged as EV cargo. The evaluation of placenta derived EV cargo is important because EVs secreted by trophoblast cells could be used to monitor placental health with minimal invasiveness since EVs can be isolated from various body fluids, including blood. There are limited means to access the placenta during pregnancy and they all require invasive procedures. EVs could be used to determine if vertical transmission occurred and what placental damage may be occurring so as to determine the risk of an adverse pregnancy outcome

[126]. The potential for EVs to provide a readout to prospectively identify pregnancies at risk for adverse outcomes, both physiological complications and pathogen-induced complications, was further expanded on as a published review paper [126] that is provided here as a Supplemental Chapter.

1.11 Significance

This work furthers our recognition that ZIKV can impact early pregnancy in the highly translational rhesus macaque pregnancy model. Our findings with the ZIKV embryo outgrowth study support epidemiological data that suggests ZIKV could impact very early pregnancy. These findings are significant for couples trying to conceive as ZIKV presence in semen does not impact oocyte fertilization. Semen collected from men positive for ZIKV may not need to be cleaned and stripped of ZIKV if used for assisted reproduction, including IVF or intracytoplasmic sperm injection. However, the embryo used for transfer should be cleaned and stripped of any potential virus as the human female reproductive tract is permissive to infection [142-144].

In addition, we showed that trophoblast cells are permissive to ZIKV infection, which impacted cellular function and EV cargo. These findings are significant as our model is more representative of the first trimester human placenta than most of what has been published. We know that ZIKV infection early in pregnancy is associated with worse outcomes and increased pregnancy loss [13, 14, 36, 40, 78-80]. However, Hofbauer cells are often the only placental cells that test positive for ZIKV [83, 145, 146], which raises questions as to whether trophoblast cells are permissive. Our

highly translational model shows these cells are permissive, which suggests placental infection may be involved in adverse outcomes. Prolonged viremia is often observed in pregnancy [40, 55, 80, 140, 147, 148], and we hypothesized the placenta could be a reservoir. Our data support this hypothesis because not only were trophoblast cells permissive, but they released EVs that contained the ZIKV E protein and may be infectious. This finding is significant as infectious trophoblast EVs shed into maternal blood could then infect other maternal cells. Overall, these findings shed light on the impact ZIKV has on early gestation trophoblasts and delves into the potential for EVs to be a readout of cellular infection.

1.12 References

1. Cornish EF, Filipovic I, Asenius F, Williams DJ, McDonnell T. Innate Immune Responses to Acute Viral Infection During Pregnancy. *Front Immunol* 2020; 11:572567.
2. Littauer EQ, Skountzou I. Hormonal Regulation of Physiology, Innate Immunity and Antibody Response to H1N1 Influenza Virus Infection During Pregnancy. *Front Immunol* 2018; 9:2455.
3. Jaan A, Rajnik M. TORCH Complex. In: StatPearls. Treasure Island (FL); 2021.
4. Zhang H, He Z, Zeng W, Peng HJ. Roles of Interferons in Pregnant Women with Dengue Infection: Protective or Dangerous Factors. *Can J Infect Dis Med Microbiol* 2017; 2017:1671607.
5. Kourtis AP, Read JS, Jamieson DJ. Pregnancy and infection. *N Engl J Med* 2014; 370:2211-2218.
6. Kudo T, Wei EQ, Inoki R. Activation of calcium ion-dependent proteinases by bradykinin in dental pulp of the rat. *Adv Exp Med Biol* 1989; 247B:627-631.
7. Huntley BJF, Mulder IA, Di Mascio D, Vintzileos WS, Vintzileos AM, Berghella V, Chauhan SP. Adverse Pregnancy Outcomes Among Individuals With and Without Severe Acute Respiratory Syndrome Coronavirus 2 (SARS-CoV-2): A Systematic Review and Meta-analysis. *Obstet Gynecol* 2021; 137:585-596.

8. Karimi L, Vahedian-Azimi A, Makvandi S, Sahebkar A. A Systematic Review of 571 Pregnancies Affected by COVID-19. *Adv Exp Med Biol* 2021; 1321:287-298.
9. Villar J, Ariff S, Gunier RB, Thiruvengadam R, Rauch S, Kholin A, Roggero P, Prefumo F, do Vale MS, Cardona-Perez JA, Maiz N, Cetin I, et al. Maternal and Neonatal Morbidity and Mortality Among Pregnant Women With and Without COVID-19 Infection: The INTERCOVID Multinational Cohort Study. *JAMA Pediatr* 2021.
10. Coyne CB, Lazear HM. Zika virus - reigniting the TORCH. *Nat Rev Microbiol* 2016; 14:707-715.
11. Silasi M, Cardenas I, Kwon JY, Racicot K, Aldo P, Mor G. Viral infections during pregnancy. *Am J Reprod Immunol* 2015; 73:199-213.
12. Freitas DA, Souza-Santos R, Carvalho LMA, Barros WB, Neves LM, Brasil P, Wakimoto MD. Congenital Zika syndrome: A systematic review. *PLoS One* 2020; 15:e0242367.
13. Lima GP, Rozenbaum D, Pimentel C, Frota ACC, Vivacqua D, Machado ES, Sztajnbok F, Abreu T, Soares RA, Hofer CB. Factors associated with the development of Congenital Zika Syndrome: a case-control study. *BMC Infect Dis* 2019; 19:277.
14. Rasmussen SA, Jamieson DJ. Teratogen update: Zika virus and pregnancy. *Birth Defects Res* 2020; 112:1139-1149.
15. Brar R, Sikka P, Suri V, Singh MP, Suri V, Mohindra R, Biswal M. Maternal and fetal outcomes of dengue fever in pregnancy: a large prospective and descriptive observational study. *Arch Gynecol Obstet* 2021.
16. Tougma SA, Zoungrana/Yameogo WN, Dahourou DL, Salou/Kagone IA, Compaore TR, Kabore A, Kagone T, Drabo MK, Meda N. Dengue virus infection and pregnancy outcomes during the 2017 outbreak in Ouagadougou, Burkina Faso: A retrospective cohort study. *PLoS One* 2020; 15:e0238431.
17. O'Leary DR, Kuhn S, Kniss KL, Hinckley AF, Rasmussen SA, Pape WJ, Kightlinger LK, Beecham BD, Miller TK, Neitzel DF, Michaels SR, Campbell GL, et al. Birth outcomes following West Nile Virus infection of pregnant women in the United States: 2003-2004. *Pediatrics* 2006; 117:e537-545.
18. Diniz LMO, Romanelli RMC, de Carvalho AL, Teixeira DC, de Carvalho LFA, Ferreira Cury V, Filho MPL, Perigolo G, Heringer TP. Perinatal Yellow Fever: A Case Report. *Pediatr Infect Dis J* 2019; 38:300-301.
19. Chong HY, Leow CY, Abdul Majeed AB, Leow CH. Flavivirus infection-A review of immunopathogenesis, immunological response, and immunodiagnosis. *Virus Res* 2019; 274:197770.

20. Charlier C, Beaudoin MC, Couderc T, Lortholary O, Lecuit M. Arboviruses and pregnancy: maternal, fetal, and neonatal effects. *Lancet Child Adolesc Health* 2017; 1:134-146.
21. Chaturvedi UC, Mathur A, Chandra A, Das SK, Tandon HO, Singh UK. Transplacental infection with Japanese encephalitis virus. *J Infect Dis* 1980; 141:712-715.
22. Ribeiro CF, Lopes VGS, Brasil P, Pires ARC, Rohloff R, Nogueira RMR. Dengue infection in pregnancy and its impact on the placenta. *Int J Infect Dis* 2017; 55:109-112.
23. Ribeiro CF, Lopes VG, Brasil P, Coelho J, Muniz AG, Nogueira RM. Perinatal transmission of dengue: a report of 7 cases. *J Pediatr* 2013; 163:1514-1516.
24. Nunes PC, Paes MV, de Oliveira CA, Soares AC, de Filippis AM, Lima Mda R, de Barcelos Alves AM, da Silva JF, de Oliveira Coelho JM, de Carvalho Rodrigues F, Nogueira RM, Dos Santos FB. Detection of dengue NS1 and NS3 proteins in placenta and umbilical cord in fetal and maternal death. *J Med Virol* 2016; 88:1448-1452.
25. Mathur A, Arora KL, Chaturvedi UC. Congenital infection of mice with Japanese encephalitis virus. *Infect Immun* 1981; 34:26-29.
26. Nishioka Sde A, Nunes-Araujo FR, Pires WP, Silva FA, Costa HL. Yellow fever vaccination during pregnancy and spontaneous abortion: a case-control study. *Trop Med Int Health* 1998; 3:29-33.
27. Suzano CE, Amaral E, Sato HK, Papaiordanou PM, Campinas Group on Yellow Fever Immunization during P. The effects of yellow fever immunization (17DD) inadvertently used in early pregnancy during a mass campaign in Brazil. *Vaccine* 2006; 24:1421-1426.
28. Porudominsky R, Gotuzzo EH. Yellow fever vaccine and risk of developing serious adverse events: a systematic review. *Rev Panam Salud Publica* 2018; 42:e75.
29. da Silva FC, Magaldi FM, Sato HK, Bevilacqua E. Yellow Fever Vaccination in a Mouse Model Is Associated With Uninterrupted Pregnancies and Viable Neonates Except When Administered at Implantation Period. *Front Microbiol* 2020; 11:245.
30. Tsai TF. Congenital arboviral infections: something new, something old. *Pediatrics* 2006; 117:936-939.
31. Centers for Disease C, Prevention. Intrauterine West Nile virus infection--New York, 2002. *MMWR Morb Mortal Wkly Rep* 2002; 51:1135-1136.
32. Julander JG, Winger QA, Rickords LF, Shi PY, Tilgner M, Binduga-Gajewska I, Sidwell RW, Morrey JD. West Nile virus infection of the placenta. *Virology* 2006; 347:175-182.
33. Platt DJ, Smith AM, Arora N, Diamond MS, Coyne CB, Miner JJ. Zika virus-related neurotropic flaviviruses infect human placental explants and cause fetal demise in mice. *Sci Transl Med* 2018; 10.

34. Musso D, Bossin H, Mallet HP, Besnard M, Brout J, Baudouin L, Levi JE, Sabino EC, Ghawche F, Lanteri MC, Baud D. Zika virus in French Polynesia 2013-14: anatomy of a completed outbreak. *Lancet Infect Dis* 2018; 18:e172-e182.
35. Cauchemez S, Besnard M, Bompard P, Dub T, Guillemette-Artur P, Eyrolle-Guignot D, Salje H, Van Kerkhove MD, Abadie V, Garel C, Fontanet A, Mallet HP. Association between Zika virus and microcephaly in French Polynesia, 2013-15: a retrospective study. *Lancet* 2016; 387:2125-2132.
36. Brady OJ, Osgood-Zimmerman A, Kassebaum NJ, Ray SE, de Araujo VEM, da Nobrega AA, Frutuoso LCV, Lecca RCR, Stevens A, Zoca de Oliveira B, de Lima JM, Jr., Bogoch, II, et al. The association between Zika virus infection and microcephaly in Brazil 2015-2017: An observational analysis of over 4 million births. *PLoS Med* 2019; 16:e1002755.
37. Martines RB, Bhatnagar J, Keating MK, Silva-Flannery L, Muehlenbachs A, Gary J, Goldsmith C, Hale G, Ritter J, Rollin D, Shieh WJ, Luz KG, et al. Notes from the Field: Evidence of Zika Virus Infection in Brain and Placental Tissues from Two Congenitally Infected Newborns and Two Fetal Losses--Brazil, 2015. *MMWR Morb Mortal Wkly Rep* 2016; 65:159-160.
38. van der Eijk AA, van Genderen PJ, Verdijk RM, Reusken CB, Mogling R, van Kampen JJ, Widagdo W, Aron GI, GeurtsvanKessel CH, Pas SD, Raj VS, Haagmans BL, et al. Miscarriage Associated with Zika Virus Infection. *N Engl J Med* 2016; 375:1002-1004.
39. Gonce A, Martinez MJ, Marban-Castro E, Saco A, Soler A, Alvarez-Mora MI, Peiro A, Gonzalo V, Hale G, Bhatnagar J, Lopez M, Zaki S, et al. Spontaneous Abortion Associated with Zika Virus Infection and Persistent Viremia. *Emerg Infect Dis* 2018; 24:933-935.
40. Musso D, Ko AI, Baud D. Zika Virus Infection - After the Pandemic. *N Engl J Med* 2019; 381:1444-1457.
41. Dudley DM, Van Rompay KK, Coffey LL, Ardeshir A, Keesler RI, Bliss-Moreau E, Grigsby PL, Steinbach RJ, Hirsch AJ, MacAllister RP, Pecoraro HL, Colgin LM, et al. Miscarriage and stillbirth following maternal Zika virus infection in nonhuman primates. *Nat Med* 2018; 24:1104-1107.
42. Melo AS, Aguiar RS, Amorim MM, Arruda MB, Melo FO, Ribeiro ST, Batista AG, Ferreira T, Dos Santos MP, Sampaio VV, Moura SR, Rabello LP, et al. Congenital Zika Virus Infection: Beyond Neonatal Microcephaly. *JAMA Neurol* 2016; 73:1407-1416.
43. de Carvalho NS, de Carvalho BF, Doris B, Silverio Biscaia E, Arias Fugaca C, de Noronha L. Zika virus and pregnancy: An overview. *Am J Reprod Immunol* 2017; 77.
44. Guerin B, Pozzi N. Viruses in boar semen: detection and clinical as well as epidemiological consequences regarding disease transmission by artificial insemination. *Theriogenology* 2005; 63:556-572.

45. Al Ahmad MZ, Pellerin JL, Larrat M, Chatagnon G, Cecile R, Sailleau C, Zientara S, Fieni F. Can bluetongue virus (BTV) be transmitted via caprine embryo transfer? *Theriogenology* 2011; 76:126-132.
46. Haegeman A, Vandaele L, De Leeuw I, Oliveira AP, Nauwynck H, Van Soom A, De Clercq K. Failure to Remove Bluetongue Serotype 8 Virus (BTV-8) From in vitro Produced and in vivo Derived Bovine Embryos and Subsequent Transmission of BTV-8 to Recipient Cows After Embryo Transfer. *Front Vet Sci* 2019; 6:432.
47. Hebia I, Fieni F, Duchamp G, Destrumelle S, Pellerin JL, Zientara S, Vautherot JF, Bruyas JF. Potential risk of equine herpes virus 1 (EHV-1) transmission by equine embryo transfer. *Theriogenology* 2007; 67:1485-1491.
48. Counotte MJ, Kim CR, Wang J, Bernstein K, Deal CD, Broutet NJN, Low N. Sexual transmission of Zika virus and other flaviviruses: A living systematic review. *PLoS Med* 2018; 15:e1002611.
49. Barzon L, Pacenti M, Franchin E, Lavezzo E, Trevisan M, Sgarabotto D, Palu G. Infection dynamics in a traveller with persistent shedding of Zika virus RNA in semen for six months after returning from Haiti to Italy, January 2016. *Euro Surveill* 2016; 21.
50. Mansuy JM, Dutertre M, Mengelle C, Fourcade C, Marchou B, Delobel P, Izopet J, Martin-Blondel G. Zika virus: high infectious viral load in semen, a new sexually transmitted pathogen? *Lancet Infect Dis* 2016; 16:405.
51. Sakkas H, Bozidis P, Giannakopoulos X, Sofikitis N, Papadopoulou C. An Update on Sexual Transmission of Zika Virus. *Pathogens* 2018; 7.
52. Joguet G, Mansuy JM, Matusali G, Hamdi S, Walschaerts M, Pavili L, Guyomard S, Prisant N, Lamarre P, Dejuq-Rainsford N, Pasquier C, Bujan L. Effect of acute Zika virus infection on sperm and virus clearance in body fluids: a prospective observational study. *Lancet Infect Dis* 2017; 17:1200-1208.
53. Turmel JM, Abgueguen P, Hubert B, Vandamme YM, Maquart M, Le Guillou-Guillemette H, Leparc-Goffart I. Late sexual transmission of Zika virus related to persistence in the semen. *Lancet* 2016; 387:2501.
54. Oliveira DB, Almeida FJ, Durigon EL, Mendes EA, Braconi CT, Marchetti I, Andreatta-Santos R, Cunha MP, Alves RP, Pereira LR, Melo SR, Neto DF, et al. Prolonged Shedding of Zika Virus Associated with Congenital Infection. *N Engl J Med* 2016; 375:1202-1204.
55. Desclaux A, de Lamballerie X, Leparc-Goffart I, Vilain-Parce A, Coatleven F, Fleury H, Malvy D. Probable Sexually Transmitted Zika Virus Infection in a Pregnant Woman. *N Engl J Med* 2018; 378:1458-1460.
56. Coelho FC, Durovni B, Saraceni V, Lemos C, Codeco CT, Camargo S, de Carvalho LM, Bastos L, Arduini D, Villela DA, Armstrong M. Higher incidence of Zika in adult women

- than adult men in Rio de Janeiro suggests a significant contribution of sexual transmission from men to women. *Int J Infect Dis* 2016; 51:128-132.
57. Tan L, Lacko LA, Zhou T, Tomoiaga D, Hurtado R, Zhang T, Sevilla A, Zhong A, Mason CE, Noggle S, Evans T, Stuhlmann H, et al. Pre- and peri-implantation Zika virus infection impairs fetal development by targeting trophectoderm cells. *Nat Commun* 2019; 10:4155.
 58. Yockey LJ, Varela L, Rakib T, Khoury-Hanold W, Fink SL, Stutz B, Szigeti-Buck K, Van den Pol A, Lindenbach BD, Horvath TL, Iwasaki A. Vaginal Exposure to Zika Virus during Pregnancy Leads to Fetal Brain Infection. *Cell* 2016; 166:1247-1256 e1244.
 59. Schmidt JK, Mean KD, Puntney RC, Alexander ES, Sullivan R, Simmons HA, Zeng X, Weiler AM, Friedrich TC, Golos TG. Zika virus in rhesus macaque semen and reproductive tract tissues: a pilot study of acute infection. *Biol Reprod* 2020; 103:1030-1042.
 60. Osuna CE, Lim SY, Deleage C, Griffin BD, Stein D, Schroeder LT, Orange RW, Best K, Luo M, Hraber PT, Andersen-Elyard H, Ojeda EF, et al. Zika viral dynamics and shedding in rhesus and cynomolgus macaques. *Nat Med* 2016; 22:1448-1455.
 61. Peregrine J, Gurung S, Lindgren MC, Husain S, Zavy MT, Myers DA, Papin JF. Zika Virus Infection, Reproductive Organ Targeting, and Semen Transmission in the Male Olive Baboon. *J Virol* 2019; 94.
 62. Block LN, Aliota MT, Friedrich TC, Schotzko ML, Mean KD, Wiepz GJ, Golos TG, Schmidt JK. Embryotoxic impact of Zika virus in a rhesus macaque in vitro implantation model. *Biol Reprod* 2020; 102:806-816.
 63. Newman CM, Tarantal AF, Martinez ML, Simmons HA, Morgan TK, Zeng X, Rosinski JR, Bliss MI, Bohm EK, Dudley DM, Aliota MT, Friedrich TC, et al. Early Embryonic Loss Following Intravaginal Zika Virus Challenge in Rhesus Macaques. *Frontiers in Immunology* 2021; 12.
 64. Gurung S, Nadeau H, Maxted M, Peregrine J, Reuter D, Norris A, Edwards R, Hyatt K, Singleton K, Papin JF, Myers DA. Maternal Zika Virus (ZIKV) Infection following Vaginal Inoculation with ZIKV-Infected Semen in Timed-Pregnant Olive Baboons. *J Virol* 2020; 94.
 65. Maltepe E, Fisher SJ. Placenta: the forgotten organ. *Annu Rev Cell Dev Biol* 2015; 31:523-552.
 66. Knofler M, Haider S, Saleh L, Pollheimer J, Gamage T, James J. Human placenta and trophoblast development: key molecular mechanisms and model systems. *Cell Mol Life Sci* 2019; 76:3479-3496.
 67. Feinberg WM, Bruck DC, Jeter MA, Corrigan JJ, Jr. Fibrinolysis after acute ischemic stroke. *Thromb Res* 1991; 64:117-127.

68. Okae H, Toh H, Sato T, Hiura H, Takahashi S, Shirane K, Kabayama Y, Suyama M, Sasaki H, Arima T. Derivation of Human Trophoblast Stem Cells. *Cell Stem Cell* 2018; 22:50-63 e56.
69. Gamage TK, Chamley LW, James JL. Stem cell insights into human trophoblast lineage differentiation. *Hum Reprod Update* 2016; 23:77-103.
70. Turco MY, Moffett A. Development of the human placenta. *Development* 2019; 146.
71. Chang CW, Wakeland AK, Parast MM. Trophoblast lineage specification, differentiation and their regulation by oxygen tension. *J Endocrinol* 2018; 236:R43-R56.
72. Robinson N, Mayorquin Galvan EE, Zavala Trujillo IG, Zavala-Cerna MG. Congenital Zika syndrome: Pitfalls in the placental barrier. *Rev Med Virol* 2018; 28:e1985.
73. Morales-Prieto DM, Ospina-Prieto S, Chaiwangyen W, Schoenleben M, Markert UR. Pregnancy-associated miRNA-clusters. *J Reprod Immunol* 2013; 97:51-61.
74. Cunningham FG, Leveno KJ, Bloom S, Dashe JS, Hoffman BL, Casey BM, Spong C. *Williams Obstetrics*. McGraw-Hill Medical; 2018.
75. Sheridan MA, Yunusov D, Balaraman V, Alexenko AP, Yabe S, Verjovski-Almeida S, Schust DJ, Franz AW, Sadovsky Y, Ezashi T, Roberts RM. Vulnerability of primitive human placental trophoblast to Zika virus. *Proc Natl Acad Sci U S A* 2017; 114:E1587-E1596.
76. Burton GJ, Cindrova-Davies T, Turco MY. Review: Histotrophic nutrition and the placental-endometrial dialogue during human early pregnancy. *Placenta* 2020; 102:21-26.
77. Navti OB, Al-Belushi M, Konje JC, Frcog. Cytomegalovirus infection in pregnancy - An update. *Eur J Obstet Gynecol Reprod Biol* 2021; 258:216-222.
78. Brasil P, Pereira JP, Jr., Moreira ME, Ribeiro Nogueira RM, Damasceno L, Wakimoto M, Rabello RS, Valderramos SG, Halai UA, Salles TS, Zin AA, Horovitz D, et al. Zika Virus Infection in Pregnant Women in Rio de Janeiro. *N Engl J Med* 2016; 375:2321-2334.
79. Hoen B, Schaub B, Funk AL, Ardillon V, Boullard M, Cabie A, Callier C, Carles G, Cassadou S, Cesaire R, Douine M, Herrmann-Storck C, et al. Pregnancy Outcomes after ZIKV Infection in French Territories in the Americas. *N Engl J Med* 2018; 378:985-994.
80. Pomar L, Malingier G, Benoist G, Carles G, Ville Y, Rousset D, Hcini N, Pomar C, Jolivet A, Lambert V. Association between Zika virus and fetopathy: a prospective cohort study in French Guiana. *Ultrasound Obstet Gynecol* 2017; 49:729-736.
81. Honein MA, Dawson AL, Petersen EE, Jones AM, Lee EH, Yazdy MM, Ahmad N, Macdonald J, Evert N, Bingham A, Ellington SR, Shapiro-Mendoza CK, et al. Birth Defects Among Fetuses and Infants of US Women With Evidence of Possible Zika Virus Infection During Pregnancy. *JAMA* 2017; 317:59-68.

82. Pierson TC, Diamond MS. The emergence of Zika virus and its new clinical syndromes. *Nature* 2018; 560:573-581.
83. Bhatnagar J, Rabeneck DB, Martines RB, Reagan-Steiner S, Ermias Y, Estetter LB, Suzuki T, Ritter J, Keating MK, Hale G, Gary J, Muehlenbachs A, et al. Zika Virus RNA Replication and Persistence in Brain and Placental Tissue. *Emerg Infect Dis* 2017; 23:405-414.
84. Rabelo K, Goncalves A, Souza LJ, Sales AP, Lima SMB, Trindade GF, Ciambarella BT, Amorim Tasmio NR, Diaz BL, Carvalho JJ, Duarte MPO, Paes MV. Zika Virus Infects Human Placental Mast Cells and the HMC-1 Cell Line, and Triggers Degranulation, Cytokine Release and Ultrastructural Changes. *Cells* 2020; 9.
85. Culjat M, Darling SE, Nerurkar VR, Ching N, Kumar M, Min SK, Wong R, Grant L, Melish ME. Clinical and Imaging Findings in an Infant With Zika Embryopathy. *Clin Infect Dis* 2016; 63:805-811.
86. Martines RB, Bhatnagar J, de Oliveira Ramos AM, Davi HP, Iglezias SD, Kanamura CT, Keating MK, Hale G, Silva-Flannery L, Muehlenbachs A, Ritter J, Gary J, et al. Pathology of congenital Zika syndrome in Brazil: a case series. *Lancet* 2016; 388:898-904.
87. Yockey LJ, Jurado KA, Arora N, Millet A, Rakib T, Milano KM, Hastings AK, Fikrig E, Kong Y, Horvath TL, Weatherbee S, Kliman HJ, et al. Type I interferons instigate fetal demise after Zika virus infection. *Sci Immunol* 2018; 3.
88. Miner JJ, Cao B, Govero J, Smith AM, Fernandez E, Cabrera OH, Garber C, Noll M, Klein RS, Noguchi KK, Mysorekar IU, Diamond MS. Zika Virus Infection during Pregnancy in Mice Causes Placental Damage and Fetal Demise. *Cell* 2016; 165:1081-1091.
89. Shan C, Xia H, Haller SL, Azar SR, Liu Y, Liu J, Muruato AE, Chen R, Rossi SL, Wakamiya M, Vasilakis N, Pei R, et al. A Zika virus envelope mutation preceding the 2015 epidemic enhances virulence and fitness for transmission. *Proc Natl Acad Sci U S A* 2020; 117:20190-20197.
90. Vermillion MS, Lei J, Shabi Y, Baxter VK, Crilly NP, McLane M, Griffin DE, Pekosz A, Klein SL, Burd I. Intrauterine Zika virus infection of pregnant immunocompetent mice models transplacental transmission and adverse perinatal outcomes. *Nat Commun* 2017; 8:14575.
91. Mohr EL, Block LN, Newman CM, Stewart LM, Koenig M, Semler M, Breitbach ME, Teixeira LBC, Zeng X, Weiler AM, Barry GL, Thoong TH, et al. Ocular and uteroplacental pathology in a macaque pregnancy with congenital Zika virus infection. *PLoS One* 2018; 13:e0190617.

92. Chen Q, Gouilly J, Ferrat YJ, Espino A, Glaziou Q, Cartron G, El Costa H, Al-Daccak R, Jabrane-Ferrat N. Metabolic reprogramming by Zika virus provokes inflammation in human placenta. *Nat Commun* 2020; 11:2967.
93. Puerta-Guardo H, Tabata T, Petitt M, Dimitrova M, Glasner DR, Pereira L, Harris E. Zika Virus Nonstructural Protein 1 Disrupts Glycosaminoglycans and Causes Permeability in Developing Human Placentas. *J Infect Dis* 2020; 221:313-324.
94. Tabata T, Petitt M, Puerta-Guardo H, Michlmayr D, Harris E, Pereira L. Zika Virus Replicates in Proliferating Cells in Explants From First-Trimester Human Placentas, Potential Sites for Dissemination of Infection. *J Infect Dis* 2018; 217:1202-1213.
95. El Costa H, Gouilly J, Mansuy JM, Chen Q, Levy C, Cartron G, Veas F, Al-Daccak R, Izopet J, Jabrane-Ferrat N. ZIKA virus reveals broad tissue and cell tropism during the first trimester of pregnancy. *Sci Rep* 2016; 6:35296.
96. Chiu CF, Chu LW, Liao IC, Simanjuntak Y, Lin YL, Juan CC, Ping YH. The Mechanism of the Zika Virus Crossing the Placental Barrier and the Blood-Brain Barrier. *Front Microbiol* 2020; 11:214.
97. Luo H, Winkelmann ER, Fernandez-Salas I, Li L, Mayer SV, Danis-Lozano R, Sanchez-Casas RM, Vasilakis N, Tesh R, Barrett AD, Weaver SC, Wang T. Zika, dengue and yellow fever viruses induce differential anti-viral immune responses in human monocytic and first trimester trophoblast cells. *Antiviral Res* 2018; 151:55-62.
98. Aldo P, You Y, Szigeti K, Horvath TL, Lindenbach B, Mor G. HSV-2 enhances ZIKV infection of the placenta and induces apoptosis in first-trimester trophoblast cells. *Am J Reprod Immunol* 2016; 76:348-357.
99. Bollati M, Alvarez K, Assenberg R, Baronti C, Canard B, Cook S, Coutard B, Decroly E, de Lamballerie X, Gould EA, Grard G, Grimes JM, et al. Structure and functionality in flavivirus NS-proteins: perspectives for drug design. *Antiviral Res* 2010; 87:125-148.
100. Owczarek K, Chykunova Y, Jassoy C, Maksym B, Rajfur Z, Pyrc K. Zika virus: mapping and reprogramming the entry. *Cell Commun Signal* 2019; 17:41.
101. Ferraris P, Yssel H, Misse D. Zika virus infection: an update. *Microbes Infect* 2019; 21:353-360.
102. Okamoto T, Suzuki T, Kusakabe S, Tokunaga M, Hirano J, Miyata Y, Matsuura Y. Regulation of Apoptosis during Flavivirus Infection. *Viruses* 2017; 9.
103. Kvensakul M. Viral Infection and Apoptosis. *Viruses* 2017; 9.
104. Bailey CC, Zhong G, Huang IC, Farzan M. IFITM-Family Proteins: The Cell's First Line of Antiviral Defense. *Annu Rev Virol* 2014; 1:261-283.
105. Savidis G, Perreira JM, Portmann JM, Meraner P, Guo Z, Green S, Brass AL. The IFITMs Inhibit Zika Virus Replication. *Cell Rep* 2016; 15:2323-2330.

106. Monel B, Compton AA, Bruel T, Amraoui S, Burlaud-Gaillard J, Roy N, Guivel-Benhassine F, Porrot F, Genin P, Meertens L, Sinigaglia L, Jouvenet N, et al. Zika virus induces massive cytoplasmic vacuolization and paraptosis-like death in infected cells. *EMBO J* 2017; 36:1653-1668.
107. Buchrieser J, Degrelle SA, Couderc T, Nevers Q, Disson O, Manet C, Donahue DA, Porrot F, Hillion KH, Perthame E, Arroyo MV, Souquere S, et al. IFITM proteins inhibit placental syncytiotrophoblast formation and promote fetal demise. *Science* 2019; 365:176-180.
108. Liang B, Guida JP, Costa Do Nascimento ML, Mysorekar IU. Host and viral mechanisms of congenital Zika syndrome. *Virulence* 2019; 10:768-775.
109. Chiramel AI, Best SM. Role of autophagy in Zika virus infection and pathogenesis. *Virus Res* 2018; 254:34-40.
110. Liang Q, Luo Z, Zeng J, Chen W, Foo SS, Lee SA, Ge J, Wang S, Goldman SA, Zlokovic BV, Zhao Z, Jung JU. Zika Virus NS4A and NS4B Proteins Deregulate Akt-mTOR Signaling in Human Fetal Neural Stem Cells to Inhibit Neurogenesis and Induce Autophagy. *Cell Stem Cell* 2016; 19:663-671.
111. Cao B, Parnell LA, Diamond MS, Mysorekar IU. Inhibition of autophagy limits vertical transmission of Zika virus in pregnant mice. *J Exp Med* 2017; 214:2303-2313.
112. Yan N, Chen ZJ. Intrinsic antiviral immunity. *Nat Immunol* 2012; 13:214-222.
113. Sadler AJ, Williams BR. Interferon-inducible antiviral effectors. *Nat Rev Immunol* 2008; 8:559-568.
114. Idriss HT, Naismith JH. TNF alpha and the TNF receptor superfamily: structure-function relationship(s). *Microsc Res Tech* 2000; 50:184-195.
115. Hunter CA, Jones SA. IL-6 as a keystone cytokine in health and disease. *Nat Immunol* 2015; 16:448-457.
116. Micallef A, Grech N, Farrugia F, Schembri-Wismayer P, Calleja-Agius J. The role of interferons in early pregnancy. *Gynecol Endocrinol* 2014; 30:1-6.
117. Bayer A, Lennemann NJ, Ouyang Y, Bramley JC, Morosky S, Marques ET, Jr., Cherry S, Sadovsky Y, Coyne CB. Type III Interferons Produced by Human Placental Trophoblasts Confer Protection against Zika Virus Infection. *Cell Host Microbe* 2016; 19:705-712.
118. Lazear HM, Govero J, Smith AM, Platt DJ, Fernandez E, Miner JJ, Diamond MS. A Mouse Model of Zika Virus Pathogenesis. *Cell Host Microbe* 2016; 19:720-730.
119. Miner JJ, Diamond MS. Zika Virus Pathogenesis and Tissue Tropism. *Cell Host Microbe* 2017; 21:134-142.

120. Gorman MJ, Caine EA, Zaitsev K, Begley MC, Weger-Lucarelli J, Uccellini MB, Tripathi S, Morrison J, Yount BL, Dinnon KH, 3rd, Ruckert C, Young MC, et al. An Immunocompetent Mouse Model of Zika Virus Infection. *Cell Host Microbe* 2018; 23:672-685 e676.
121. Tripathi S, Balasubramaniam VR, Brown JA, Mena I, Grant A, Bardina SV, Maringer K, Schwarz MC, Maestre AM, Sourisseau M, Albrecht RA, Krammer F, et al. A novel Zika virus mouse model reveals strain specific differences in virus pathogenesis and host inflammatory immune responses. *PLoS Pathog* 2017; 13:e1006258.
122. Taguchi T, Mukai K. Innate immunity signalling and membrane trafficking. *Curr Opin Cell Biol* 2019; 59:1-7.
123. Riedl W, Acharya D, Lee JH, Liu G, Serman T, Chiang C, Chan YK, Diamond MS, Gack MU. Zika Virus NS3 Mimics a Cellular 14-3-3-Binding Motif to Antagonize RIG-I- and MDA5-Mediated Innate Immunity. *Cell Host Microbe* 2019; 26:493-503 e496.
124. Grant A, Ponia SS, Tripathi S, Balasubramaniam V, Miorin L, Sourisseau M, Schwarz MC, Sanchez-Seco MP, Evans MJ, Best SM, Garcia-Sastre A. Zika Virus Targets Human STAT2 to Inhibit Type I Interferon Signaling. *Cell Host Microbe* 2016; 19:882-890.
125. Kumar A, Hou S, Airo AM, Limonta D, Mancinelli V, Branton W, Power C, Hobman TC. Zika virus inhibits type-I interferon production and downstream signaling. *EMBO Rep* 2016; 17:1766-1775.
126. Block LN, Bowman BD, Schmidt JK, Keding LT, Stanic AK, Golos TG. The promise of placental extracellular vesicles: models and challenges for diagnosing placental dysfunction in uterodagger. *Biol Reprod* 2021; 104:27-57.
127. Anderson MR, Kashanchi F, Jacobson S. Exosomes in Viral Disease. *Neurotherapeutics* 2016; 13:535-546.
128. Schorey JS, Cheng Y, Singh PP, Smith VL. Exosomes and other extracellular vesicles in host-pathogen interactions. *EMBO Rep* 2015; 16:24-43.
129. Longatti A, Boyd B, Chisari FV. Virion-independent transfer of replication-competent hepatitis C virus RNA between permissive cells. *J Virol* 2015; 89:2956-2961.
130. Meckes DG, Jr., Gunawardena HP, Dekroon RM, Heaton PR, Edwards RH, Ozgur S, Griffith JD, Damania B, Raab-Traub N. Modulation of B-cell exosome proteins by gamma herpesvirus infection. *Proc Natl Acad Sci U S A* 2013; 110:E2925-2933.
131. Gould SJ, Booth AM, Hildreth JE. The Trojan exosome hypothesis. *Proc Natl Acad Sci U S A* 2003; 100:10592-10597.
132. Slonchak A, Clarke B, Mackenzie J, Amarilla AA, Setoh YX, Khromykh AA. West Nile virus infection and interferon alpha treatment alter the spectrum and the levels of coding and noncoding host RNAs secreted in extracellular vesicles. *BMC Genomics* 2019; 20:474.

133. Jabalee J, Towle R, Garnis C. The Role of Extracellular Vesicles in Cancer: Cargo, Function, and Therapeutic Implications. *Cells* 2018; 7.
134. Vora A, Zhou W, Londono-Renteria B, Woodson M, Sherman MB, Colpitts TM, Neelakanta G, Sultana H. Arthropod EVs mediate dengue virus transmission through interaction with a tetraspanin domain containing glycoprotein Tsp29Fb. *Proc Natl Acad Sci U S A* 2018; 115:E6604-E6613.
135. Zhou W, Woodson M, Neupane B, Bai F, Sherman MB, Choi KH, Neelakanta G, Sultana H. Exosomes serve as novel modes of tick-borne flavivirus transmission from arthropod to human cells and facilitates dissemination of viral RNA and proteins to the vertebrate neuronal cells. *PLoS Pathog* 2018; 14:e1006764.
136. Rozmyslowicz T, Majka M, Kijowski J, Murphy SL, Conover DO, Poncz M, Ratajczak J, Gaulton GN, Ratajczak MZ. Platelet- and megakaryocyte-derived microparticles transfer CXCR4 receptor to CXCR4-null cells and make them susceptible to infection by X4-HIV. *AIDS* 2003; 17:33-42.
137. Mack M, Kleinschmidt A, Bruhl H, Klier C, Nelson PJ, Cihak J, Plachy J, Stangassinger M, Erfle V, Schlondorff D. Transfer of the chemokine receptor CCR5 between cells by membrane-derived microparticles: a mechanism for cellular human immunodeficiency virus 1 infection. *Nat Med* 2000; 6:769-775.
138. Carter AM. Animal models of human placentation--a review. *Placenta* 2007; 28 Suppl A:S41-47.
139. Nguyen SM, Antony KM, Dudley DM, Kohn S, Simmons HA, Wolfe B, Salamat MS, Teixeira LBC, Wiepz GJ, Thoong TH, Aliota MT, Weiler AM, et al. Highly efficient maternal-fetal Zika virus transmission in pregnant rhesus macaques. *PLoS Pathog* 2017; 13:e1006378.
140. Hirsch AJ, Roberts VHJ, Grigsby PL, Haese N, Schabel MC, Wang X, Lo JO, Liu Z, Kroenke CD, Smith JL, Kelleher M, Broeckel R, et al. Zika virus infection in pregnant rhesus macaques causes placental dysfunction and immunopathology. *Nat Commun* 2018; 9:263.
141. Dudley DM, Aliota MT, Mohr EL, Newman CM, Golos TG, Friedrich TC, O'Connor DH. Using Macaques to Address Critical Questions in Zika Virus Research. *Annu Rev Virol* 2019; 6:481-500.
142. Prisant N, Bujan L, Benichou H, Hayot PH, Pavili L, Lurel S, Herrmann C, Janky E, Joguet G. Zika virus in the female genital tract. *Lancet Infect Dis* 2016; 16:1000-1001.
143. Prisant N, Breurec S, Moriniere C, Bujan L, Joguet G. Zika Virus Genital Tract Shedding in Infected Women of Childbearing age. *Clin Infect Dis* 2017; 64:107-109.

144. Murray KO, Gorchakov R, Carlson AR, Berry R, Lai L, Natrajan M, Garcia MN, Correa A, Patel SM, Aagaard K, Mulligan MJ. Prolonged Detection of Zika Virus in Vaginal Secretions and Whole Blood. *Emerg Infect Dis* 2017; 23:99-101.
145. de Noronha L, Zanluca C, Burger M, Suzukawa AA, Azevedo M, Rebutini PZ, Novadzki IM, Tanabe LS, Presibella MM, Duarte Dos Santos CN. Zika Virus Infection at Different Pregnancy Stages: Anatomopathological Findings, Target Cells and Viral Persistence in Placental Tissues. *Front Microbiol* 2018; 9:2266.
146. Quicke KM, Bowen JR, Johnson EL, McDonald CE, Ma H, O'Neal JT, Rajakumar A, Wrammert J, Rimawi BH, Pulendran B, Schinazi RF, Chakraborty R, et al. Zika Virus Infects Human Placental Macrophages. *Cell Host Microbe* 2016; 20:83-90.
147. Meaney-Delman D, Oduyebo T, Polen KND, White JL, Bingham AM, Slavinski SA, Heberlein-Larson L, St George K, Rakeman JL, Hills S, Olson CK, Adamski A, et al. Prolonged Detection of Zika Virus RNA in Pregnant Women. *Obstet Gynecol* 2016; 128:724-730.
148. Pomar L, Lambert V, Matheus S, Pomar C, Hcini N, Carles G, Rousset D, Vouga M, Panchaud A, Baud D. Prolonged Maternal Zika Viremia as a Marker of Adverse Perinatal Outcomes. *Emerg Infect Dis* 2021; 27:490-498.

Chapter 2

Ocular and uteroplacental pathology in macaque congenital Zika virus infection

Publication:

Mohr EL*, Block LN*, Newman CM*, Stewart LM, Koenig M, Semler M, Breitbach ME, Teixeira LBC, Zeng X, Weiler AM, Barry GL, Thoong TH, Wiepz GJ, Dudley DM, Simmons HA, Mejia A, Morgan TK, Salamat MS, Kohn S, Antony KM, Aliota MT, Mohns MS, Hayes JM, Schultz-Darken N, Schotzko ML, Peterson E, Capuano S 3rd, Osorio JE, O'Connor SL, Friedrich TC, O'Connor DH, Golos TG. Ocular and uteroplacental pathology in a macaque pregnancy with congenital Zika virus infection. *PLoS One*. 2018 Jan 30;13(1):e0190617. doi: 10.1371/journal.pone.0190617. PMID: 29381706; PMCID: PMC5790226.

*These authors contributed equally to this work.

Author Contributions

Emma L. Mohr, Conceptualization, Data curation, Formal analysis, Investigation, Methodology, Project administration, Supervision, Visualization, Writing – original draft, Writing – review & editing

Lindsey N. Block, Data curation, Formal analysis, Investigation, Methodology, Validation, Visualization, Writing – original draft, Writing – review & editing

Christina M. Newman, Conceptualization, Data curation, Formal analysis, Investigation, Methodology, Project administration, Supervision, Validation, Writing – original draft

Laurel M. Stewart, Data curation, Formal analysis, Investigation, Validation

Michelle Koenig, Data curation, Formal analysis, Investigation, Software, Validation

Matthew Semler, Data curation, Formal analysis, Investigation, Validation

Meghan E. Breitbach, Data curation, Formal analysis, Investigation, Validation

Leandro B. C. Teixeira, Data curation, Formal analysis, Investigation, Validation

Xiankun Zeng, Data curation, Formal analysis, Investigation, Validation

Andrea M. Weiler, Data curation, Formal analysis, Investigation, Validation

Gabrielle L. Barry, Data curation, Formal analysis, Investigation, Validation

Troy H. Thoong, Formal analysis, Investigation

Gregory J. Wiepuz, Data curation, Formal analysis, Validation

Dawn M. Dudley, Conceptualization, Data curation, Formal analysis, Investigation, Methodology, Project administration, Supervision, Validation, Writing – original draft

Heather A. Simmons, Data curation, Formal analysis, Investigation, Validation, Visualization, Writing – original draft, Writing – review & editing

Andres Mejia, Data curation, Formal analysis, Investigation, Validation, Visualization, Writing – original draft, Writing – review & editing

Terry K. Morgan, Formal analysis, Writing – review & editing

M. Shahriar Salamat, Formal analysis

Sarah Kohn, Data curation, Investigation, Validation

Kathleen M. Antony, Data curation, Formal analysis, Investigation, Validation, Visualization

Matthew T. Aliota, Data curation, Formal analysis, Investigation, Methodology, Validation, Writing – original draft

Mariel S. Mohns, Formal analysis, Investigation, Validation

Jennifer M. Hayes, Investigation, Validation

Nancy Schultz-Darken, Investigation, Validation

Michele L. Schotzko, Investigation

Eric Peterson, Investigation

Saverio Capuano, III, Funding acquisition, Resources, Supervision

Jorge E. Osorio, Supervision

Shelby L. O'Connor, Methodology, Supervision, Validation

Thomas C. Friedrich, Formal analysis, Supervision, Validation, Writing – original draft

David H. O'Connor, Conceptualization, Data curation, Formal analysis, Funding acquisition, Methodology, Project administration, Resources, Software, Supervision, Validation, Writing – original draft

Thaddeus G. Golos, Conceptualization, Formal analysis, Funding acquisition, Methodology, Project administration, Resources, Supervision, Validation, Writing – original draft, Writing – review & editing

2.1 Abstract (Original by LNB; edited by ELM, TGG, and others)

Congenital Zika virus (ZIKV) infection impacts fetal development and pregnancy outcomes. We infected a pregnant rhesus macaque with a Puerto Rican ZIKV isolate in the first trimester. The pregnancy was complicated by preterm premature rupture of membranes (PPROM) and fetal demise 49 days post infection (gestational day 95). Significant pathology at the maternal-fetal interface included acute chorioamnionitis, placental infarcts, and leukocytoclastic vasculitis of the myometrial radial arteries. ZIKV RNA was disseminated throughout the fetus tissues and maternal immune system at necropsy, as assessed by quantitative RT-PCR for viral RNA. Replicating ZIKV was identified in fetal tissues, maternal lymph node, and maternal spleen by fluorescent in situ hybridization for viral replication intermediates. Fetal ocular pathology included a choroidal coloboma, suspected anterior segment dysgenesis, and a dysplastic retina. This is the first report of ocular pathology and prolonged viral replication in both maternal and fetal tissues following congenital ZIKV infection in rhesus macaques. PPRM followed by fetal demise and severe pathology of the visual system have not been described in macaque congenital infection previously; further nonhuman primate studies are needed to determine if an increased risk for PPRM is associated with congenital Zika virus infection.

2.2 Introduction (Original by ELM; edited by LNB, TGG, and others)

First isolated from a febrile rhesus macaque in Uganda in 1947, Zika virus (ZIKV) generally did not result in recognized widespread clinical disease in subsequent outbreaks across Asia and the South Pacific, until late 2015, when clinicians in Northeast Brazil reported a surge in babies born with severe birth defects (1). By early 2016, the US Centers for Disease Control and Prevention (CDC) asserted that there was a causal relationship between prenatal ZIKV infection and serious brain anomalies including microcephaly (2). The constellation of fetal and neonatal abnormalities and birth defects associated with ZIKV infection *in utero* is designated congenital Zika syndrome (CZS) (3-9). Characteristics of CZS include ocular anomalies, brain anomalies, stillbirth, cranial dysmorphologies, musculoskeletal contractures and neurologic sequelae (10). Infection during the first trimester increases the risk for birth defects (5) because critical cell proliferation and differentiation occurs during this trimester (11). One striking characteristic of CZS is a high frequency of ocular malformations, observed in as many as 55% of infants with evidence of congenital ZIKV infection and microcephaly (12, 13). Multiple case reports and case series have identified infants with ocular anomalies, which include macular pigment mottling, optic nerve hypoplasia, chorioretinal and iris coloboma, lens subluxation, retinal vascular abnormalities, cataracts and maculopathy (5, 14-21). Specific retinal defects include retinal thinning, discontinuity of the retinal pigment epithelium, and colobomatous-like excavation in the neurosensory retina, retinal pigment epithelium and choroid in multiple infants (17). Because the retina develops as an outpocketing from the neural tube (22), the presence of retinal lesions implies CNS damage even without brain abnormalities.

Other recognized outcomes of congenital ZIKV infection are miscarriage, stillbirth and PPROM (23-26). The etiology of PPROM is multifactorial (27). Prenatal ZIKV infection in the first trimester of gestation results in up to 25% of pregnancies with miscarriage, fetal loss or stillbirth, with lower frequencies in the second and third trimesters in a study including 125 pregnancies (28). The CDC reports 15 fetal demise cases with birth defects out of 4,695 live births in women with confirmed ZIKV infection (29). However, this number likely does not capture the total number of fetal demises following congenital ZIKV infection because it does not include fetuses without overt birth defects even though there may be vertical transmission, or early pregnancy losses from women who were not aware of infection, or never sought a diagnosis. The pathophysiology of preterm birth or fetal loss before viability following congenital ZIKV infection has not been defined. In murine models, pregnancy following a systemic viral infection can result in an ascending bacterial uterine infection, inflammation, and preterm birth (30). It has also been reported that viral persistence of ZIKV in the lower female genital tract in the rhesus monkey is prolonged in animals treated with Depo-Provera, a synthetic progestogen (31). The specific etiology of adverse pregnancy outcomes in congenital ZIKV infection, however, is yet to be defined and requires further study.

One novel feature of ZIKV infection is the persistence of both ZIKV RNA (32-37) and replication competent virus in body fluids (33, 38) for weeks after infection. ZIKV RNA has been identified in semen between 3-188 days after infection (39, 40) with a median of 34 days (32), in urine up to 29 days after infection (41) with a median of 8 days (32), in saliva up to 29 days after infection (41), and in serum with a median of 14 days (32). Both ZIKV RNA and infectious particles have

been isolated from breast milk 2 days after infection (42). In comparison, RNA from dengue virus (DENV), the flavivirus most closely related to ZIKV, has only been isolated from urine up to 3-4 weeks after infection (43); no DENV RNA has been isolated from semen, prolonged plasma viremia has only been reported in hematopoietic stem cell recipients (44, 45), and only DENV RNA has been isolated from breast milk around the time of acute infection (46).

Defining the body fluid and tissue persistence of ZIKV is critical to the development of public health recommendations and solid organ and hematopoietic stem cell transplant guidelines. Non-human primate (NHP) models have begun to define the tissue distribution of ZIKV following infection because defining tissue distribution in humans is not possible. Following ZIKV infection in nonpregnant NHPs, ZIKV has been identified in multiple tissues up to 35 days after infection, including the brain, spinal cord, eye, spleen, lymph nodes, muscles and joints (47, 48) and in cerebrospinal fluid (CSF) up to 42 days after infection (48), suggesting that one of these tissues may support prolonged ZIKV replication. Since prolonged ZIKV viremia is a feature of ZIKV infection during pregnancy, we hypothesized that ZIKV tissue persistence would be longer in pregnant NHPs compared to nonpregnant NHPs. Indeed, following ZIKV infection in pregnant NHPs, ZIKV RNA detection in plasma is prolonged (47) and can be detected up to 70 days after infection (49), far longer than the plasma viremia duration reported for nonpregnant NHPs (48, 50).

NHP models of both congenital infection and tissue distribution following ZIKV infection provide insight into the pathophysiology of ZIKV infection not possible through epidemiological and

clinical human studies. As with humans, the rhesus macaque placenta has a hemochorial placentation with extensive endovascular invasion of the maternal endometrial spiral arterioles and arteries and innate immune cellular populations homologous with that found in the human decidua (51-53). There are multiple similarities between human and NHP ZIKV infection natural history, including the duration of viremia and viruria (47, 48, 50, 54), robust neutralizing antibody responses (47, 50, 54, 55), vertical transmission (49), and fetal pathology (49, 56). To define the tissue distribution of ZIKV and fetal pathology following infection with a clinically relevant Puerto Rican isolate of ZIKV, we infected a pregnant rhesus macaque in the first trimester and performed a necropsy of the dam and fetus to comprehensively define maternal and fetal viral tissue distribution following spontaneous fetal death 49 days post-infection. Here, we describe the pregnancy outcome, maternal and fetal viral tissue distribution, and fetal pathology associated with first trimester ZIKV infection in a case of fetal demise.

2.3 Materials & Methods

Study Design (Original by ELM; edited by LNB, TGG, and others)

A 3.8-year-old, primigravida rhesus macaque (*Macaca mulatta*) of Indian ancestry was infected subcutaneously with 1×10^4 PFU Zika virus/H.sapiens-tc/PUR/2015/PRVABC59_v3c2 (PRVABC59) during the first trimester, 46 days gestation (term 165 ± 10 days). This macaque was part of the Specific Pathogen Free (SPF) colony at the Wisconsin National Primate Research Center (WNPRC) and was free of Macacine herpesvirus 1 (Herpes B), Simian Retrovirus Type D (SRV), Simian T-lymphotropic virus Type 1 (STLV), and Simian Immunodeficiency Virus (SIV).

Ethics (Original by ELM; edited by LNB, TGG, and others)

All monkeys are cared for by the staff at the WNPRC in accordance with the regulations and guidelines outlined in the Animal Welfare Act and the Guide for the Care and Use of Laboratory Animals and the recommendations of the Weatherall report (<https://royalsociety.org/topics-policy/publications/2006/weatherall-report/>). This study was approved by the University of Wisconsin-Madison Graduate School Institutional Animal Care and Use Committee (animal protocol number G005401).

Care & Use of Macaques (Original by ELM; edited by LNB, TGG, and others)

The female monkey described in this report was co-housed with a compatible male and observed daily for menses and breeding. Pregnancy was detected by ultrasound examination of the uterus at approximately 20-24 gestation days (gd) following the predicted day of ovulation. The gd was estimated (+/- 2 days) based on the dam's menstrual cycle, observation of copulation, and the greatest length of the fetus at initial ultrasound examination which was compared to normative growth data in this species (57). For physical examinations, virus inoculations, some ultrasound examinations, blood and swab collections, the dam was anesthetized with an intramuscular dose of ketamine (10 mg/kg). Blood samples from the femoral or saphenous vein were obtained using a vacutainer system or needle and syringe. The pregnant macaque was monitored daily prior to and after inoculation for any clinical signs of infection (e.g., diarrhea, inappetence, inactivity and atypical behaviors). This macaque developed chronic diarrhea prior to conception and was treated daily with oral tylosin throughout pregnancy.

Inoculation and monitoring (Original by ELM; edited by LNB, TGG, and others)

ZIKV strain PRVABC59 (GenBank: KU501215), originally isolated from a traveler to Puerto Rico and passaged three times on Vero cells (American Type Culture Collection (ATCC): CCL-81), was obtained from Brandy Russell (CDC, Ft. Collins, CO). Virus stocks were prepared by inoculation onto a confluent monolayer of C6/36 cells (*Aedes albopictus* larval cells; ATCC: CCL-1660) with two rounds of amplification. The inoculating stock was prepared and validated as previously described (49, 50). The animal was anesthetized as described above, and 1 mL of inoculum at 1×10^4 PFU dilution in PBS was administered subcutaneously over the cranial dorsum. Post-inoculation, the animal was closely monitored by veterinary and animal care staff for adverse reactions or any signs of disease.

Pregnancy monitoring and fetal measurements (Original by ELM; edited by LNB, TGG, and others)

Weekly ultrasounds were conducted to observe the health of the fetus and to obtain measurements including fetal femur length (FL), biparietal diameter (BPD), head circumference (HC), and heart rate, with methods as previously described (49). Growth curves were developed for FL, BPD, and HC (58). Mean measurements and standard deviations at specified days of gestation in rhesus macaques were retrieved from Tarantal et al. (57) and the data were plotted against normative data for fetal rhesus macaques (58). The actual growth measurements were obtained from weekly ultrasound data and used to retrieve the predicted growth measurement by plotting the obtained experimental growth measurement against the growth curves. Data were then graphed as actual gestation age versus predicted gestation age to depict rate of growth compared to uninfected,

control rhesus macaques (method described previously in (49)). Doppler ultrasounds to measure fetal heart rate were performed as requested by veterinary staff.

Amniocentesis (Original by ELM; edited by LB, TGG, and others)

For the amniocentesis procedures reported, animals were shaved, and the skin was prepped with Betadyne® solution, and sterile syringes, needles and gloves were used during the amniocentesis procedure. Under real-time ultrasound guidance, a 22 gauge, 3.5 inch Quincke spinal needle was inserted into the amniotic sac as described previously (49). The first 1.5-2 mL of fluid was discarded due to potential maternal contamination, and an additional 3-4 mL of amniotic fluid was collected in a new sterile syringe for viral qRT-PCR analysis as described elsewhere (50). These samples were obtained at the gestational ages specified in Figure 1. All fluids were free of any blood contamination.

vRNA isolation from body fluids and tissues (Original by ELM; edited by LNB, TGG, and others)

RNA was isolated from maternal plasma, urine, saliva and amniotic fluid using the Viral Total Nucleic Acid Purification Kit (Promega, Madison, WI, USA) and from maternal and fetal tissues using the Maxwell 16 LEV simplyRNA Tissue Kit (Promega, Madison, WI) on a Maxwell 16 MDx instrument as previously reported (50). Fetal and maternal tissues were processed with RNAlater® (Invitrogen, Carlsbad, CA) according to manufacturer protocols. 20-40 mg of each tissue was homogenized using homogenization buffer from the Maxwell 16 LEV simplyRNA

Tissue Kit and two 5 mm stainless steel beads (Qiagen, Hilden, Germany) in a 2 mL snap-cap tube, shaking twice for 3 minutes at 20 Hz each side in a TissueLyser (Qiagen, Hilden, Germany). The isolation was continued according to the Maxwell 16 LEV simplyRNA Tissue Kit protocol, and samples were eluted into 50 μ L RNase free water.

Viral quantification by plaque assay (Original by ELM; edited by LNB, TGG, and others)

Titration for replication competent virus quantification of amniotic fluid was completed by plaque assay on Vero cell cultures as described previously (50). Vero cells were obtained from American Type Culture Collection (CCL-81), were not further authenticated and were not specifically tested for mycoplasma. Duplicate wells were infected with 0.1 ml of aliquots from serial 10-fold dilutions in growth media and virus was adsorbed for 1 h. Following incubation, the inoculum was removed, and monolayers were overlaid with 3 ml containing a 1:1 mixture of 1.2% oxoid agar and 2 DMEM (Gibco, Carlsbad, CA, USA) with 10% (vol/vol) FBS and 2% (vol/vol) penicillin/streptomycin. Cells were incubated at 37°C in 5% CO₂ for 4 days for plaque development. Cell monolayers then were stained with 3 ml of overlay containing a 1:1 mixture of 1.2% oxoid agar and 2 DMEM with 2% (vol/vol) FBS, 2% (vol/vol) penicillin/streptomycin and 0.33% neutral red (Gibco). Cells were incubated overnight at 37°C and plaques were counted.

Plaque Reduction Neutralization test (PRNT) (Original by MTA; edited by ELM, LNB, TGG, and others)

Macaque serum samples were screened for ZIKV neutralizing antibodies utilizing a plaque reduction neutralization test (PRNT). End point titrations of reactive sera, utilizing a 90% cutoff (PRNT90), were performed as described (59) against ZIKV strain PRVABC59. Briefly, ZIKV was mixed with serial 2-fold dilutions of serum for 1 hour at 37°C prior to being added to Vero cells and neutralization curves were generated using GraphPad Prism software (La Jolla, CA). The resulting data were analyzed by nonlinear regression to estimate the dilution of serum required to inhibit both 90% and 50% of infection.

Maternal and neonatal necropsy (Original by ELM; edited by LNB, TGG, and others)

At 49 days post infection (dpi) (gd 95), no fetal heartbeat was detected. The dam was sedated, euthanized, and sterile instruments were used for the dissection and collection of all maternal, fetal, and maternal-fetal interface tissues during the gross post-mortem examination. Amniotic fluid was aspirated with a syringe and needle inserted through the uterine wall into the lumen. Each tissue was collected with a unique set of sterile instruments and placed in a separate sterile petri dish before transfer to appropriate containers for viral RNA analysis and histology, to prevent cross-contamination between tissues. Tissue distribution for subsequent analysis was as previously described (49).

Histology (Original by ELM; edited by LNB, TGG, and others)

For general pathology, tissues were fixed in 4% PFA as for IHC, routinely processed and embedded in paraffin. Paraffin sections (5 µm) were stained with hematoxylin and eosin (H&E).

Two veterinary pathologists were blinded to vRNA findings when tissue sections were evaluated microscopically. Lesions in each tissue were described and assigned morphologic diagnoses as described previously (49). Photomicrographs were obtained using brightfield microscopes Olympus BX43 and Olympus BX46 (Olympus Inc., Center Valley, PA) with attached Olympus DP72 digital camera (Olympus Inc.) and Spot Flex 152 64 Mp camera (Spot Imaging, Sterling Heights, MI), and captured using commercially available image-analysis software (cellSens DimensionR, Olympus Inc. and Spot software 5.3). Uteroplacental pathology was specifically performed by an experienced placental pathologist (T.K.M.).

In situ hybridization (Original by ELM; edited by LNB, TGG, and others)

In situ hybridization (ISH) was conducted with tissues fixed in 4% PFA, and alcohol processed and paraffin embedded, as for IHC. ISH probes against Zika genome were purchased commercially (Advanced Cell Diagnostics, Cat No. 468361, Newark, California, USA). ISH was performed using the RNAscope® Red 2.5 Kit (Advanced Cell Diagnostics, Cat No. 322350) according to the manufacturer's instructions. Briefly, after deparaffinization with xylene, a series of ethanol washes, and peroxidase blocking, sections were heated in boiling antigen retrieval buffer for 15 minutes and then digested by proteinase K (2.5 ug/ml, to completely cover the section) for 16 minutes at 40°C. Sections were exposed to ISH target probe and incubated at 40°C in a hybridization oven for 2 h. After rinsing, ISH signal was amplified using company-provided Pre-amplifier and Amplifier conjugated to horseradish peroxidase (HRP), and incubated with a red substrate-chromogen solution for 10 min at room temperature.

Multiplex fluorescent in situ hybridization (Original by ELM; edited by LNB, TGG, and others)

Multiplex fluorescent in situ hybridization (mFISH) was conducted with tissues fixed in 4% PFA as for IHC. mFISH was performed using the RNAscope® Fluorescent Multiplex Kit (Catalog # 320850, Advanced Cell Diagnostics) according to the manufacturer's instructions with modifications. Probes with C1 channel (Cat# 468361, red) targeting ZIKV positive sense RNA and probes with C3 channel (Cat# 467911, green) targeting ZIKV negative sense RNA were synthesized by Advanced Cell Diagnostics. Paraformaldehyde fixed paraffin embedded rhesus monkey fetus tissue sections underwent deparaffinization with xylene and a series of ethanol washes. These tissue sections were treated with 0.1% Sudan Black B (Sigma-Aldrich, St. Louis, MO, USA) to reduce autofluorescence, heated in antigen retrieval buffer (Citrate buffer with pH 6.0), and digested by proteinase. Sections were exposed to ISH target probes and incubated at 40°C in a hybridization oven for 2 h. After rinsing, ISH signal was amplified using company-provided Pre-amplifier and Amplifier conjugated to fluorescent dye. Sections were counterstained with 4', 6-diamidino-2-phenylindole (DAPI, Thermo Fisher Scientific, Waltham, MA, USA), mounted, and stored at 4°C until image analysis. mFISH images were captured on an LSM 880 Confocal Microscope with Airyscan (Zeiss, Oberkochen, Germany) and processed using open-source ImageJ software (National Institutes of Health, Bethesda, MD, USA).

Placental alpha microglobulin-1 (PAMG-1) immunochromatographic assay (Original by LNB, edited by ELM, TGG, and others)

A PAMG-1 immunochromatographic assay (AmniSure® ROM (Rupture of [fetal] Membranes) test, Qiagen, Boston, MA, FMRT-1-10-US) was performed according to the manufacturer's

protocol with urine and amniotic fluid samples that had been stored at -80°C . A sterile polyester swab, provided by the manufacturer, was inserted into a tube containing the sample fluid for 1 minute. The swab was then added to the solvent microfuge tube and rotated by hand for 1 minute. Finally, the test strip was placed into the solvent and incubated at room temperature for 10 minutes before the test strip was read and photographs were taken. A term amniotic fluid sample was the positive control and non-pregnant urine was the negative control. Open-source ImageJ software was used to measure the relative pixel density of each band (control and test band) (National Institutes of Health, Bethesda, MD, USA). The pixel density of each band was measured, the background density was subtracted, and the relative pixel density of each test band was calculated by subtracting the control band density from the test band density.

Insulin-like growth factor-binding protein 1 (IGFBP-1) ELISA (Original by LNB, edited by ELM, TGG, and others)

An IGFBP-1 ELISA kit (Abcam, Cambridge, MA, ab100539) was used to determine if a marker for amniotic fluid was detectable in maternal urine. The protocol was followed as specified by the manufacturer and all samples were frozen undiluted at -80°C until use. Duplicates were run for the standards, samples, positive, and negative controls. A term amniotic fluid sample was used as the positive control and male urine and non-pregnant female urine were used as negative controls. All urines were diluted 1:5000 and all amniotic fluid samples were diluted 1:20,000. Immediately upon addition of the stop solution the plate was read at 450 nm. A standard curve was calculated from the average of each standard. This standard curve equation was used to calculate the concentration of each sample.

Data availability (Original by ELM; edited by LNB, TGG, and others)

Primary data that support the findings of this study are available at the Zika Open-Research Portal (<https://zika.labkey.com/project/OConnor/ZIKV-019/begin.view?>). Zika virus/H.sapiens-tc/PUR/2015/PRVABC59-v3c2 sequence data have been deposited in the Sequence Read Archive (SRA) with accession code SRX2975259. The authors declare that all other data supporting the findings of this study are available within the article and its supplementary information files.

2.4 Results (Original by ELM and LNB, edited by all)

Pregnancy outcome

A pregnant rhesus macaque was subcutaneously inoculated with 1×10^4 PFU ZIKV-Puerto Rico at gd46. She had no fever, rash, or inappetence detected following inoculation. The pregnancy was monitored by ultrasonography, vRNA titers in blood, and urine samples, and neutralizing antibody titers at multiple times throughout pregnancy; amniotic fluid and maternal CSF were collected at several time points (Figure 1).

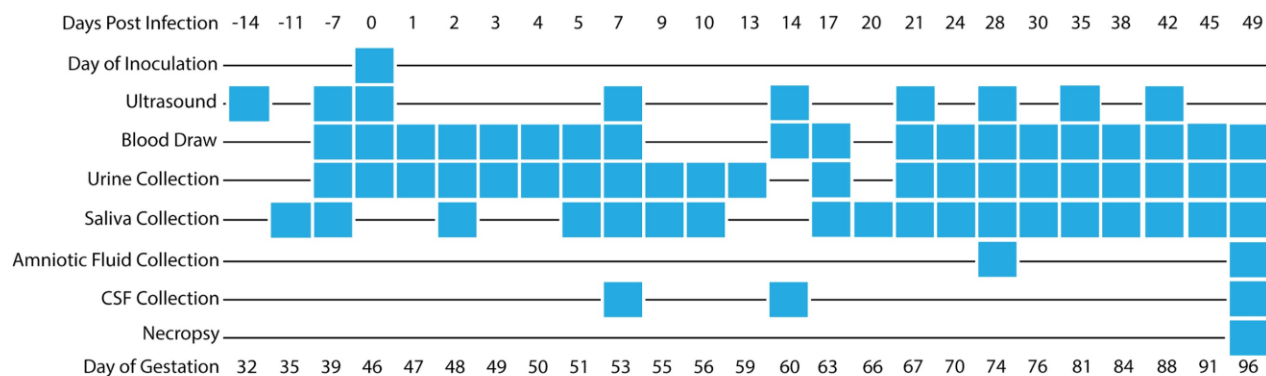


Figure 2.1. Timeline depicting body fluid sampling and procedures throughout pregnancy. Blood, urine, saliva, amniotic fluid, and CSF were collected as indicated in the schedule above, and ultrasounds were performed weekly. The axes are not drawn to scale.

Maternal plasma viremia was detected from days 1 through 18 post-infection, peaking at 5 dpi with 2.55×10^5 vRNA copies per mL, and was also detected at 24 dpi (Figure 2). At 21 dpi the viral load dropped below 100 vRNA copies per mL, the limit of quantification of the qRT-PCR assay. Amniotic fluid at 28 dpi had a viral load of 1.84×10^4 vRNA copies per mL. The amniotic fluid was reported as clear, and a plaque assay performed on the amniotic fluid was negative (data not shown). Saliva samples remained negative throughout pregnancy (data not shown). CSF samples taken at 7, 14, and 49 dpi were all negative. ZIKV RNA was first detected in a passively collected urine sample (i.e. in pan at the bottom of the cage) at 42 dpi, with a concentration of 7×10^4 vRNA copies per mL, and was present in the urine until euthanasia at 49 dpi.

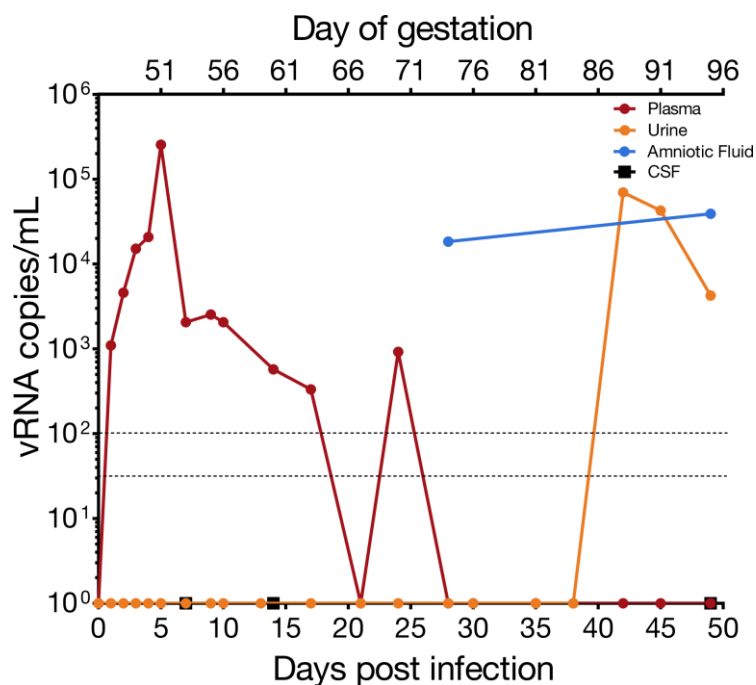


Figure 2.2. ZIKV vRNA levels in maternal body fluids. vRNA was measured by quantitative RT-PCR in plasma, urine, amniotic fluid and CSF. The limit of assay quantification is 100 copies/mL and the limit of detection is 33 copies/mL. Data collated and figure designed by LNB.

In addition to vRNA in body fluids, the development of maternal ZIKV-specific antibodies was assessed. Plaque reduction neutralization tests (PRNT) were performed on serum collected at 10, 28, and 49 dpi. All post-infection time points demonstrated the presence of ZIKV-specific neutralizing antibodies with an increasing concentration of neutralizing antibodies throughout the post-infection period (Figure 3).

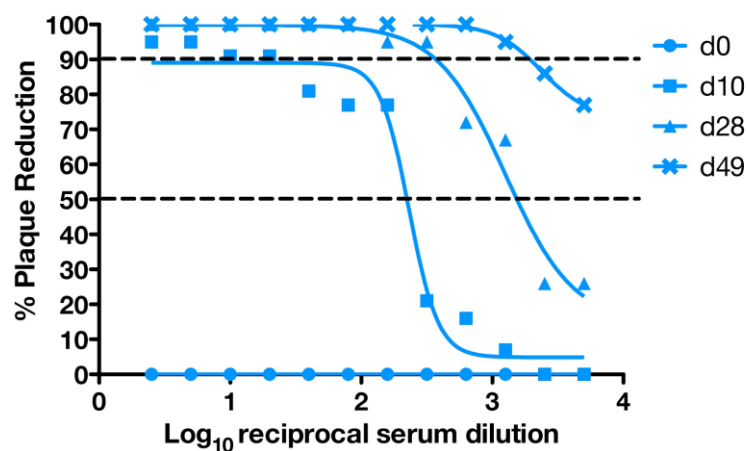


Figure 2.3. Neutralizing antibody titers following ZIKV infection. PRNT titers were measured pre and post infection. The x-axis represents the reciprocal serum dilution (\log_{10}) and the y-axis represents the percent reduction. The dashed lines indicate 90% and 50% reduction. Data collected, collated, and figure designed by MTA.

Because identifying urine vRNA so long after infection was unexpected, and its presence coincided with the presence of vRNA in the amniotic fluid, we wanted to determine whether the

passively collected urine contained amniotic fluid, a potential harbinger of an adverse pregnancy outcome. We performed an AmniSure[®] test, which detects an amniotic fluid protein, placental alpha microglobulin-1, (PAMG-1), and determined that urine contained detectable PAMG-1 (Figure 4). As expected, the 28 dpi amniotic fluid was positive for PAMG-1, as was the positive control term amniotic fluid from a different animal. The 28 dpi urine (collected just prior to the amniocentesis) was negative for PAMG-1, however the 45 and 49 dpi urine samples were positive for PAMG-1. The negative control was a non-pregnant urine sample. AmniSure[®] is not a quantitative test but the result suggested there was amniotic fluid in the urine samples at 45 and 49 dpi. To confirm this finding, we performed an insulin-like growth factor binding protein-1 (IGFBP-1) ELISA on the animal's pan-collected urine and amniotic fluid samples, along with appropriate controls. IGFBP-1 is a 25 kD protein synthesized and secreted by the fetal liver and maternal decidua, and is present in amniotic fluid from the second trimester of pregnancy until full term (60). It is not found in urine. In the pregnant animal, IGFBP-1 was detected in pan-collected urine at levels similar to that in amniotic fluid alone, confirming the presence of amniotic fluid-specific protein in the urine (Figure 4). The IGFBP-1 levels in urine from this dam were higher than negative control urine samples (urine from a male and a nonpregnant female) but lower than amniotic fluid from a control macaque late in gestation, which is consistent with dilution from urine from passive collection. Thus, the presence of amniotic fluid in the urine is consistent with premature rupture of membranes.

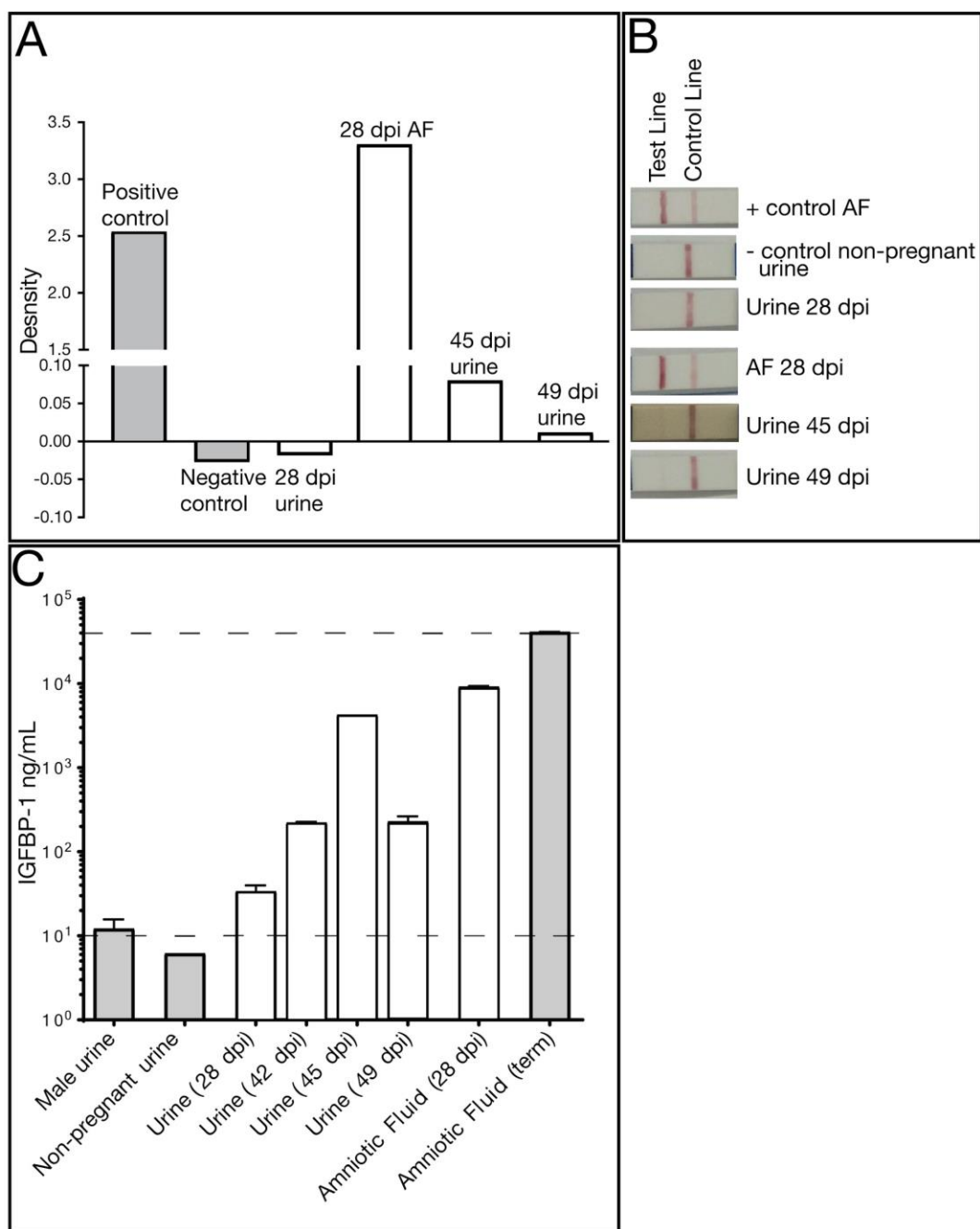


Figure 2.4. Amniotic fluid (AF) markers confirm rupture of membranes. (A) An AmniSure[®] test, which measures PAMG-1 protein, was performed on pan urine collection (28 dpi, 45 dpi, 49 dpi) and AF (28 dpi) from the pregnant animal. Nonpregnant control animal urine and pregnant animal AF are included as controls. (B) Relative pixel density of the Amnisure[®] test strip test band and control band. (C) Amniotic fluid protein IGFBP-1 ELISA. Body fluids from the pregnant animal (pan urine collection 28, 42, 45, 49 dpi and AF 28 dpi), nonpregnant negative control male and female urine samples, amniotic fluid from a control pregnancy were evaluated for the presence of IGFBP-1. In Panels B and C, white bars denote body

fluids from the experimental animal and grey bars denote control fluids from other animals in the colony. Assays completed, data collated, and figure made by LNB.

Ultrasonography

The fetus displayed typical growth in all parameters when compared with normative data (Figure 5) (58). Plotting the predicted gestational age (pGA) vs. the clinically estimated (actual) gestational age (aGA) can reveal changes in the trajectory of a specific growth parameter (49, 57); this analysis did not reveal any growth trajectory anomalies (Figure 5B growth chart).

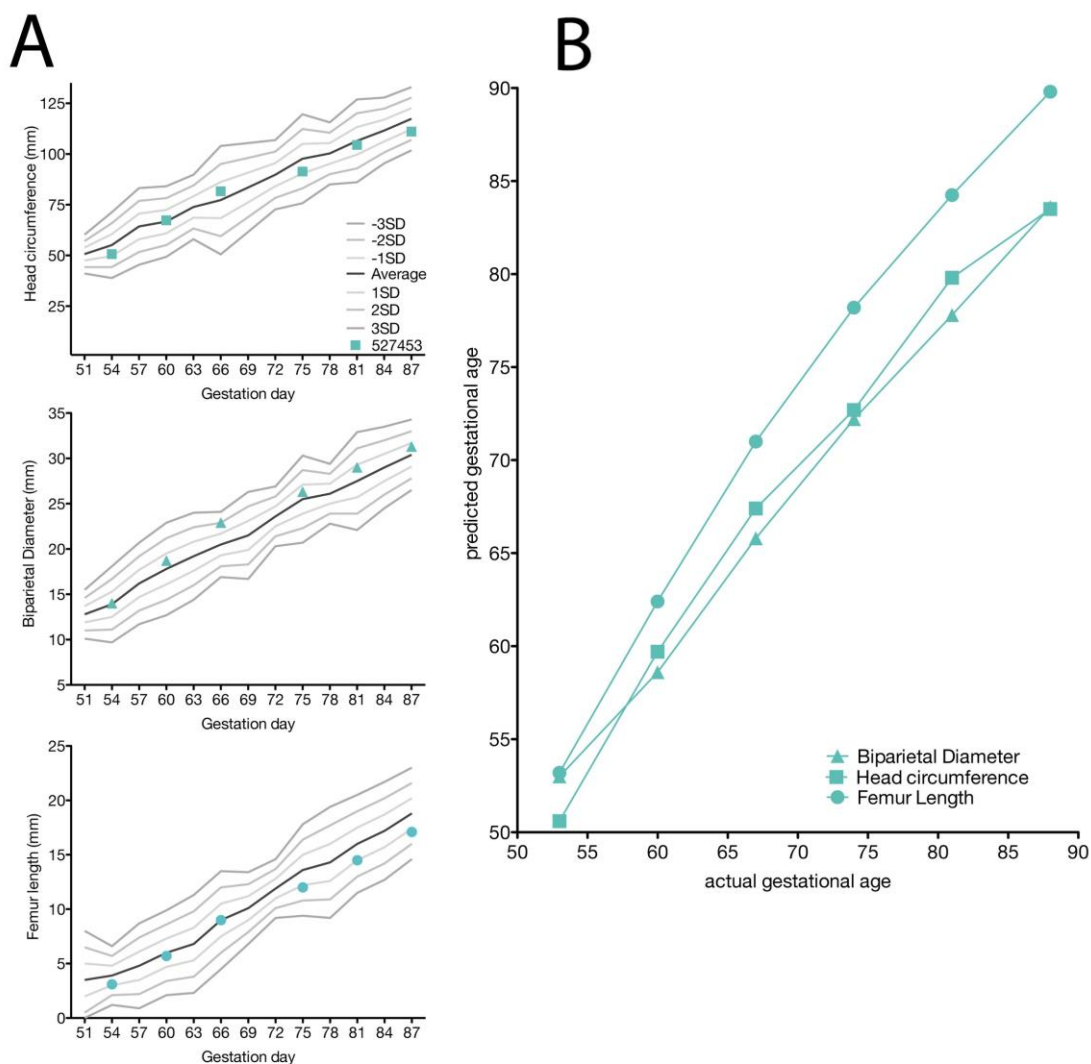


Figure 2.5. Fetal growth measured by ultrasonography. (A) Head circumference (HC), biparietal diameter (BPD), and femur length (FL) were measured in weekly ultrasounds. All measurements are depicted as millimeters (mm). The solid grey lines were derived from reference ranges from Tarantal et al. 2005 to show the mean (black lines) and one, two, and three standard deviations from the mean (grey lines). The HC, BPD, and FL were then plotted along these reference ranges to observe any deviations from the mean. Representative images of the HC, BPD, and FL ultrasounds are located to the right of the respective graph. (B) The pGA is plotted against the aGA (based on gestational age estimated from breeding and menstrual history). The pGA is shown separately for each measurement: BPD (triangle), HC (square), and FL (circle). Data collated and figure made by LNB.

We also closely observed placental and fetal health by ultrasonography. No significant placental lesions were identified until 35 dpi (gd 81) when ultrasonography identified a possible area of placental abruption and a retroplacental clot along the edge of the placenta over the cervix, which was resolving by 42 dpi (gd 88). No fetal abnormalities were noted at either time point, and the fetus did not demonstrate any persistent tachycardia or bradycardia. Because of these small placental lesions, daily heart rate monitoring was initiated and remained within a normal range until 49 dpi (gd 95) when no fetal heartbeat was detected.

The dam underwent euthanasia and necropsy for a comprehensive collection of both maternal and fetal tissues. During the necropsy, the cervix was noted to be closed and no debris was noted in the vaginal vault. The amniotic sac contained significant amounts of adherent purulent matter, and purulent fibrinous material covered the decidua and fetus (Figure 6). The fetus showed advanced tissue autolysis, including severe autolysis of the fetal brain (not shown). Bacterial culture obtained by swab of the fibrinopurulent amniotic fluid at the time of necropsy demonstrated *Staphylococcus epidermidis*. We also identified clusters of gram-positive cocci in the fetal esophageal lumen (Supplementary Figure 1). *S. epidermidis* is part of the vaginal flora in rhesus macaques (61). No additional samples were obtained for culture or bacterial 16s rDNA-PCR.

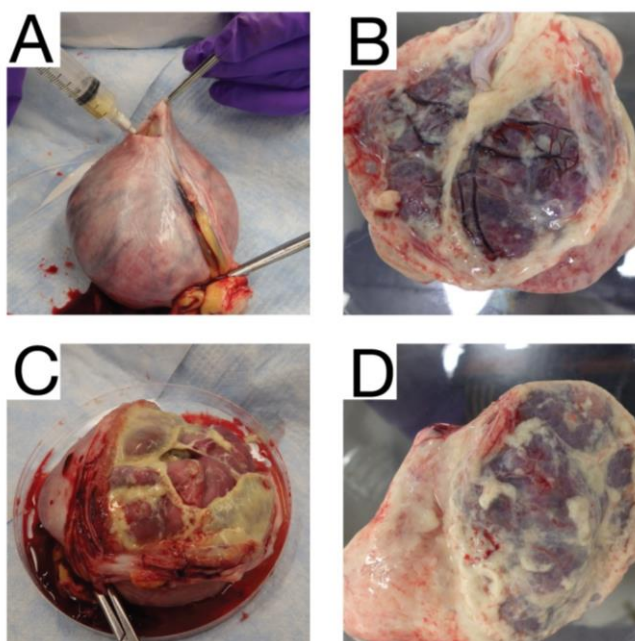
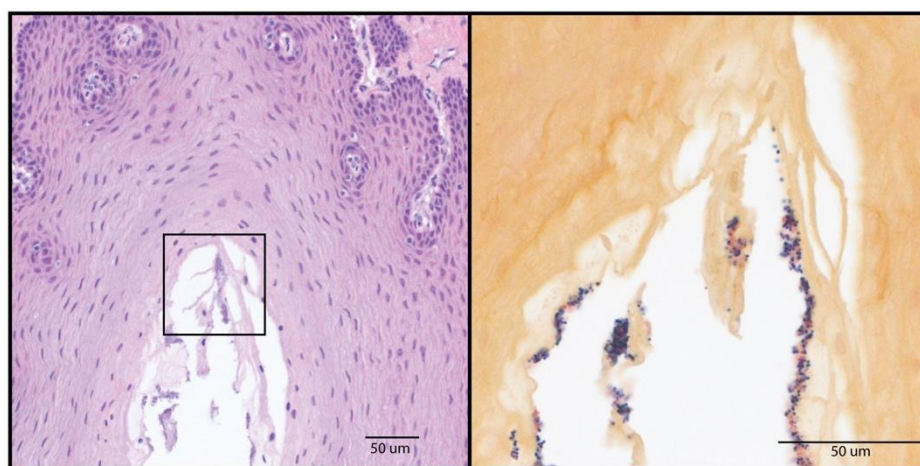


Figure 2.6. Maternal and fetal necropsy images. (A) The uterus was removed in entirety from the abdominal cavity of the dam using sterile instruments and a syringe was used to aspirate the purulent fluid from inside the uterine cavity. (B) The fetus was removed from the uterus and was covered in thick fibrinous material. (C) and (D) Placental discs 1 and 2 were covered in the same thick fibrinous maternal that covered the fetus. Figure made by ELM.



Supplementary Figure 2.1. Histology and gram stain of fetal esophagus. A & B) representative H&E images of the fetal esophagus with the lumen running centrally from upper left to lower right. Panel B shows the boxed area of Panel A at higher magnification. C) Gram stain of a section of the fetal esophagus epithelial surface, where gram positive cocci were abundant. Images taken by AM. Figure made by LNB.

Fetal and maternal vRNA tissue distribution

At necropsy, a range of fetal and maternal tissues were processed for qRT-PCR to determine ZIKV RNA burden. ZIKV RNA was widely distributed within fetal tissues, maternal lymphoid structures, and the reproductive tract: 33 fetal, maternal and maternal-fetal interface tissues were positive for vRNA (Table 1); of these, 27 were fetal tissues. Amniotic fluid collected during necropsy also contained vRNA (Figure 2) but did not contain replicating virus as assessed via plaque assay (not shown). The highest viral loads were detected in fetal colon and fetal lung tissue. Most organs of the fetal digestive system had detectable vRNA: stomach, jejunum, and colon. The presence of vRNA in fetal ocular structures and cerebellum indicates a central nervous system infection. vRNA was detected in four maternal lymph nodes and the spleen, indicating that ZIKV RNA was still present in the maternal immune system structures at 49 dpi, despite the absence of detectable maternal viremia.

Table 2.1: Tissues with detectable ZIKV RNA from mother and fetus.

Tissue Source	Organ System	Tissue Name	vRNA copies/mg
Maternal	Immune	Axillary LN	258.3
		Inguinal LN	1774.8
		Mesenteric LN	9763.8
		Spleen	981.9
		Pelvic LN	583.7
	Reproductive	Decidua	278.2
		Uterus	1471.7
Uterus/placental bed		486.5	
Fetal	Alimentary Canal	Stomach	6140.4
		Colon	355157
		Jejunum	2055.9
		Liver	5.4
	Renal	Kidneys	51.1
		Urinary Bladder	185.1
	Cardiovascular	Aorta-thoracic	921.3
		Heart	366
		Pericardium	1196.3
	Extraembryonic	Amniotic Chorionic Membrane	4933.7
		Placental Disc 1	64.4
		Umbilical Cord	6
	Connective	Adipose Tissue-Omentum	5102.2
	Immune	Axillary LN	287.6
		Spleen	261.1
		Thymus	215.3
	Musculoskeletal	Muscle-quadriiceps	387
	Pulmonary	Lung	37947
	Reproductive	Sem vesicle/Prostate	5700
		Testis	5188.1
	Central Nervous	Cerebrum	72.9
		Dura Mater	74.3
	Ocular	Cornea	135.1
Retina		316.5	
Sclera		370.8	

127 maternal biopsies and fetal tissues were assayed for vRNA. All the tissues positive for ZIKV RNA are listed in this table. The maternal and fetal tissues which were vRNA negative are listed in Supplementary Table 1. Table made by LNB.

Supplementary Table 2.1. Tissues evaluated by qRT-PCR that were negative. *Table made by LNB.*

Tissue Source	Organ System	Tissue Name
Maternal	Alimentary Canal	Bile aspirate
		Colon
		Jejunum
		Pancreas
		Salivary gland
		Stomach
	Cardiovascular	Thyroid
		Thoracic aorta
		Endocardium left ventricle
		Femoral artery
		Femoral vein
		Pulmonary artery
	Endocrine	Mammary gland
		Pituitary gland
	Hematopoiesis	Bone marrow
	Immune	Adipose tissue/omentum
		Aortic lymph node
		Cervical lymph node
		Oropharyngeal lymph node
		Spleen
		Submandibular lymph node
		Thymus
		Tracheobronchial lymph node
	Musculoskeletal	Articular cartilage
		Cardiovascular valve
		Fascia-quadriceps
		Femur head w/ trabecular
		Hand tendon
		Hand tendon (extensor pollicis brevis)
		Ligament-round head of femur
		Metacarpal bone
		Muscle and hand muscle (abductor pollicis brevis)
		Central Nervous
	Cerebellum	
	Cerebrum/hippocampus	
	Dura mater	
	Frontal lobe	
	Hand nerve	
	Sciatic nerve	
	Spinal cord (cervical, lumbar, thoracic)	
	Renal	Kidney
		Urinary bladder
	Reproductive	Ovary
Vagina		
Respiratory	Bronchus primary	
	Lung caudal lobe	
Ocular	Cornea	
	Optic nerve	
	Retina	
	Sclera	
Fetal	Central Nervous	Cerebrum 1 right
		Cerebrum 2 right
		Cerebrum 4 right
		Cerebellum 1 right
		Spinal cord (cervical, lumbar, thoracic)
	Musculoskeletal	Femur bone
	Immune	Mesenteric lymph node

Uteroplacental histopathology

Maternal-fetal interface tissues were evaluated for histological evidence of infection and lesions. There was clear evidence of both acute chorioamnionitis consistent with bacterial infection (Figure 7A), and features of relative placental insufficiency. There is no acute or chronic villitis, but the villi do show increased perivillous fibrin deposition (Figure 7B), and there are multiple remote infarctions (Figure 7C), which is a finding consistent with insufficiency. Radial arteries in the myometrium showed a pronounced leukocytoclastic vasculitis defined as an infiltrative mixture of lymphocytes, eosinophils, and plasma cells into the smooth muscle wall of these vessels (Figure 7D). The leukocytoclastic vasculitis seen around the radial arteries is usually related to hypersensitivity reactions or viral infections, and is not a consequence of bacterial infection. The decidua, placenta, placental bed and amniotic/chorionic membranes also showed significant pathology (Supplementary Table 2).

Supplementary Table 2.2. Histology description of fetal and maternal tissues. *Descriptions completed by HAS. Table made by LNB.*

Tissue Source	Tissue Name	Histology Summary
Maternal	Mesenteric lymph node	Moderate sinus histiocytosis with moderate erythrophagocytosis and minimal moderate siderophagocytosis.
	Spleen	Moderate to marked follicular lymphoid hyperplasia and moderate to marked suppurative splenitis (neutrophilia)
	Uterus/placental bed	Moderate to severe diffuse suppurative and lymphoplasmacytic endometritis with multifocal necrosis, mineralization, fibrinoid vascular necrosis, and multifocal perivascular lymphoplasmacytic myometritis with chronic myometrial interstitial fibrosis. Myometrial radial arteries show leukoclastic vasculitis
	Decidua	Severe diffuse fibrinopurulent and necrotizing deciduitis with multifocal mineralization.
Fetal	Placenta	Moderate suppurative placentitis with moderate multifocal villous infarction, syncytial knot, nodular fibrin accumulation, marked multifocal mineralization with perivillous fibrin deposition, suppurative vasculitis (amniotic vessels), severe diffuse suppurative chorioamnionitis, and multiple remote infarctions
	Amniotic/Chorionic membrane	Severe diffuse fibrinopurulent and necrotizing chorioamnionitis with multifocal mineralization
	Eye	Anterior segment dysgenesis, choroidal coloboma, moderate ventral retinal dysgenesis
	Esophagus	Marked bacterial mucosal colonization with no inflammation
	Lung	Diffuse, moderate tissue autolysis; multifocal to coalescing areas, affecting up to 80% of the tissue sections with one of the following changes: numerous alveoli filled with pale eosinophilic material (fibrin), cellular debris, and rare squamous cells admixed with moderate numbers of viable and degenerative neutrophils; multifocally, alveolar walls are lined by hyperplastic type II pneumocytes with multifocal segmental thickening of the alveolar septa with infiltrated neutrophils
	Mesenteric lymph node	Mild diffuse suppurative lymphadenitis with moderate diffuse autolysis
	Adipose tissue, omentum	(Autolyzed pancreas, mesenteric lymph nodes, large arteries, and fibrovascular tissue): Moderate diffuse tissue autolysis
	Stomach	Moderate to advanced mucosal autolysis with no discernible histologic lesion
	Jejunum	Moderate to advanced mucosal autolysis with no discernible histologic lesion
Colon	Lumen filled with abundant pink eosinophilic material, fibrillar material, and occasional granular basophilic material consistent with nuclear debris; moderate to advanced mucosal autolysis with no discernible histopathological lesions	

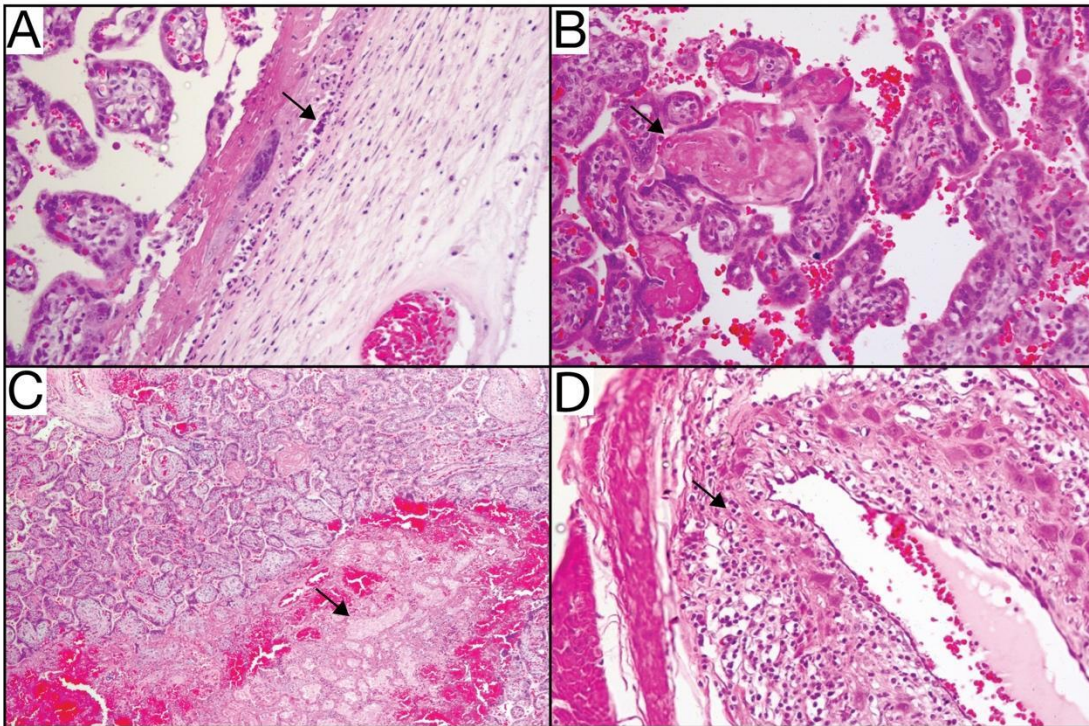


Figure 2.7. Uteroplacental histopathology. (A) Maternal neutrophils invading chorionic plate (arrow) is diagnostic of acute chorioamnionitis. (B) Villi show increased perivillous fibrin deposition (arrow) and there are multiple remote infarctions (arrow, C). (D) Radial arteries in the myometrium show a pronounced leukocytoclastic vasculitis (arrow) defined as an infiltrative mixture of lymphocytes, eosinophils, and plasma cells into the smooth muscle wall of these vessels. Figure made by TKM.

Fetal ocular histopathology

In our previous study (49), 2/2 macaque fetuses from first trimester ZIKV infection had suppurative inflammation in the ocular tissues at term (retina, choroid, optic nerve). In the current study, ocular tissues were therefore carefully evaluated by qRT-PCR and histology. One fetal eye was dissected for vRNA detection by qRT-PCR and the contralateral eye was fixed and processed for histological analysis. ZIKV RNA was detected by qRT-PCR in the retina, choroid, and lens at

low levels (Table 1). At the time of demise, the fetal eyelids were still fused, suggesting that vRNA present in the eye was not due to passage of the virus from the amniotic fluid directly across the cornea or sclera.

In the fixed and processed globe, a chorioretinal coloboma affecting the ventral aspect of the globe was revealed, and was characterized by extensive areas of choroidal and scleral thinning with a central area of choroidal and retinal pigmented epithelium absence and marked dysplasia of the adjacent retina (Figure 8). Additionally, the presence of fusion of the iris with the posterior corneal stroma and a seeming lack of adequate maturation of the iridocorneal angle structures suggested the presence of anterior segment dysgenesis. It is necessary to acknowledge that the histologic interpretation of the anterior segment changes in this globe was hampered by the tissue autolysis presence in the fetus. Although the chorioretinal lesions were obvious even with a mild degree of autolysis, the autolytic changes impacted our ability to analyze the delicate structure of the developing tissues of the iridocorneal angles, making it impossible to definitively diagnose anterior segment dysgenesis. Because the retina is part of the central nervous system, the finding of retinal dysplasia indicates that the fetus had CNS abnormalities. The presence of the coloboma, dysplastic retina, and potential anterior segment dysgenesis are abnormalities that likely arose from disruption of early ocular developmental processes (62), consistent with the first trimester window of sensitivity in our earlier study (49).

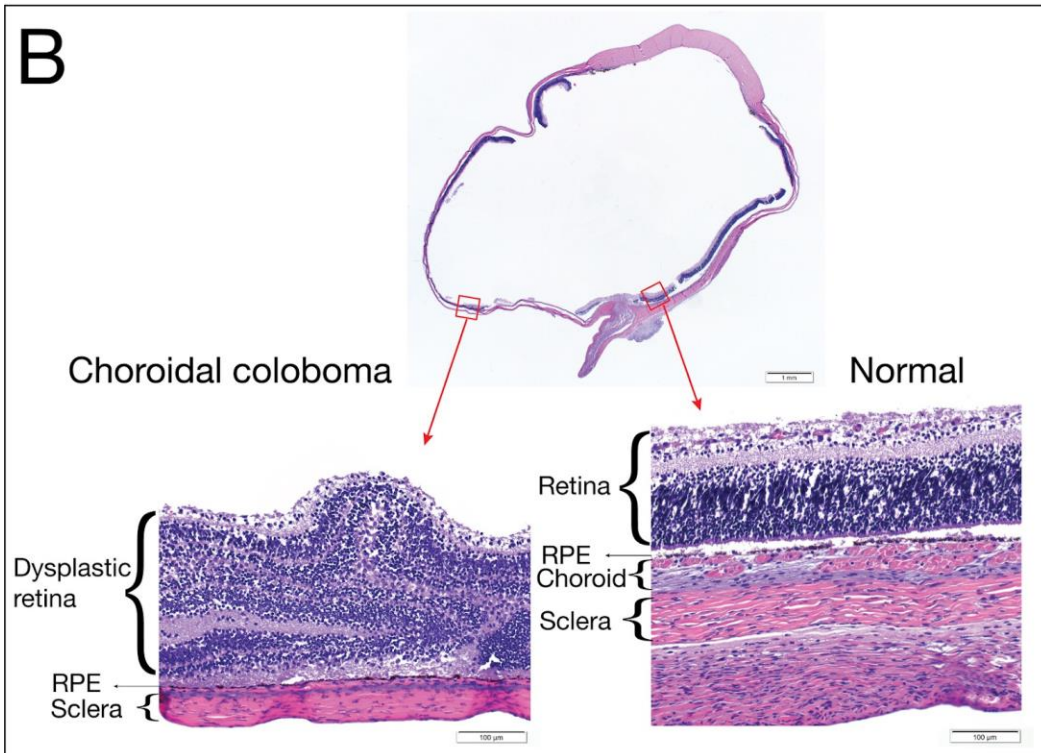
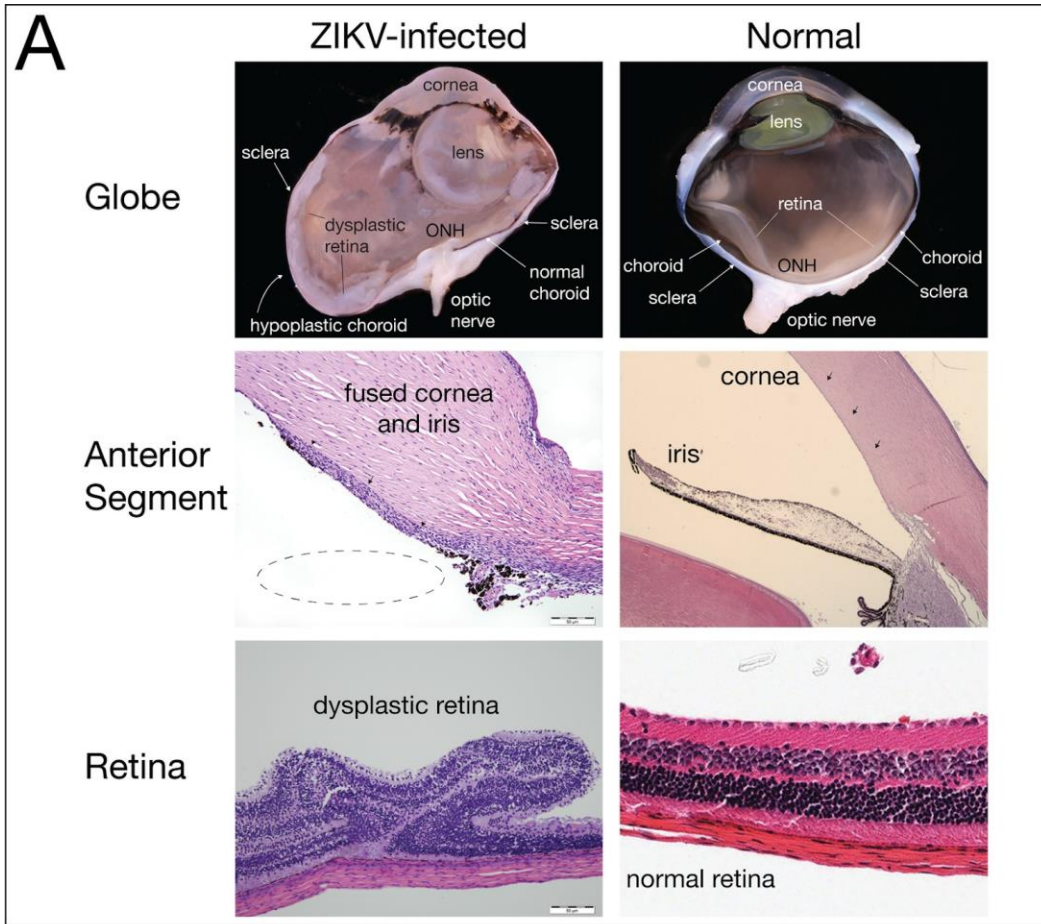


Figure 2.8. Fetal ocular pathology. (A) The left panels contain images of the ZIKV-infected eye, and the right panels show normal features from a different infant macaque for comparison. The globe of the ZIKV-infected fetus shows a hypoplastic choroid and dysplastic retina compared to the normal eye. The irregular shape of the eye in the ZIKV-infected globe is a processing artifact. The anterior segment image of the ZIKV-infected fetus shows that the iris is fused to the posterior cornea (black arrow heads), suggesting anterior segment dysgenesis; the dotted line shows where the iris would be in normal ocular development. The ZIKV-infected eye presents marked retinal dysplasia, characterized by retinal folding and loss of normal retinal organization when compared with the normal retina in the control image on the right. (B) A choroidal coloboma was identified on the ventral aspect of the globe (left image); the choroid had normal development on the dorsal aspect of the same globe (right image). The retina, retinal pigment epithelium (RPE), choroid (if present), and sclera are labeled with the left image demonstrating an absence of choroid. Images taken by HAS and AM. Figure made by TGG and LNB.

Tissue pathology and detection of vRNA in maternal and fetal tissues

Histologic lesions were noted in the fetal tissues that were potentially exposed to virus in the amniotic fluid, specifically the respiratory and gastrointestinal systems. There were significant lesions in the lungs, mesenteric lymph node, placenta, chorioamniotic membranes, decidua, maternal uterus, and maternal spleen (Supplementary Table 2). Consistent with the bacterial growth of *S. epidermidis* from amniotic fluid, gram positive cocci were observed within the lumen of the esophagus (Supplementary Figure 1), although there was no associated inflammatory reaction within the epithelium or deeper tissue layers of the esophagus. The stomach and small intestine had mucosal autolysis with no discernible histologic lesions. The lumen of the colon had granular basophilic material consistent with nuclear debris.

The fetal lungs had notable pathology. The pulmonary alveoli had fibrin, cellular debris, edema, occasional squamous cells, and neutrophilic infiltration (alveolitis). There were multiple areas of

alveoli with type II pneumocyte hyperplasia, with multifocal expansion of the alveolar septa with fibrin. The trachea, primary and secondary bronchi, had relatively intact respiratory epithelium.

ZIKV histological analyses

ZIKV RNA localization was evaluated by ISH and mFISH on selected tissues with high vRNA burden as determined by qRT-PCR. Figure 9 presents photomicrographs from near sections of the same spleen, fetal membranes, and fetal lung specimens. H&E staining is presented to demonstrate tissue organization and pathology; ISH to confirm the presence of ZIKV genome within cells, and mFISH for both negative and positive strand ZIKV RNAs to detect the dsRNA of replicative intermediates. Supplementary Figure 2 also presents representative images of positive and negative strand RNAs for the tissues displayed; the merged figure colocalizes both positive and negative sense RNA strands, indicating active ZIKV replication in these tissues.

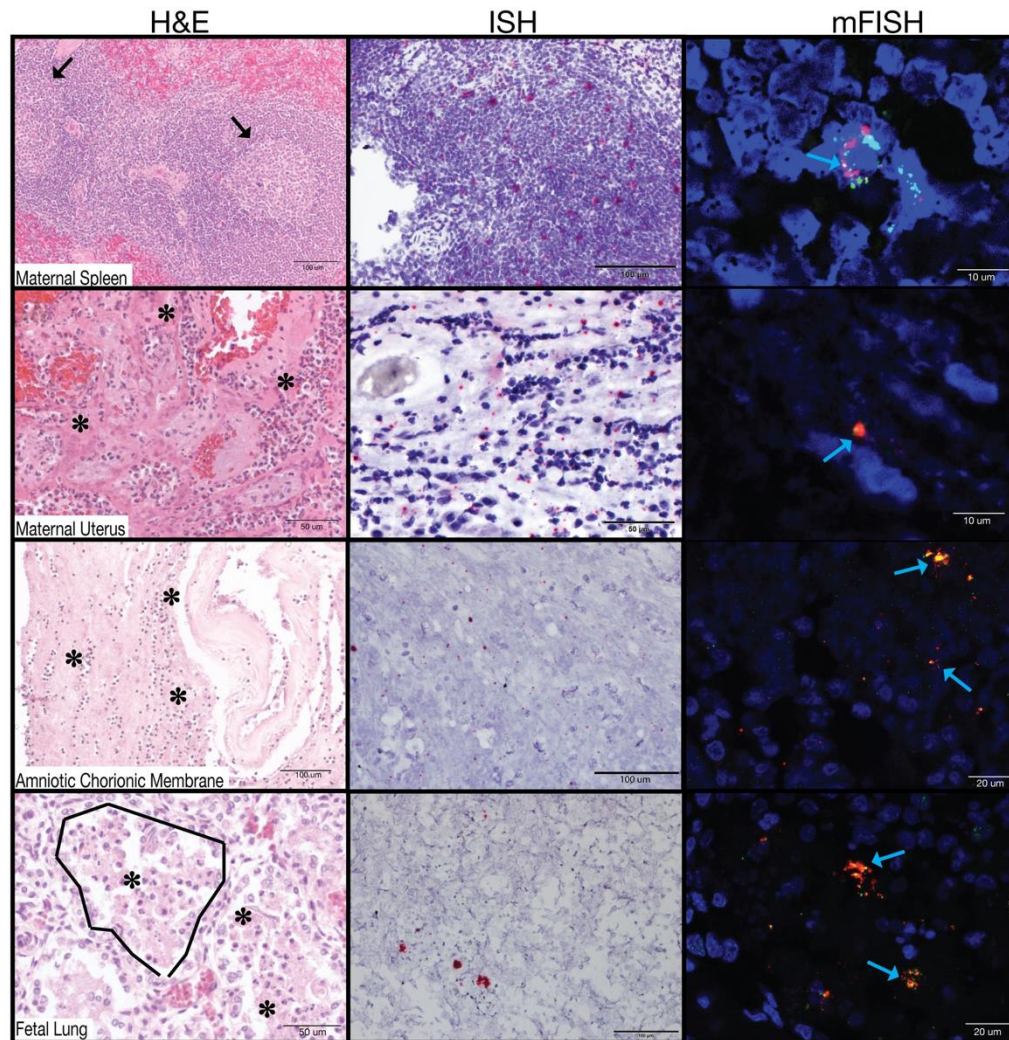
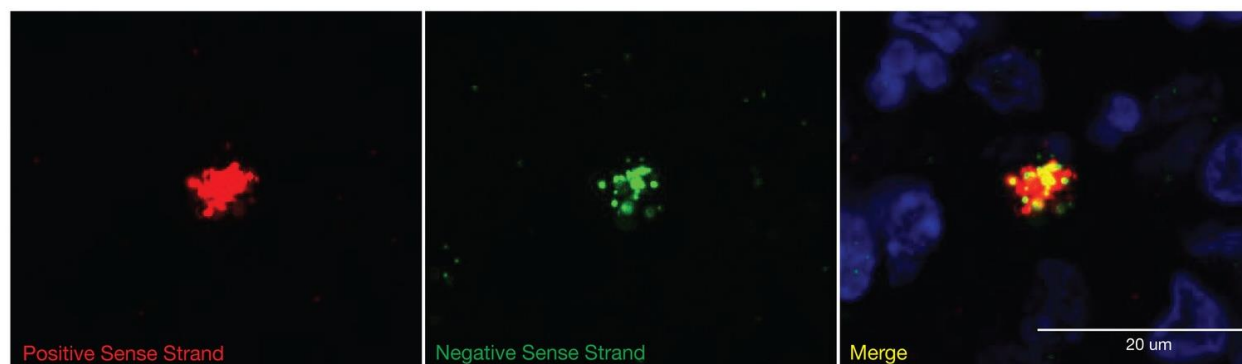


Figure 2.9. Tissue histology and viral localization of maternal spleen, maternal uterus, amniotic/chorionic membrane, and fetal lung. Each tissue was stained with H&E, ISH, and mFISH. ISH shows localization of ZIKV vRNA. mFISH shows replicative intermediates by staining the negative sense RNA strands green and positive sense RNA strands red. Co-localization (yellow) demonstrates dsRNA intermediates. Black arrows denote a germinal center. Asterisks indicate neutrophils. Blue arrows highlight green, red, or yellow fluorescence. Images taken and annotated by HAS, AM, and KZ. Figure made by LNB.

Table 2.2. Tissue vRNA burden, ISH and mFISH results.

Tissue Source	Tissue Name	vRNA copies/mg	ISH	mFISH
Maternal	Mesenteric LN	976.38	-	
	Spleen	98.19	+	+
	Uterus	147.17	+	+
	Decidua	27.82	+	+
Fetal	Amniotic/Chorionic Membrane	493.37	+	+
	Colon	35515.7	+	+
	Stomach	614.04	-	
	Pericardium	119.63	-	
	Adipose Tissue-Omentum	510.22	+	-
	Lung	3794.70	+	+
	Seminal Vesicle/Prostate	570.00	-	
	Testis	518.81	-	
	Eye (Retina/Cornea/Sclera)	31.65/13.51/37.08	-	

Tissues with a detectable vRNA burden were evaluated by ISH and mFISH. ISH detects positive sense vRNA; mFISH detects ZIKV replicative intermediates (negative and positive sense vRNA). “+” indicates detectable signal in these tissues sections, “-“ indicates no signal. Tissues with no detectable ISH signal were not further evaluated by mFISH. Table made by LNB.



Supplementary Figure 2.2. Multiplex fluorescent in situ hybridization of positive and negative strand vRNA in fetal lung. Images taken and figure made by XZ.

2.5 Discussion (Original by ELM and LNB; edited by all)

In this report of an adverse pregnancy outcome following ZIKV infection in a rhesus macaque, we describe fetal demise following suspected PPROM, fetal and maternal ZIKV burden, and significant ocular pathology in the fetus. ZIKV RNA was widely distributed throughout fetal tissues at necropsy, including in the cerebellum and ocular tissues. ZIKV vRNA was also identified in maternal lymph nodes and maternal spleen at the time of necropsy (49 dpi). Replication competent virus was identified by ISH for the presence of negative and positive strand RNA in fetal and maternal tissues. Abnormal histology was characterized in multiple fetal tissues including alveolitis and pneumocyte hyperplasia in fetal lung tissue, and severe ocular abnormalities. Both fetal ocular pathology and fetal demise have been described in human reports of ZIKV infection and demonstrate parallels between human and NHP CZS.

Fetal demise

This is the first report of rupture of membranes and fetal demise in an NHP model of congenital ZIKV infection. We presume that maternal membranes ruptured around 42 dpi (although some amniotic fluid may have been present at 28 dpi) because we detected amniotic fluid markers in the urine at this time point, and identified high vRNA burden in this urine sample, despite absence of detectable maternal viremia at this time. A week after detection of ZIKV RNA in the pan-collected urine/amniotic fluid mixture, abdominal ultrasound evaluation found no fetal heartbeat and the fetus and dam were submitted for necropsy. There was no chronic villitis, which would be expected for viral induced changes. However, sections of the decidua and myometrium revealed a

pronounced leukocytoclastic vasculitis involving the smooth muscle walls of the radial and spiral arteries. This is significant because this type of vasculitis is not expected in cases of bacterial infection, but do occur as a response to viral infections associated with cutaneous vasculitis (hypersensitivity vasculitis) (63).

Although there was fibrinopurulent material surrounding the fetus in the uterine cavity and gram positive cocci in the esophagus, multiple sections of placenta and all other fetal tissues had no histologic evidence of bacterial colonization. The growth of *S. epidermidis* from aspirated amniotic fluid was minimal and contamination at the time of collection is a possibility. Neutrophilic infiltration, such as that seen in the chorionic plate, is consistent with bacterial infection, but intra-amniotic neutrophilic inflammation can also be sterile (64). Sterile neutrophilic inflammation has been reported previously in experimental infection in animals models with this strain of ZIKV, including mice which demonstrated neutrophil infiltration of the skeletal muscle and hippocampus (65) and male rhesus macaques which demonstrated interstitial neutrophilic prostatitis (47). Therefore, while this clinical presentation is consistent with an ascending bacterial intraamniotic infection, further studies will be able to provide clarification of the histopathologic outcomes with macaque pregnancies.

Closely associated with this fetal demise is the occurrence of PPRM. Although it is not possible to determine if the amniotic membranes ruptured because of ZIKV infection, the finding of PPRM followed by fetal demise also occurs during human prenatal ZIKV infection (24). It could be hypothesized that the amniocentesis at 28 dpi contributed to the possible intrauterine bacterial

infection; however, the long duration of time separating these events, and the typical rapidity of preterm labor in the rhesus macaque with experimental bacterial infection of the amniotic fluid makes this unlikely (66, 67). Additional studies of ZIKV infection during NHP pregnancy are needed to determine if there is an association between congenital ZIKV infection and an increased risk for intra-amniotic infection leading to PPRM and fetal demise. One may speculate that ZIKV infection early in gestation affects pregnancy-induced T-cell changes or placental invasion involved in uterine vascular remodeling necessary for normal blood flow to the placenta. In turn, ZIKV infection may lead to abnormal remodeling and abnormal blood flow to the placenta culminating in pathologic infarctions and increased risk for relative placental insufficiency and preterm birth. This working hypothesis requires further study.

Fetal ocular defects

Congenital ocular abnormalities are strongly associated with human prenatal ZIKV infection, as demonstrated by the high frequency (up to 55%) of ocular disease in human infants with first trimester prenatal infections (12). There is growing evidence that structures of the fetal visual system are a significant target for ZIKV in human pregnancy. The fetal eye evaluated for pathology in the current study had anterior segment dysgenesis, a ventral choroidal coloboma, and retinal dysplasia. This is the first time that such severe ocular abnormalities have been reported with macaque CZS. As far as we are aware, bacterial infections are not associated with such abnormalities during development. In addition, an acute intrauterine bacterial infection would not have impacted eye development, since the ocular structure damage described would likely have occurred from the disruption of normal developmental processes which occur earlier in pregnancy.

Anterior segment dysgenesis refers to a spectrum of developmental anomalies resulting from abnormalities of neural crest migration and differentiation during fetal development (68). In humans, anterior segment dysgenesis is present in rare syndromes (69), and although the rate of anterior segment dysgenesis and related syndromes is unknown in rhesus macaques, it would be unlikely to appear in pregnancy.

An ocular coloboma is a congenital lesion associated with a failure in the closure of the embryonic (ocular) fissure causing defects of one or more ocular structures (i.e., the eyelids, lens, cornea, iris, ciliary body, zonules, choroid, retina and optic nerve). The defect is essentially a bare sclera with the overlying retinal pigmented epithelium, retina or choroid missing (70). It may be sporadic or inherited and, in some cases, is associated with systemic disorders (70). Choroidal colobomas in humans can be also associated with the presence of retinal dysplasia (71, 72), which was noted in the current case. Although there are multiple genetic mutations associated with colobomatous defects in humans (70), there is only one case report of a macaque with coloboma and no genetic evaluations were pursued in that report (73). We did not pursue a genetic evaluation because it seems unlikely that a rare genetic defect would occur in one of the fetuses with congenital ZIKV infection. The defects in the eye affected the posterior and ventral aspect of the globe, which is common, since the ocular fissure is embryologically located in the ventro-nasal quadrant of the eye. It also mainly affected the choroid, thereby classifying it as a choroidal coloboma. In our previous study, we identified optic nerve gliosis in the two-first trimester infections (49), but did not identify other significant ocular pathology. CZS represents a continuum of disease from mild to severe and the macaque model highlights this by capturing the wide disease spectrum. It is also

important to note that the current study was conducted with a virus stock prepared from an isolate obtained from a person infected in Puerto Rico, whereas our previous study (49) was conducted with a virus stock prepared from a French Polynesian isolate. Our results may indicate that closely related viruses can cause different outcomes in pregnant macaques, however further studies will be needed to understand whether specific genetic determinants are related to these outcomes. Although ZIKV causes ocular disease in the adult murine model (74), no ocular anomalies to this extent have yet been observed in mouse models of congenital ZIKV infection. This also underscores the important role the rhesus macaque model plays in studying ZIKV effects on pregnancy outcomes.

Maternal and fetal tissue viral distribution

ZIKV RNA was detected throughout fetal tissues, affecting multiple organ systems (digestive, respiratory, reproductive, cardiovascular, immune, and nervous), and replication competent virus was identified in fetal lung tissue 49 dpi via negative and positive strand RNA ISH. Remarkably, ZIKV RNA was also detected in maternal lymph nodes at 49 dpi and replication competent virus was identified in the lymph node tested. The presence of vRNA does not imply that the virus is replicating or may be transmissible. However, the detection of negative strand RNA by ISH and its colocalization with positive strand vRNA is confirmation of replication competent virus, and the finding of infectious virus in fetal and maternal tissues 49 dpi could have important implications for transmission. The fact that replication competent ZIKV is still present in an adult lymphoid-associated tissue at 49 dpi is critical to understanding the risk involved with organ transplantation, although with the caveat that viral persistence may be longer in pregnancy. Viral

persistence is not explained by a lack of maternal humoral immune response since the dam developed neutralizing antibodies at concentrations similar to our previous NHP studies of ZIKV infections (50, 55).

We do not know to what extent ZIKV infection of the fetus directly contributed to fetal demise, since this case is complicated by PPROM with acute chorioamnionitis. Extended exposure of the fetus to ZIKV is most likely responsible for the ocular pathology observed, and there is no literature of which we are aware which suggests that bacterial infection results in ocular malformations. The substantial viral burden in the fetal membranes also supports the hypothesis that ZIKV contributed to PPROM. The detection of replicating ZIKV intermediates in membranes and fetal tissues at the time of fetal demise also suggests that active ZIKV infection was ongoing up until fetal demise.

In summary, we describe a case of congenital ZIKV infection with severe ocular and uteroplacental pathology complicated by fetal demise following apparent PPROM. The fetal ocular pathology recapitulates defects seen in human CZS. This is the first report of an adverse pregnancy outcome and fetal pathology in an NHP infected with ZIKV strain PRVABC59, and thus supports the importance of the macaque model for not only defining the risk ZIKV poses for pregnant women and their fetuses in the Americas, but also for defining the precise pathways by which ZIKV accesses the fetal compartment, and for testing strategies to intervene in vertical transmission.

2.6 References

1. Schuler-Faccini L, Ribeiro EM, Feitosa IM, Horovitz DD, Cavalcanti DP, Pessoa A, et al. Possible Association Between Zika Virus Infection and Microcephaly - Brazil, 2015. *MMWR Morbidity and mortality weekly report*. 2016;65(3):59-62.
2. Rasmussen SA, Jamieson DJ, Honein MA, Petersen LR. Zika Virus and Birth Defects - Reviewing the Evidence for Causality. *The New England journal of medicine*. 2016.
3. van der Linden V, Filho EL, Lins OG, van der Linden A, Aragao Mde F, Brainer-Lima AM, et al. Congenital Zika syndrome with arthrogryposis: retrospective case series study. *BMJ (Clinical research ed)*. 2016;354:i3899.
4. van der Linden V, Pessoa A, Dobyns W, Barkovich AJ, Junior HV, Filho EL, et al. Description of 13 Infants Born During October 2015-January 2016 With Congenital Zika Virus Infection Without Microcephaly at Birth - Brazil. *MMWR Morbidity and mortality weekly report*. 2016;65(47):1343-8.
5. Honein MA, Dawson AL, Petersen EE, Jones AM, Lee EH, Yazdy MM, et al. Birth Defects Among Fetuses and Infants of US Women With Evidence of Possible Zika Virus Infection During Pregnancy. *JAMA : the journal of the American Medical Association*. 2017;317(1):59-68.
6. Russo FB, Jungmann P, Beltrao-Braga PC. Zika infection and the development of neurological defects. *Cellular microbiology*. 2017.
7. Chan JF, Choi GK, Yip CC, Cheng VC, Yuen KY. Zika fever and congenital Zika syndrome: An unexpected emerging arboviral disease. *The Journal of infection*. 2016;72(5):507-24.
8. Costa F, Sarno M, Khouri R, de Paula Freitas B, Siqueira I, Ribeiro GS, et al. Emergence of Congenital Zika Syndrome: Viewpoint From the Front Lines. *Annals of internal medicine*. 2016;164(10):689-91.
9. Franca GV, Schuler-Faccini L, Oliveira WK, Henriques CM, Carmo EH, Pedi VD, et al. Congenital Zika virus syndrome in Brazil: a case series of the first 1501 livebirths with complete investigation. *Lancet*. 2016.
10. Moore CA, Staples JE, Dobyns WB, Pessoa A, Ventura CV, Fonseca EB, et al. Characterizing the Pattern of Anomalies in Congenital Zika Syndrome for Pediatric Clinicians. *JAMA pediatrics*. 2016.
11. Meyer U, Yee BK, Feldon J. The neurodevelopmental impact of prenatal infections at different times of pregnancy: the earlier the worse? *The Neuroscientist : a review journal bringing neurobiology, neurology and psychiatry*. 2007;13(3):241-56.
12. Ventura CV, Maia M, Travassos SB, Martins TT, Patriota F, Nunes ME, et al. Risk Factors Associated With the Ophthalmoscopic Findings Identified in Infants With Presumed Zika Virus Congenital Infection. *JAMA ophthalmology*. 2016;134(8):912-8.

13. Zin AA, Tsui I, Rossetto J, Vasconcelos Z, Adachi K, Valderramos S, et al. Screening Criteria for Ophthalmic Manifestations of Congenital Zika Virus Infection. *JAMA pediatrics*. 2017.
14. Agrawal R, Oo HH, Balne PK, Ng L, Tong L, Leo YS. Zika Virus and Eye. *Ocular immunology and inflammation*. 2017;1-6.
15. Ventura CV, Maia M, Bravo-Filho V, Gois AL, Belfort R, Jr. Zika virus in Brazil and macular atrophy in a child with microcephaly. *Lancet*. 2016;387(10015):228.
16. Ventura CV, Fernandez MP, Gonzalez IA, Rivera-Hernandez DM, Lopez-Alberola R, Peinado M, et al. First Travel-Associated Congenital Zika Syndrome in the US: Ocular and Neurological Findings in the Absence of Microcephaly. *Ophthalmic surgery, lasers & imaging retina*. 2016;47(10):952-5.
17. Ventura CV, Ventura LO, Bravo-Filho V, Martins TT, Berrocal AM, Gois AL, et al. Optical Coherence Tomography of Retinal Lesions in Infants With Congenital Zika Syndrome. *JAMA ophthalmology*. 2016;134(12):1420-7.
18. Ventura CV, Maia M, Ventura BV, Linden VV, Araujo EB, Ramos RC, et al. Ophthalmological findings in infants with microcephaly and presumable intra-uterus Zika virus infection. *Arquivos brasileiros de oftalmologia*. 2016;79(1):1-3.
19. Miranda HA, 2nd, Costa MC, Frazao MA, Simao N, Franchischini S, Moshfeghi DM. Expanded Spectrum of Congenital Ocular Findings in Microcephaly with Presumed Zika Infection. *Ophthalmology*. 2016;123(8):1788-94.
20. Wong CW, Ng SR, Cheung CM, Wong TY, Mathur R. ZIKA-RELATED MACULOPATHY. *Retinal cases & brief reports*. 2017.
21. Yopez JB, Murati FA, Pettito M, Penaranda CF, de Yopez J, Maestre G, et al. Ophthalmic Manifestations of Congenital Zika Syndrome in Colombia and Venezuela. *JAMA ophthalmology*. 2017;135(5):440-5.
22. Centers for Disease Control and Prevention. Pregnant Women with Any Laboratory Evidence of Possible Zika Virus Infection in the United States and Territories [updated March 2, 2017. Available from: <https://www.cdc.gov/zika/geo/pregwomen-uscases.html>.
23. Sarno M, Sacramento GA, Khouri R, do Rosario MS, Costa F, Archanjo G, et al. Zika Virus Infection and Stillbirths: A Case of Hydrops Fetalis, Hydranencephaly and Fetal Demise. *PLoS neglected tropical diseases*. 2016;10(2):e0004517.
24. Schaub B, Monthieux A, Najihoullah F, Harte C, Cesaire R, Jolivet E, et al. Late miscarriage: another Zika concern? *European journal of obstetrics, gynecology, and reproductive biology*. 2016;207:240-1.
25. van der Eijk AA, van Genderen PJ, Verdijk RM, Reusken CB, Mogling R, van Kampen JJ, et al. Miscarriage Associated with Zika Virus Infection. *The New England journal of medicine*. 2016.

26. Martines RB, Bhatnagar J, Keating MK, Silva-Flannery L, Muehlenbachs A, Gary J, et al. Notes from the Field: Evidence of Zika Virus Infection in Brain and Placental Tissues from Two Congenitally Infected Newborns and Two Fetal Losses - Brazil, 2015. *MMWR Morbidity and mortality weekly report*. 2016;65(6):159-60.
27. Morgan TK. Role of the Placenta in Preterm Birth: A Review. *American journal of perinatology*. 2016;33(3):258-66.
28. Kapogiannis BG, Chakhtoura N, Hazra R, Spong CY. Bridging Knowledge Gaps to Understand How Zika Virus Exposure and Infection Affect Child Development. *JAMA pediatrics*. 2017;171(5):478-85.
29. Prevention; CfDca. Outcomes of Pregnancies with Laboratory Evidence of Possible Zika Virus Infection in the United States and the US Territories 2017 [Available from: <https://www.cdc.gov/zika/reporting/pregnancy-outcomes.html>].
30. Racicot K, Cardenas I, Wunsche V, Aldo P, Guller S, Means RE, et al. Viral infection of the pregnant cervix predisposes to ascending bacterial infection. *Journal of immunology (Baltimore, Md : 1950)*. 2013;191(2):934-41.
31. Carroll T, Lo M, Lanteri M, Dutra J, Zarbock K, Silveira P, et al. Zika virus preferentially replicates in the female reproductive tract after vaginal inoculation of rhesus macaques. *PLoS pathogens*. 2017;13(7):e1006537.
32. Paz-Bailey G, Rosenberg ES, Doyle K, Munoz-Jordan J, Santiago GA, Klein L, et al. Persistence of Zika Virus in Body Fluids - Preliminary Report. *The New England journal of medicine*. 2017.
33. Sotelo JR, Sotelo AB, Sotelo FJB, Doi AM, Pinho JRR, Oliveira RC, et al. Persistence of Zika Virus in Breast Milk after Infection in Late Stage of Pregnancy. *Emerging infectious diseases*. 2017;23(5):856-7.
34. Oliveira Souto I, Alejo-Cancho I, Gascon Brustenga J, Peiro Mestres A, Munoz Gutierrez J, Martinez Yoldi MJ. Persistence of Zika virus in semen 93 days after the onset of symptoms. *Enfermedades infecciosas y microbiologia clinica*. 2016.
35. Atkinson B, Thorburn F, Petridou C, Bailey D, Hewson R, Simpson AJ, et al. Presence and Persistence of Zika Virus RNA in Semen, United Kingdom, 2016. *Emerging infectious diseases*. 2017;23(4):611-5.
36. Gaskell KM, Houlihan C, Nastouli E, Checkley AM. Persistent Zika Virus Detection in Semen in a Traveler Returning to the United Kingdom from Brazil, 2016. *Emerging infectious diseases*. 2017;23(1):137-9.
37. Turmel JM, Abgueguen P, Hubert B, Vandamme YM, Maquart M, Le Guillou-Guillemette H, et al. Late sexual transmission of Zika virus related to persistence in the semen. *Lancet*. 2016;387(10037):2501.

38. Hirayama T, Mizuno Y, Takeshita N, Kotaki A, Tajima S, Omatsu T, et al. Detection of dengue virus genome in urine by real-time reverse transcriptase PCR: a laboratory diagnostic method useful after disappearance of the genome in serum. *Journal of clinical microbiology*. 2012;50(6):2047-52.
39. de Laval F, Matheus S, Labrousse T, Enfissi A, Rousset D, Briolant S. Kinetics of Zika Viral Load in Semen. *The New England journal of medicine*. 2017;377(7):697-9.
40. Barzon L, Pacenti M, Franchin E, Lavezzo E, Trevisan M, Sgarabotto D, et al. Infection dynamics in a traveller with persistent shedding of Zika virus RNA in semen for six months after returning from Haiti to Italy, January 2016. *Euro surveillance : bulletin European sur les maladies transmissibles = European communicable disease bulletin*. 2016;21(32).
41. Barzon L, Pacenti M, Berto A, Sinigaglia A, Franchin E, Lavezzo E, et al. Isolation of infectious Zika virus from saliva and prolonged viral RNA shedding in a traveller returning from the Dominican Republic to Italy, January 2016. *Euro surveillance : bulletin European sur les maladies transmissibles = European communicable disease bulletin*. 2016;21(10).
42. Dupont-Rouzeyrol M, Biron A, O'Connor O, Huguon E, Descloux E. Infectious Zika viral particles in breastmilk. *Lancet*. 2016.
43. Van den Bossche D, Cnops L, Van Esbroeck M. Recovery of dengue virus from urine samples by real-time RT-PCR. *European journal of clinical microbiology & infectious diseases : official publication of the European Society of Clinical Microbiology*. 2015;34(7):1361-7.
44. de Souza Pereira BB, Darrigo Junior LG, de Mello Costa TC, Felix AC, Simoes BP, Stracieri AB, et al. Prolonged viremia in dengue virus infection in hematopoietic stem cell transplant recipients and patients with hematological malignancies. *Transplant infectious disease: an official journal of the Transplantation Society*. 2017.
45. Bandeira AC, Campos GS, Rocha VF, Souza BS, Soares MB, Oliveira AA, et al. Prolonged shedding of Chikungunya virus in semen and urine: A new perspective for diagnosis and implications for transmission. *IDCases*. 2016;6:100-3.
46. Arragain L, Dupont-Rouzeyrol M, O'Connor O, Sigur N, Grangeon JP, Huguon E, et al. Vertical Transmission of Dengue Virus in the Peripartum Period and Viral Kinetics in Newborns and Breast Milk: New Data. *Journal of the Pediatric Infectious Diseases Society*. 2016.
47. Hirsch AJ, Smith JL, Haese NN, Broeckel RM, Parkins CJ, Kreklywich C, et al. Zika Virus infection of rhesus macaques leads to viral persistence in multiple tissues. *PLoS pathogens*. 2017;13(3):e1006219.
48. Aid M, Abbink P, Larocca RA, Boyd M, Nityanandam R, Nanayakkara O, et al. Zika Virus Persistence in the Central Nervous System and Lymph Nodes of Rhesus Monkeys. *Cell*. 2017.

49. Nguyen SM, Antony KM, Dudley DM, Kohn S, Simmons HA, Wolfe B, et al. Highly efficient maternal-fetal Zika virus transmission in pregnant rhesus macaques. *PLoS pathogens*. 2017;13(5):e1006378.
50. Dudley DM, Aliota MT, Mohr EL, Weiler AM, Lehrer-Brey G, Weisgrau KL, et al. A rhesus macaque model of Asian-lineage Zika virus infection. *Nature communications*. 2016;7:12204.
51. Enders AC. Implantation in the macaque: expansion of the implantation site during the first week of implantation. *Placenta*. 2007;28(8-9):794-802.
52. Blankenship TN, Enders AC, King BF. Trophoblastic invasion and the development of uteroplacental arteries in the macaque: immunohistochemical localization of cytokeratins, desmin, type IV collagen, laminin, and fibronectin. *Cell and tissue research*. 1993;272(2):227-36.
53. Bondarenko GI, Burleigh DW, Durning M, Breburda EE, Grendell RL, Golos TG. Passive immunization against the MHC class I molecule Mamu-AG disrupts rhesus placental development and endometrial responses. *Journal of immunology (Baltimore, Md : 1950)*. 2007;179(12):8042-50.
54. Osuna CE, Lim SY, Deleage C, Griffin BD, Stein D, Schroeder LT, et al. Zika viral dynamics and shedding in rhesus and cynomolgus macaques. *Nature medicine*. 2016;22(12):1448-55.
55. Aliota MT, Dudley DM, Newman CM, Mohr EL, Gellerup DD, Breitbart ME, et al. Heterologous Protection against Asian Zika Virus Challenge in Rhesus Macaques. *PLoS neglected tropical diseases*. 2016;10(12):e0005168.
56. Adams Waldorf KM, Stencel-Baerenwald JE, Kapur RP, Studholme C, Boldenow E, Vornhagen J, et al. Fetal brain lesions after subcutaneous inoculation of Zika virus in a pregnant nonhuman primate. *Nature medicine*. 2016.
57. Tarantal AF. Ultrasound Imaging in Rhesus (*Macaca mulatta*) and Long-tailed (*Macaca fascicularis*) Macaques: Reproductive and Research Applications. *Ultrasound Imaging: Elsevier Ltd.*; 2005.
58. Tarantal AF, Hendrickx AG. Characterization of prenatal growth and development in the crab-eating macaque (*Macaca fascicularis*) by ultrasound. *The Anatomical record*. 1988;222(2):177-84.
59. Lindsey HS, Calisher CH, Mathews JH. Serum dilution neutralization test for California group virus identification and serology. *Journal of clinical microbiology*. 1976;4(6):503-10.
60. Rutanen EM, Pekonen F, Karkkainen T. Measurement of insulin-like growth factor binding protein-1 in cervical/vaginal secretions: comparison with the ROM-check Membrane Immunoassay in the diagnosis of ruptured fetal membranes. *Clinica chimica acta; international journal of clinical chemistry*. 1993;214(1):73-81.

61. Doyle L, Young CL, Jang SS, Hillier SL. Normal vaginal aerobic and anaerobic bacterial flora of the rhesus macaque (*Macaca mulatta*). *Journal of medical primatology*. 1991;20(8):409-13.
62. Gribnau AA, Geijsberts LG. Morphogenesis of the brain in staged rhesus monkey embryos. *Advances in anatomy, embryology, and cell biology*. 1985;91:1-69.
63. Carlson JA, Chen KR. Cutaneous vasculitis update: neutrophilic muscular vessel and eosinophilic, granulomatous, and lymphocytic vasculitis syndromes. *The American Journal of dermatopathology*. 2007;29(1):32-43.
64. Romero R, Miranda J, Chaemsaitong P, Chaiworapongsa T, Kusanovic JP, Dong Z, et al. Sterile and microbial-associated intra-amniotic inflammation in preterm prelabor rupture of membranes. *The journal of maternal-fetal & neonatal medicine : the official journal of the European Association of Perinatal Medicine, the Federation of Asia and Oceania Perinatal Societies, the International Society of Perinatal Obstet*. 2015;28(12):1394-409.
65. Aliota MT, Caine EA, Walker EC, Larkin KE, Camacho E, Osorio JE. Characterization of Lethal Zika Virus Infection in AG129 Mice. *PLoS neglected tropical diseases*. 2016;10(4):e0004682.
66. Novy MJ, Duffy L, Axthelm MK, Sadowsky DW, Witkin SS, Gravett MG, et al. *Ureaplasma parvum* or *Mycoplasma hominis* as sole pathogens cause chorioamnionitis, preterm delivery, and fetal pneumonia in rhesus macaques. *Reproductive sciences (Thousand Oaks, Calif)*. 2009;16(1):56-70.
67. Adams Waldorf KM, Rubens CE, Gravett MG. Use of nonhuman primate models to investigate mechanisms of infection-associated preterm birth. *BJOG : an international journal of obstetrics and gynaecology*. 2011;118(2):136-44.
68. Churchill A, Booth A. Genetics of aniridia and anterior segment dysgenesis. *The British journal of ophthalmology*. 1996;80(7):669-73.
69. Reis LM, Semina EV. Genetics of anterior segment dysgenesis disorders. *Current opinion in ophthalmology*. 2011;22(5):314-24.
70. Gregory-Evans CY, Williams MJ, Halford S, Gregory-Evans K. Ocular coloboma: a reassessment in the age of molecular neuroscience. *Journal of medical genetics*. 2004;41(12):881-91.
71. Onwochei BC, Simon JW, Bateman JB, Couture KC, Mir E. Ocular colobomata. *Survey of ophthalmology*. 2000;45(3):175-94.
72. Yanoff MS, J.W. *Ocular Pathology*. 7th ed: Saunders Elsevier; 2015.
73. Lin CC, Tso MO, Vygantas CM. Coloboma of optic nerve associated with serous maculopathy. A clinicopathologic correlative study. *Archives of ophthalmology (Chicago, Ill : 1960)*. 1984;102(11):1651-4.

74. Miner JJ, Sene A, Richner JM, Smith AM, Santeford A, Ban N, et al. Zika Virus Infection in Mice Causes Panuveitis with Shedding of Virus in Tears. *Cell reports*. 2016;16(12):3208-18.

Chapter 3

Embryotoxic impact of Zika virus in a rhesus macaque in vitro implantation model

Publication:

Block LN, Aliota MT, Friedrich TC, Schotzko ML, Mean KD, Wiepz GJ, Golos TG, Schmidt JK. Embryotoxic impact of Zika virus in a rhesus macaque in vitro implantation model. *Biol Reprod.* 2020 Apr 15;102(4):806-816. doi: 10.1093/biolre/ioz236. PMID: 31901091; PMCID: PMC7124964.

3.1 Abstract (Original by LNB; edited by TGG and JKS)

Zika virus infection (ZIKV) is associated with adverse pregnancy outcomes in humans, and infection in the first trimester can lead to miscarriage and stillbirth. Vertical and sexual transmission of ZIKV have been demonstrated, yet the impact of infection during the initial stages of pregnancy remains unexplored. Here we defined the impact of ZIKV on early embryonic and placental development with a rhesus macaque model. During *in vitro* fertilization (IVF), macaque gametes were inoculated with a physiologically relevant dose of $5.48 \log_{10}$ plaque-forming units (PFU) of Zika virus/H.sapiens-tc/PUR/2015/PRVABC59_v3c2. Exposure at fertilization did not alter blastocyst formation rates compared to controls. To determine the impact of ZIKV exposure

at implantation, hatched blastocysts were incubated with $3.26\log_{10}$, $4.26\log_{10}$, or $5.26\log_{10}$ PFU, or not exposed to ZIKV, followed by extended embryo culture for 10 days. ZIKV exposure negatively impacted attachment, growth, and survival in comparison to controls, with exposure to $5.26\log_{10}$ PFU ZIKV resulting in embryonic degeneration by day 2. Embryonic secretion of pregnancy hormones was lower in ZIKV-exposed embryos. Increasing levels of infectious virus were detected in the culture media post-exposure, suggesting that the trophectoderm is susceptible to productive ZIKV infection. These results demonstrate that ZIKV exposure severely impacts the zona-free blastocyst, whereas exposure at the time of fertilization does not hinder blastocyst formation. Overall, early stages of pregnancy may be profoundly sensitive to infection and pregnancy loss, and the negative impact of ZIKV infection on pregnancy outcomes may be underestimated.

3.2 Introduction (Original by LNB; edited by TGG and JKS)

Zika virus (ZIKV) is a human pathogen with human-to-human transmissibility. It was originally isolated from a febrile rhesus macaque in Uganda in 1947 [1]. In the past decade, there have been numerous outbreaks of ZIKV[2], and the most recent outbreak, in Brazil in 2015, suggested congenital ZIKV infection is associated with fetal malformations, including microcephaly as a severe manifestation of disease [3, 4]. Although most infections in adults do not cause significant disease and are often asymptomatic, a ZIKV infection while pregnant can be catastrophic for the fetus, and result in stillbirth and miscarriage [4-6].

Placental defects are noted in many cases of adverse pregnancy outcome [4, 7]. Consistent with these findings, ZIKV has been shown *in vivo* and *in vitro* to infect trophoblast cells, which have specialized niches in the placenta [8-16]. A study by El Costa et. al. found that first-trimester human placental explants and primary trophoblasts were susceptible to infection with a ZIKV isolate obtained during the Brazil outbreak [12]. Conversely, a study by Bayer et. al. reported that term primary human trophoblast cells were resistant to ZIKV [13]. This increased resistance to ZIKV in later stages of development was also observed in nonhuman primate (NHP) studies, where maternal ZIKV infection in the third trimester resulted in less severe outcomes compared to infections in the first trimester [14].

Despite the grave repercussions of ZIKV infection during pregnancy, it is unknown how early in development ZIKV can infect the embryo and early trophoblast lineage. This gap in knowledge is largely due to a limited means of determining human pregnancy loss in the first month of gestation. Bridging this knowledge gap is important as epidemiological and experimental data suggest that an infection earlier in pregnancy may be more likely to result in birth defects or pregnancy loss than an infection in later stages of pregnancy [17, 18]. Sheridan et. al demonstrated that human embryonic stem cells differentiated to form more primitive trophoblast cells were highly susceptible to African ZIKV strains (Nigeria, Senegal and the lab adapted Uganda) [19]. Thus, the earliest placental lineage may have differential susceptibility to infection. This necessitates evaluation of how infection impacts embryonic trophoblasts.

Previous *in vivo* NHP pregnancy studies modeling ZIKV infection in our lab and others have reported similar findings regarding pregnancy outcomes and associated pathologies as those

observed in humans [7, 14, 16, 20, 21]. Both macaques and humans are similar in placental development forming an interstitial implantation site, in which the trophoblast cells invade through the luminal epithelium of the uterus [22]. Thus, the NHP model recapitulates early human trophoblast development and is an essential and appropriate model to study the impact of ZIKV during pregnancy.

Sexual transmission of ZIKV may negatively impact an established pregnancy, but its impact on embryo development and the establishment of pregnancy is unknown. ZIKV RNA (vRNA) has been detected in human semen and cases of sexual transmission have been reported [23-27]. This is a concern as Zika vRNA has been sporadically detected in human semen for up to 370 days after infection [28]. Furthermore, Zika vRNA was detected in 25% of sperm cell fraction samples prepared by washing on a 90% gradient, the method of preparation recommended for HIV-infected men [23]. This may have implications in assisted reproductive technologies (ART), as it is unclear if infectious semen can impact fertilization and embryo development. NHP studies have also observed Zika vRNA shedding in semen and detectable vRNA in male reproductive tract tissues including the testes, epididymis, seminal vesicle, and prostate [29-33]. Hence, the NHP model presents an opportunity to evaluate how sexual transmission of ZIKV can impact the initial stages of embryo development to ensure ARTs, including *in vitro* fertilization (IVF) and intracytoplasmic sperm injection (ICSI), are safe and do not compromise developmental outcomes.

In order to study the direct impact of ZIKV on the earliest trophoblast cells, we implemented an *in vitro* implantation NHP model. Combining this model with IVF allowed us to study the effect of ZIKV on the earliest stages of pregnancy by monitoring implantation stage trophoblast/embryo

outgrowths in a controlled environment, which are difficult to study *in vivo*. Our primary objective for this study was to determine the earliest stage that ZIKV could impact embryo development and the establishment of pregnancy, as well as how infection alters trophoblast function during implantation. Embryo implantation in the uterus is a critical event in establishing pregnancy, as disruption of this process is estimated to account for 60% of pregnancy loss [34]. Based on the adverse pregnancy outcomes from *in-utero* ZIKV exposure, we hypothesized that ZIKV would have a detrimental impact on the development of the implanting embryo and on subsequent trophoblast growth. ARTs, such as IVF, are used to overcome infertility, and the risk of viral infection decreasing success rates would be devastating. The outcomes of this research directly define the impact of ZIKV infection on early embryo development and implantation, and address concerns regarding parental infection and the use of ARTs.

3.3 Materials and Methods (Original by LNB and JKS; edited by TGG)

Rhesus macaque IVF and embryo culture

Rhesus monkeys (*Macaca mulatta*) were from the colony maintained at the Wisconsin National Primate Research Center. All procedures were performed in accordance with the NIH Guide for the Care and Use of Laboratory Animals and under the approval of the University of Wisconsin College of Letters and Sciences and Vice Chancellor Office for Research and Graduate Education Institutional Animal Care and Use Committee. A total of five semen donors and 22 oocyte donors were used for these studies, where oocytes from 9 donors were designated to assess the impact of ZIKV at the time of fertilization, and hatched blastocysts from 13 oocyte donors were evaluated

for the impact of ZIKV during the peri-implantation stage of development. Note that oocyte donors could undergo up to three ovarian stimulation events for oocyte collection.

Rhesus IVF embryos were generated as previously described [35-38] and methods are briefly outlined here. Female oocyte donors underwent ovarian hyperstimulation by administration of 30 international units (IU) recombinant human follicle stimulating hormone (FSH; follitropin beta, Merck Sharp & Dohme Corp, Whitehouse Station, NJ, USA), twice daily for eight to nine days followed by one injection of 1000 IU recombinant human choriogonadotropin (hCG; Ovitrelle, Merck Serono Ltd, Middlesex, UK) the next day. Oocytes were retrieved by laparoscopic aspiration between 30-33 hours post hCG injection. Those that had resumed meiosis and were in metaphase I were placed into maturation medium, consisting of CMRL (Thermo Fisher Scientific, Cat #11530037, Waltham, MA, USA) medium supplemented with 0.5 mM sodium pyruvate (Sigma Aldrich, Cat #2256, St. Louis, MO, USA), 2 mM Alanine-glutamine (Sigma, #G8541) and 20% fetal bovine serum (FBS; Peak Serum, Cat #PS-FB1, Wellington, CO, USA). MI oocytes were evaluated for progression to metaphase II (MII) at 36 h post hCG and those that had extruded a polar body were transferred to fertilization medium composed of IVF-TL medium (Caisson Laboratories Inc, Smithfield, UT) supplemented with 0.5 mM sodium pyruvate, 2 mM Alanine-glutamine, and 0.1 mg/ml Polyvinyl alcohol (PVA; Sigma, Cat #P8136). Oocytes that were MII at the time of recovery were placed directly into fertilization medium.

Semen was collected from male rhesus macaques by electroejaculation [39]. The coagulum was removed 30 min post-collection and sperm were washed twice in HEPES-TL (Caisson

Laboratories, Cat #IVL01) supplemented with 0.1 mM sodium pyruvate and 3 mg/ml bovine serum albumin (Sigma, Cat #A8806). A total of 40 million sperm were added to 2 ml of capacitation medium consisting of IVF-TL (Caisson Laboratories, Cat #IVL02) supplemented with 0.1 mM sodium pyruvate and 0.1 mg/ml PVA. To facilitate capacitation, caffeine (Sigma, Cat #C0750) and dibutyryl-cAMP (Sigma, Cat #D0627) were added to the capacitation medium 30 minutes prior to fertilization at a final concentration of 1 mM and 0.5 mM, respectively [39]. At the time of fertilization, 2.5 μ l sperm, 2 μ l 100 mM caffeine, and 2 μ l of 50 mM dibutyryl-cAMP were added to each fertilization drop (93.5 μ l drops for gametes not exposed to ZIKV and 81 μ l drops for gametes exposed to ZIKV). The difference in drop size is to account for the amount of ZIKV added.

Gametes were co-incubated for ~16 hours and individual presumptive zygotes were transferred into microwells of CultureCoin Miri-TL® dishes (Esco Medical, Denmark). A CultureCoin Miri-TL® dish contains 14 microwells that contain 25 μ l of media overlaid with 3 ml Ovoil (Vitrolife, Cat #10029, Englewood, CO, USA). Embryos were cultured in G-TL medium (Vitrolife, Cat #10145) supplemented with 5% FBS for eight to eleven days corresponding to the hatched blastocyst stage.

Inoculation of gametes and embryos with ZIKV

Zika virus/H.sapiens-tc/PUR/2015/PRVABC59_v3c2 (PRVABC59) (GenBank: KU501215) was originally isolated from a traveler to Puerto Rico and passaged three times on Vero cells (American Type Culture Collection (ATCC): CCL-81), was obtained from Brandy Russell (CDC, Ft. Collins, CO). Virus stocks were prepared by inoculation onto a confluent monolayer of C6/36 cells (*Aedes*

albopictus larval cells; ATCC: CCL-1660) with two rounds of amplification and confirmed to be identical to the reference sequence at the consensus level. This isolate was chosen as it would complement other *in vivo* studies that utilized ZIKV-PRVABC59 and observed adverse pregnancy outcomes [7, 40].

To determine if ZIKV could impact oocyte fertilization, gametes were inoculated with $5.48 \log_{10}$ PFU (16 μ l at $7.26 \log_{10}$ PFU/ml added to 81 μ l fertilization medium) ZIKV-PRVABC59 at fertilization. To determine if ZIKV could impact trophoblast function and embryo implantation, blastocyst stage embryos were plated on Matrigel (BD Biosciences, Cat # 354253, Bedford, MA) [36] within 24 hours of hatching, which occurred on ~day 8-10 of development. Embryos were then either exposed to ZIKV or were cultured as non-exposed controls. The day the blastocysts were plated on Matrigel, they were incubated with either $5.26 \log_{10}$ (high), $4.26 \log_{10}$ (medium), or $3.26 \log_{10}$ (low) PFU ZIKV for five hours (Figure 1) or left as uninfected controls. Co-incubation of embryo and virus was accomplished by addition of 10 μ l of ZIKV (or serially diluted ZIKV dependent on dose) to 90 μ l culture medium. Mock infected embryos were exposed to C6/36 cell conditioned medium for five hours the day they were plated on Matrigel to verify that the conditioned medium in which the ZIKV stock was produced was not embryotoxic.

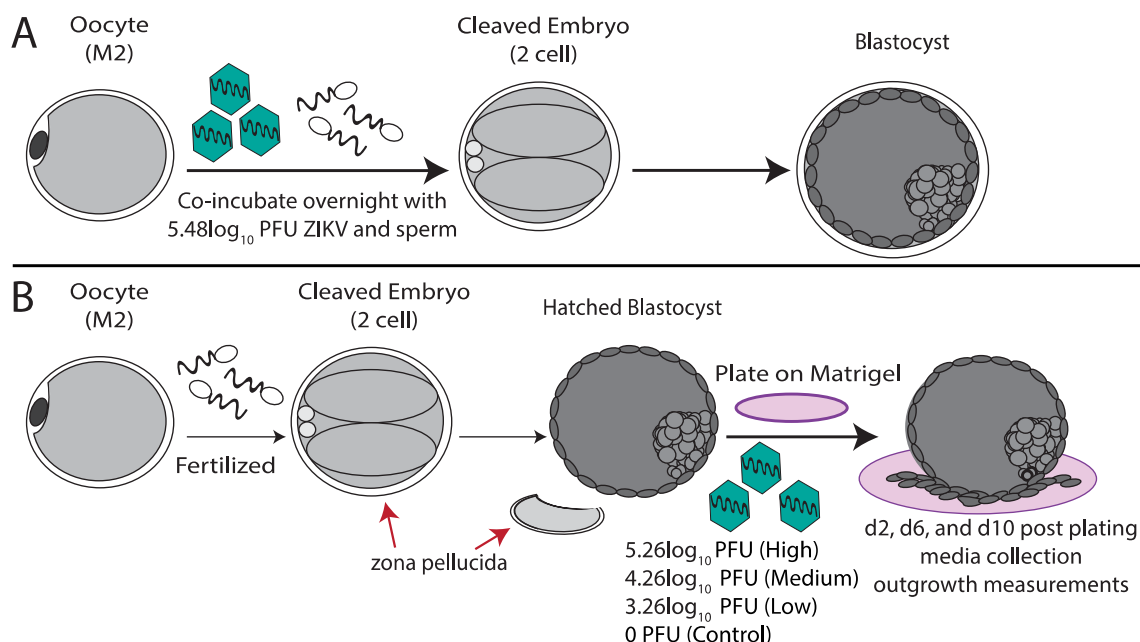


Figure 3.1. Schematic depiction of ZIKV exposure to gametes (A) and hatched blastocysts (B). (A) Rhesus gametes were co-incubated with ZIKV at the time of fertilization, followed by evaluation of embryo cleavage and blastocyst formation rates. (B) In vitro fertilized hatched blastocysts were plated on Matrigel and immediately exposed to one of three doses of ZIKV for five hours or cultured as unexposed controls. On day (d) 2, d6 and d10 post-plating, media were collected, embryo outgrowths were imaged, and area and diameter were measured. Figure made by LNB.

Extended embryo culture utilizing an *in vitro* peri-implantation model.

Embryos were cultured as previously described [38] with modifications. Hatched blastocyst stage embryos were plated on Matrigel (Corning, Cat # 354230, Corning, NY, USA) with 200 μ l of Buffalo Rat Liver (BRL) conditioned medium, which is equal parts EMEM (Quality Biologics, Cat #112018, Gaithersburg, MD, USA) and CMRL (Thermo Fisher Scientific, Cat #11530037) with 5% FBS. The medium was conditioned for 24-hours, ultracentrifuged (SW41 rotor at 130,000 \times g average) overnight to remove large particles and extracellular vesicles, sterile-filtered, and

frozen back. Media were changed on days 2 and 6 post-plating (Figure 1B). Prior to media exchange, embryo outgrowths were imaged using a Nikon Eclipse TE300. Outgrowth area was calculated using 4x images and ImageJ using a ratio of one millimeter (mm) equal to 620 pixels. Embryos that grew up the side of the well were excluded from the analysis (one control, two low-dose, and two medium-dose). Of note, four control embryos were removed from initial experiments to serve as age matched controls for transcriptome analysis (not shown) and no data from these four controls is present in the dataset.

Hormone secretion

Progesterone secretion was analyzed using an enzyme immunoassay (EIA) (Cat #582601, Cayman, Ann Arbor, Michigan, USA). Samples were diluted in enzyme-linked immunosorbent assay (ELISA) buffer, run in duplicate, the manufacturer's protocol was followed as directed, and the plate was read at 410 nm. The minimum level of detection was 0.01 ng/ml (Figure 3A). To control for baseline quantities of hormones in the conditioned media, blank media samples conditioned by BRL cells but not conditioned by an embryo, were collected. For the blank samples that could reliably be quantified, the amount of progesterone detected was 0.063 ng/ml \pm 0.016.

Monkey CG (mCG) secretion was analyzed by radioimmunoassay as previously published[41]. Samples were diluted in EMEM and run in duplicate. The amount of mCG detected in blank media samples was 13.202 ng/ml \pm 6.977. Interassay variation (CV) was 6.3%. For statistical purposes, samples that fell below the limit of detection (0.1 ng/ml) were assigned that value.

Luminex assay for cytokine, chemokine and growth factor secretion by embryo outgrowths

To analyze the secretion of cytokines, chemokines, and growth factors an NHP 37-plex Procarta Luminex assay (Thermo Fisher Scientific, Cat # EPX370-40045-901, Waltham, MA, USA) was used and the manufacturer's instructions were followed. Samples were run in duplicate on a Bioplex 200 (BioRad, Cat #171000201, Hercules, CA, USA) and analyzed with the Bioplex Manager Software. The lower level of detection was obtained for each analyte based on the manufacturer's quantifications (Figure 3B-H).

Infectious virus detected by plaque assay

Plaque assays were used to assess embryo susceptibility to ZIKV by determining if infectious virus was produced in culture [7]. Three embryos were exposed to the medium dose of ZIKV for 5-hours. Due to the different collection timepoints, the media used for this aspect of the study were not used for any other analysis. For each media change, all media were removed and fresh media were added. The quantity of virus detected was the total amount of new virus produced between media collections which occurred at 12-hour, 1-day, 2-day, 4-day, 6-day, and 10-days post-plating.

Statistical analysis

A Fisher's exact test with a Bonferroni correction was used to determine significance ($p < 0.05$) for the ZIKV exposure at the time of fertilization dataset, as well as attachment and survival. For the growth and secretion data, analysis was completed using GraphPad Prism 8.0 (GraphPad Software) and a nonparametric Kruskal-Wallis test with Dunn's corrections applied ($p < 0.05$). All graphs show the mean +/- standard error of the mean (SEM).

3.4 Results (Original by LNB and JKS; edited by TGG)

ZIKV exposure at the time of fertilization

Since ZIKV is present in semen and can be sexually transmitted, we exposed gametes to ZIKV at the time of fertilization to determine if exposure impacted *in vitro* embryo development. A total of 102 MII oocytes were obtained from nine ovarian stimulation events, in which 57 oocytes were inoculated with ZIKV and cultured in parallel to 45 control oocytes. Embryo development in terms of cleavage rate was significantly higher in ZIKV exposed versus control embryos as shown in Table 1 ($p < 0.01$). Of note, the control cleavage rate was lower in experimental replicates towards the end of the IVF season. However, no significant difference for blastocyst rate was observed between the ZIKV exposed gametes and control ($p < 0.81$). These results suggest that ZIKV exposure at the time of fertilization does not impact preimplantation embryo developmental rates.

Embryo group	# oocyte retrievals	#M2	# Cleaved	Cleavage Rate	# Blastocysts	Blastocyst Rate
Controls	9	45	26	57.78%	8	30.77%
ZIKV	9	57	47	82.46%	14	29.79%
p-value				$p < 0.01$		0.81

Table 3.1. In vitro embryo development rates following ZIKV exposure at fertilization. *The number of MII oocytes for each group that subsequently underwent cleavage and blastocyst formation. Cleavage rate was determined by dividing the total number of embryos by the number of mature oocytes. Blastocyst rate was determined by dividing the total number of embryos that reached the blastocyst stage by those that cleaved. For the nine oocyte retrieval replicates, the ratio of MII oocytes for control/ZIKV exposed are as follows: 2/7, 5/8, 11/5, 6/11, 5/6, 4/5, 5/7, 3/4, 4/4. Table made by LNB.*

ZIKV exposure decreased peri-implantation embryo survival, attachment, and growth.

To determine the impact of ZIKV on development in the peri-implantation phase, we exposed 32 hatched blastocysts to ZIKV and cultured 18 embryos as unexposed controls. At this stage of development the embryo has shed its zona pellucida, thus leaving the trophoctoderm in direct contact with its environment. Embryo survival was evaluated based on the following parameters: attachment to the Matrigel, trophoblast outgrowth dissociation, and overall appearance, e.g. dark or grainy appearance indicating cellular degeneration. 83% of control trophoblast outgrowths survived until day 10 post-plating on Matrigel while only 60%, 33%, and 0% of the low, medium, and high-dose survived, respectively (Table 2). There was a significant difference between control and high-dose embryo survival on days 2, 6, and 10 ($p < 0.05$) and between low-dose and high-dose on day 2 as demonstrated in Table 2 ($p < 0.05$). The difference in survival between control and medium-dose embryos (83% and 33%, respectively) approached significance on day 10 ($p = 0.052$). Together, these results suggest a dose-related effect of ZIKV exposure on embryo survival.

Table 3.2. The percent of embryos attached to the Matrigel and alive on each day post-plating is shown.

Embryo group	d2	d6	d10
% Attached			
Control	50	78 ^a	93
Low	70	70 ^{ab}	60
Medium	42	42 ^{ab}	33
High	0	0 ^b	0
% Survival			
Control	95 ^{ac}	83 ^a	83 ^{a*}
Low	100 ^{ac}	60 ^{ab}	60 ^{ab}
Medium	83 ^{abc}	50 ^{ab}	33 ^{ab}
High	20 ^b	0 ^b	0 ^{b*}

A Fisher's exact test with a Bonferroni correction on the number of embryos attached or alive was calculated to determine significance. Values that do not share superscripts are statistically different at $P < 0.05$ and a superscript asterisk indicates $P < 0.001$. Table made by LNB.

Embryo outgrowths were imaged on days 2, 6, and 10 post-plating to measure embryo growth and representative images are shown in Figure 2A. Supplemental Figure 1 shows a representative image of primitive syncytiotrophoblast and extravillous trophoblast cells. A decrease in outgrowth diameter was observed for embryos exposed to $5.26\log_{10}$ PFU ZIKV (high-dose) on day 2. Likewise, embryos that were exposed to $4.26\log_{10}$ PFU ZIKV (medium-dose) had significantly reduced diameter ($p<0.001$) and area ($p<0.05$) in comparison to control outgrowths at day 6 post-plating. The trend towards decreased size for embryos exposed to ZIKV continued through day 10 post-plating.

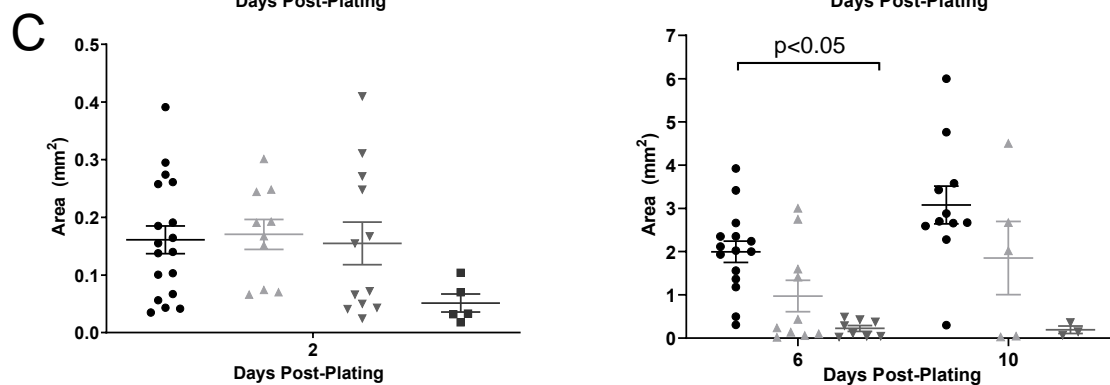
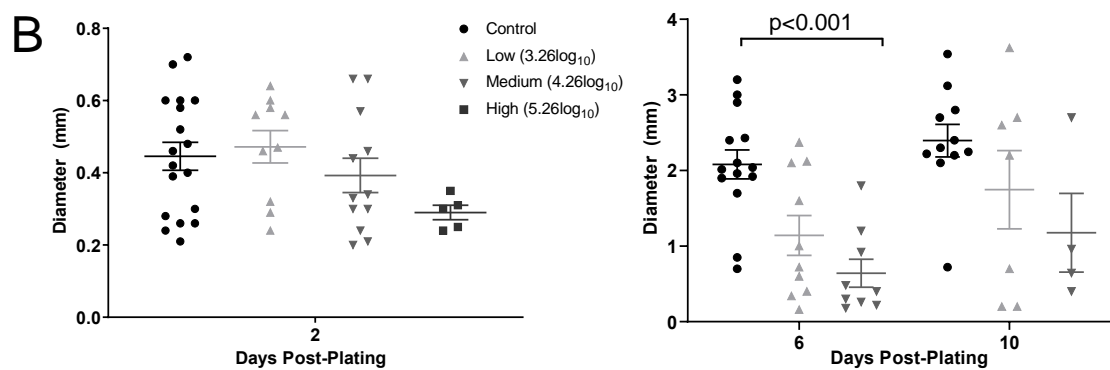
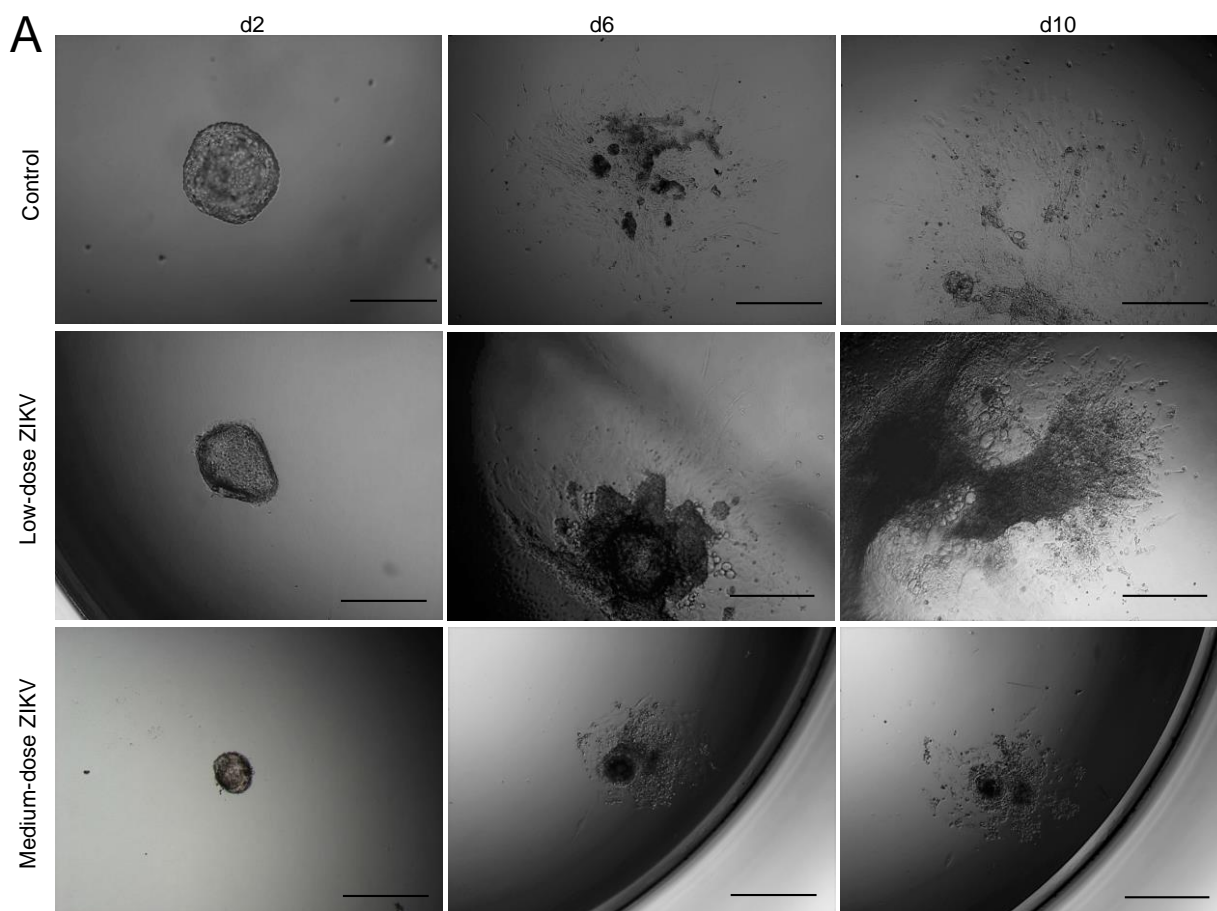
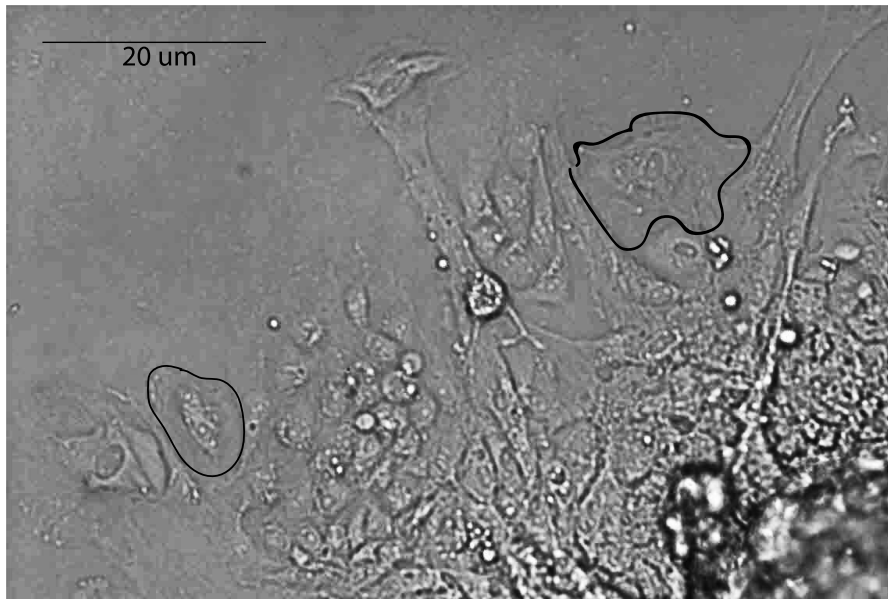


Figure 3.2. Peri-implantation in vitro embryo outgrowths exposed to ZIKV reduces growth. (A) Representative images of day 2, 6, and 10 post-plating of a control, a low-dose exposed, and a medium-dose exposed trophoblast outgrowth (scale bars = 50 μ m). (B) Trophoblast outgrowth diameter. (C) Outgrowth area. Blastocyst experimental groups are denoted as follows: controls = black circles, low-dose ZIKV = light gray triangles, medium-dose = medium gray upside-down triangles, and high-dose = dark gray squares. Figure made by LNB.



Supplemental Figure 3.1. Trophoblast cell morphology. A) Multinucleated cells from a trophoblast outgrowth are circled. B) Arrows point to extravillous trophoblast-like cells from a trophoblast outgrowth. Scale bars = 20 μ m. Figure made by LNB and JKS.

Establishment of pregnancy requires attachment of the embryo to the uterine epithelium. In this study, 50% of control embryos attached to the Matrigel culture surface by day 2 post-plating, and 83% were attached by day 10 (Table 2). Decreased attachment to the Matrigel was noted with exposure to increasing doses of ZIKV. There was a significant ($p < 0.05$) decrease in attachment for embryos exposed to the high dose of ZIKV compared to controls on days 6 and 10 post-plating. No attachment for high-dose blastocysts reflects the degeneration of these embryos by day 2. The difference in attachment between medium-dose and control blastocysts (33% and 93%, respectively) approached significance on day 10. By day 2, 70% of the blastocysts exposed to low-dose ZIKV were attached and there was a slight decrease in attachment over time.

Trophoblast function assessed by secretion of pregnancy-related hormones, cytokines, chemokines and growth factors.

To determine how ZIKV exposure impacted trophoblast function, we analyzed the media for the pregnancy-associated hormones, progesterone and mCG, that are produced by trophoblasts. Embryo conditioned and non-conditioned media were collected on days 2, 6, and 10 post-plating to quantify the amount of hormone secreted relative to the area of the embryo outgrowth (Figure 3). All high-dose exposed blastocysts had degenerated by day 2, hence no data could be collected for this group. No significant differences were observed between ZIKV and control embryos, although there was a trend towards decreased progesterone and mCG secretion on day 6 for ZIKV exposed embryos. If progesterone and mCG secretion were not normalized to the area of the trophoblast outgrowth, hormone secretion decreased between control and ZIKV exposed embryos

with a significant difference between controls and medium-dose day 6 post-plating ($p < 0.01$; Supplemental Figure 2).

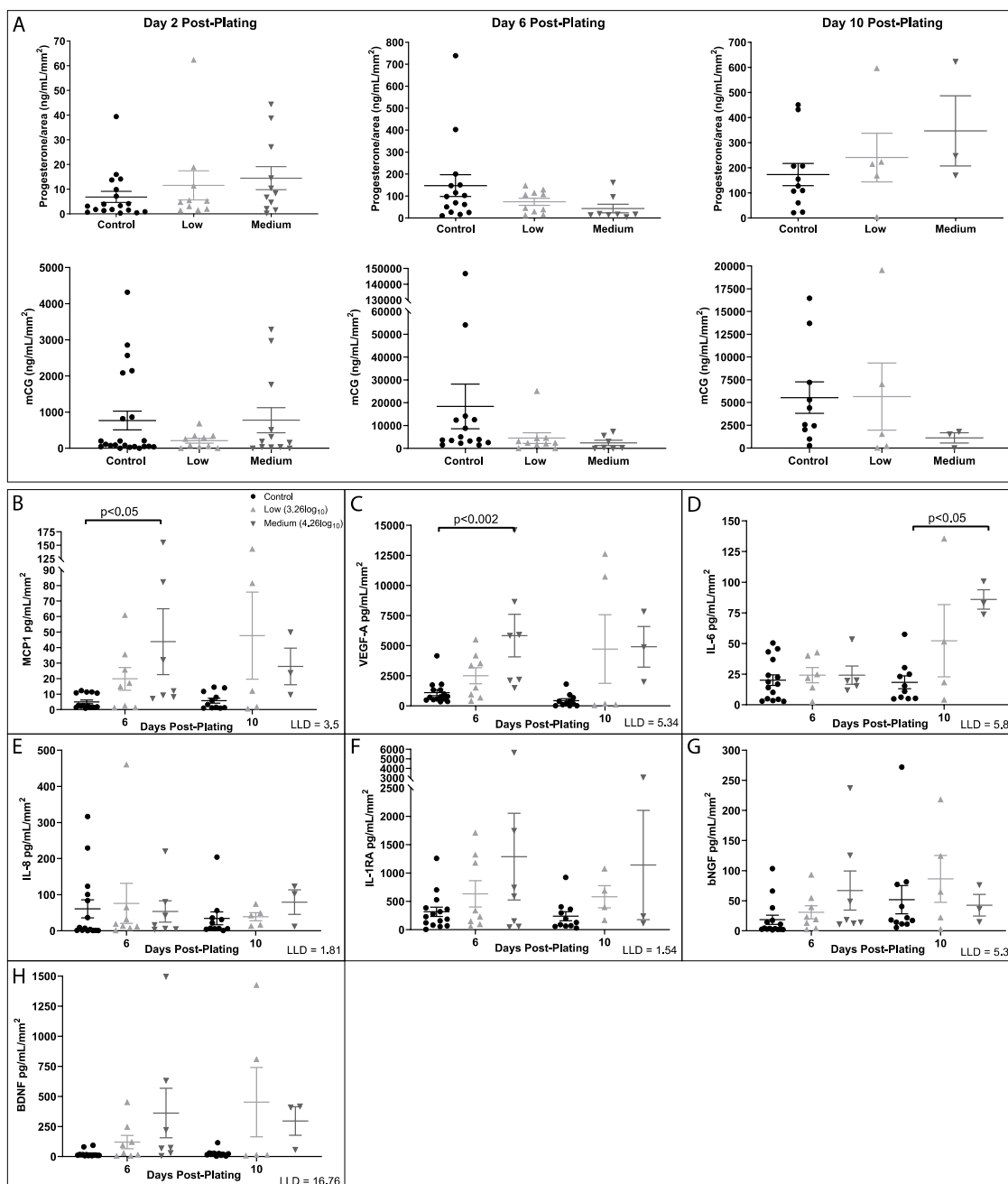
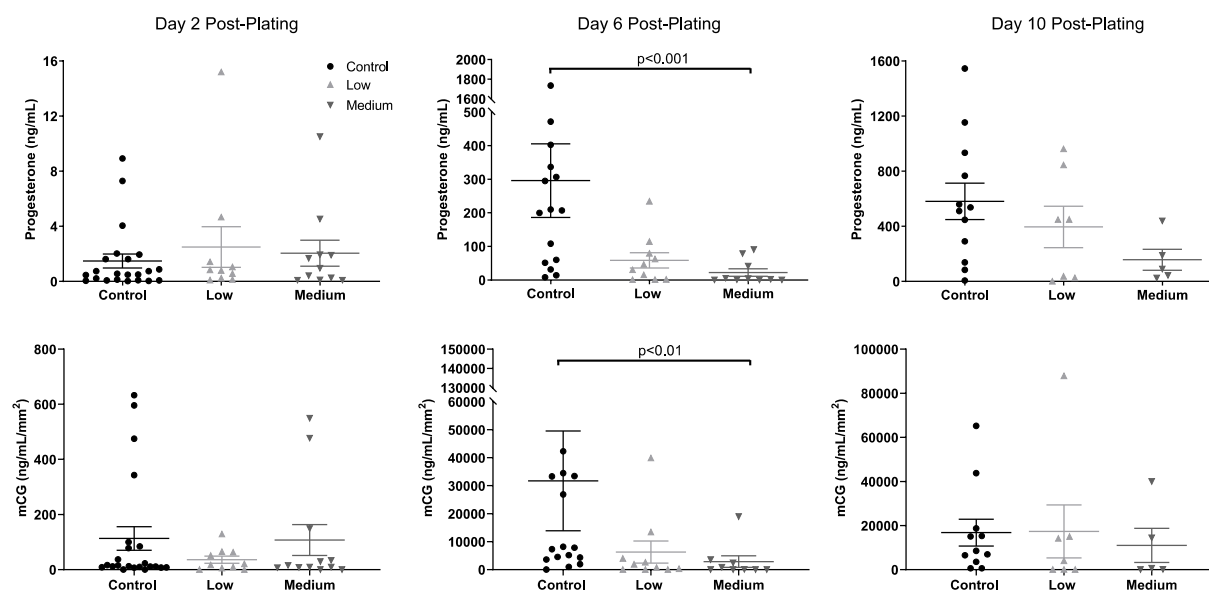


Figure 3.3. Secretion of hormones and immunomodulators by embryo outgrowths. (A) Progesterone and mCG secretions normalized for outgrowth area (pg/mL/mm²) on days 2, 6, and 10 post-plating are shown as individual graphs as the y-axis is changed for ease of reading. Trophoblast cytokine and growth

factor secretions normalized for outgrowth area (pg/mL/mm^2) and are depicted over days post-plating. (B) MCP1, (C) VEGF-A, (D) IL-6 (E) IL-8, (F) IL-1RA (G) bNGF (H) BDNF. The lower limit of detection (LLD) in picograms (pg) is depicted in the corner of each graph. Fisher's exact test with Bonferroni's correction was used to determine significance, which is indicated directly on the graphs. The following analytes were not detected in any sample: IL-2, IL-17A, IL-23, IP-10, GM-CSF, IFN-gamma, IL-1beta, IL-10, IL-12p70, IL-13, ITAC, MIG, MIP-1alpha, IL-7, and VEGF-D. The following analytes were detected in 5 samples or less: FGF-2, Eotaxin, IL-4, IL-18, IL-5, TNF-alpha, BLC, MIP-1beta, SDF-1alpha, CD-40ligand, G-CSF, IFN-alpha, IL-15, PDGF-BB, and SCF. Figure made by LNB.



Supplemental Figure 3.2. Secretion of progesterone and mCG by embryo outgrowths. Hormone secretion is depicted as ng/ml over days post-plating. Embryo outgrowth groups are denoted as follows: controls = black circles, low-dose ZIKV= light gray triangles, and medium-dose = medium gray upside-down triangles. Significance was tested with Kruskal-Wallis test with Dunn's Correction and is depicted on the graph. Figure made by LNB.

To assess if ZIKV triggers an embryonic immune response, a Luminex assay was performed to measure secretion of cytokines, chemokines, and growth factors. The amount of analyte secreted was normalized to the area of the outgrowth. Seven cytokines and growth factors were consistently detected in the conditioned media: monocyte chemoattractant protein 1 (MCP1), brain-derived

neurotrophic factor (BDNF), interleukin-8 (IL-8), interleukin-6 (IL-6), interleukin 1 receptor antagonist (IL-1RA), vascular endothelial growth factor A (VEGF-A), and beta nerve growth factor (bNGF) (Figure 3). There was a significant increase in MCP1, VEGF-A, and IL-6 secretion by ZIKV-exposed embryos compared to controls on day 6 post-plating ($p<0.05$, $p<0.002$, and $p<0.05$, respectively). There was also a trend towards increased IL-8 and IL-6 secretion on day 10, and increased MCP1, BDNF, VEGF-A, IL-1RA, and bNGF secretion on days 6 and 10 between controls and ZIKV.

Verification of embryonic ZIKV infection

To determine if the embryo outgrowths were productively infected by ZIKV, embryo-conditioned media were tested for infectious virus via plaque assay. The embryos were exposed to ZIKV immediately after being plated on Matrigel. The titer of the inoculum for the three embryos was $5.1 \log_{10}$ PFU ZIKV on average (data not shown). At each time point (12-hours and 1, 2, 4, 6, and 10 days post-plating/post ZIKV exposure), all media were collected, and new media were added. Minimal virus was produced within the first 24 hours post ZIKV exposure but enhanced viral production occurred 2 and 4-days post-plating (3.29 and $3.92 \log_{10}$ PFU ZIKV on average, respectively) (Figure 4). ZIKV titers dropped off day 6 post-plating and remained low day 10 post-plating.

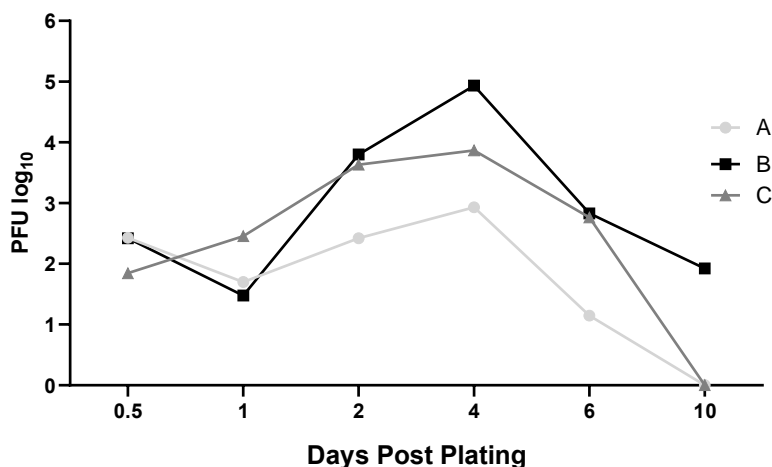


Figure 3.4. Infectious virus was detected in culture media following ZIKV exposure. Three embryos (A, B, and C) were exposed to medium-dose of ZIKV for 5 hours. All media was removed from the well and collected at 12-hours and 1, 2, 4, 6, and 10-days post plating/days post ZIKV exposure. The graph depicts the amount of virus detected (log₁₀ PFU) over days post-plating. Figure made by LNB.

3.5 Discussion (Original by LNB; edited by TGG and JKS)

Embryo implantation is essential for the establishment of pregnancy and is difficult to directly study in humans, therefore the present study utilized rhesus macaque IVF-produced embryos an extended culture system to evaluate the impact of ZIKV exposure around the time of implantation. ZIKV-exposed oocytes had a higher cleavage rate than controls but an equivalent blastocyst rate, which suggests that ZIKV exposure at fertilization does not hinder preimplantation development rates. However, ZIKV exposure at the time of implantation is embryotoxic and impacts trophoblast function. ZIKV exposure in the zona-free stages of development severely impacted survival, growth, and attachment in a dose-related manner. Alterations in embryo secretions including mCG, MCP1, VEGF-A, and IL-6 support the hypothesis that ZIKV can impact the implanting blastocyst

and impede trophoblast function as well as alter immune-related signaling by the trophoblasts. In addition, plaque assay data support the embryos were susceptible to productive ZIKV infection. These findings are supported by a recent study which demonstrated that the trophectoderm of both human and mouse embryos is susceptible to ZIKV infection [42]. Collectively, the observations that ZIKV impacts NHP, mouse, and human embryos should caution couples trying to naturally conceive or utilize ARTs for conception as the abundance of virus present in the semen of infected males may determine pregnancy success or failure.

Implantation encompasses the initial attachment and growth of the embryo as it invades into the endometrium. A decrease in the growth of embryo outgrowths was observed in response to ZIKV exposure, indicating that the trophoblast cells are either not proliferating or are undergoing cell death. High-dose ZIKV exposure was rapidly embryotoxic, which suggests cell death was the more likely scenario. However, it remains unclear whether exposure to low and medium-doses of ZIKV were mainly impacting cellular proliferation or survival, both of which could be detrimental to the events of implantation. The negative impact of ZIKV infection near the time of implantation was recently demonstrated in an *in vivo* mouse pregnancy model. Tan et al. [42] reported ~50-70% reduction in pregnancy rates in a mouse model following subcutaneous ZIKV inoculation during the preimplantation stage of development at E2.5 and E3.5, whereas inoculation at the E4.5, during the peri-implantation stage, reduced the pregnancy rate by ~11%. Mating of male mice infected with ZIKV to wild-type females resulted in reduced pregnancy rates and fewer viable fetuses, although, sperm counts were also reduced [43]. Similarly, fetal demise was observed at day 10 and 12 post-mating in pregnancies where the virus was sexually transmitted to the female by mating

with infected males 7 days post-inoculation [44]. These studies demonstrate that, in the presence of ZIKV, embryo survival is impeded near the time of implantation.

To better understand how ZIKV impacts trophoblast function, we measured the secretion of two trophoblast-secreted pregnancy hormones and several immune modulators. Embryos exposed to ZIKV had altered hormone secretion, which could impact the establishment of a pregnancy. Progesterone is a marker of trophoblast differentiation and important for maintaining pregnancy. Embryos exposed to ZIKV had decreased progesterone secretion compared to controls on day 6. However, on day 10, there was an increase in the amount of progesterone secreted. CG promotes trophoblast differentiation [35], cytotrophoblast growth [45], and the establishment of the pregnancy [46, 47], and decreased CG could impact the maintenance of the pregnancy. Based on morphology, the presence of multinucleated cells and the detection of mCG suggests syncytiotrophoblast are present in our model [38]. The decrease in mCG secretion by trophoblast outgrowths exposed to ZIKV suggests trophoblast differentiation and syncytiotrophoblast formation are impaired, an outcome that would be consistent with increased risk of early pregnancy loss.

Cytokines and growth factors are important signaling molecules between the blastocyst and uterus during implantation [48]. VEGF-A is an important growth factor during implantation as it promotes vascular remodeling of the maternal spiral arteries, while insufficient levels can lead to preeclampsia [49]. MCP1 is a mediator of angiogenesis, vascular remodeling, and plays a role in

inflammation [50]. Flavivirus infection during pregnancy has been documented, and in one dengue virus-infected pregnancy that resulted in stillbirth, the placenta was inflamed, hemorrhagic, and necrotic and had increased levels of MCP1 and VEGF compared to control tissues [51]. This *in vivo* data is consistent with our observation that ZIKV exposure resulted in increased MCP1 and VEGF-A secretion. BDNF is involved in trophoblast growth and proliferation of the trophoctoderm [52], and increased BDNF secretion was observed by embryos exposed to ZIKV, an observation which seems contrary to the decreased trophoblast outgrowth size of embryos exposed to ZIKV. Nonetheless, these cytokines and growth factors play important roles in trophoblast function, and their altered secretion supports the concept that ZIKV exposure can lead to aberrant placental development and function.

The plaque assay data demonstrated that the blastocysts were susceptible to ZIKV. In addition, these three embryos appeared dead around day 4 post-plating, which aligns with decreased ZIKV production detected days-6 and 10 post-plating, potentially due to a lack of live cells to produce virus. Several blastocysts were exposed to C6/36 conditioned medium to verify that C6/36 media itself is not embryonic lethal. These five embryos were exposed to the same duration and quantity of inoculating medium as the high-dose ZIKV embryos. Although the exact pathways and receptor mediating infection remain unclear, numerous *in vitro* and *in vivo* studies indicate ZIKV can infect cells of the placenta [4, 9, 13, 53]. The extent of trophoblast susceptibility may be variable throughout gestation [4, 53] and dependent upon the ZIKV strain [15, 19, 31].

Human and NHP studies show that first-trimester placentas are more vulnerable to pathogenic outcomes from a ZIKV infection [4, 40, 54]. Sheridan et. al. evaluated primitive (i.e., embryonic stem cell-derived) trophoblast cell susceptibility and their conclusions further support our findings that the trophoblast cells present at the time of implantation are susceptible to ZIKV [19]. In another study, exposure of first trimester placental explants to ZIKV showed that various placental cell types were susceptible to infection, and that infection of proliferating cytotrophoblasts resulted in cellular arrest [11]. This supports the current study's finding that ZIKV exposure resulted in decreased trophoblast size and survival.

ZIKV has been detected in the semen of infected men [23] and NHPs [30, 33, 55]. The highest quantities of ZIKV detected were $8.5\log_{10}$ [24], $8.6\log_{10}$ [27], and $7.5\log_{10}$ [26] copies/mL of semen. PRVABC59, the isolate used in these studies, has been shown to infect human male reproductive tract cells *in vitro* [28], which is relevant for this study in regards to ARTs and sexual transmission. ZIKV vRNA has been detected in both the seminal plasma and sperm cell fractions of human and NHPs isolated using a sperm wash method recommended for HIV-infected men [23, 55], which implies that sperm wash preparations prior to IVF may not completely remove ZIKV. Moreover, Mansuy et al. [56] detected ZIKV within the head of a human spermatozoon by immunostaining against ZIKV. It is uncertain whether transmission outcomes may differ when ZIKV is present and delivered to the oocyte as cargo within the sperm head or when bound to the exterior surface.

While sexual transmission of ZIKV is known to occur [26, 28, 57, 58], its impact on the female reproductive tract, oocytes, and embryos remains unclear. Vaginal/endocervical swabs from non-pregnant humans were positive for ZIKV by qRT-PCR [59-62]. Comparatively, ZIKV infection during pregnancy in the mouse results in higher viral titers in female reproductive tract tissues than infection during the non-pregnant state [44, 63]. However, uterine viral loads in the non-pregnant state are detectable following sexual transmission [63] or intravaginal inoculation [44]. *In vitro* studies have shown that ZIKV can infect human endometrial stromal cells (HESC) and decidualized HESC [64]. In a clinical study of women undergoing oocyte vitrification cycles, no ZIKV was detected in 13 patient endometrial biopsies where five of the patients presented with positive vaginal vRNA at 19 days, 8, 14, 17 or 29 weeks prior to the endometrial biopsy [62]. It is plausible that ZIKV infection may have been cleared by endometrial cells at the time of biopsy collection, and biopsy collection closer to the time of infection, whether vector-borne or sexual transmission, may be more informative. Mouse and NHP models of ZIKV infection in the non-pregnant state have demonstrated that intravaginal and subcutaneous inoculations result in positive ZIKV detection in female reproductive tract tissues as well as vaginal washes/swabs [20, 30, 44, 63, 65, 66] which supports potential embryo exposure to ZIKV in the female reproductive tract.

3.6 Conclusions

Following the ZIKV outbreak in Brazil in 2016, a significant decline in pregnancy rates was observed, which Castro, et. al. hypothesized to be due to postponement and selected termination of pregnancy [67]. In the present study, ZIKV exposure at the time of *in vitro* implantation resulted in decreased embryo survival, attachment and growth, and altered the quantity of secreted products compared to controls. We speculate that the decline in pregnancy rates immediately following the

ZIKV epidemic may in part be due to a decline in the successful establishment of pregnancies, via ZIKV impeding embryo implantation, sexual transmission of ZIKV, or potentially infectious follicular fluid, oocytes, or female reproductive tract tissues. However, further *in vivo* research into the impact of ZIKV infection on embryo implantation is required to elucidate how ZIKV infection may have impacted the pregnancy rates during the Brazil outbreak. The present study shows ZIKV can infect embryos and impact the earliest trophoblast cell function, and therefore suggests that ZIKV exposure could impact pregnancy sooner than previously demonstrated.

3.7 References

1. Dick GW, Kitchen SF, Haddow AJ. Zika virus. I. Isolations and serological specificity. *Trans R Soc Trop Med Hyg* 1952; 46:509-520.
2. Campos GS, Bandeira AC, Sardi SI. Zika Virus Outbreak, Bahia, Brazil. *Emerg Infect Dis* 2015; 21:1885-1886.
3. Schuler-Faccini L, Ribeiro EM, Feitosa IM, Horovitz DD, Cavalcanti DP, Pessoa A, Doriqui MJ, Neri JI, Neto JM, Wanderley HY, Cernach M, El-Husny AS, et al. Possible Association Between Zika Virus Infection and Microcephaly - Brazil, 2015. *MMWR Morb Mortal Wkly Rep* 2016; 65:59-62.
4. Bhatnagar J, Rabeneck DB, Martines RB, Reagan-Steiner S, Ermias Y, Estetter LB, Suzuki T, Ritter J, Keating MK, Hale G, Gary J, Muehlenbachs A, et al. Zika Virus RNA Replication and Persistence in Brain and Placental Tissue. *Emerg Infect Dis* 2017; 23:405-414.
5. Moore CA, Staples JE, Dobyns WB, Pessoa A, Ventura CV, Fonseca EB, Ribeiro EM, Ventura LO, Neto NN, Arena JF, Rasmussen SA. Characterizing the Pattern of Anomalies in Congenital Zika Syndrome for Pediatric Clinicians. *JAMA Pediatr* 2017; 171:288-295.
6. Agrawal R, Oo HH, Balne PK, Ng L, Tong L, Leo YS. Zika Virus and the Eye. *Ocul Immunol Inflamm* 2018; 26:654-659.
7. Mohr EL, Block LN, Newman CM, Stewart LM, Koenig M, Semler M, Breitbach ME, Teixeira LBC, Zeng X, Weiler AM, Barry GL, Thoong TH, et al. Ocular and

- uteroplacental pathology in a macaque pregnancy with congenital Zika virus infection. *PLoS One* 2018; 13:e0190617.
8. Martines RB, Bhatnagar J, Keating MK, Silva-Flannery L, Muehlenbachs A, Gary J, Goldsmith C, Hale G, Ritter J, Rollin D, Shieh WJ, Luz KG, et al. Notes from the Field: Evidence of Zika Virus Infection in Brain and Placental Tissues from Two Congenitally Infected Newborns and Two Fetal Losses--Brazil, 2015. *MMWR Morb Mortal Wkly Rep* 2016; 65:159-160.
 9. Aagaard KM, Lahon A, Suter MA, Arya RP, Seferovic MD, Vogt MB, Hu M, Stossi F, Mancini MA, Harris RA, Kahr M, Eppes C, et al. Primary Human Placental Trophoblasts are Permissive for Zika Virus (ZIKV) Replication. *Sci Rep* 2017; 7:41389.
 10. Adams Waldorf KM, Stencel-Baerenwald JE, Kapur RP, Studholme C, Boldenow E, Vornhagen J, Baldessari A, Dighe MK, Thiel J, Merillat S, Armistead B, Tisoncik-Go J, et al. Fetal brain lesions after subcutaneous inoculation of Zika virus in a pregnant nonhuman primate. *Nat Med* 2016; 22:1256-1259.
 11. Tabata T, Petitt M, Puerta-Guardo H, Michlmayr D, Wang C, Fang-Hoover J, Harris E, Pereira L. Zika Virus Targets Different Primary Human Placental Cells, Suggesting Two Routes for Vertical Transmission. *Cell Host Microbe* 2016; 20:155-166.
 12. El Costa H, Gouilly J, Mansuy JM, Chen Q, Levy C, Cartron G, Veas F, Al-Daccak R, Izopet J, Jabrane-Ferrat N. ZIKA virus reveals broad tissue and cell tropism during the first trimester of pregnancy. *Sci Rep* 2016; 6:35296.
 13. Bayer A, Lennemann NJ, Ouyang Y, Bramley JC, Morosky S, Marques ET, Jr., Cherry S, Sadovsky Y, Coyne CB. Type III Interferons Produced by Human Placental Trophoblasts Confer Protection against Zika Virus Infection. *Cell Host Microbe* 2016; 19:705-712.
 14. Nguyen SM, Antony KM, Dudley DM, Kohn S, Simmons HA, Wolfe B, Salamat MS, Teixeira LBC, Wiepz GJ, Thoong TH, Aliota MT, Weiler AM, et al. Highly efficient maternal-fetal Zika virus transmission in pregnant rhesus macaques. *PLoS Pathog* 2017; 13:e1006378.
 15. Sheridan MA, Yunusov D, Balaraman V, Alexenko AP, Yabe S, Verjovski-Almeida S, Schust DJ, Franz AW, Sadovsky Y, Ezashi T, Roberts RM. Vulnerability of primitive human placental trophoblast to Zika virus. *Proc Natl Acad Sci U S A* 2017; 114:E1587-E1596.
 16. Gurung S, Reuter N, Preno A, Dubaut J, Nadeau H, Hyatt K, Singleton K, Martin A, Parks WT, Papin JF, Myers DA. Zika virus infection at mid-gestation results in fetal

- cerebral cortical injury and fetal death in the olive baboon. *PLoS Pathog* 2019; 15:e1007507.
17. Meyer U, Yee BK, Feldon J. The neurodevelopmental impact of prenatal infections at different times of pregnancy: the earlier the worse? *Neuroscientist* 2007; 13:241-256.
 18. Honein MA, Dawson AL, Petersen EE, Jones AM, Lee EH, Yazdy MM, Ahmad N, Macdonald J, Evert N, Bingham A, Ellington SR, Shapiro-Mendoza CK, et al. Birth Defects Among Fetuses and Infants of US Women With Evidence of Possible Zika Virus Infection During Pregnancy. *JAMA* 2017; 317:59-68.
 19. Sheridan MA, Balaraman V, Schust DJ, Ezashi T, Roberts RM, Franz AWE. African and Asian strains of Zika virus differ in their ability to infect and lyse primitive human placental trophoblast. *PLoS One* 2018; 13:e0200086.
 20. Hirsch AJ, Roberts VHJ, Grigsby PL, Haese N, Schabel MC, Wang X, Lo JO, Liu Z, Kroenke CD, Smith JL, Kelleher M, Broeckel R, et al. Zika virus infection in pregnant rhesus macaques causes placental dysfunction and immunopathology. *Nat Commun* 2018; 9:263.
 21. Dudley DM, Aliota MT, Mohr EL, Newman CM, Golos TG, Friedrich TC, O'Connor DH. Using Macaques to Address Critical Questions in Zika Virus Research. *Annu Rev Virol* 2019.
 22. Lee KY, DeMayo FJ. Animal models of implantation. *Reproduction* 2004; 128:679-695.
 23. Joguet G, Mansuy JM, Matusali G, Hamdi S, Walschaerts M, Pavili L, Guyomard S, Prisant N, Lamarre P, Dejuq-Rainsford N, Pasquier C, Bujan L. Effect of acute Zika virus infection on sperm and virus clearance in body fluids: a prospective observational study. *Lancet Infect Dis* 2017; 17:1200-1208.
 24. D'Ortenzio E, Matheron S, Yazdanpanah Y, de Lamballerie X, Hubert B, Piorowski G, Maquart M, Descamps D, Damond F, Leparac-Goffart I. Evidence of Sexual Transmission of Zika Virus. *N Engl J Med* 2016; 374:2195-2198.
 25. Atkinson B, Hearn P, Afrough B, Lumley S, Carter D, Aarons EJ, Simpson AJ, Brooks TJ, Hewson R. Detection of Zika Virus in Semen. *Emerg Infect Dis* 2016; 22:940.
 26. Musso D, Roche C, Robin E, Nhan T, Teissier A, Cao-Lormeau VM. Potential sexual transmission of Zika virus. *Emerg Infect Dis* 2015; 21:359-361.
 27. Mansuy JM, Dutertre M, Mengelle C, Fourcade C, Marchou B, Delobel P, Izopet J, Martin-Blondel G. Zika virus: high infectious viral load in semen, a new sexually transmitted pathogen? *Lancet Infect Dis* 2016; 16:405.

28. Counotte MJ, Kim CR, Wang J, Bernstein K, Deal CD, Broutet NJN, Low N. Sexual transmission of Zika virus and other flaviviruses: A living systematic review. *PLoS Med* 2018; 15:e1002611.
29. Gurung S, Preno AN, Dubaut JP, Nadeau H, Hyatt K, Reuter N, Nehete B, Wolf RF, Nehete P, Dittmer DP, Myers DA, Papin JF. Translational Model of Zika Virus Disease in Baboons. *J Virol* 2018; 92.
30. Osuna CE, Lim SY, Deleage C, Griffin BD, Stein D, Schroeder LT, Orange RW, Best K, Luo M, Hraber PT, Andersen-Elyard H, Ojeda EF, et al. Zika viral dynamics and shedding in rhesus and cynomolgus macaques. *Nat Med* 2016; 22:1448-1455.
31. Koide F, Goebel S, Snyder B, Walters KB, Gast A, Hagelin K, Kalkeri R, Rayner J. Development of a Zika Virus Infection Model in Cynomolgus Macaques. *Front Microbiol* 2016; 7:2028.
32. Hirsch AJ, Smith JL, Haese NN, Broeckel RM, Parkins CJ, Kreklywich C, DeFilippis VR, Denton M, Smith PP, Messer WB, Colgin LM, Ducore RM, et al. Zika Virus infection of rhesus macaques leads to viral persistence in multiple tissues. *PLoS Pathog* 2017; 13:e1006219.
33. Silveira ELV, Rogers KA, Gumber S, Amancha P, Xiao P, Woollard SM, Byrareddy SN, Teixeira MM, Villinger F. Immune Cell Dynamics in Rhesus Macaques Infected with a Brazilian Strain of Zika Virus. *J Immunol* 2017; 199:1003-1011.
34. Emiliani S, Delbaere A, Devreker F, Englert Y. Embryo-maternal interactive factors regulating the implantation process: implications in assisted reproductive. *Reprod Biomed Online* 2005; 10:527-540.
35. Chang TA, Bondarenko GI, Gerami-Naini B, Drenzek JG, Durning M, Garthwaite MA, Schmidt JK, Golos TG. Trophoblast differentiation, invasion and hormone secretion in a three-dimensional in vitro implantation model with rhesus monkey embryos. *Reprod Biol Endocrinol* 2018; 16:24.
36. Rozner AE, Dambaeva SV, Drenzek JG, Durning M, Golos TG. Modulation of cytokine and chemokine secretions in rhesus monkey trophoblast co-culture with decidual but not peripheral blood monocyte-derived macrophages. *Am J Reprod Immunol* 2011; 66:115-127.
37. Wolfgang MJ, Eisele SG, Knowles L, Browne MA, Schotzko ML, Golos TG. Pregnancy and live birth from nonsurgical transfer of in vivo- and in vitro-produced blastocysts in the rhesus monkey. *J Med Primatol* 2001; 30:148-155.

38. Rozner AE, Durning M, Kropp J, Wiepz GJ, Golos TG. Macrophages modulate the growth and differentiation of rhesus monkey embryonic trophoblasts. *Am J Reprod Immunol* 2016; 76:364-375.
39. VandeVoort CA, Tollner TL, Overstreet JW. Separate effects of caffeine and dbcAMP on macaque sperm motility and interaction with the zona pellucida. *Mol Reprod Dev* 1994; 37:299-304.
40. Dudley DM, Van Rompay KK, Coffey LL, Ardeshir A, Keesler RI, Bliss-Moreau E, Grigsby PL, Steinbach RJ, Hirsch AJ, MacAllister RP, Pecoraro HL, Colgin LM, et al. Miscarriage and stillbirth following maternal Zika virus infection in nonhuman primates. *Nat Med* 2018; 24:1104-1107.
41. Toni E, Ziegler RLM, and Frederick H, Wegner. Detection of Urinary Gonadotropins in Callitrichid Monkeys With a Sensitive Immunoassay Based Upon a Unique Monoclonal Antibody. *American Journal of Primatology* 1993:181-188.
42. Tan L, Lacko LA, Zhou T, Tomoiaga D, Hurtado R, Zhang T, Sevilla A, Zhong A, Mason CE, Noggle S, Evans T, Stuhlmann H, et al. Pre- and peri-implantation Zika virus infection impairs fetal development by targeting trophoblast cells. *Nat Commun* 2019; 10:4155.
43. Govero J, Esakky P, Scheaffer SM, Fernandez E, Drury A, Platt DJ, Gorman MJ, Richner JM, Caine EA, Salazar V, Moley KH, Diamond MS. Zika virus infection damages the testes in mice. *Nature* 2016; 540:438-442.
44. Duggal NK, Ritter JM, Pestorius SE, Zaki SR, Davis BS, Chang GJ, Bowen RA, Brault AC. Frequent Zika Virus Sexual Transmission and Prolonged Viral RNA Shedding in an Immunodeficient Mouse Model. *Cell Rep* 2017; 18:1751-1760.
45. Yagel S, Casper RF, Powell W, Parhar RS, Lala PK. Characterization of pure human first-trimester cytotrophoblast cells in long-term culture: growth pattern, markers, and hormone production. *Am J Obstet Gynecol* 1989; 160:938-945.
46. Seshagiri PB, Terasawa E, Hearn JP. The secretion of gonadotrophin-releasing hormone by peri-implantation embryos of the rhesus monkey: comparison with the secretion of chorionic gonadotrophin. *Hum Reprod* 1994; 9:1300-1307.
47. Fazleabas AT, Donnelly KM, Srinivasan S, Fortman JD, Miller JB. Modulation of the baboon (*Papio anubis*) uterine endometrium by chorionic gonadotrophin during the period of uterine receptivity. *Proc Natl Acad Sci U S A* 1999; 96:2543-2548.

48. Simon C, Frances A, Piquette GN, el Danasouri I, Zurawski G, Dang W, Polan ML. Embryonic implantation in mice is blocked by interleukin-1 receptor antagonist. *Endocrinology* 1994; 134:521-528.
49. Li Y, Zhu H, Klausen C, Peng B, Leung PC. Vascular Endothelial Growth Factor-A (VEGF-A) Mediates Activin A-Induced Human Trophoblast Endothelial-Like Tube Formation. *Endocrinology* 2015; 156:4257-4268.
50. Yamada M, Kim S, Egashira K, Takeya M, Ikeda T, Mimura O, Iwao H. Molecular mechanism and role of endothelial monocyte chemoattractant protein-1 induction by vascular endothelial growth factor. *Arterioscler Thromb Vasc Biol* 2003; 23:1996-2001.
51. Nunes P, Nogueira R, Coelho J, Rodrigues F, Salomao N, Jose C, de Carvalho J, Rabelo K, de Azeredo E, Basilio-de-Oliveira R, Basilio-de-Oliveira C, Dos Santos F, et al. A Stillborn Multiple Organs' Investigation from a Maternal DENV-4 Infection: Histopathological and Inflammatory Mediators Characterization. *Viruses* 2019; 11.
52. Kawamura K, Kawamura N, Sato W, Fukuda J, Kumagai J, Tanaka T. Brain-derived neurotrophic factor promotes implantation and subsequent placental development by stimulating trophoblast cell growth and survival. *Endocrinology* 2009; 150:3774-3782.
53. Aldo P, You Y, Szigeti K, Horvath TL, Lindenbach B, Mor G. HSV-2 enhances ZIKV infection of the placenta and induces apoptosis in first-trimester trophoblast cells. *Am J Reprod Immunol* 2016; 76:348-357.
54. Hoen B, Schaub B, Funk AL, Ardillon V, Boullard M, Cabie A, Callier C, Carles G, Cassadou S, Cesaire R, Douine M, Herrmann-Storck C, et al. Pregnancy Outcomes after ZIKV Infection in French Territories in the Americas. *N Engl J Med* 2018; 378:985-994.
55. Peregrine J, Gurung S, Lindgren MC, Husain S, Zavy MT, Myers DA, Papin JF. Zika Virus Infection, Reproductive Organ Targeting, and Semen Transmission in the Male Olive Baboon. *J Virol* 2019; 94.
56. Mansuy JM, Suberbielle E, Chapuy-Regaud S, Mengelle C, Bujan L, Marchou B, Delobel P, Gonzalez-Dunia D, Malnou CE, Izopet J, Martin-Blondel G. Zika virus in semen and spermatozoa. *Lancet Infect Dis* 2016; 16:1106-1107.
57. Foy BD, Kobylinski KC, Chilson Foy JL, Blitvich BJ, Travassos da Rosa A, Haddow AD, Lanciotti RS, Tesh RB. Probable non-vector-borne transmission of Zika virus, Colorado, USA. *Emerg Infect Dis* 2011; 17:880-882.

58. Magalhaes T, Foy BD, Marques ETA, Ebel GD, Weger-Lucarelli J. Mosquito-borne and sexual transmission of Zika virus: Recent developments and future directions. *Virus Res* 2018; 254:1-9.
59. Visseaux B, Mortier E, Houhou-Fidouh N, Brichler S, Collin G, Larrouy L, Charpentier C, Descamps D. Zika virus in the female genital tract. *Lancet Infect Dis* 2016; 16:1220.
60. Prisant N, Bujan L, Benichou H, Hayot PH, Pavili L, Lurel S, Herrmann C, Janky E, Joguet G. Zika virus in the female genital tract. *Lancet Infect Dis* 2016; 16:1000-1001.
61. Nicastri E, Castilletti C, Balestra P, Galgani S, Ippolito G. Zika Virus Infection in the Central Nervous System and Female Genital Tract. *Emerg Infect Dis* 2016; 22:2228-2230.
62. Prisant N, Joguet G, Herrmann-Stock C, Moriniere C, Pavili L, Lurel S, Bujan L. Upper and lower genital tract Zika virus screening in a large cohort of reproductive-age women during the Americas epidemic. *Reprod Biomed Online* 2019; 39:624-632.
63. Duggal NK, McDonald EM, Ritter JM, Brault AC. Sexual transmission of Zika virus enhances in utero transmission in a mouse model. *Sci Rep* 2018; 8:4510.
64. Pagani I, Ghezzi S, Ulisse A, Rubio A, Turrini F, Garavaglia E, Candiani M, Castilletti C, Ippolito G, Poli G, Broccoli V, Panina-Bordignon P, et al. Human Endometrial Stromal Cells Are Highly Permissive To Productive Infection by Zika Virus. *Sci Rep* 2017; 7:44286.
65. Carroll T, Lo M, Lanteri M, Dutra J, Zarbock K, Silveira P, Rourke T, Ma ZM, Fritts L, O'Connor S, Busch M, Miller CJ. Zika virus preferentially replicates in the female reproductive tract after vaginal inoculation of rhesus macaques. *PLoS Pathog* 2017; 13:e1006537.
66. Yockey LJ, Varela L, Rakib T, Khoury-Hanold W, Fink SL, Stutz B, Szigeti-Buck K, Van den Pol A, Lindenbach BD, Horvath TL, Iwasaki A. Vaginal Exposure to Zika Virus during Pregnancy Leads to Fetal Brain Infection. *Cell* 2016; 166:1247-1256 e1244.
67. Castro MC, Han QC, Carvalho LR, Victora CG, Franca GVA. Implications of Zika virus and congenital Zika syndrome for the number of live births in Brazil. *Proc Natl Acad Sci U S A* 2018; 115:6177-6182.

Chapter 4

Rhesus macaque early-gestation trophoblast cells are permissive to Zika virus infection and extracellular vesicle cargo is altered with virus exposure

Planned submission: Cell Host and Microbe, 09/2021

Lindsey N. Block^{1,2}, Jenna Kropp Schmidt¹, Megan C. McKeon³, Brittany D. Bowman^{1#}, Gregory J. Wiepz¹, Thaddeus G. Golos^{1,4,5}

Author affiliations:

¹Wisconsin National Primate Research Center, University of Wisconsin-Madison, Madison, WI, USA

²Department of Pathology and Laboratory Medicine, University of Wisconsin-Madison, Madison, WI, USA

³Department of Biomolecular Chemistry, University of Wisconsin-Madison, Madison, WI, USA

⁴Department of Comparative Biosciences, University of Wisconsin-Madison, Madison, WI, USA

⁵Department of Obstetrics and Gynecology, University of Wisconsin-Madison, Madison, WI, USA

#Current address: University of Nebraska Medical Center, Omaha, NE, USA

4.1 Abstract (Original by LNB; edited by TGG and JKS)

Zika virus (ZIKV) infection of maternal and placental cells at the maternal-fetal interface is associated with a spectrum of adverse pregnancy outcomes including fetal demise and pregnancy loss. Trophoblast cell types that comprise the placenta include cytotrophoblasts, syncytiotrophoblasts (STs), and extravillous trophoblasts (EVTs). To determine which trophoblast cells are permissive to ZIKV infection and to understand how infection impacts cellular gene expression, we utilized a rhesus macaque in vitro trophoblast stem cell model. Trophoblast stem cells (TSCs) have been derived from primary cytotrophoblasts and represent a proliferative trophoblast. The TSCs can be differentiated into STs and EVTs. TSCs and ST3Ds were highly permissive to infection with ZIKV strain DAK AR 41524 (DAKAR), whereas EVTs maintained a level of resistance to productive ZIKV infection. The impact of ZIKV on cellular gene expression was determined by transcriptomic and miRNAome analysis. Infection of TSCs and ST3Ds results in increased expression of immune related genes, including those in the type I and type III interferon response. Infection impacts the size of EVs released by all three trophoblast types as well as their protein, mRNA, and miRNA cargo, regardless of productive infection. Overall, ZIKV exposure results in increased quantities of proteins and miRNAs detected in EVs. Altogether, these findings suggest TSCs and STs of the nonhuman primate are permissive to ZIKV infection and that EV analysis has the potential to identify ZIKV infection. These findings provide a foundation for further ZIKV study and allow for potential ZIKV infection biomarker identification in a highly translational model.

4.2 Introduction (Original by LNB; edited by TGG and JKS)

Maternal Zika virus (ZIKV) infection is associated with adverse pregnancy outcomes including pregnancy loss and fetal malformations [1, 2]. Zika viremia is prolonged during human and nonhuman primate (NHP) pregnancy [2-7], which suggests there is a pregnancy-specific viral reservoir. ZIKV has been detected in placental and fetal tissues and its presence is correlated with pathological observations [8]. Prolonged maternal viremia and the presence of virus at the maternal fetal interface support the premise that the placenta may serve as the viral reservoir.

The placenta is an essential organ in pregnancy as it not only conveys sufficient nutrients and oxygen for proper development [9], but also provides signals for the adaptation of maternal physiological systems to pregnancy. Errors in placental development and function are often associated with adverse pregnancy outcomes [9]. The placenta comprises several trophoblast cell types, including villous cytotrophoblasts (vCTBs), syncytiotrophoblast (STs), extravillous trophoblasts (EVTs), as well as fetal macrophages (hofbauer cells), other immune and vascular cells, and fibroblasts [10]. vCTBs can be induced to a proliferative stem cell-like state in vitro, termed trophoblast stem cells (TSCs) that can be differentiated into STs or EVTs [10, 11].

Extensive data support that ZIKV infection early in pregnancy is associated with worse outcomes than infections which occur later in pregnancy [2, 4, 12-16]. In addition, in vitro studies also have demonstrated that early pregnancy trophoblasts are permissive to ZIKV infection, however the impact on placental cells has not been deeply characterized. Regardless of the human culture

systems available, the ability to relate back to early human pregnancy is limited. The ability of clinicians and investigators to assess the risk of vertical transmission is also hindered by the lack of knowledge of timing of infection, and inability to intervene in infected pregnancies. In addition, based on the inconsistency with which cells are infected *in vivo* and, in some cases, *in vitro*, it is important to establish models which can provide a platform to better understand the impact of ZIKV on the different populations of trophoblasts present *in vivo* and develop methods by which placental function can be monitored *in vivo* with minimal invasion. Extracellular vesicles (EVs) are widely studied as a means to monitor cell function as a minimally invasive “liquid biopsy” from *in vivo* body fluids or *in vitro* culture media [17, 18]. EVs also contain cell-type specific markers, which can be used to monitor the function of specific cells [17]. The cargo packaged within EVs, which includes nucleic acids and proteins, is often altered under diseased and infected states [19-21].

Macaques are relevant models of human pregnancy [22] and ZIKV infection during pregnancy [23]. In this current study, a newly established rhesus macaque early gestation TSC model [11] was utilized to determine which trophoblast cells were permissive to infection and how infection impacted those cells. This model has been shown to express functional characteristics representative of early pregnancy trophoblasts. For instance, the STs secrete chorionic gonadotropin (CG), a feature that is restricted to the first 4-5 weeks of pregnancy in the macaque [24, 25]. The objectives of this study were to 1) determine which macaque trophoblast cell types were permissive to ZIKV infection, 2) determine the molecular and secretory impact of ZIKV infection, and 3) analyze placental EVs (PEVs), to determine if they could be used as surrogates

of trophoblast cell function. Although strains that were related to Asian lineage ZIKV have been identified in the recent ZIKV epidemic in South America [26], in vivo mouse [27, 28] and porcine [29] studies and in vitro human studies [30-32] suggest that strains of the African lineage may be more detrimental to pregnancy. Hence, a strain from the African lineage was utilized to inoculate macaque trophoblasts in vitro to assess the impact of ZIKV on cell function and EV cargo. The outcomes of this in vitro study provide insight into how ZIKV impact trophoblasts in the first trimester and suggests that PEV cargo may serve as readout of placental ZIKV infection.

4.3 Methods (Original by LNB; edited by TGG and JKS)

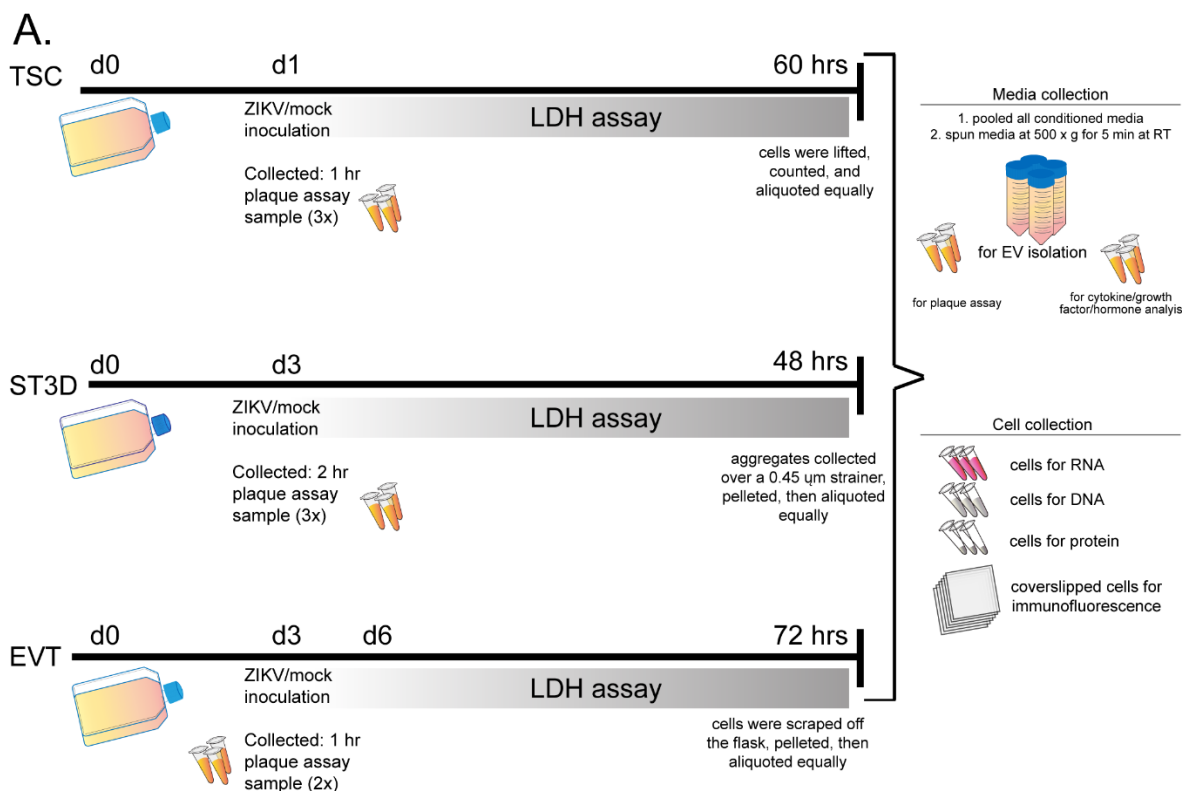
Trophoblast cell culture

Rhesus monkey TSCs [11] were graciously provided by Dr. Jenna Kropp Schmidt. The four TSC lines used for this study were: rh010319 (male; gestation date (gd) 58; line 1); rh090419 (female; gd 75; line 2), r121118 (male; gd 62; line 3), and rh020119 (female; gd 74; line 4). The same protocols as previously published [11] were followed with some modifications as described. TSCs were differentiated into either EVT_s or ST3D aggregates (Supplemental Figure 1A). TSCs were grown in 13 ml media, EVT_s in 15 ml media, and ST3D_s in 10 ml media (Supp Figure 1B).

TSCs were differentiated to EVT by seeding into T75 flasks coated with 1 µg/ml collagen (col IV; Corning, NY, USA, Cat #354233) with 2% Matrigel added to the EVT media (Corning, Cat #

354234). No additional Matrigel was added on day 3 when the media were changed as previously described. Growth Factor Reduced Matrigel (0.5%; Corning, Cat #354230) was added on day six.

For ST3D culture, TSCs were plated in non-adherent T75 flasks (Thermo Fisher, Cat #174952 and Cat #156800) and cultured for five days total. After three days, the media were removed, and fresh media added. For additional details on the media composition and growth conditions, please see Schmidt, et al. 2020 [11].



B. Table 1. Logistics of trophoblast cell infections.

	TSC	EVT	ST3D
Vessel for cell culture	T75	T75	T75 non-adherent
Number cells/flask	$7.5 \times 10^5 - 1.2 \times 10^6$	$1.5 - 2.0 \times 10^6$	750,000
MOI	5	5	10
Inoculation vessel	T75	T75	15 mL tube
Day(s) post plating cells were inoculated	1	6	3
Volume of inoculum	1 ml	1 ml	300 μ l
Length of ZIKV exposure	1 hr	1 hr	2 hrs
Length of culture post-inoculation	60 hr	72 hr	48 hr
Volume post inoculation	13 ml	15 ml	10 ml

Supplemental Figure 4.1. Methods overview. *A)* A timeline depiction of how TSCs, ST3Ds, and EVTs were cultured, when samples were collected, and for what assay samples were collected. *B)* The logistics

of trophoblast cell infection including the type of vessel used for cell culture, the number of cells plated, the MOI, inoculation vessel, the day of differentiation cells were inoculated, volume of inoculum, length of ZIKV exposure, length of culture post-inoculation, and media volume post inoculation. Figure made by LNB.

ZIKV stock and infection

IKV, DAK AR 41524, NR-50338 (“DAKAR”) was obtained through BEI Resources, NIAID, NIH, as part of the WRCEVA program. To propagate this stock for subsequent experiments, the previously published protocol was followed [33] with minor adaptations. Briefly, Vero cells (ATCC, Manassas, VA, USA, Cat #CCL-81) were plated at 4×10^6 cells/T75 flask in MEM (ThermoFisher, Cat #11-095-080) containing 2% FBS (Peak Serum, Wellington, Colorado, USA, Cat #PS-FB1) and 100 mM sodium pyruvate (Sigma Aldrich, St. Louis, MO, USA, Cat #2256). The following day, they were exposed to DAK at an MOI of 0.1 for 1 hr in 2 ml of MEM medium. Cytopathic effect was observed at 48 hr in the ZIKV exposed cultures, and media were collected and spun at $15,000 \times g$ for 30 mins at 4°C . The supernatants were then aliquoted and frozen at -80°C until used for infection studies. The final stock was sequenced by Dr. Shelby O’Connor’s laboratory at UW-Madison using an Illumina MiSeq instrument and compared to the ZIKV stock reference sequence (Genbank Accession KY348860). Three single nucleotide (nt) substitutions at nt positions 470 (synonymous mutation; serine -> serine), 3868 (missense, alanine - valine), and 3790 (missense, alanine - valine) were identified in the ZIKV stock used. The frequencies of these substitutions were all below 16%. The stock concentration (4.6×10^7 PFU/ml) was determined by plaque assays that were run in triplicate, as previously described [34].

For infection of the TSCs and EVTs, one flask of cells from each TSC line was lifted and counted just prior to infection. The MOI used was determined based on the quantity of virus calculated from the Vero cell plaque assay described above. To infect the ST3Ds, the number of “cells” (at this point they are aggregates) present was based on the number of TSCs added to the flask three days prior (Supplemental Figure 1B). Duration of culture and MOI were first optimized prior to generating experimental infection replicates. Both ZIKV-infected cells and uninfected controls underwent the same processing except that uninfected cells were exposed to ZIKV-free Vero cell conditioned media that was collected alongside the ZIKV stock (mock infected).

Trophoblast ZIKV Inoculations

For TSCs and EVTs, media were aspirated, and 1 ml of inoculum was added to the flask. Cultures were incubated at 37°C and rocked gently every 15 mins for 1 hr to spread the inoculum. The inoculum was then removed, and cells were washed once with PBS followed by addition of fresh medium. To infect the ST3Ds that were grown in suspension, aggregates/cells were pelleted by centrifugation at 500 x g for 3 mins, the supernatant was removed, and the cells were resuspended in 300 µl of inoculum. Aggregates were incubated in the ZIKV inoculum for 2 hrs at 37°C and gently disturbed every 30 mins. Since ST3Ds are grown in suspension, a larger volume of inoculum was used, and the length of inoculation was extended to account for this increase. Next, 2 ml of PBS was added, the cells were re-pelleted by centrifugation as above, and the supernatant was removed. A volume of 10 ml ST3D medium was added to the cells and they were then transferred back into a T75 flask. Once fresh media were added back for all cell types, a 500 µl aliquot was removed to serve as a baseline of initial viral titer in the culture. The aliquot was spun

at 500 x g for 5 mins to remove any cellular debris and a plaque assay was conducted. For EVT_s, Growth Factor Reduced Matrigel (0.5%; Corning, Cat #354230) was supplemented to the cultures after this step. EVT_s were cultured for a day longer than previously reported [11] (72 hrs total) to extend the duration of ZIKV infection.

Sample collection: cells and media

After (mock) infection, all cells were rinsed once with PBS. At the end of the culture period, TSC_s were lifted, EVT_s were scraped off the flasks, and ST3D_s were pelleted prior to aliquoting cells for RNA, DNA, and protein isolation (Supplemental Figure 1A). Conditioned media collected from all flasks were spun at 500 x g for 5 mins to remove dead cells and debris, pooled, and then aliquoted and frozen back at -80°C for EV isolation, hormone analysis, Luminex assay, or plaque assay.

EV isolation

To isolate EV_s, 20 ml of media was placed onto a concentration column (Sartorius, Swedesboro, NJ, USA, Cat # 1208L91) and spun for 60 mins at 3,000 x g at room temperature (RT). For EVT EV samples, due to a high density of Matrigel in the conditioned media, the media were first filtered using a 0.22 um filter (Millipore Sigma, Cat # SLGP033RS) and then spun for 60 - 90 mins. The concentrated sample was then passed through a size exclusion column (Izon, Medford, MA, USA, Cat # SP5, serial #1000788) according to the manufacturer's protocol and the 1.5 ml flow through was collected. The sample was then concentrated using an Amicon concentration

column (Millipore Sigma, Cat # UFC801024) for 45-60 min at 3,000 x g at RT. Four replicates of 20 ml media volumes were processed for EV isolation and then combined into one sample. This sample was quantified and characterized thrice by Zetaview Nanoparticle Tracking Analysis (NTA; methods described below). The sample was then divided into three aliquots, one each for RNAseq by freezing in Qiazol (Qiagen, Germantown, MD, USA, Cat #217004), mass spectrometry by freezing in PBS (FisherScientific, Cat #BP3991), and Western Blot by freezing in Pierce RIPA buffer (Fisher Scientific, Waltham, MA, USA, Cat #P18990) with 1X HALT (Thermo Fisher, Cat #78440).

EV sample quantification and characterization

PBS utilized for all EV dilutions was first filtered through 0.02 μm filters (Millipore Sigma, Cat # WHA68091002) and the absence of particles was confirmed using the Zetaview NTA (Particle Metrix, Meerbusch, Germany). EVs were quantified by NTA using the following parameters: minimum brightness = 23, maximum size = 800, minimum size = 8, tracelength = 16, nm/class = 4, class/decade = 64, sensitivity = 80.2, frame rate = 30, and shutter = 100. Each sample was analyzed thrice, and the coefficient of variation (CV) was calculated. The CV within each sample set was less than <6%. To determine the percentage of potential Zika virions in the EV samples, the percentage of particles 50-54 nm in size [35] was calculated for each sample.

To determine if Zika virions were present in the EV preparations and to co-localize ZIKV E protein with EVs released by infected cells, an AlexaFluor-488 labeled E antibody (1:10 dilution) was

added to EV samples and incubated for 2 hrs at RT in the dark prior to quantification with the Zetaview NTA. Samples were diluted at least 1:1000 according to the Zetaview NTA fluorescence protocol. As a positive control, 5.5 ml ZIKV stock was put through the EV isolation protocol, stained with the conjugated E antibody, and evaluated by NTA following the same protocol as described for the EV preparations. The fluorescent settings were minimum brightness = 20, maximum size = 800, minimum size = 5, tracelength = 11, nm/class = 4, class/decade = 64, sensitivity = 80, frame rate = 30, and shutter = 100.

Detection of ZIKV via immunofluorescence

To evaluate cells exposed to ZIKV by immunocytochemistry, additional cells were infected and cultured as described above. For staining, TSCs were cultured for 60 hrs on col IV coated coverslips (5 µg/ml), rinsed in PBS, and fixed with 4% paraformaldehyde (PFA; Fisher Scientific, Cat #50-980-487) in PBS for 10 mins. Previous work showed that EVTs did not grow well on glass coverslips. So after culture, EVTs were lifted, rinsed in PBS, fixed in 4% PFA, and cytospun at 1000 x g for 1 min onto coverslips. ST3Ds were cultured for 48 hrs, then transferred to wells containing col IV coated coverslips (5 µg/ml) and allowed to attach for 2 hrs. The cells were rinsed with PBS and fixed in 4% PFA for 10 mins. After fixation, all coverslipped cells were rinsed twice more with PBS and stored at 4°C in PBS. For immunostaining, the cells were permeabilized for 10 mins with 0.1% Triton-100 (Millipore Sigma, cat #T-9284) and then blocked for 10 mins with Background Punisher (Biocare Medical, Pacheco, CA, USA, Cat #BP974H). For antibody details please see Supplemental Table 1. Cells were incubated with either primary specific or IgG isotype control antibodies diluted in DaVinci Green Diluent (Biomedical Care, PD900M) for 1 hr at RT,

washed 3 times at 5 mins each with Tris-buffered saline with 0.1% Tween (TBST), and then exposed to secondary mouse and rabbit antibodies and phalloidin-488 for 45 mins at RT. Finally, the cells were stained with DAPI for 5 mins, washed in Milli-Q water, and then coverslips were adhered to slides using ProLong Diamond Mountant (Fisher Scientific, Cat # P36961). The following day the slides were imaged using a Nikon confocal microscope and Elements software (Nikon, Tokyo, Japan).

Lactate Dehydrogenase (LDH) Apoptosis Assay

To determine if ZIKV induced cell death, an LDH (Cytotox96 non-radioactive cytotoxicity assay, Promega, Madison, WI, Cat #G1780) time course was completed on each cell type; infection of Vero cells was done as a positive control. For this assay, additional cells were inoculated at the same MOI and length of duration as previously stated and shown in Supplemental Figure 1A.

TSCs (100,000 cells/well) were seeded into 24-well col IV coated plates (Corning, Cat #3527). The following day they were exposed to ZIKV or mock infected. EVT3s were plated (100,000 cells/well) in collagen IV coated 24-well plates and differentiated in the wells following the previously stated media changes. ST3Ds were differentiated in non-adherent T25 flasks and after they were exposed to ZIKV (day 3 of differentiation, as previously stated) they were transferred (three-quarters of a T25 flask/well) to non-adherent 24-well plates (Eppendorf, Hamburg, Germany, Cat #0030 722.019). Vero cells were plated in 24-well plates and then exposed to ZIKV at an MOI of 1, 5, or 10 for 1 hr the following day. Cells were plated such that three ZIKV-exposed and three control wells were quantified at each time point.

After the ZIKV exposure (as previously determined for each cell type), cells were rinsed once with PBS and then an LDH assay was performed. For the LDH assay, media were removed, the cells rinsed with PBS, and then 100 μ l of 1X lysis solution was added. The cells were incubated in lysis solution at 37°C for 45 mins. After the 45 min incubation, 50 μ l was removed and put into a 96-

well plate. A volume of 50 μ l of the CytoTox 96 reagent was added and the plate incubated for 30 mins at RT in the dark. Finally, 50 μ l of Stop Solution was added, and the plate was immediately read at 490 nm. The average among the three wells was calculated and the change in LDH in infected cells compared to controls was determined. To determine the change in LDH, ZIKV LDH absorbance was divided by the control LDH absorbance.

Plaque assay

To determine the quantity of virus in the conditioned media, plaque assays on Vero cells were conducted as previously reported [34]. Samples were assessed in duplicate (EVT samples) or triplicate (TSC and ST3D samples).

Hormone quantification

Monkey chorionic gonadotropin (mCG) and progesterone assays were performed as previously reported [34]. Samples were run in duplicate and unconditioned media were analyzed to determine background mCG and progesterone. The lower limit of detection for the mCG and progesterone is 0.1 ng/ml and 10 pg/ml, respectively.

Total RNA isolation from cells

Total RNA was isolated from cells using an RNeasy kit (Qiagen, Cat #74104) following kit recommendations with modifications. A volume of 700 μ l of Qiazol was added to the cell pellet

and then frozen at -80°C until RNA extraction. The protocol was followed with the same minor adaptations as with the miRNeasy kit. A 15 min DNase treatment was performed on the column using RNase-Free DNase (Qiagen, Cat # 79254) prior to washing the column.

Total RNA isolation from EVs

Each EV sample was diluted in 5x Qiazol and incubated for 5 mins at RT prior to freezing at -80°C until RNA extraction. The miRNeasy serum/plasma kit (Qiagen, Cat #217184) was used to isolate total RNA from EVs following the manufacturer's protocol with minor adaptations. The Qiazol with Chloroform was overlaid onto phase maker tubes (ThermoFisher, Cat #A33248) and then spun at 4°C at $16,000 \times g$ for 15 mins. In addition, two RPE washes of $500 \mu\text{l}$ were applied prior to RNA elution. All samples were eluted in $30 \mu\text{l}$ RNase free water and the initial elution was placed back on the column to increase RNA concentration. Sample concentration and purity was determined with the NanoDrop One (ThermoFisher, Cat # ND-ONE-W).

miRNA-seq library prep, sequencing and statistical analyses

The total RNA quality and quantity was assessed using a Bioanalyzer 2100 (Agilent, CA, USA). Approximately $1 \mu\text{g}$ of total RNA were used to prepare small RNA cDNA libraries utilizing the specified protocol for the TruSeq Small RNA Sample Prep Kit (Illumina, San Diego, USA). Single-read sequencing of 50 bp was performed on an Illumina HiSeq 2500 at LC Sciences LLC (Houston, Texas, USA).

Raw reads were subjected to a proprietary, ACGT101-miR program (LC Sciences) to remove adapter dimers and to filter out junk, low complexity, common RNA families (rRNA, tRNA, snRNA, snoRNA) and repeated reads. Subsequently, unique sequences of 18-26 nucleotides in length were mapped to macaca mulatta precursors in miRBase 22.0 via an NCBI BLAST search to the macaque reference genome 10 (mmul 10) to identify known and novel miRNAs. Length variation at both 3' and 5' ends and one mismatch inside of the sequence were allowed in the alignment. The unique sequences mapping to mature miRNAs in hairpin arms were identified as known miRNAs. The unique sequences mapping to the other arm of known selected species precursor hairpin opposite to the annotated mature miRNA-containing arm were considered to be novel 5p- or 3p derived miRNA candidates. The remaining sequences were mapped to other selected species precursors in miRBase 22.0 by BLAST search, and the mapped pre-miRNAs were further BLASTed against the specific species genomes to determine their genomic locations. The above two were defined as known miRNAs. The unmapped sequences were BLASTed against the specific genomes, and the hairpin RNA structures containing sequences were predicated from the flank 80 nt sequences using RNAfold software (<http://rna.tbi.univie.ac.at/cgi-bin/RNAWebSuite/RNAfold.cgi>). The criteria for secondary structure prediction were: (1) number of nucleotides in one bulge in stem (≤ 12) (2) number of base pairs in the stem region of the predicted hairpin (≥ 16) (3) cutoff of free energy (kCal/mol ≤ -15) (4) length of hairpin (up and down stems + terminal loop ≥ 50) (5) length of hairpin loop (≤ 20). (6) number of nucleotides in one bulge in mature region (≤ 8) (7) number of biased errors in one bulge in mature region (≤ 4) (8) number of biased bulges in mature region (≤ 2) (9) number of errors in mature region (≤ 7) (10) number of base pairs in the mature region of the predicted hairpin (≥ 12) (11) percent of mature in stem (≥ 80).

Differential expression of miRNAs based on normalized deep-sequencing counts was analyzed by either using the student t-test (two group comparison) or ANOVA (three group comparison) with R software.

Poly(A)RNAsequencing: library prep, sequencing and statistical analyses

RNA integrity was checked with Agilent Technologies 2100 Bioanalyzer. Poly(A) tail-containing mRNAs were purified using oligo-(dT) magnetic beads with two rounds of purification. After purification, poly(A) RNA was fragmented using a divalent cation buffer in elevated temperature. The poly(A) RNA cDNA sequencing library was prepared following Illumina's TruSeq-stranded-mRNA sample preparation protocol. Quality control analysis and quantification of the sequencing library were performed using Agilent Technologies 2100 Bioanalyzer High Sensitivity DNA Chip. Pair-end sequencing reads of 150 bp reads were generated on an Illumina NovaSeq 6000 sequencing system.

For cell poly(A)seq data, sequencing reads were filtered to remove adaptors and primer sequences and to remove sequences with a quality score lower than 20 [36]. The cleaned sequencing reads were aligned to the reference genome [https://ftp.ncbi.nlm.nih.gov/genomes/all/GCF/003/339/765/GCF_003339765.1_Mmul_10] using the HISAT2 package [37]. Multiple alignments with a maximum of two mismatches were allowed for each read sequence (up to 20 by default). HISAT2 also built a database of potential

splice junctions. Transcript abundance estimation and differential expression analysis of aligned reads of individual samples were assembled using StringTie [38]. Transcriptomes from all samples were then merged to reconstruct a comprehensive transcriptome using a proprietary Perl script designed by LC Sciences. Following transcriptome reconstruction, raw read counts were filtered, normalized, and differential expression determined with DESeq2 [39] and edgeR [40, 41]. The glmLRT test was used for edgeR differential expression analysis. EdgeR normalized values were used to produce the heatmaps.

For EV poly(A)seq data, sequences were filtered, adaptors removed, and sequences aligned with Salmon. Since only eight samples were sequenced, EVs released by control TSCs and ST3Ds (five total samples) were combined and compared to EV data obtained from ZIKV exposed TSCs and ST3Ds (three total samples). Due to limited sample size differential expression analysis was not performed.

Validation of gene expression by qRT-PCR

A second RNA sample was extracted to generate technical replicates to validate gene expression changes by qRT-PCR that were initially identified by Poly(A)-sequencing analysis. cDNA was synthesized with a SuperScript III First-Strand Synthesis kit (ThermoFisher, Cat # 18080051) using 1 µg RNA per reaction. The manufacturer's protocol was followed and the Oligo dT primer was used. qRT-PCR was performed with iQ SYBR Green Supermix (Bio Rad, Cat #1708882) following the manufacturer's recommendation for primer concentration, master mix formulation

and primer concentration. Beta-actin mRNA was amplified in parallel to serve as the reference gene and the primer sequences are listed in Supplemental Table 2. cDNA was diluted 1:10 and reactions were run in triplicate. The cycling protocol indicated with the kit was followed. Beta-actin was used to normalize and $2^{-\Delta\Delta C_t}$ method [42] was used to determine changes in transcript abundance. Data are presented as the \log_2 fold change in expression with the p-values calculated via a t-test on the ΔC_t values for each transcript.

Supplemental Table 4.2. Primer sequences for qRT-PCR.

<i>Gene</i>	<i>Forward (5' -> 3')</i>	<i>Reverse (5' -> 3')</i>	<i>Amplicon size</i>
<i>ACTB</i>	CTA CCA TGA GCT GCG TGT GG	GTA CAT GGC TGG GGT GTT GA	130
<i>INFL1</i>	ATC GTG GTG CTG GTG ACT TT	TTG AGT GAC TCT TCC AAG GCA	170
<i>ISG20</i>	TGC TGT GCT GTA CGA CAA GT	CCA AGC AGG CTG TTC TGG AT	339
<i>OASL</i>	CAT CGT GCC TGC CTA CAG AG	GAC CTG GCT TTC ACA TAC TGC T	219
<i>DDX58</i>	CTG GTT CCG TGG CTT TTT GG	CCC CTT AGT GGA GCA AAT CTG T	238
<i>IFNB1</i>	CTC CTG TTG TGC TTC TCC ACT	AAT GCA GCG TCC TCC TTC TG	203
<i>DHX58</i>	AAG ATC CTG CAA AGG CAG TTC A	TAC TTC TTG CTG GTC CCT CTG G	204
<i>PARP14</i>	CCA AGA ATG GCC AGA CAA TGA	CTT TCC ATA TGC CAC AGC ATT C	128
<i>MT1E</i>	CTG GCT GCG TTT TTG CCT TA	TCT TCT TGC AGG AGG TGC ATT	147
<i>MTX1</i>	CGT GTT TGC CTC TTC ATT GGG	CAC AGG AAC CAT CAG GCG AG	86

Protein quantification and sample preparation

EV and cell protein samples for Western Blots were solubilized in Pierce RIPA buffer with 1X HALT, sonicated for 3-6 s, spun down at 10,000 x g for 10 mins, and frozen at -80°C. Samples were quantified using the BCA assay as previously described [11]. For cell samples, 2-4 samples were quantified to estimate the total amount of cell protein in the study.

Western Blots

EV samples were diluted in 2 or 4X TPA buffer (2X recipe: 20 mM TRIS, 2 mM EDTA, 1 mM Na_3VO_4 , 2 mM DTT, 2% SDS, 20% glycerol, and a few drops of bromophenol blue) and heated

for 5 mins at 70°C. Cluster of differentiation (CD) 9, Heat shock protein 70 (Hsp70), and calnexin were stained for based on the MISEV 2018 guidelines [43]. To detect ZIKV, the envelope (E) and nonstructural protein 2B (NS2B) antibodies were used; see Supplemental Table 1 for antibody information.

A total of 3 µg of cell, EV, or an in-house quality control (QC) protein sample was added per well of a 12% polyacrylamide gel along with 8 µl PageRuler Standard (Thermo Fisher, Cat #26616). Samples were prepared such that 2 identical blots were run at the same time. Gels were run in Running buffer (National Diagnostics, Cat # EC870). Protein transfer was done using the GENIE Electrophoretic Transfer (IdeaScientific, Minneapolis, MN, USA) and Transfer buffer (National Diagnostics, Cat # EC880) with 20% methanol (Fisher Scientific, Cat #A412P-4). Protein was transferred onto PVDF paper (Millipore Sigma, Cat # IVPH00010, Billerica, MA, USA) for 90 mins at 0.5 amps with a Power Pac HC power supply (Bio Rad, Cat #1645052). The blots were blocked at 4°C overnight in 5% nonfat dry milk (RPI, Cat # M17200, Mount Prospect, Illinois, USA) in 1X TBST. Blots were incubated in primary antibody (at the concentrations specified in Supplemental Table 1) for 1 hr on a rocker in 5% milk at 37°C. The blots were then washed in 1X TBST three times for 5 mins each at RT and then exposed to either mouse or rabbit secondary antibody for 1 hr on a rocker in 5% milk at 37°C. The blots were washed again in TBST three times for 5 mins each at RT and then exposed to Immobilon Crescendo HRP (Millipore Sigma, Cat # WBLUR0100) for 3 mins at RT and imaged in a Bio-Rad ChemiDoc XRS+ with ImageLab software.

Mass spectrometry for proteomics: sample processing, data collection, and data analysis

EV preparations were submitted to the University of Wisconsin Mass Spectroscopy/Proteomics Facility through the Biotechnology Center. Isolated EVs in PBS (5 - 10 µg protein) were acidified with trichloroacetic acid (TCA; Fisher Scientific, Cat #A322-100) (10% vol:vol final) to inactivate ZIKV, diluted with water to 200 µl total volume, and then 250 µl of acetone and 50 µl of TCA were added. Samples were sonicated for 2 mins at 6°C in a sonication bath to lyse and release protein content, incubated on ice for 45 mins to facilitate protein denaturation and precipitation and then spun for 10 mins at RT with max speed (16,000 x g). Protein pellets were washed once each in acetone and methanol and then re-solubilized and denatured in 20 µl of 8 M Urea, 50 mM NH₄HCO₃ (pH 8.5), 1mM TrisHCl. Samples were then diluted to 60 µl with 2.5 µl of 25 mM DTT, 5 µl MeOH, and 32.5 µl 25 mM NH₄HCO₃ (pH8.5), incubated at 52°C for 15 mins, cooled on ice to RT, and then 3 µl of 55 mM Iodoacetamide (IAA) was added for alkylation and incubated in darkness at RT for 15 mins. Reactions were then quenched by adding 8 µl of 25 mM DTT. Finally, 6 µl of Trypsin/LysC solution [100 ng/µl 1:1 *Trypsin* (Promega) and LysC (FujiFilm) mix in 25 mM NH₄HCO₃] and 23 µl of 25 mM NH₄HCO₃ (pH8.5) was added to 100 µl final volume. Digestion was conducted for 2 h at 42°C, 3 µl of trypsin/LysC mix was added, and then the digestion proceeded overnight at 37°C. Reaction was terminated by acidification with 2.5% TFA [Trifluoroacetic Acid] to 0.3% final concentration.

NanoLC-MS/MS was completed as previously described [44]. The Lumos acquired MS/MS data files were searched using Proteome Discoverer (ver. 2.2.0.388) Sequest HT search engine against Uniprot *Rhesus macaque* proteome database (UP000006718, 11/19/2020 download, 44,378 total

entries) using previously published settings. Static cysteine carbamidomethylation, and variable methionine oxidation plus asparagine and glutamine deamidation, 2 tryptic miss-cleavages and peptide mass tolerances set at 15 ppm with fragment mass at 0.6 Da were selected. Peptide and protein identifications were accepted under strict 1% FDR cut offs with high confidence XCorr thresholds of 1.9 for $z=2$ and 2.3 for $z=3$ and at least 2 PSMs per protein identification. Strict principles of parsimony were applied for protein grouping. Chromatograms were aligned for feature mapping and area-based quantification using unique and razor peptides. Normalization was performed on total peptide amount and scaling on all averages.

Luminex assay on conditioned media

To quantify secreted immunomodulatory proteins and growth factors, conditioned media were analyzed with the Procarta 37-plex as previously described [34] and a custom Bio-Rad 6-plex based on the Human Inflammation Panel 1 (BioRad, Cat# 171AL001M). For both assays, samples were run in duplicate on a Bioplex 200 instrument (BioRad, Cat #171000201). Data were analyzed with the Bioplex Manager Software. The lower level of quantification for each analyte is listed in the figure legend and is based on the manufacturer's quantifications.

DNA preparation

Cell pellets were frozen at -80°C until DNA extraction. DNA was extracted using a Qiagen FlexiGene kit (Qiagen, Cat # 51206) according to the "Isolation of DNA from cultured cells" protocol. Two to four samples were extracted per sample type and DNA was dissolved in 100-500

μ l of the kit's FG3 buffer. If the sample was viscous after the heat incubation, it was sonicated for 3-6 s on ice. DNA was quantified using a Nanodrop One spectrophotometer.

Statistical analysis

Data are represented as the mean \pm standard error of the mean (SEM) of four biological replicates. For Zetaview NTA, each sample was processed at least thrice and the CV was calculated. All secreted protein data was normalized to the total DNA calculated for that sample set. Statistical analysis of secretion data was performed using GraphPad Prism 9.0 (GraphPad Software) by first log transforming the data prior to conducting a one-way ANOVA test with a post-hoc Bonferroni correction applied ($p < 0.05$). Zetaview NTA data were also analyzed in GraphPad Prism using a Kruskal-Wallis test and post-hoc Dunn's correction.

For the mass spectrometry and Poly(A)seq data, significance was determined with an adjusted p-value < 0.05 and $1 < \log_2$ fold change < -1 . For the miRNAseq data, a p-value < 0.05 and $1 < \log_2$ fold change < -1 were cut-off values. For heatmaps, the rows were organized by hierarchical clustering using agglomerative clustering with Ward's minimum variance method and the Euclidean distance metric.

Data availability

Data has not yet been uploaded to GEO but will be uploaded prior to manuscript submission.

4.4 Results (Original by LNB; edited by TGG and JKS)

Differentiation of trophoblast stem cells alters cell permissibility to ZIKV.

Since maternal ZIKV infection early in pregnancy is associated with a high rate of pregnancy loss and fetal malformations, an early-gestation in vitro macaque TSC model was used to determine which trophoblast cell types are permissive to infection. Preliminary time-course experiments testing two to three multiplicities of infection (MOIs) were performed for each cell type to assess viral replication through 72 hrs of culture (Figure 1A). The amount of infectious virus detected in TSCs and syncytiotrophoblasts (ST3Ds) plateaued at 60 and 48 hrs, respectively. For TSCs, an increase in infectious virus was observed with an MOI of 5 resulting in more virus production than an MOI of 1 or 10. In ST3Ds, more infectious virus was produced at an MOI of 10 than an MOI of 1. An increase in infectious virus was not observed during the EVT time course; however, to determine if the extracellular matrix (collagen-coated wells and Matrigel supplemented to the media) used to differentiate EVTs masked accurate quantification of ZIKV, a subsequent experiment was performed in which ZIKV was inoculated to collagen-coated wells containing media supplemented with Matrigel that lacked cells (“no cells”). A ~100-fold decrease in infectious virus was observed in the “no cells” wells after inoculation confirming that the matrix did not “trap” virus being released by EVTs, and thus that there was indeed limited infection in EVT cultures (Figure 1A). Compared to the amount of virus detected in the “no cells” wells at 60 hrs (mean 2.2 plaque forming units (PFU) \log_{10}/ml), there was over 100-fold more virus (mean 3.8 PFU \log_{10}/ml) in the EVT samples at 60 hrs. The half-life of ZIKV is ~12 hours [45], which supports the decrease in infectious virus observed over time in the “no cell” wells. For subsequent EVT infection experiments, cells were inoculated at an MOI 5 and cultured for 60 hrs.

The analysis of extracellular vesicles (EVs) as a readout of cell function was of great interest in this study. For that reason and for the desire to minimize cytotoxic effects, the length of culture was chosen based on when the amount of virus being produced began to plateau, with the idea being that EVs released by cells during peak viral infection would show the most impact. MOIs were chosen based on whether there was a substantial increase in viral production. An MOI of 5, 10, and 5 were used to infect the TSCs, ST3Ds, and EVT_s, respectively. Inoculated and mock-inoculated control TSCs were cultured for 60 hrs, while ST3Ds and EVT_s were cultured for 48 and 72 hrs, respectively. At the culture endpoint, cells and culture media were collected to assess the cellular impact of ZIKV and to isolate EVs for cargo analysis, respectively. Supplemental Figure 1A illustrates the sample collection paradigm. After cells were exposed to ZIKV or treated as mock-infected controls, an aliquot of culture medium was immediately collected to assess baseline (initial=i) viral titers. After 48-72 hrs of culture, a final (f) aliquot of medium was collected to assess viral replication by plaque assay. The quantity of infectious virus detected in the TSC and ST3D samples increased significantly by ~100-fold between the initial and final time points within the respective cell type ($TSC_i = \text{mean } 4.20 \log_{10} \pm \text{SEM } 0.16$, $TSC_f = \text{mean } 6.35 \log_{10} \pm \text{SEM } 0.17$, $ST3D_i = \text{mean } 4.53 \log_{10} \pm 0.04$, $ST3D_f = \text{mean } 6.32 \log_{10} \pm 0.07$; Figure 1B). A minimal change in infectious virus was detected in the EVT samples ($EVT_i = \text{mean } 4.28 \log_{10} \pm 0.14$, $EVT_f = \text{mean } 4.58 \log_{10} \pm 0.23$; Figure 1B).

Cellular ZIKV infection was validated by evaluating the presence of ZIKV envelope (E) and non-structural (NS2B) within inoculated and mock-inoculated trophoblasts. ZIKV E and NS2B

proteins were detected via Western Blot in the ZIKV exposed cells but not in uninfected (control) cells (Figure 1C). Neither ZIKV protein was observed in inoculated EVT samples, supporting the minimal increase of infectious virus from the plaque assays. Positive ZIKV E protein detection via immunofluorescent staining further supported that TSC and ST3D are clearly permissive to ZIKV, while few EVTs stained positive for ZIKV. (Figure 1D). Full Western Blot and isotype control immunofluorescence staining images are shown in Supplemental Figures 2 and 3, respectively.

To determine if the MOIs chosen for infection induced a cytotoxic effect, cellular Lactate Dehydrogenase (LDH) was assayed in each cell type (TSC, ST3D, and EVT). Vero cells were used as a positive control as they are highly permissive to ZIKV, and cytopathic effect is observed following ZIKV infection (Figure 1E). If ZIKV induced cell death there would be less LDH detected in infected cells than in the controls, which would result in a ZIKV: control ratio less than one. However, a consistent decrease in LDH absorbance was not observed in trophoblasts, whereas a decrease in the LDH ratio was observed in Vero cells at 48 hrs that continued through 86 hrs. These data suggest that ZIKV did not induce cell death in the trophoblast cells used in this study. These findings further support the MOI and length of culture chosen for this study.

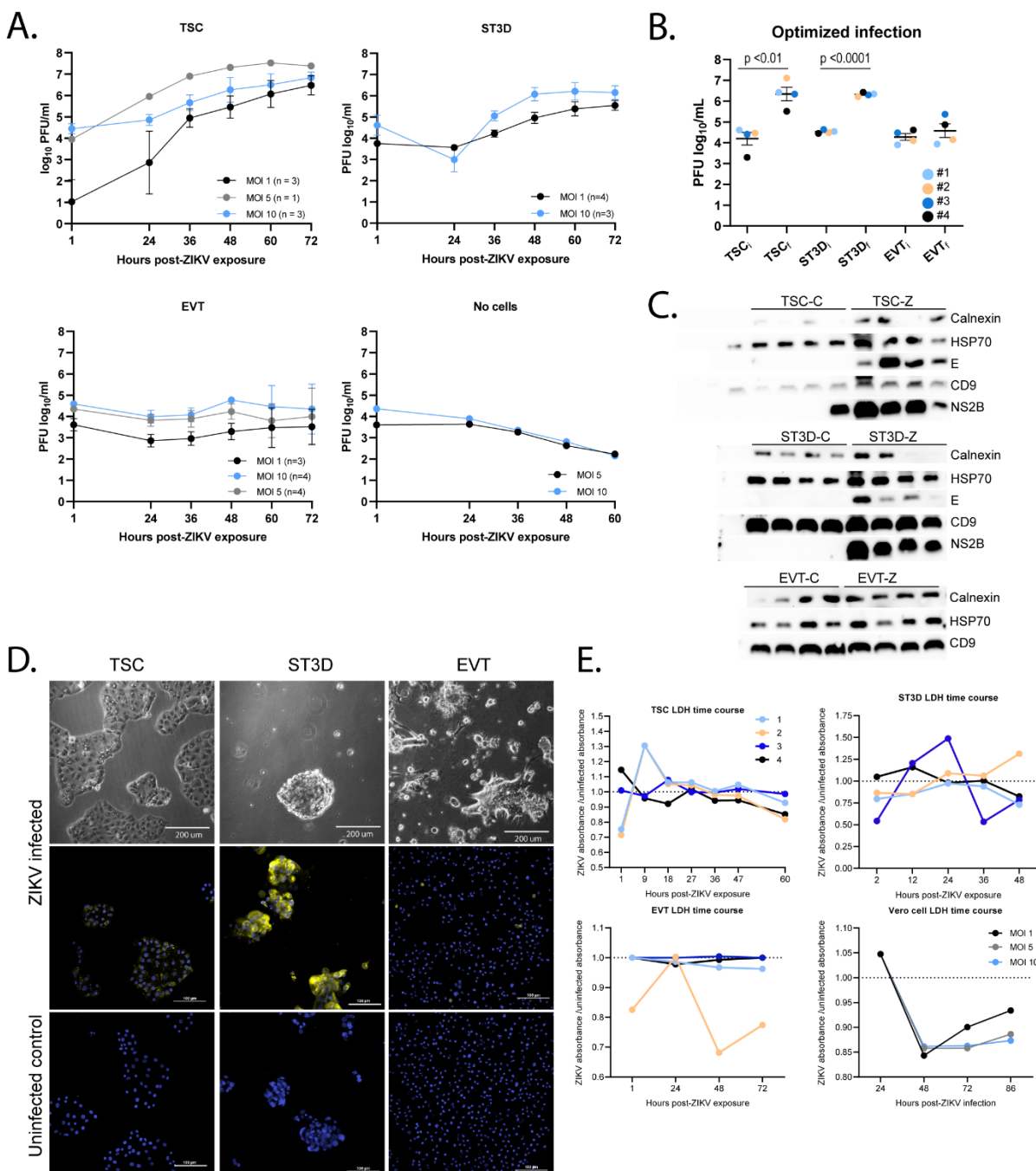
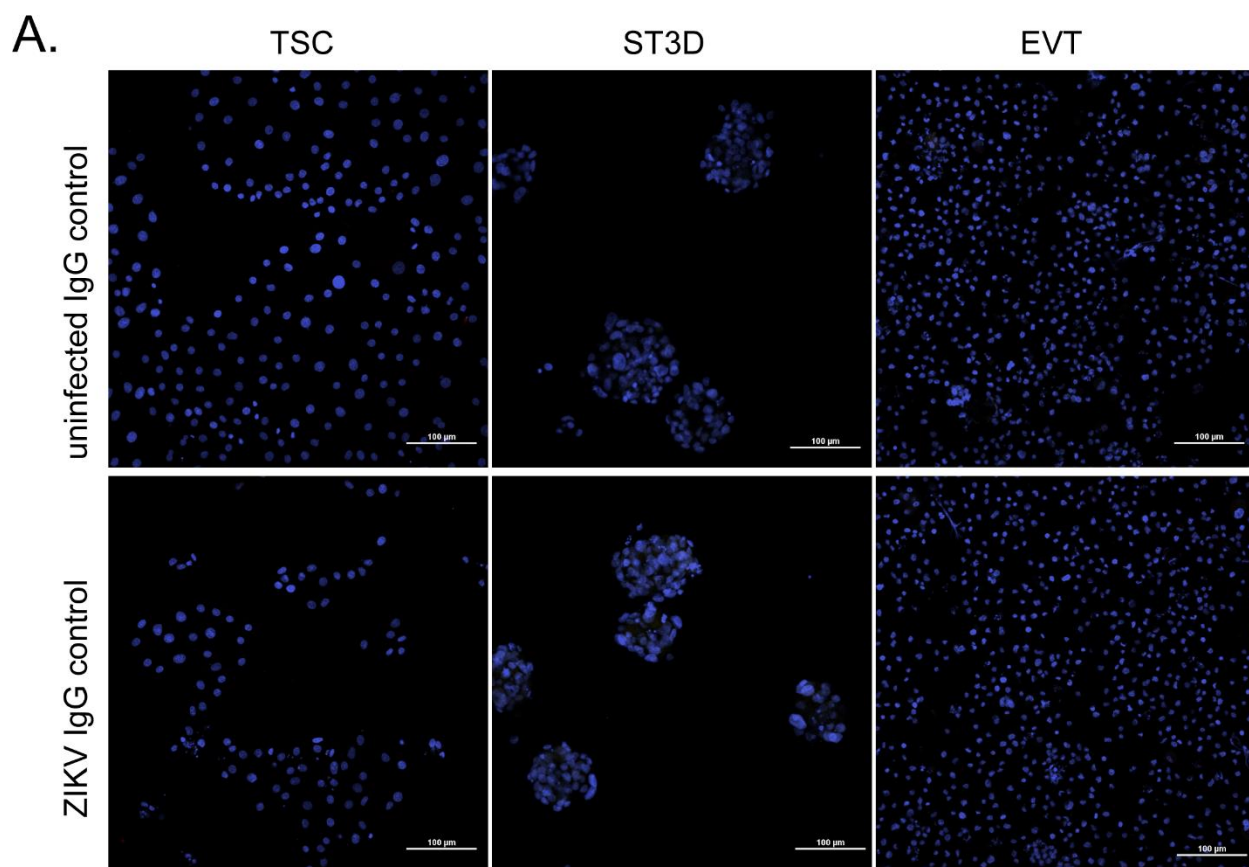
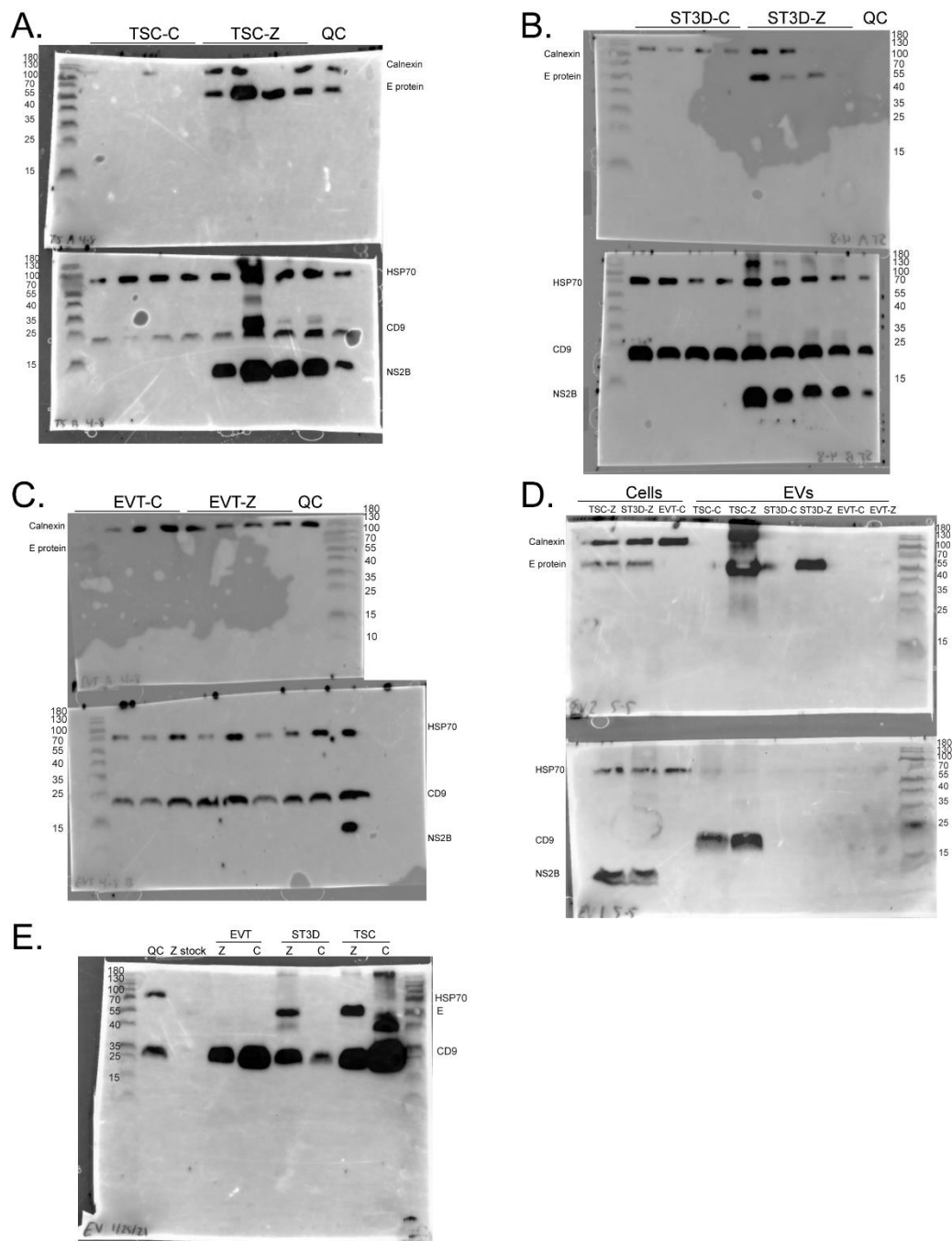


Figure 4.1. Early gestation trophoblast cells are permissive to ZIKV infection. *A)* Quantification of infectious virus by plaque assay upon testing the duration of culture and multiplicity of infection (MOI) dose response for each cell type (TSC, ST3D, EVT, or “no cells”). The number of cell lines, *n*, is indicated within parentheses next to the MOI. The quantity of infectious virus detected at each time point represents accumulated virus over time since the previous time point from the same well. *B)* Quantification of infectious virus by plaque assay with optimized MOI and duration of culture (*i* subscript = initial time point; *f* subscript = final time point) for each cell type and cell line (indicated by circle color). The mean

plaque forming units (PFUs) \pm the standard error of the mean (SEM) is shown for the four samples per group. Significance, determined with unpaired *t*-tests, is indicated directly on the graph. **C)** Western Blotting of ZIKV E, NS2B, CD9, Calnexin, and Heat shock protein 70 (HSP70; loading control) proteins for each cell line ($n = 4$) and cell type. Equal amounts of protein (3 μ g) were loaded into each lane. **D)** Immunostaining for ZIKV E protein. The top panel shows bright field images of trophoblasts after ZIKV exposure. ZIKV infected cells (middle panels) and control cells (bottom panel) were stained with an antibody against ZIKV E protein (yellow) and a nuclear stain (DAPI; blue). **E)** LDH time course data collected on TSCs, ST3Ds, EVT, and Vero cells. Data is presented as the mean of biological and technical replicates at each time point. The y-axis is presented as ZIKV LDH absorbance/control LDH absorbance, where a value > 1 indicates less cell death in ZIKV exposed cells and a value < 1 indicates more cell death in ZIKV exposed cells. Figure made by LNB.



Supplemental Figure 4.2. Rabbit IgG controls and ZIKV uninfected control images. A) Rabbit IgG controls on TSC, ST3D, and EVT cells to verify the ZIKV E antibody was specific. Figure made by LNB.



Supplemental Figure 4.3. Full Western Blots and control immunocytochemistry images. *Full Western Blots.* A-C) The full Western Blots of TSCs, ST3Ds, EVTs lysates are shown with the ladder merged with the stained blot. D) The Western blots completed on six EV lysates with three cellular lysates included as a control. E) A Western Blot completed on six of the EV lysates submitted for mass spectroscopy. Figure made by LNB.

ZIKV infection impacted cellular innate immune gene expression.

Next generation RNA sequencing was performed to assess the impact of ZIKV on the cellular transcriptome. Transcriptomic analysis by Poly(A)seq found 82 (52 upregulated, 30 downregulated) and 113 (90 upregulated; 23 downregulated) genes to be differentially expressed in infected TSCs and ST3Ds, respectively, compared to control with a greater proportion of the DEGs being upregulated in response to infection (Figure 2A, 2B). Figure 2C presents a Venn diagram of upregulated mRNAs within the three trophoblast cell types. Transcriptomic analysis identified 13 genes significantly upregulated by ZIKV infection in both ST3Ds and TSCs, including: APOL2, CXCL11, DDX58, IFIT2, IFNB1, IFNL1, INFL2, IFNL3, IRF1, ISG20, OASL, PARP14, and SCNN1D. No significantly down regulated genes were similar between ST3Ds and TSCs. PILR alpha-associated neural protein (*PIANP*) was the only gene found to be significantly different (ZIKV mean $15.25 \log_{10} \pm \text{SEM } 2.72$, control mean $0 \log_{10} \pm \text{SEM } 0$) in EVT_s exposed to ZIKV (Figure 2D).

Integrated Pathway Analysis (IPA) was performed on the TSC (Figure 2E) and ST3D (Figure 2F) data sets. IPA identified “role of hypercytokinemia/hyperchemokemia in the pathogenesis of Influenza” to be highly upregulated and the “coronavirus pathogenesis pathway” to be downregulated by ZIKV infection in TSCs and ST3Ds. The “role of PKR in interferon induction and antiviral response” was another top canonical pathway upregulated by ZIKV infection in TSCs (TSC-Z) (Figure 2E). Of the top five most significant diseases or functions identified by IPA in the TSC-Z cell mRNA data, four of them were related to viral replication and three were predicted to have decreased activation (data not shown).

The top canonical pathways upregulated by ZIKV infection in ST3D (ST3D-Z) cells included “interferon signaling”, “activation of IRF by cytosolic pattern recognition receptors”, “role of pattern recognition receptors in recognition of bacteria and viruses”, “systemic lupus erythematosus in B cell signaling pathway”, and “retinoic acid mediated apoptosis signaling” (Figure 2F). The “LXR/RXR activation” also was downregulated in ZIKV infected ST3D cells. Diseases and function IPA analysis of the ST3D-Z data predicts increased activation of the “antiviral response” and decreased “activation of viral infection,” “replication of viral replicon,” and “replication of RNA virus” (data not shown).

The expression of seven of genes (*PARP14*, *ISG20*, *DHX58*, *INFL1*, *DDX58*, *IFNb1*, and *OASL*) involved in the antiviral response and two genes (*MTIE* and *MTIX*) involved in the anti-apoptosis pathway [46, 47] were validated with qRT-PCR (Figure 2G). The trends in expression observed with qRT-PCR agreed with those identified by Poly(A)-seq analysis (Supplemental Table 3). TSC-Z or ST3D-Z samples had a significant increase in expression of six and seven genes, respectively, of these genes with only minor elevations in *PAPR14*, *DHX58*, *IFNL1*, *DDX58*, *IFNb1*, and *OASL* genes in EVTs (Figure 2G). A trend in decreased expression of *MTIE* and *MTIX* was confirmed in TSC-Z samples.

Potential receptors for ZIKV entry were detected in the Poly(A)seq data, including *AXL*, *TYRO3*, *MERTK*, and *HAVCRI* (*TIMI*) (Figure 2H) [31]. *DC-SIGN* was not detected. *AXL* and *HACVRI*

expression were greatest in TSCs whereas TYRO3 expression was greatest in EVTs. No significant difference in receptor expression was observed between infected and control cells. These findings suggest that receptor expression is not the limiting factor in EVT infection.

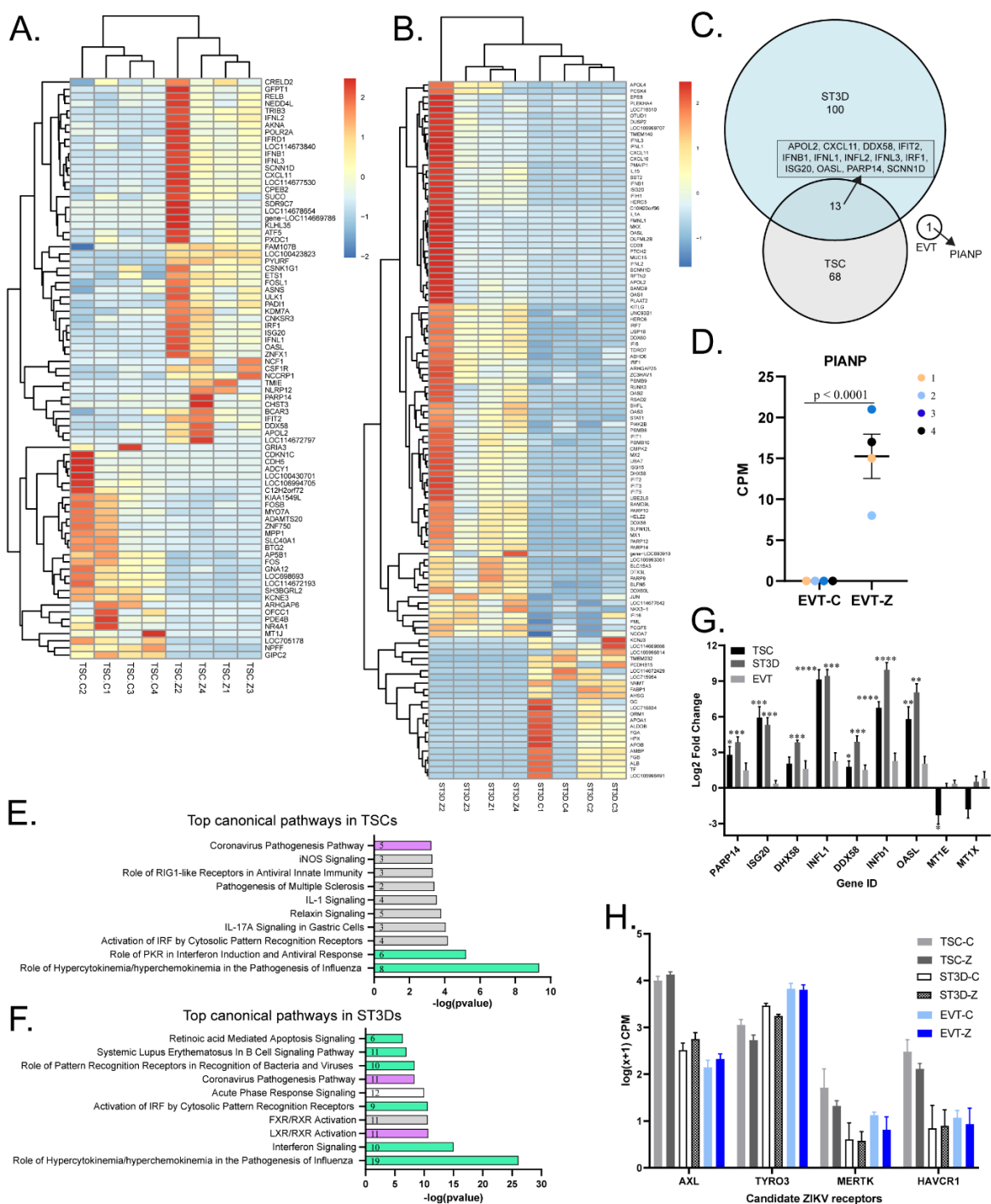


Figure 4.2. The impact of ZIKV on the cellular transcriptome. A-B) Heatmaps of significantly differentially expressed mRNAs in TSCs and ST3Ds. C) A Venn diagram of the number of genes upregulated by ZIKV infection in TSCs, ST3Ds, and EVTs. D) A scatter plot of PIANP mRNA expression in EVTs with

significance indicated on the graph. **E, F**). Top 10 canonical pathways identified in the TSC and ST3D datasets ($-\log_{10}$ (p-value)). Purple indicates a positive Z-score (decreased in ZIKV); green indicates a negative Z-score (increased in ZIKV); white indicates 0 z-score (no clear indication of whether the pathway is decreased or increased in ZIKV); and gray indicates unknown direction. The number of genes identified in each pathway are stated on the graph. **G**) A bar graph of differential mRNA expression (\log_2 fold change) validated by qRT-PCR in TSCs, ST3Ds, and EVT. Significance is depicted on the graphs (* $p < 0.05$; ** $p < 0.01$; *** $p < 0.001$; **** $p < 0.0001$). **H**) Normalized $\log(x + 1)$ transformed counts per million reads (CPM) determined by edgeR for candidate ZIKV receptors. Figure made by LNB.

Supplemental Table 4.3. qRT-PCR, DESeq2, and edgeR log fold change (log2FC) and significance (p-value/adjusted p-value) comparisons

Gene name	TSC						ST3D						EVT									
	qRT-PCR			DESeq2			edgeR			qRT-PCR			DESeq2			edgeR						
	log ₂ FC	p-value	log ₂ FC	p-value adj	log ₂ FC	FDR	log ₂ FC	p-value	log ₂ FC	FDR	log ₂ FC	p-value	log ₂ FC	p-value adj	log ₂ FC	FDR	log ₂ FC	p-value	log ₂ FC	FDR		
<i>PARP14</i>	2.8	2.40E-02	2.4	2.00E-02	2.4	3.50E-02	3.9	2.70E-04	3.7	1.80E-05	3.7	2.90E-05	3.7	1.80E-05	3.7	2.90E-05	1.5	1.60E-01	1	1.00E+00	1	1.00E+00
<i>ISG20</i>	5.9	3.20E-04	4.3	3.50E-03	4.3	1.80E-02	5.3	7.90E-04	4.7	9.50E-04	4.7	4.40E-03	4.7	9.50E-04	4.7	4.40E-03	0.4	7.20E-01	0	1.00E+00	0	1.00E+00
<i>DHX58</i>	2	4.50E-02	1.9	9.90E-02	1.9	1.70E-01	3.8	3.40E-03	2.9	2.30E-03	2.9	1.60E-03	2.9	2.30E-03	2.9	1.60E-03	1.6	2.40E-01	0.8	1.00E+00	0.8	1.00E+00
<i>INFL1</i>	9.1	1.40E-05	6.6	6.30E-06	6.6	2.40E-05	9.4	8.10E-04	6.4	5.60E-06	6.4	1.40E-05	6.4	5.60E-06	6.4	1.40E-05	2.3	1.90E-01	0.9	1.00E+00	0.9	1.00E+00
<i>INFB1</i>	6.7	4.40E-05	4	1.70E-04	3.9	1.30E-03	9.9	2.80E-05	9.9	1.20E-16	9.7	2.30E-14	9.7	2.30E-14	9.7	2.30E-14	2.3	8.60E-02	3	8.30E-01	2.9	5.60E-01
<i>MTIE</i>	-2.3	3.40E-02	-2.2	4.20E-02	-2.2	7.90E-02	0	9.30E-01	0.5	1.00E+00	0.5	1.00E+00	0.5	1.00E+00	0.5	1.00E+00	0.4	7.60E-01	0.2	1.00E+00	0.2	1.00E+00
<i>MTIX</i>	-1.8	9.40E-02	-3.1	3.00E-02	-3.1	9.00E-02	0.5	5.20E-01	0.9	1.00E+00	0.9	1.00E+00	0.9	1.00E+00	0.9	1.00E+00	0.8	6.90E-01	1.3	1.00E+00	1.3	1.00E+00
<i>OASL</i>	5.8	2.30E-03	6.4	3.10E-03	6.3	7.00E-03	8	1.60E-03	7.8	3.70E-05	7.8	1.50E-04	7.8	3.70E-05	7.8	1.50E-04	2	2.00E-01	0.8	1.00E+00	0.8	1.00E+00
<i>DDX58</i>	1.8	2.70E-02	1.6	1.30E-02	1.6	1.80E-02	3.9	8.00E-04	2.9	9.50E-09	2.9	3.70E-09	2.9	9.50E-09	2.9	3.70E-09	1.5	6.70E-02	0.7	1.00E+00	0.7	1.00E+00

ZIKV infection altered the cellular miRNAome.

Placental miRNAs are temporally expressed throughout gestation and have critical roles in trophoblast differentiation and function [48, 49], thus the miRNAome was profiled to assess alterations in expression relative to infection. miRNA-seq identified 849 miRNAs in the TSCs, 704 miRNAs in ST3Ds, and 668 miRNAs in the EVT_s were detected. In the TSCs, 5 miRNAs were significantly decreased and 10 significantly increased in infected versus control cells (Figure 3A). Despite modest infection of EVT_s, as determined by plaque assay of culture media (Figure 1A), 19 miRNAs were significantly increased in infected versus control EVT_s (Figure 3B). Although ST3Ds were highly infected, only PC-3p-49144_396 (ZIKV 3.89 CPM \pm 1.38 SEM, control 1.48 CPM \pm 0.30 SEM) and mml-miR-324-3p (ZIKV 2.88 CPM \pm 1.59 SEM vs control 0.40 CPM \pm SEM 0.81) had significantly ($p < 0.05$) increased expression in ST3D-Z cells (Figure 3C). PC-3p-49144_396 has sequence homology to the human miRNA hsa-miR-328-3p (Supplemental Table 4).

The chromosome 19 miRNA cluster (C19MC) is exclusive to primates and predominantly expressed in the placenta [49], and antiviral roles have been associated with miRNAs of this cluster [50]. Expression of C19MCs miRNAs were compared across all infected and control trophoblasts (Figure 3D). The miR-371-3 miRNA cluster is also highly expressed in the placenta [49] and was assessed in infected and control trophoblasts (Figure 3E). One of the TSC lines (4) expressed very high levels of the miR-371-3 miRNAs compared to the other TSC lines or other cell types. C19MC and C371-373 expression was not consistently impacted by infection across or within cells, but rather individual cell lines had different responses to infection.

To determine how ZIKV infection impacted miRNA expression amongst cell types, miRNAs found to be significantly differentially expressed in one cell type were examined in the other cell type datasets (Supplemental Figure 4A). miR-324-3p, miR-99b-3p, miR-335-5p, miR-145-3p, miR-132-5p, miR-421, miR-497-5p, miR-671-5p, miR-491-5p, mir-1249, and miR-7189-3p were upregulated by ZIKV infection in all three cell types (TSC, ST3D, EVT). miR-30b-3p, miR-30d-3p, and mir-517b were downregulated by ZIKV infection in all three cell types. miR-145-3p was only detected in EVTs and was significantly increased by ZIKV infection.

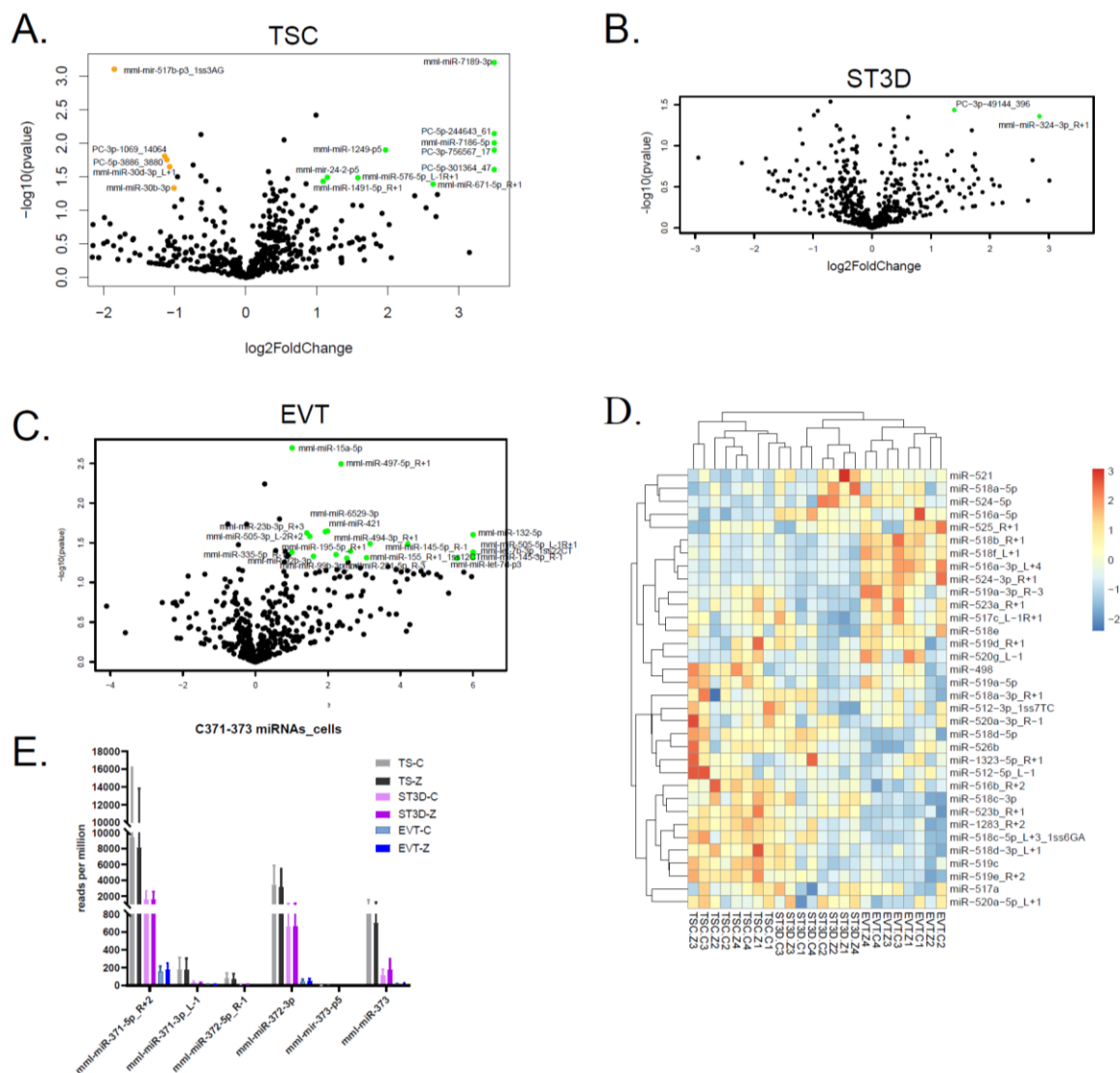
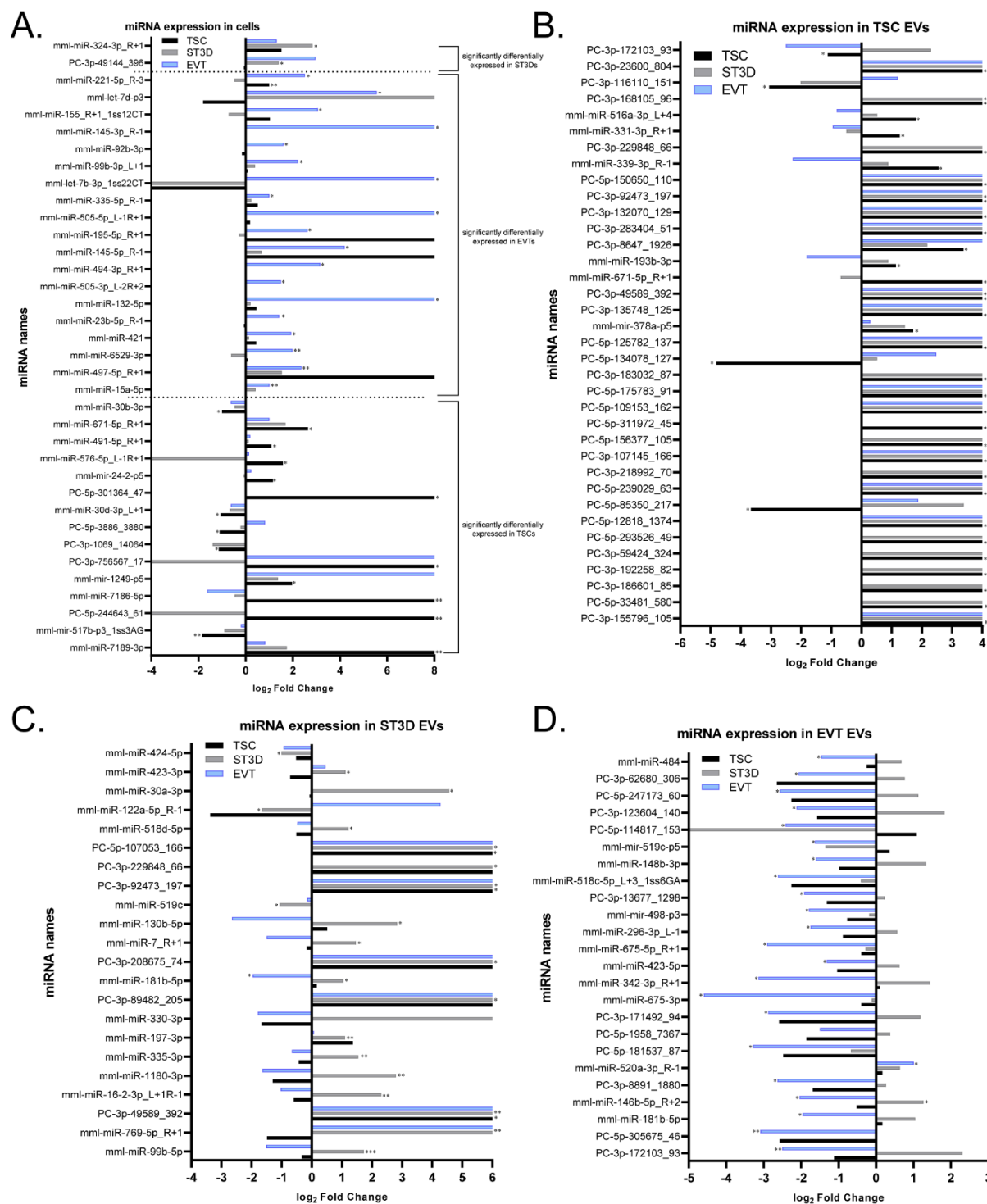


Figure 4.3. The impact of ZIKV exposure on the cellular miRNAome. *A)* Significantly differentially expressed miRNAs are highlighted in the volcano plots for TSCs and *(B)* EVT mRNA expression. Orange indicates a decrease in ZIKV samples and green indicates an increase. *(C)* Significantly differentially expressed miRNAs detected within the ST3Ds depicted as two scatter plots. Significance is indicated on the graphs. *(D)* C19MC and *(E)* miR-371-2 cluster expression was compared among all samples with the Euclidean distance metric. Figure made by LNB.



Supplemental Figure 4.4. miRNA comparison across cell types. *A)* A bar graph of miRNAs found significantly differentially expressed in the different cell types. *B-D)* Bar graphs of miRNAs found significantly differentially expressed in TSC, ST3D, and EVT EVs. A positive log₂ fold change indicated upregulation in ZIKV infected cells/EVs and a negative log₂ fold change indicated downregulation. miRNAs

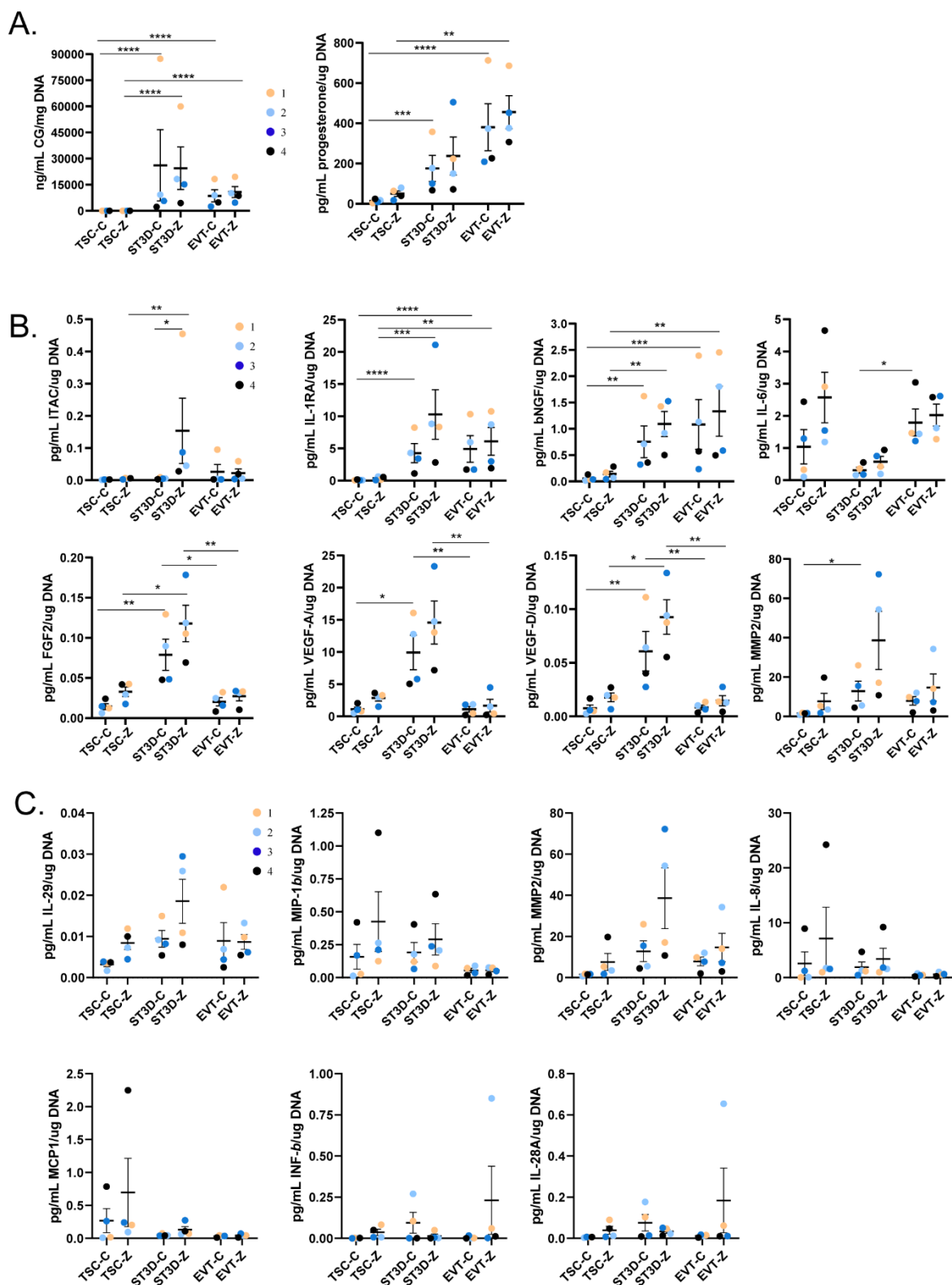
with an infinite fold change (positive or negative) reach the edge of the x-axis. Significance is indicated on the graphs ($p < 0.05$; ** $p < 0.01$, *** $p < 0.001$). Figure made by LNB.*

ZIKV infection did not alter trophoblast secretion of hormones and modestly impacted cytokine secretion.

To assess the impact of infection on trophoblast function, secretion of hormones, cytokines, chemokines, and growth factors within conditioned cell culture media was assayed. Chorionic gonadotropin (CG) and progesterone are two key hormones in the recognition and maintenance of pregnancy [51]. There were no differences in CG or progesterone secretion between infected and control samples for TSC, ST3D, and EVT_s (Supplemental Figure 5A). TSC_s secreted minimal CG or progesterone, in agreement with our previous report [11]. ST3D_s and EVT_s secreted significantly more CG than TSC_s. Control and ZIKV EVT_s secreted significantly more progesterone than control and ZIKV TSC_s ($p < 0.001$, $p < 0.01$, respectively). Control ST3D_s also secreted significantly more progesterone than control TSC_s ($p < 0.001$).

Cytokines and growth factors associated with infection and the inflammatory response were also quantified (Supplemental Figure 5B). ITAC (CXCL11) was significantly upregulated in infected ST3D_s compared to control (a similar trend was observed in CXCL11 mRNA expression, Figure 2B), and was more highly expressed in infected ST3D_s compared to infected TSC_s. Otherwise, no significant differences in cytokine or growth factor secretion between infected and control cells were observed.

While there was not an impact of infection, there were significant differences in the secretion of a number of cytokines and growth factors between trophoblast cell types (Supplemental Figure 4B). Control and infected ST3D and EVT_s expressed significantly more IL-1RA and bNGF than TSC_s. IL-6 was significantly upregulated in control EVT_s compared to control ST3D_s. FGF-2, VEGF-A, and VEGF-D expression was significantly increased in ST3D cells compared to TSC_s or EVT_s. Conversely, some cytokines and growth factors showed no significant differences across cell type or infection status (Supplemental Figure 5C). A list of analytes that were not detected is presented in the Methods section.



Supplemental Figure 4.5. Hormone, cytokine, and growth factor secretion by cell type and infection group. *A) Individual scatter plots of CG and progesterone and cytokines and (B) growth factors are shown. C) Luminex assay data on seven analytes (MIP-1b, MCP1, IFN-beta, MMP2, IL-8, IL-28A, and IL-29) which were detected in more than five samples but has no significant changes in expression between ZIKV and control or between cell types. All secretions were normalized to cellular DNA quantity. Significance is depicted on the graphs (* $p < 0.05$; ** $p < 0.01$; *** $p < 0.001$; **** $p < 0.0001$). Figure made by LNB.*

Characterization and impact of ZIKV infection on EVs

Trophoblast-secreted EVs were isolated from ZIKV and control cell conditioned media to assess changes in their physical properties (e.g. size or quantity) and cargo (e.g. RNA and protein) following ZIKV exposure. EV samples were characterized by Zetaview nanoparticle tracking analyzer (NTA; Figure 4A), transmission electron microscopy (TEM; Figure 4B), and Western Blot (Figure 4C). Collectively, the results of these analyses support the enrichment of trophoblast EVs by the methods employed.

A consistent trend towards increased particle size was observed in TSC-Z and ST3D-Z EVs compared to their controls (Figure 4A). This trend also was seen with EVT samples, which were not widely infected. No differences in particle concentration were observed in any cell type, although Figure 4A shows that TSCs tended to release fewer EVs. Six EV samples from control and ZIKV exposed cells (two from each cell type) were imaged with TEM to verify the appropriate shape and size of EV particles (Figure 4B).

To determine if ZIKV proteins were packaged into EVs, EV preparations were assessed for E and NS2B proteins by Western Blot. The ZIKV E protein was readily detected in the TSC-Z and ST3D-Z EV samples with little detected in the EVT-Z EV samples and none in any controls via Western Blot (Figure 4C; full blots are shown in Supplemental Figure 3D). Since ZIKV infection was not widespread in the EVT cultures, it is not surprising that the E protein was not detected. The presence of two proteins commonly enriched in EVs, CD9 and HSP70, was also determined. CD9 was more highly presented in the two TSC EV (one C and one Z) samples compared to the cell samples or EVs from ST3D or EVTs. Additionally, Calnexin, an ER resident protein not expected to be present within EVs, was confirmed to be absent from all EV samples. In addition, Calnexin was observed in cell samples along with CD9 (Figure 1C). Interestingly, a higher molecular weight cross-reactive band was seen in the TSC-Z sample, however calnexin was not detected in EVs by mass spectroscopy data so it is unlikely that the cross-reactive protein is calnexin. As a control, three cell samples were evaluated alongside the six EV samples (Supplemental Figure 3D). In addition, EV samples submitted for mass spectroscopy were stained for CD9 (Supplemental Figure 3E).

To assess whether ZIKV virions were present in the EV preparations, EVs were stained with a fluorescently labeled ZIKV E antibody and analyzed by Zetaview NTA. EV preparations and concentrated ZIKV stock (positive control) were analyzed under scatter and fluorescent modes (Figure 4D and 4E, respectively) and the average number of particles were calculated. Through this analysis, the total number of particles, the number of non-EV contained ZIKV-E virions (based

on a particle size of ~50 nm and fluorescence), and the number of ZIKV-E-associated EV particles (based on a particle size > 50 nm along with positive fluorescence) were quantified.

Zika virions are ~ 50 nm in size [35] and a shift to the left was observed in the “ZIKV stock” histogram indicative of the abundant presence of ZIKV virions (Figure 4D) (larger particles in this preparation may represent Vero cell-secreted EVs). The fluorescence histogram of EVs isolated from ZIKV cultured trophoblasts, termed “ZIKV” in the figure, showed that the size of particles ranged from ~50-300 nm (Figure 4E). The detection of ZIKV E protein in particles that are larger in size than virions suggests that the protein was associated with the EVs. To further support these data, the number of particles detected in the size range of ZIKV (~50 nm) were quantified in the main 24 EV samples (same data seen in Figure 4A) and the percentage of particles between 50 and 54 nm was calculated (Figure 4F). ZIKV ST3D and EVT EV samples contained fewer “ZIKV-sized” particles than controls, again suggesting Zika virions were not abundant in the EV samples. Overall, these data indicate that ZIKV E protein is a component of EVs.

DAVID enrichment analysis was used to further verify the mass spectroscopy and Poly(A)-seq data gathered from EVs (Figure 5A and 5B). Proteins identified in among all 24 EV samples (ZIKV and control) were pooled and analyzed with DAVID. The results showed high enrichment of “extracellular exosome” (Figure 5A). Other highly enriched cellular components include membrane, plasma membrane, and cytosol, as expected. Based on the top 1000 genes identified in the eight EV Poly(A)-seq samples, the most enriched cellular component also was “extracellular exosome” (Figure 5B). Lastly, IPA on all proteins detected in the TS, ST3D, and EVT EV mass

spectroscopy data show that ~50% of proteins isolated were cytoplasmic with ~20-25% associated with the plasma membrane (Figure 5C). Enzymes, transporter proteins, kinases, transcription regulators, translation regulators, transmembrane receptors, and peptidases were some of the more abundantly detected protein types (Figure 5D). Altogether, these data support the integrity and authenticity of these trophoblast-produced EV preparations.

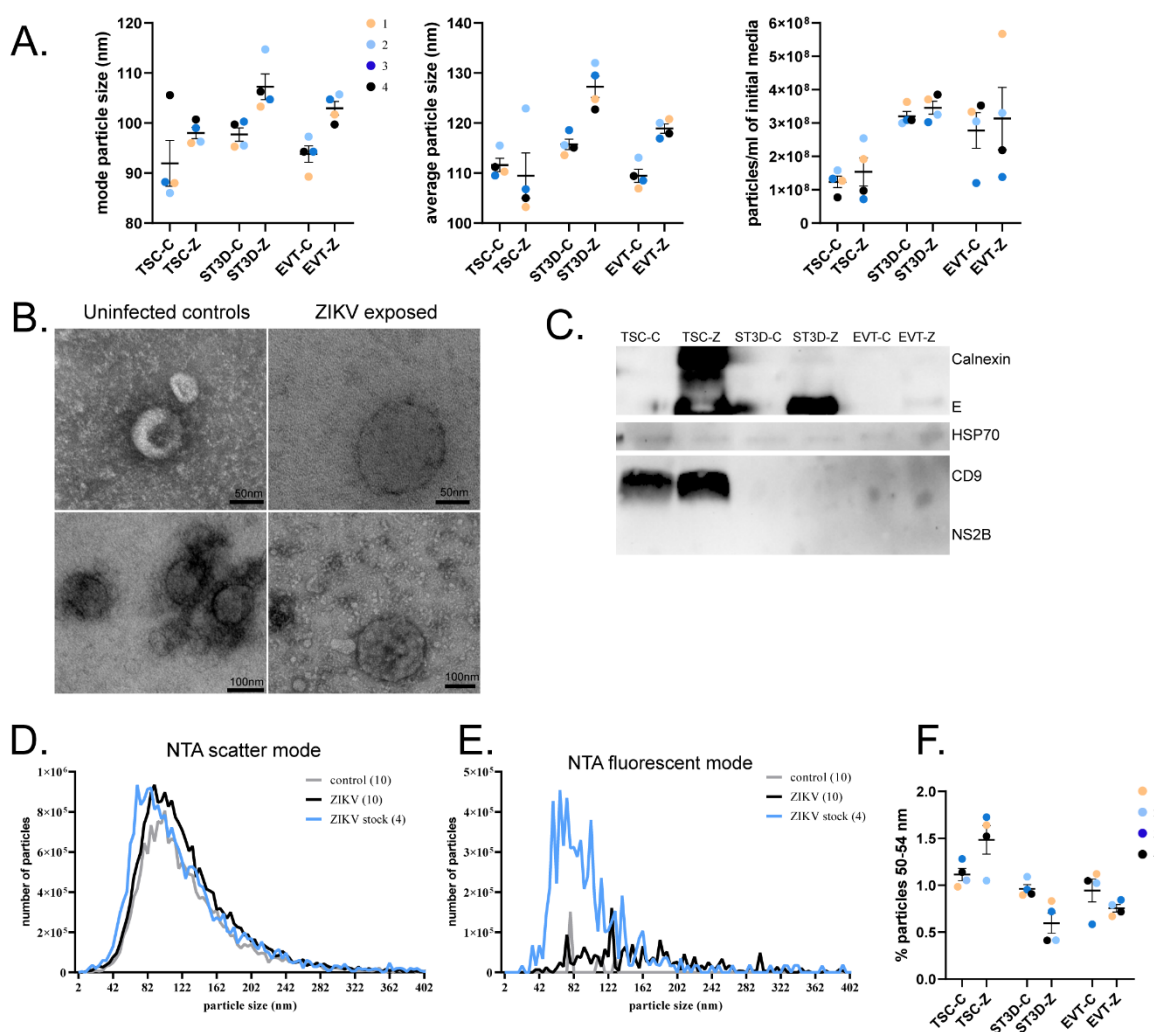


Figure 4.4. EV characterization from trophoblast-conditioned media. A) NTA analysis of the mode and average particle size and the concentration of particles presented as the particles/ml on

all 24 EV samples. B) TEM images of four EV samples (two control and two ZIKV) with scale bars included. C) Western Blots from cell and EV samples for ZIKV E, ZIKV NS2B, Calnexin, HSP70, and CD9. D) EV samples were characterized with NTA scatter mode and (E) fluorescent mode. The average number of particles detected across the control samples, ZIKV samples, and ZIKV stock were plotted. The number of samples is indicated in the parentheses. F) The percentage of “ZIKV-sized” particles (50-54 nm) was calculated for all 24 EV samples and is plotted by treatment group. Figure made by LNB.

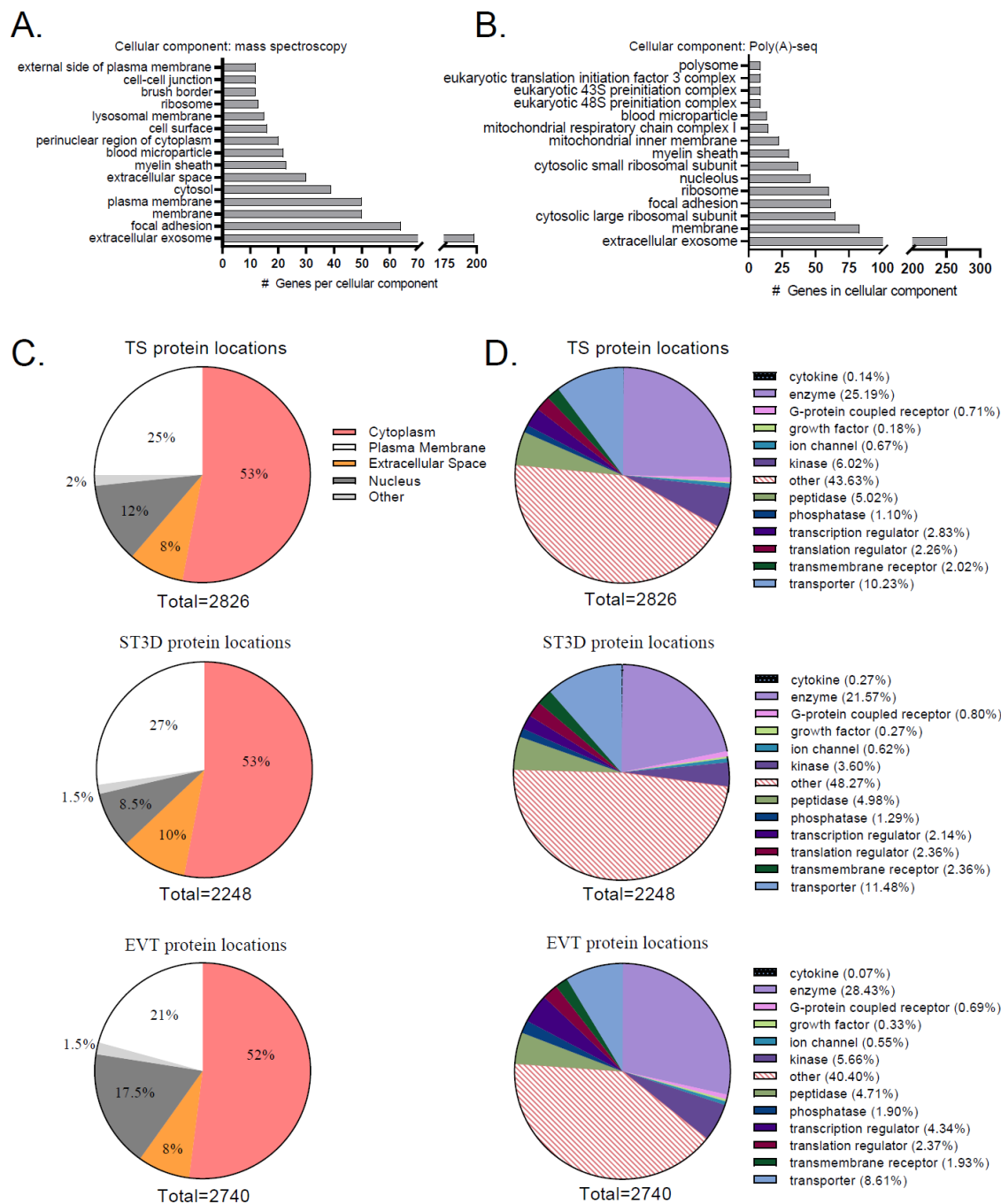


Figure 4.5. EV verification analyses and protein information analyses. *A)* The 392 proteins identified in all 24 EV samples and were analyzed with DAVID enrichment. The bar plot shows the top cellular components. *B)* DAVID pathways enriched on the top 1,000 genes detected among the eight EV samples by Poly(A)-seq. For DAVID enrichment analysis, a minimum of five genes for that pathway/process and an

adjusted p-value < 0.05 (Benjamini-Hochberg correction) were required. C-D) IPA on all proteins detected in the TSC, ST3D, and EVT EV data provide the protein location and type. Figure made by LNB.

Mass spectroscopy analysis on EV proteins

Proteomic data analysis revealed that many proteins were significantly differentially detected in TSC (191 total: 180 up, 11 down), ST3D (75 total: 63 up, 12 down), and EVT EVs (128 total: 78 up, 50 down) released from ZIKV exposed cells (Figure 6A-C). Interestingly, unsupervised clustering of protein expression revealed that samples do not group by infection status.

Top diseases and biological functions predicted in TSC-Z EVs were decreased “death of embryo”, “necrosis”, “cell death of tumor cell lines,” “organismal death,” “apoptosis of tumor cell lines,” and “apoptosis” with increased prediction of “organization of cytoplasm,” “viral infection,” “infection of cells,” and “organization of cytoskeleton” (Figure 6E upper graph). The topmost significant predicted canonical pathways increased in TSC-Z EVs were tRNA charging, EIF2 signaling, purine nucleotide biosynthesis, actin cytoskeleton signaling, Rho GTPase signaling, and RhoA signaling (Figure 6E lower graph).

Top diseases and biological functions predicted in ST3D-Z cells were decreased death, lifespan, and apoptosis with enrichment for infection and viral infection (Figure 6F upper graph). ZIKV infection of ST3Ds was predicted to impact various pathways but directional shifts were not identified (Figure 6F lower graph). The BAG2 (Bcl2-associated athanogene 2) signaling pathway is enriched in the ST3D samples.

Top diseases and biological functions predicted in EVT-Z EVs were decreased degranulation of various cells and decreased adhesion of immune cells (Figure 6G upper graph). Despite low EVT infection, EVs released from EVT-Z had altered granzyme A and glucocorticoid receptor signaling (Figure 6G lower graph). EVT-Z EVs had increased NAD, Protein Kinase A, actin cytoskeleton, and 14-3-3 mediated signaling. Ferroptosis and p70S6K signaling were decreased in EVT-Z EVs.

To determine if there are trends in protein cargo shared among the three cell types, significant proteins detected by mass spectroscopy were compared. This comparison revealed two proteins common among the three cell types, eight proteins between TS and EVT, two proteins between ST3D and EVT, and 13 proteins between TS and ST3D (Figure 7H). The log₂ fold change is plotted for each of those proteins with a positive change indicative of increased presence in ZIKV EVs and negative change indicative of increased presence in control EVs. *TPM2*, *RPS14*, *RANBP1*, *PSMD12*, *PDLIM2*, *NMT1*, *MYH14*, *HNRNPF*, *EML4*, *DPP3*, *CAPNS1*, *Gm5621*, *SLC35F6*, *MACF1*, and *EEF1D* were increased in ZIKV EVs. *RPL31*, *CLSTN1*, and *IFI16* were consistently decreased in ZIKV-EVs. The other six genes (*LAMC2*, *PYCR3*, *KRT16*, *HAT1*, *FLNB*, *MAPT*, *KRT15*) were increased in some cell types but decreased in others.

In terms of placenta specific protein detection in EVs, MAMU-AG4 (NCBI ID: Q5TM80) was detected in all 24 samples. Endogenous retrovirus group FRD member 1 (Uniprot ID: A0A1D5R0I7) was detected in six of eight ST3D EV samples. Placenta growth factor (Uniprot

ID: A0A1D5R9B1) and pregnancy specific beta-1-glycoprotein 7 (Uniprot ID: F6YVT1) were detected in six of eight EVT EV samples. Pappalysin 1 (Uniprot ID: F6ZUN7) was detected in all ST3D and EVT EV samples but no TS EV samples.

Figure 4.6. EV proteomics analysis. *A-C) Heatmaps of significantly differentially detected proteins in TSC, ST3D, and EVT EV samples. E-G upper graphs) Top diseases and functions identified in the TSC, ST3D, and EVT EVs. E-G lower graphs) Top canonical pathways identified in the TSC, ST3D, and EVT EVs. Purple indicates a positive Z-score (predicted down in ZIKV); green indicates a negative Z-score (predicted up in ZIKV); white indicates 0 z-score (no clear indication of whether the pathway is decreased or increased in ZIKV); and gray indicates unknown direction. H) Log₂ Fold Change of genes identified in multiple cell types. A positive log₂ fold change indicated increased detection in ZIKV EVs and negative indicated decreased detection in ZIKV EVs. Figure made by LNB.*

The impact of ZIKV on EV poly(A) and miRNA cargo

A total of 24 EV samples were submitted for Poly(A)-seq and cDNA libraries could be prepared for eight samples (3 TSC-C, 1 TSC-Z, 2 ST3D-C, and 2 ST3D-Z). A total of 31,320 transcripts were identified of which 2,329 transcripts were detected in all eight EV samples. Conversely, 10,085 and 3,949 transcripts were specific to either control or ZIKV EV samples, respectively. When comparison was restricted to transcripts detected in a majority of samples (three-fifths of control or two-thirds of ZIKV-exposed; see Figure 7A for sample flow diagram), 871 and 602 transcripts were detected only in control or ZIKV EVs, respectively. A total of 66 and 35 transcripts were identified in all three ZIKV EV samples or all five control EV samples, respectively.

IFNL1 transcripts were only detected in EVs released by ZIKV infected cells. Two different interleukin 1 receptor antagonist (IL1RN) transcripts were detected in the control or ZIKV EVs, with each transcript being unique to either group (XM_001091833.4 and XM_015113137.2 in control or ZIKV, respectively) .

To determine what pathways were enriched in the ZIKV or control EV group, transcripts identified in a majority of samples in that group (602 and 871 for ZIKV and control, respectively) were uploaded to IPA (Figure 7B). Of the top 10 canonical pathways identified, only the aryl hydrocarbon receptor signaling pathway was decreased by ZIKV exposure. Otherwise, the pyridoxal 5'-phosphate salvage pathway, the salvage pathways of pyrimidine ribonucleotides, ferroptosis signaling pathway, sirtuin signaling pathway, and autophagy were increased by ZIKV exposure.

miRNAseq on EVs

TSC-derived EVs predominantly contained miRNAs that have not been previously annotated in the macaque reference genome. Overall, ZIKV infection resulted in more of an increase in miRNA detection rather than decrease, except for EVT EVs. A total of 35 miRNAs were detected at significantly different levels between ZIKV exposed and control TSC EVs (Figure 7E). Three miRNAs (PC-5p-85350_217, PC-5p-134078, and PC-3p-116110_151) were significantly decreased in the TSC ZIKV EV samples while 32 were increased. Of the three miRNAs with decreased expression in TSC ZIKV EVs, only PC-3p-116110_151 was detected in one of the TSC samples and none of the others were detected in any cell type. Twenty-three miRNAs were significantly differentially detected between ZIKV exposed and control ST3D EVs (Figure 7F). Three miRNAs (miR-122a-5p, miR-519c, and miR-424-5p) were significantly decreased in the ST3D ZIKV EV and were slightly decreased in ST3D ZIKV cells (data not shown). PC-3p-229848_66 was significantly increased in ST3D EVs and was not detected in ST3D cells. For EVT EVs, 24 miRNAs were significantly differentially detected between ZIKV and control (Figure

7G). One miRNA (miR-520a-3p) was significantly increased in the EVT ZIKV EV samples and 23 were decreased.

miRNAs significantly differentially represented in one cell type's EVs were assessed in the other cell type EV datasets (Supplemental Figure 4B-D). In all, miRNAs significantly increased by ZIKV infection in TSC EVs were also increased (not significantly) in ST3D and EVT EVs with a few exceptions (Supplemental Figure 4B). PC-5p-134078_127 and PC-5p-85350_217 were significantly decreased in ZIKV TSC EVs but had increased presence in ST3D-Z and EVT-Z EVs (3.4 and 3.5 log₂ fold change, respectively), though not significantly. PC-3p-229848_66 was significantly increased in TSC and ST3D but was not detected in EVT EVs (Figure 7E, 7F, and Supplemental Figure 4C).

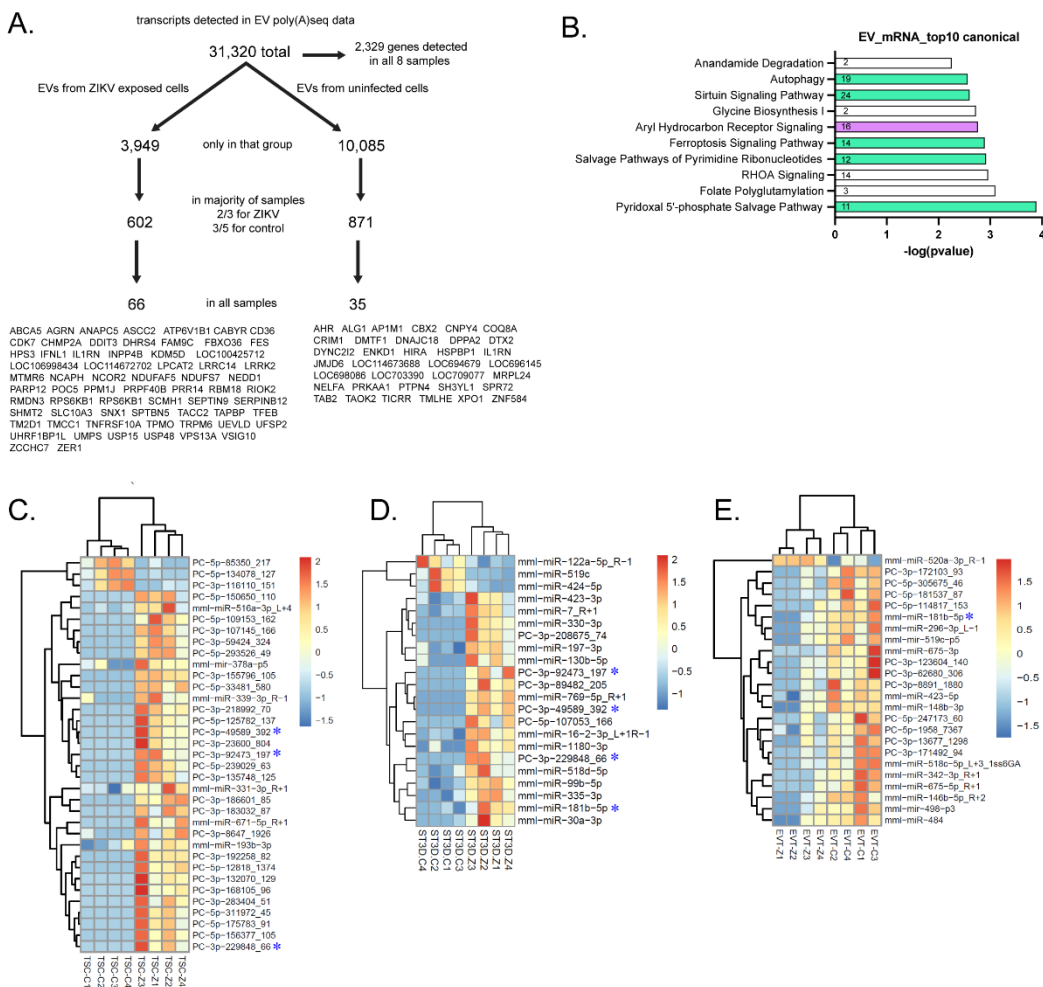


Figure 4.7. mRNA and miRNA transcripts vary between EVs from ZIKV exposed cells and uninfected controls. *A)* Schematic of the total number of transcripts detected across the eight EV samples, the number of transcripts solely detected in either the ZIKV or control samples, the number of transcripts detected in a majority (three of five control; two of three ZIKV samples) of the samples per group, and the number of transcripts detected in all samples of that group. The 66 and 34 gene IDs that correspond with transcripts identified are written below. *B)* Top 10 canonical pathways identified in a majority of either the ZIKV or control EV samples ($-\log_{10}(p\text{-value})$). Purple indicates a positive Z-score (decreased in ZIKV); green indicates a negative Z-score (increased in ZIKV); and white indicates 0 z-score (no clear indication of whether the pathway is decreased or increased in ZIKV). The number of transcripts identified in each pathway are stated on the graph. *C-E)* Significantly differentially expressed miRNAs detected in TSC, ST3D, and EVT EVs. A blue asterisk indicates that miRNA was found in other cell types. Figure made by LNB.

4.5 Discussion (Original by LNB; edited by TGG and JKS)

To determine which trophoblast cells are permissive to ZIKV infection and to understand how infection impacts function, we established a novel *in vitro* trophoblast cell model. TSCs and ST3Ds were highly permissive to infection, as observed by plaque assay, immunocytochemistry, and Western Blots. Conversely, EVT_s maintained a level of resistance to either ZIKV infection. The impact of ZIKV on cell gene expression was observed in the transcriptomic and miRNAome analyses. Infection impacted the size of EVs as well as their protein, mRNA, and miRNA cargo.

Experimental infection of *in vitro* macaque trophoblasts presented in this study supports the hypothesis that ZIKV can infect early gestation trophoblast cells. Significant virus production after TSC and ST3D ZIKV exposure, but minimal virus production after EVT exposure was observed. First trimester trophoblast cells, first trimester placental explants, and human embryonic stem cell (ESC)-derived trophoblast cells were shown to be permissive to ZIKV infection [31, 52, 53]. Maternal ZIKV infection early in pregnancy is associated with increased risk for pregnancy loss and more severe complications [2, 4, 12-16]. Despite the reported placental pathologies observed after a ZIKV infection, placental macrophages (Hofbauer cells) were often the only cells shown to contain ZIKV vRNA or protein with *in vivo* infected placentas [54]. However, human observations can be difficult to interpret because of uncertainty about the infecting viral dose, potentially uncertain times of infection during gestation, and limitations in the extent at which an entire placenta can be evaluated. Thus, additional *in vivo* studies during the first trimester are needed to verify trophoblast permissibility and potentially the interplay between trophoblasts and Hofbauer cells relative to trophoblast infection. Animal models of maternal ZIKV infection will

be critical for addressing the *in vivo* impact of infection on the cells of the maternal fetal interface during early gestation.

Elevated expression of IFNs and IFN pathway-associated genes in the transcriptome data in the current study was noted, which agrees with other studies [55-57]. The protective effect of IFNs against ZIKV infection has been reported by others [57-59]. Secreted type III IFNs, which are constitutively expressed in term trophoblast cells, have been reported to protect other cells against ZIKV infection [57]. Trophoblast cells derived from human ESCs, which are described as primitive trophoblasts, expressed only low levels of type I and III IFNs [31]. However, in the current study IFN-beta (type I IFN) and IFNL1 and IFNL3 (type III IFNs) transcript abundance increased in ZIKV exposed cells. The different responses between human ESC-derived trophoblasts and the TSC-derived trophoblasts in the current study suggests that the trophoblasts derived from TSCs utilized in the current study are more representative of a different developmental stage than trophoblasts derived from human ESCs. It should be noted that changes in IFN concentrations measured by Luminex assay were not detected in response to ZIKV infection, which could be due to suboptimal cross-reactivity or sensitivity of the Luminex assay with the macaque protein, or translational block of the mRNAs detected in RNAseq experiments.

Based on the transcriptomic and qRT-PCR data, ZIKV exposure induced a cellular immune response. Cells maintain multiple mechanisms to identify and curtail a viral infection, including inhibiting protein translation, degrading viral mRNA transcripts, and alerting immune cells via cytokine secretion [60, 61]. While an immune response is critical for mitigating infection, the

interplay between the trophoblast response and the maternal immune response to infection, and the impact of both on the semi-allograft fetoplacental unit remains unclear.

miRNAs also are important for the trophoblast antiviral response [62]. miR-24 was significantly increased in TSCs exposed to ZIKV and is involved in antiviral functions against RSV and influenza viruses via the MAPK pathway [63]. In the current study, PC-3p-49144_396 miRNA was significantly upregulated in ST3D-Z cells and had a trend towards increased levels in EVT-Z cells. PC-3p-49144_396 is homologous to the human hsa-miR-328-3p. Hepatitis B infection of HLE-2, a liver cell line, resulted in increased expression of hsa-miR-328-3p and increased cell injury [64]. The authors found that miR-328-3p mediated its effect via Forkhead box protein O4 (FOXO4) regulation [64]. FOXO4 was not differentially expressed in the cells used in the current study. mml-miR-324-3p was significantly increased in ST3D-Z cells and increased (although not significantly) in EVT-Z and TSC-Z cells. miR-324-3p also was detected in greater quantities in Hepatitis B infected cells, which promoted cellular proliferation, migration, and invasion [65]. Increased levels of PC-3p-49144_396 and mml-miR-324-3p in infected cells offer two potential candidates for further study in placental viral infections.

ZIKV infection decreased miR-122a-5p expression, which plausibly contributed to alterations cellular gene expression and stimulation of the type I IFN response [63]. *GNPDA1*, *MAP1B*, *MAPRE1*, *PKM*, *SERPINB6*, and *WARS1* were increased in TSC-Z EVs and IPA predicted miR-122a-5p, which regulates those genes, to be decreased in TSC-Z EVs. A decrease in the miRNA's expression was indeed observed in TSC-Z EVs. In addition to activating the type I IFN response

[63], miR-122a-5p inhibits cellular proliferation, migration, and invasion in Pancreatic ductal adenocarcinoma cells [66]. Thus, although the functional significance in placental development and trophoblast function remains to be investigated, several miRNA/mRNA target changes can be seen with ZIKV infection in cultured trophoblasts.

Despite changes in the miRNAome and transcriptome, the EVT_s in this study showed no evidence for substantial viral replication with ZIKV inoculation, which is unlike findings with other *in vitro* models. Two studies with placental explants showed that EVT_s were permissive to ZIKV [52, 53]; however, due to the model the quantity of virus produced specifically by EVT_s could not be determined. JEG3 cells, an EVT-like trophoblast cell line, were highly permissive to ZIKV infection [67]. The low level of EVT infection in the current study is an important finding as endovascular EVT_s that migrate into and remodel maternal spiral arteries are in direct contact with maternal blood and circulating cells of the maternal immune system. One possible explanation for lack of ZIKV replication in EVT cultures may be due to the extracellular matrix molecules present (col IV and Matrigel). Experimental infection of cancer cell lines with herpes simplex virus type 1 (HSV-1) in the presence of Matrigel resulted in decreased viral replication, and the authors concluded that the extracellular matrix hindered viral replication post-viral entry [68]. Another explanation could be the lack of ZIKV receptors; however, candidate receptors as well as GAS6 and PROS1, two ligands potentially involved in ZIKV entry [31] were detected in rhesus TSC-derived EVT_s. Additional studies to assess diverse ZIKV strains at varying MOIs are needed to fully elucidate the EVT response to ZIKV. Coculture studies may also provide insight as to whether infection of other nearby cells impacts the permissiveness of EVT_s.

The data suggest that even though minimal virus was produced in EVT_s, ZIKV exposure did alter gene expression and EV cargo. For example, *PIANP* gene expression was significantly increased in EVT-Z cells. *PIANP* enhances cellular resistance to stress by strengthening the plasma membrane, potentially to protect cells from proteolytic breakdown [69]. Interestingly, this protein is cleaved by a Furin-like proprotein convertase, as is the pre-membrane ZIKV protein, before it can localize to the plasma membrane [70]. *PIANP* can activate paired immunoglobulin-like type 2 receptor alpha (Pir- α), an inflammation inhibitory receptor [71].

IPA on EVT EV mRNA cargo suggests that ZIKV exposure is predicted to decrease degranulation of various cell types and decrease adhesion of immune cells. Exposure of Mast cells, another cell type found in the placenta, to ZIKV resulted in degranulation [72]. The genes associated with “adhesion of immune cells” biological function include: *C3*, *F2*, *FLT1*, *ILK*, *LBP*, *MYADM*, *PPIB*, *RAP1A*, *SI00A9*, and *BMPER*. It is interesting that EVT_s exposed to ZIKV secreted EVs enriched in proteins associated with this pathway as EVT_s are in direct contact with maternal immune cells. Additional studies are needed to understand the impact EVT EVs may have on maternal immune cells. p70S6K signaling also was significantly downregulated in ZIKV EVT EVs, which is involved in host protein translation [61] and promotes cell survival [73].

The ZIKV life cycle utilizes the secretory pathway [74], which is also the mechanism by which exosomes form and are secreted [75]. This overlap in pathways could allow for Zika viral proteins,

genome, and/or whole virions to be packaged within exosomes. In the present study, EVs within the expected size range stained positive for ZIKV E protein suggestive that Zika viral proteins were packaged into EVs. Furthermore, ZIKV E protein but not the NS2B protein were detected in the EV preparations by Western Blot. This is an important observation, as the NS2B protein is not packaged in the mature virion whereas the E protein is key to the mature virion. A low abundance of virions in the EV samples cannot be ruled out; however, the size of the ZIKV-E positive EVs suggests incorporation of the E protein.

Ultimately, an important goal is to identify biomarkers from circulating EVs that will allow insight into placental health, or in the context of ZIKV, placental infection. A few putative biomarkers were identified in EVs from ZIKV-exposed cells, including Proteasome 26S subunit, non-ATPase 12 (PSMD12), PDZ LIM domain protein 2 (PDLIM2), 5.8S ribosomal RNA mRNA, ribosomal subunit 27 variant 1 mRNA, PC-3p-49589_392, PC-3p-92473_197, and PC-3p-229848_66. PSMD12 is involved in normal removal of damaged/misfolded proteins [76]. In this context, as a protein packaged into EVs, it may have chaperoned damaged proteins into the secretory pathway for degradation in lysosomes. The increased presence of the proteasome in ZIKV infected cells could be part of a cellular immune response to activate increased degradation of viral proteins. The 26S proteasome also plays a role in processing peptides for MHC class I expression [76], which would elicit an immune response to infection if ZIKV peptides are presented by trophoblast MHC class I molecules. PDLIM2 is a ubiquitin E3 ligase that targets STAT2 for degradation [77] and was upregulated by infection with other Flaviviridae viruses [77]. In this study, PDLIM2 was increased in TSC-Z and ST3D-Z EVs with no change in cellular expression. This finding could

have two implications. One interpretation is that cells exposed to ZIKV attempt to remove or degrade PDLIM2 so as to trigger an antiviral response, which is why it was increased in EVs. The other is that infected cells transferred additional PDLIM2 to other cells, which could hinder their immune response to ZIKV infection. Additional studies are needed to better understand why and how PDLIM2 ends up in EVs and what impact this could have on recipient cells.

Overall, this study shows that macaque TSCs and STs representative of early first trimester trophoblasts are permissive to ZIKV infection. STs are in direct contact with maternal blood and therefore could be readily infected. Although the location and presence of the TSC niche in the human or primate placenta is poorly understood [78], these cells are not in direct contact with maternal blood but could become infected if the ST layer is breached. As a progenitor cell that will differentiate to vCTB or column cytotrophoblasts to then give rise to ST and EVT [79], their permissiveness to ZIKV could have major implications on placental health.

To better understand the communication and impact infected cells have on neighboring cells, in vitro studies that expose decidual cells, Hofbauer cells, and trophoblast cells to one another's EVs would provide insight into the impact of their potential communication in vivo. In vivo data strongly indicate that trophoblast cells maintain a level of resistance to infection and that Hofbauer cells are the main infected cell type at the maternal-fetal interface. However, significant placental pathology observed with in vivo and ex vivo explant studies indicate that there may be indirect as well as direct pathways by which ZIKV may impact pregnancy. In addition, we saw that infection altered trophoblast function, even in EVTs that did not show prominent infection. This in turn

could impact the maternal response to the pregnancy and maternal immune response to ZIKV at the maternal-fetal interface. In vivo studies in which PEVs are isolated from maternal blood after infection also are needed to validate and extend upon the changes in cargo observed in this study.

4.6 References

1. Venceslau EM, Guida JP, Amaral E, Modena JLP, Costa ML. Characterization of Placental Infection by Zika Virus in Humans: A Review of the Literature. *Rev Bras Ginecol Obstet* 2020; 42:577-585.
2. Musso D, Ko AI, Baud D. Zika Virus Infection - After the Pandemic. *N Engl J Med* 2019; 381:1444-1457.
3. Desclaux A, de Lamballerie X, Leparc-Goffart I, Vilain-Parce A, Coatleven F, Fleury H, Malvy D. Probable Sexually Transmitted Zika Virus Infection in a Pregnant Woman. *N Engl J Med* 2018; 378:1458-1460.
4. Pomar L, Malinger G, Benoist G, Carles G, Ville Y, Rousset D, Hcini N, Pomar C, Jolivet A, Lambert V. Association between Zika virus and fetopathy: a prospective cohort study in French Guiana. *Ultrasound Obstet Gynecol* 2017; 49:729-736.
5. Meaney-Delman D, Oduyebo T, Polen KND, White JL, Bingham AM, Slavinski SA, Heberlein-Larson L, St George K, Rakeman JL, Hills S, Olson CK, Adamski A, et al. Prolonged Detection of Zika Virus RNA in Pregnant Women. *Obstet Gynecol* 2016; 128:724-730.
6. Hirsch AJ, Roberts VHJ, Grigsby PL, Haese N, Schabel MC, Wang X, Lo JO, Liu Z, Kroenke CD, Smith JL, Kelleher M, Broeckel R, et al. Zika virus infection in pregnant rhesus macaques causes placental dysfunction and immunopathology. *Nat Commun* 2018; 9:263.
7. Pomar L, Lambert V, Matheus S, Pomar C, Hcini N, Carles G, Rousset D, Vouga M, Panchaud A, Baud D. Prolonged Maternal Zika Viremia as a Marker of Adverse Perinatal Outcomes. *Emerg Infect Dis* 2021; 27:490-498.
8. Driggers RW, Ho CY, Korhonen EM, Kuivanen S, Jaaskelainen AJ, Smura T, Rosenberg A, Hill DA, DeBiasi RL, Vezina G, Timofeev J, Rodriguez FJ, et al. Zika Virus Infection with Prolonged Maternal Viremia and Fetal Brain Abnormalities. *N Engl J Med* 2016; 374:2142-2151.
9. Maltepe E, Fisher SJ. Placenta: the forgotten organ. *Annu Rev Cell Dev Biol* 2015; 31:523-552.
10. Turco MY, Moffett A. Development of the human placenta. *Development* 2019; 146.

11. Schmidt JK, Keding LT, Block LN, Wiepz GJ, Koenig MR, Meyer MG, Dusek BM, Kroner KM, Bertogliat MJ, Kallio AR, Mean KD, Golos TG. Placenta-derived macaque trophoblast stem cells: differentiation to syncytiotrophoblasts and extravillous trophoblasts reveals phenotypic reprogramming. *Sci Rep* 2020; 10:19159.
12. Brasil P, Pereira JP, Jr., Moreira ME, Ribeiro Nogueira RM, Damasceno L, Wakimoto M, Rabello RS, Valderramos SG, Halai UA, Salles TS, Zin AA, Horovitz D, et al. Zika Virus Infection in Pregnant Women in Rio de Janeiro. *N Engl J Med* 2016; 375:2321-2334.
13. Brady OJ, Osgood-Zimmerman A, Kassebaum NJ, Ray SE, de Araujo VEM, da Nobrega AA, Frutuoso LCV, Lecca RCR, Stevens A, Zoca de Oliveira B, de Lima JM, Jr., Bogoch, II, et al. The association between Zika virus infection and microcephaly in Brazil 2015-2017: An observational analysis of over 4 million births. *PLoS Med* 2019; 16:e1002755.
14. Hoen B, Schaub B, Funk AL, Ardillon V, Boullard M, Cabie A, Callier C, Carles G, Cassadou S, Cesaire R, Douine M, Herrmann-Storck C, et al. Pregnancy Outcomes after ZIKV Infection in French Territories in the Americas. *N Engl J Med* 2018; 378:985-994.
15. Lima GP, Rozenbaum D, Pimentel C, Frota ACC, Vivacqua D, Machado ES, Sztajn bok F, Abreu T, Soares RA, Hofer CB. Factors associated with the development of Congenital Zika Syndrome: a case-control study. *BMC Infect Dis* 2019; 19:277.
16. Rasmussen SA, Jamieson DJ. Teratogen update: Zika virus and pregnancy. *Birth Defects Res* 2020; 112:1139-1149.
17. Jin J, Menon R. Placental exosomes: A proxy to understand pregnancy complications. *Am J Reprod Immunol* 2018; 79:e12788.
18. Zhou B, Xu K, Zheng X, Chen T, Wang J, Song Y, Shao Y, Zheng S. Application of exosomes as liquid biopsy in clinical diagnosis. *Signal Transduct Target Ther* 2020; 5:144.
19. Salomon C, Kobayashi M, Ashman K, Sobrevia L, Mitchell MD, Rice GE. Hypoxia-induced changes in the bioactivity of cytotrophoblast-derived exosomes. *PLoS One* 2013; 8:e79636.
20. Chahar HS, Bao X, Casola A. Exosomes and Their Role in the Life Cycle and Pathogenesis of RNA Viruses. *Viruses* 2015; 7:3204-3225.
21. Vora A, Zhou W, Londono-Renteria B, Woodson M, Sherman MB, Colpitts TM, Neelakanta G, Sultana H. Arthropod EVs mediate dengue virus transmission through interaction with a tetraspanin domain containing glycoprotein Tsp29Fb. *Proc Natl Acad Sci U S A* 2018; 115:E6604-E6613.
22. Grigsby PL. Animal Models to Study Placental Development and Function throughout Normal and Dysfunctional Human Pregnancy. *Semin Reprod Med* 2016; 34:11-16.

23. Dudley DM, Van Rompay KK, Coffey LL, Ardeshir A, Keesler RI, Bliss-Moreau E, Grigsby PL, Steinbach RJ, Hirsch AJ, MacAllister RP, Pecoraro HL, Colgin LM, et al. Miscarriage and stillbirth following maternal Zika virus infection in nonhuman primates. *Nat Med* 2018; 24:1104-1107.
24. Hodgen GD, Tullner WW, Vaitukaitis JL, Ward DN, Ross GT. Specific radioimmunoassay of chorionic gonadotropin during implantation in rhesus monkeys. *J Clin Endocrinol Metab* 1974; 39:457-464.
25. Wolfgang MJ, Eisele SG, Knowles L, Browne MA, Schotzko ML, Golos TG. Pregnancy and live birth from nonsurgical transfer of in vivo- and in vitro-produced blastocysts in the rhesus monkey. *J Med Primatol* 2001; 30:148-155.
26. Weaver SC, Costa F, Garcia-Blanco MA, Ko AI, Ribeiro GS, Saade G, Shi PY, Vasilakis N. Zika virus: History, emergence, biology, and prospects for control. *Antiviral Res* 2016; 130:69-80.
27. Jaeger AS, Murrieta RA, Goren LR, Crooks CM, Moriarty RV, Weiler AM, Rybarczyk S, Semler MR, Huffman C, Mejia A, Simmons HA, Fritsch M, et al. Zika viruses of African and Asian lineages cause fetal harm in a mouse model of vertical transmission. *PLoS Negl Trop Dis* 2019; 13:e0007343.
28. Aubry F, Jacobs S, Darmuzey M, Lequime S, Delang L, Fontaine A, Jupatanakul N, Miot EF, Dabo S, Manet C, Montagutelli X, Baidaliuk A, et al. Recent African strains of Zika virus display higher transmissibility and fetal pathogenicity than Asian strains. *Nat Commun* 2021; 12:916.
29. Udenze D, Trus I, Berube N, Gerdts V, Karniychuk U. The African strain of Zika virus causes more severe in utero infection than Asian strain in a porcine fetal transmission model. *Emerg Microbes Infect* 2019; 8:1098-1107.
30. Sheridan MA, Balaraman V, Schust DJ, Ezashi T, Roberts RM, Franz AWE. African and Asian strains of Zika virus differ in their ability to infect and lyse primitive human placental trophoblast. *PLoS One* 2018; 13:e0200086.
31. Sheridan MA, Yunusov D, Balaraman V, Alexenko AP, Yabe S, Verjovski-Almeida S, Schust DJ, Franz AW, Sadovsky Y, Ezashi T, Roberts RM. Vulnerability of primitive human placental trophoblast to Zika virus. *Proc Natl Acad Sci U S A* 2017; 114:E1587-E1596.
32. Tabata T, Petitt M, Puerta-Guardo H, Michlmayr D, Harris E, Pereira L. Zika Virus Replicates in Proliferating Cells in Explants From First-Trimester Human Placentas, Potential Sites for Dissemination of Infection. *J Infect Dis* 2018; 217:1202-1213.
33. Moser LA, Boylan BT, Moreira FR, Myers LJ, Svenson EL, Fedorova NB, Pickett BE, Bernard KA. Growth and adaptation of Zika virus in mammalian and mosquito cells. *PLoS Negl Trop Dis* 2018; 12:e0006880.

34. Block LN, Aliota MT, Friedrich TC, Schotzko ML, Mean KD, Wiepz GJ, Golos TG, Schmidt JK. Embryotoxic impact of Zika virus in a rhesus macaque in vitro implantation model. *Biol Reprod* 2020; 102:806-816.
35. Sirohi D, Kuhn RJ. Zika Virus Structure, Maturation, and Receptors. *J Infect Dis* 2017; 216:S935-S944.
36. Martin M. Cutadapt removes adapter sequences from high-throughput sequencing reads. *Bioinformatics* 2011; 17:3.
37. Kim D, Langmead B, Salzberg SL. HISAT: a fast spliced aligner with low memory requirements. *Nat Methods* 2015; 12:357-360.
38. Pertea M, Pertea GM, Antonescu CM, Chang TC, Mendell JT, Salzberg SL. StringTie enables improved reconstruction of a transcriptome from RNA-seq reads. *Nat Biotechnol* 2015; 33:290-295.
39. Love MI, Huber W, Anders S. Moderated estimation of fold change and dispersion for RNA-seq data with DESeq2. *Genome Biol* 2014; 15:550.
40. Robinson MD, McCarthy DJ, Smyth GK. edgeR: a Bioconductor package for differential expression analysis of digital gene expression data. *Bioinformatics* 2010; 26:139-140.
41. McCarthy DJ, Chen Y, Smyth GK. Differential expression analysis of multifactor RNA-Seq experiments with respect to biological variation. *Nucleic Acids Res* 2012; 40:4288-4297.
42. Livak KJ, Schmittgen TD. Analysis of relative gene expression data using real-time quantitative PCR and the $2^{-\Delta\Delta C(T)}$ Method. *Methods* 2001; 25:402-408.
43. Thery C, Witwer KW, Aikawa E, Alcaraz MJ, Anderson JD, Andriantsitohaina R, Antoniou A, Arab T, Archer F, Atkin-Smith GK, Ayre DC, Bach JM, et al. Minimal information for studies of extracellular vesicles 2018 (MISEV2018): a position statement of the International Society for Extracellular Vesicles and update of the MISEV2014 guidelines. *J Extracell Vesicles* 2018; 7:1535750.
44. Novy V, Nielsen F, Cullen D, Sabat G, Houtman CJ, Hunt CG. The characteristics of insoluble softwood substrates affect fungal morphology, secretome composition, and hydrolytic efficiency of enzymes produced by *Trichoderma reesei*. *Biotechnol Biofuels* 2021; 14:105.
45. Goo L, Dowd KA, Smith AR, Pelc RS, DeMaso CR, Pierson TC. Zika Virus Is Not Uniquely Stable at Physiological Temperatures Compared to Other Flaviviruses. *mBio* 2016; 7.
46. Raymond AD, Gekonge B, Giri MS, Hancock A, Papasavvas E, Chehimi J, Kossenkov AV, Nicols C, Yousef M, Mounzer K, Shull J, Kostman J, et al. Increased metallothionein gene expression, zinc, and zinc-dependent resistance to apoptosis in circulating monocytes during HIV viremia. *J Leukoc Biol* 2010; 88:589-596.

47. Dziegiel P, Pula B, Kobierzycki C, Stasiolek M, Podhorska-Okolow M. Metallothioneins in Normal and Cancer Cells. *Adv Anat Embryol Cell Biol* 2016; 218:65-77.
48. Morales-Prieto DM, Favaro RR, Markert UR. Placental miRNAs in feto-maternal communication mediated by extracellular vesicles. *Placenta* 2020; 102:27-33.
49. Morales-Prieto DM, Ospina-Prieto S, Chaiwangyen W, Schoenleben M, Markert UR. Pregnancy-associated miRNA-clusters. *J Reprod Immunol* 2013; 97:51-61.
50. Delorme-Axford E, Donker RB, Mouillet JF, Chu T, Bayer A, Ouyang Y, Wang T, Stolz DB, Sarkar SN, Morelli AE, Sadovsky Y, Coyne CB. Human placental trophoblasts confer viral resistance to recipient cells. *Proc Natl Acad Sci U S A* 2013; 110:12048-12053.
51. Costa MA. The endocrine function of human placenta: an overview. *Reprod Biomed Online* 2016; 32:14-43.
52. El Costa H, Gouilly J, Mansuy JM, Chen Q, Levy C, Cartron G, Veas F, Al-Daccak R, Izopet J, Jabrane-Ferrat N. ZIKA virus reveals broad tissue and cell tropism during the first trimester of pregnancy. *Sci Rep* 2016; 6:35296.
53. Tabata T, Pettitt M, Puerta-Guardo H, Michlmayr D, Wang C, Fang-Hoover J, Harris E, Pereira L. Zika Virus Targets Different Primary Human Placental Cells, Suggesting Two Routes for Vertical Transmission. *Cell Host Microbe* 2016; 20:155-166.
54. de Noronha L, Zanluca C, Burger M, Suzukawa AA, Azevedo M, Rebutini PZ, Novadzki IM, Tanabe LS, Presibella MM, Duarte Dos Santos CN. Zika Virus Infection at Different Pregnancy Stages: Anatomopathological Findings, Target Cells and Viral Persistence in Placental Tissues. *Front Microbiol* 2018; 9:2266.
55. Xia H, Luo H, Shan C, Muruato AE, Nunes BT, Medeiros DBA, Zou J, Xie X, Giraldo MI, Vasconcelos PFC, Weaver SC, Wang T, et al. An evolutionary NS1 mutation enhances Zika virus evasion of host interferon induction. *Nat Commun* 2018; 9:414.
56. Hu Y, Dong X, He Z, Wu Y, Zhang S, Lin J, Yang Y, Chen J, An S, Yin Y, Shen Z, Zeng G, et al. Zika virus antagonizes interferon response in patients and disrupts RIG-I-MAVS interaction through its CARD-TM domains. *Cell Biosci* 2019; 9:46.
57. Bayer A, Lennemann NJ, Ouyang Y, Bramley JC, Morosky S, Marques ET, Jr., Cherry S, Sadovsky Y, Coyne CB. Type III Interferons Produced by Human Placental Trophoblasts Confer Protection against Zika Virus Infection. *Cell Host Microbe* 2016; 19:705-712.
58. Weisblum Y, Oiknine-Djian E, Vorontsov OM, Haimov-Kochman R, Zakay-Rones Z, Meir K, Shveiky D, Elgavish S, Nevo Y, Roseman M, Bronstein M, Stockheim D, et al. Zika Virus Infects Early- and Midgestation Human Maternal Decidual Tissues, Inducing Distinct Innate Tissue Responses in the Maternal-Fetal Interface. *J Virol* 2017; 91.

59. Yockey LJ, Jurado KA, Arora N, Millet A, Rakib T, Milano KM, Hastings AK, Fikrig E, Kong Y, Horvath TL, Weatherbee S, Kliman HJ, et al. Type I interferons instigate fetal demise after Zika virus infection. *Sci Immunol* 2018; 3.
60. Wu N, Nguyen XN, Wang L, Appourchaux R, Zhang C, Panthu B, Gruffat H, Journo C, Alais S, Qin J, Zhang N, Tartour K, et al. The interferon stimulated gene 20 protein (ISG20) is an innate defense antiviral factor that discriminates self versus non-self translation. *PLoS Pathog* 2019; 15:e1008093.
61. Walsh D, Mohr I. Viral subversion of the host protein synthesis machinery. *Nat Rev Microbiol* 2011; 9:860-875.
62. Mouillet JF, Ouyang Y, Bayer A, Coyne CB, Sadovsky Y. The role of trophoblastic microRNAs in placental viral infection. *Int J Dev Biol* 2014; 58:281-289.
63. Barbu MG, Condrat CE, Thompson DC, Bugnar OL, Cretoiu D, Toader OD, Suciu N, Voinea SC. MicroRNA Involvement in Signaling Pathways During Viral Infection. *Front Cell Dev Biol* 2020; 8:143.
64. Fu X, Ouyang Y, Mo J, Li R, Fu L, Peng S. Upregulation of microRNA-328-3p by hepatitis B virus contributes to THLE-2 cell injury by downregulating FOXO4. *J Transl Med* 2020; 18:143.
65. Zhao L, Yang Q, Liu J. Clinical value evaluation of microRNA-324-3p and other available biomarkers in patients with HBV-infection-related hepatocellular carcinoma. *Open Forum Infectious Diseases* 2021.
66. Dai C, Zhang Y, Xu Z, Jin M. MicroRNA-122-5p inhibits cell proliferation, migration and invasion by targeting CCNG1 in pancreatic ductal adenocarcinoma. *Cancer Cell Int* 2020; 20:98.
67. Chiu CF, Chu LW, Liao IC, Simanjuntak Y, Lin YL, Juan CC, Ping YH. The Mechanism of the Zika Virus Crossing the Placental Barrier and the Blood-Brain Barrier. *Front Microbiol* 2020; 11:214.
68. Voros A, Kormos B, Valyi-Nagy T, Valyi-Nagy K. Increased Resistance of Breast, Prostate, and Embryonic Carcinoma Cells against Herpes Simplex Virus in Three-Dimensional Cultures. *ISRN Oncol* 2013; 2013:104913.
69. Evdokimov K, Biswas S, Schledzewski K, Winkler M, Gorzelanny C, Schneider SW, Goerdts S, Geraud C. Leda-1/Pianp is targeted to the basolateral plasma membrane by a distinct intracellular juxtamembrane region and modulates barrier properties and E-Cadherin processing. *Biochem Biophys Res Commun* 2016; 475:342-349.
70. Evdokimov K, Biswas S, Adrian M, Weber J, Schledzewski K, Winkler M, Goerdts S, Geraud C. Proteolytic cleavage of LEDA-1/PIANP by furin-like proprotein convertases precedes its plasma membrane localization. *Biochem Biophys Res Commun* 2013; 434:22-27.

71. Biswas S, Adrian M, Evdokimov K, Schledzewski K, Weber J, Winkler M, Goerdts S, Geraud C. Counter-regulation of the ligand-receptor pair Leda-1/Pianp and Piralpha during the LPS-mediated immune response of murine macrophages. *Biochem Biophys Res Commun* 2015; 464:1078-1083.
72. Rabelo K, Goncalves A, Souza LJ, Sales AP, Lima SMB, Trindade GF, Ciambarella BT, Amorim Tasmio NR, Diaz BL, Carvalho JJ, Duarte MPO, Paes MV. Zika Virus Infects Human Placental Mast Cells and the HMC-1 Cell Line, and Triggers Degranulation, Cytokine Release and Ultrastructural Changes. *Cells* 2020; 9.
73. Harada H, Andersen JS, Mann M, Terada N, Korsmeyer SJ. p70S6 kinase signals cell survival as well as growth, inactivating the pro-apoptotic molecule BAD. *Proc Natl Acad Sci U S A* 2001; 98:9666-9670.
74. Sager G, Gabaglio S, Sztul E, Belov GA. Role of Host Cell Secretory Machinery in Zika Virus Life Cycle. *Viruses* 2018; 10.
75. Margolis L, Sadovsky Y. The biology of extracellular vesicles: The known unknowns. *PLoS Biol* 2019; 17:e3000363.
76. McCarthy MK, Weinberg JB. The immunoproteasome and viral infection: a complex regulator of inflammation. *Front Microbiol* 2015; 6:21.
77. Joyce MA, Berry-Wynne KM, Dos Santos T, Addison WR, McFarlane N, Hobman T, Tyrrell DL. HCV and flaviviruses hijack cellular mechanisms for nuclear STAT2 degradation: Up-regulation of PDLIM2 suppresses the innate immune response. *PLoS Pathog* 2019; 15:e1007949.
78. Chang CW, Parast MM. Human trophoblast stem cells: Real or not real? *Placenta* 2017; 60 Suppl 1:S57-S60.
79. Knofler M, Haider S, Saleh L, Pollheimer J, Gamage T, James J. Human placenta and trophoblast development: key molecular mechanisms and model systems. *Cell Mol Life Sci* 2019; 76:3479-3496.

Chapter 5

Concluding Remarks

The objective of this thesis was to enhance understanding of how and when ZIKV can impact pregnancy by conducting targeted studies on the earliest stages of the development of the placenta, an organ essential to a successful pregnancy. In chapter 2, we discussed a case study of a macaque that experienced a miscarriage after late first trimester ZIKV exposure. The findings of that study led us to investigate with more tractable model systems at what point ZIKV can begin to impact the placenta. In chapter 3, we showed that peri-implantation rhesus macaque embryos in an in vitro culture system were negatively impacted by ZIKV. This culture model encourages the growth of the trophoctoderm, which are the earliest trophoblast (placenta) cells. Based on the findings of this study, we then asked which of the other early gestation trophoblast cells that arise during formation of the definitive placenta are susceptible to ZIKV infection. In chapter 4, early gestation trophoblast stem cells and syncytiotrophoblast cells were shown to be permissive to ZIKV infection, whereas extravillous trophoblast cells were not readily infected, although exposure to ZIKV impacted cellular function. We also showed that EVs released by infected cells contain cargo that differed from that of uninfected cells. Altogether, our in vitro-derived data support that ZIKV exposure early in pregnancy impacts placental cells that can in turn have severe consequences on pregnancy outcomes. These findings have implications from conception through early gestation and encompass the potential risks of sexual and vertical transmission of ZIKV.

Maternal ZIKV exposure has been associated with congenital ZIKV syndrome (CZS) and pregnancy loss in humans, hence translational models of human pregnancy are needed to research ZIKV infection. Rhesus macaques are translational models of human pregnancy as they have similar placentation, have a long gestation period, and give birth to precocious young. Since ZIKV infection during pregnancy was associated with neurological impairments in fetal development, it was important to use a model in which the nervous system developed in utero. Several studies published at the University of Wisconsin support the translatability of rhesus macaques ZIKV infection to humans [1-3]. In chapter 2, a case study highlighted that a ZIKV infection in the late first trimester resulted in a miscarriage late in the second trimester. Placental pathology was observed, which may have developed as a result of ZIKV infection. A key finding in this case study was fetal ocular pathology, including a choroidal coloboma, suspected anterior segment dysgenesis, and a dysplastic retina. It is important to note that the miscarriage was confounded by a bacterial infection at the maternal-fetal interface that may have contributed to premature preterm rupture of the fetal membranes (PPROM). However, there is no literature that indicates a reproductive tract bacterial infection impacts fetal morphogenesis. Based on coincident ZIKV exposure during ocular development, we concluded that ZIKV caused this damage, which has been seen in ZIKV infections during the first trimester in humans [4]. Currently, this is the first and only report of an ocular developmental defect in the nonhuman primate model of ZIKV infection during pregnancy, supporting the macaque as a viable model for congenital Zika syndrome (CZS). These findings thus were an important contribution to the development of the use of primates for Zika research and support the macaque as a translational model of human pregnancy and their use in the studies discussed below. This thesis is mainly focused on the cell biology of the placenta.

Therefore, proposals for future in vivo studies in nonhuman primates that focus on CZS will not be discussed.

The observations reported in human clinical literature, as well as nonhuman primate studies that ZIKV could be sexually transmitted raised several questions relevant to our interest in the impact of ZIKV on the maternal-fetal interface. One question we were particularly interested in was whether sexual transmission could impact pregnancy. Since we knew ZIKV could infect the placenta and that an infection earlier in gestation resulted in worse outcomes, we wanted to know just how early ZIKV could impact pregnancy and at what point ZIKV can begin to impact the placenta. To determine whether gametes were permissive to ZIKV, we exposed oocytes and sperm to ZIKV at the time of fertilization. We found that exposure at the time of fertilization had no impact on embryo development. This information is significant for couples trying to conceive with IVF as ZIKV presence in semen should not be a concern. However, for couples trying to conceive naturally, the presence of ZIKV in semen can still be transmitted sexually and a mouse study showed decreased embryo implantation with the presence of ZIKV [5]. As such, while the presence of ZIKV does not impact embryo development, it can still infect the implanting embryo and the female reproductive tract.

The earliest placental cells, the trophoctoderm, are exposed to uterine fluid during implantation and exposed to maternal blood after implantation. To determine if ZIKV presence in these fluids could infect the implanting embryo, we exposed embryos to three doses of ZIKV. From this part of the study, we concluded that ZIKV was embryotoxic at high doses and was able to impede

cellular growth at lower doses. Based on our findings, ZIKV exposure at the time of implantation, potentially by sexual or vertical transmission, can negatively impact pregnancy. Unfortunately, it is not feasible to know if this occurred in humans due to the typically delayed knowledge that pregnancy has begun. Generally, women do not know they are pregnant until at least 3 weeks after embryo implantation and the establishment of pregnancy.

In light of our findings, studies in which embryos are exposed to ZIKV during the peri-implantation stage *in vivo* are necessary to truly determine the potential of ZIKV to disrupt the establishment of pregnancy. Such studies would be very resource-demanding, however other alternatives also exist. Previous studies have used *in vitro* models to monitor the interaction between maternal immune cells and the developing embryo *in vitro* [6, 7]. Utilization of this model alongside ZIKV exposure would provide an intermediary platform to understand how the maternal immune system may respond to the presence of ZIKV and a partial-allograft embryo. The implications of such a study would shed light as to the interaction and communication that occurs between the maternal immune system and an implanting embryo, during a viral infection. While we observed embryo growth at low doses of ZIKV, the immune response to the infection may be very strong and could result in more embryo death than observed in the *in vitro* system used in Chapter 3. Alternatively, maternal immune cells could be protective in the *in vitro* context, and other *in vivo* factors, such as a change in maternal uterine/decidual vasculature may contribute to an adverse outcome.

In vivo experiments could be performed to determine whether embryos exposed to ZIKV can implant and survive the insult. Timed mating or embryo transfer followed by intravaginal inoculation of ZIKV followed by monitoring pregnancy establishment rates could serve as readout of ZIKV impact at this stage. This is an alternative in vivo approach to the in vitro embryo-immune cell system. An advantage of this system is the direct translatability of the findings. However, such a study would be demanding of animal and experimental management resources, take a long time, and there are more variables to control. For instance, monkeys that previously had a successful pregnancy should be used to verify their uterus has been receptive to embryo implantation. The in vitro experiment would be less expensive, less invasive, and easier to control; however, there is still the question of relevance to the in vivo system.

The recently established trophoblast stem cell in vitro model allowed us to transition from studying the earliest embryonic trophoblast cells (the trophoctoderm) to studying the early trophoblast cells that make up the placenta proper. With this model, we studied how ZIKV exposure impacted trophoblast cell function by analyzing cellular gene expression, miRNA expression, and secreted products, including extracellular vesicles. From these studies we found that trophoblast stem cells and syncytiotrophoblast cells were permissive to ZIKV, while the extravillous trophoblast cells were less permissive. Regardless of the level of viral replication by the different cell populations, ZIKV exposure altered gene and miRNA expression. A significant increase in genes associated with the innate immune response was observed in the trophoblast stem cells and syncytiotrophoblast cells. Alterations in extracellular vesicle (EV) cargo released by all cell types exposed to ZIKV were also observed. The cargo that was increased in EVs released by ZIKV

exposed cells, such as PDLIM2 and PSMD12, should be further studied as they could be potential biomarkers for in vivo placental infection.

We already know hormones and cytokines/growth factors are involved in cell-cell communication, and there is extensive research supporting EVs as another means of conveying information. However, due to their small size and the overlap in size among the different types of EVs (exosomes, microvesicles, and apoptotic bodies), there are many unanswered questions in the EV field in general as to the purpose behind this putative mode of communication. Deciphering how and what impact EVs will have on recipient cells is difficult as they contain an array of cargo (miRNAs, lncRNAs, mRNAs, DNA, and proteins) and express different proteins on their surfaces. How/why cargo is packaged within EVs also remains unclear.

A concept I have found particularly intriguing is the possibility of specific packaging of EV cargo. This notion is key to really understanding the purpose behind, and functional physiological significance of, EVs. While there is extensive literature supporting the idea that EVs are not simply secreted waste, their purposes/targets remain speculative. One goal of the EV field is to use EVs and their cargo as biomarkers for various diseased or infected states. Their cargo has been shown to be altered under various pregnancy complications, as discussed in great depth in the appendix [10]. The potential for PEVs to serve as surrogates of placental health would be a tremendous steppingstone in the prognosis of pregnancy complications. Instead of monitoring maternal symptoms for insight into the health status of the pregnancy and the placenta, specific placental molecular patterns could be directly monitored in maternal blood.

Another area that needs further study is determining whether EVs express markers that enable/encourage targeting of specific cell types. Studies in which EVs are isolated from one cell type, ZIKV infected or uninfected, and are exposed to the other cell types would help discern how they may communicate about an infection in vivo. One potential experiment to address whether PEVs have specific targets in vivo would be to inject engineered PEVs into a pregnant monkey and monitor which tissues/cells take them up. For instance, isolate EVs secreted by trophoblast cells in vitro, label them with Ferumoxytol, a superparamagnetic iron oxide nanoparticle [11], inject them intravenously into a pregnant macaque, and use magnetic resonance imaging (MRI) to monitor which tissues the PEVs target. These data would allow for future studies to focus on those tissues of interest. This would provide a basis to understand how PEVs are involved in a healthy pregnancy, which could then be expanded upon for studies with ZIKV infection and other pregnancy complications. These findings also may provide additional intel as to how the placenta communicates with mom's immune system and various organs. The in vitro models and the in vivo nonhuman primate model used in this thesis could provide tremendous insight into EV-based communication, diagnostics, and therapeutics.

There are several limitations in the studies presented in this thesis. One is the limited number of biological replicates, partially due to the expense, availability, and ethical restrictions on primate research. The findings presented in chapter 2 are only from one pregnant rhesus macaque case study. Congenital Zika syndrome birth defects are readily observed when there are millions of human pregnancies in Brazil, but the number of animal replicates in primate pregnancy studies

precludes a realistic replication of the human condition. Regardless, the primate studies do demonstrate that the animal model can recapitulate outcomes seen in human pregnancy and this validates the *in vivo* pregnancy experiments, although careful consideration of animal numbers and experimental design is important.

Although we were able to test several different doses (three) for the embryo study in chapter 3, due to practical limitations on the numbers of animals that could be enrolled in the study, we were unable to explore additional viral strains or other viruses altogether. Such experiments could have shed light as to whether ZIKV specifically caused the embryo loss or whether the abundance of a virus was cytotoxic. In addition, exposure of embryos to inactivated ZIKV would have been beneficial. Due to limited samples, we were unable to comprehensively analyze the transcriptome or miRNAome to better understand how exposure impacts trophoblast function, and to be able to relate more comprehensively the outcomes of chapter 3 studies to chapter 4.

Chapter 4 studies allowed us to overcome some of the resource limitations that the use of IVF-derived embryos imposed. However, there remained resource limitations. One limitation in chapter 4 is that ST3Ds were exposed to a higher MOI than EVT_s, which resulted in widespread ZIKV infection. An MOI of five was not tested with the ST3Ds based on the literature in term human primate trophoblasts that indicated ST_s were resistant to infection [12]. Additional studies with ST3D exposure to an MOI of five would shed light as to whether early gestation ST3Ds also maintain a level of resistance to ZIKV infection. Having said that, an MOI of 1 also resulted in ZIKV replication, so ST3Ds still are more permissive than EVT_s.

Another limitation is the use of only one ZIKV strain for each study. As previously mentioned, the impact of ZIKV appears to be strain dependent and comparison of different strains would give us more detailed information as to what may be causing embryonic death or altering trophoblast cell function. One question is whether more virus would be needed to induce similar effects with one strain over another (i.e., would a strain from the Asian lineage lead to more changes/be more cytotoxic than a strain from the African lineage?).

It is important to consider variations in the genome of ZIKV isolates when attempting to understand the impact of ZIKV on pregnancy. This is partly since ZIKV was not associated with pregnancy complications for the first 60 years since it was first identified. This suggests that as ZIKV spread, it mutated and gained the ability to cause adverse pregnancy outcomes. There are two main lineages of ZIKV, Asian and African, and there has been mention of there being a third lineage (Brazilian) but this is not yet a widely recognized classification. An Asian lineage ZIKV strain was used in chapters 2 and 3, which reflected the state of the field at the time those studies were done. An African lineage strain was used in chapter 4 as it became recognized that there may be relevant strain differences. The most recent outbreaks in the Americas were from the Asian lineage, which was initially thought to be more pathogenic. However, numerous studies that have compared various strains between the two lineages routinely find African to be more pathogenic (in vitro cell and in vivo animal model studies). Once this information came to light, we decided to use a strain from the African lineage. The finding that ZIKV strains from the African lineage may be more pathogenic raise questions and concerns as to how African ZIKV outbreaks have

“gone under the radar”. An increase in early pregnancy loss rates would be difficult to notice as miscarriages are quite common, and the etiology is often unknown. However, CZS, and microcephaly, in particular would be noticeable, and outbreaks in the Americas with Asian lineage virus may have allowed pregnancies to be carried to term and revealed the impact on fetal development. As such, studies that compare these different strains in the in vitro TSC model would enhance our understanding as to what caused this shift in adverse pregnancy outcomes. Additional studies with other strains in the same/similar models are needed to strengthen the findings within this thesis.

One prominent question is why early gestation trophoblast cells are more permissive to infection. This question cannot be directly answered from the work in this thesis since we did not compare early to term trophoblast cells. However, isolation of trophoblast cells from term placentas is a common technique. These cells could be isolated and exposed to ZIKV with the same paradigm used here to determine how gestational age directly correlates with permissibility. Term trophoblast cells are hypothesized to be resistant to ZIKV infection because they constitutively release high levels of type III interferons [12]. However, type III interferons also were expressed in the TSC model used in chapter 4. For this reason, direct comparison studies are needed to fully elucidate at what level interferons are protective.

Altogether, we found that ZIKV can infect early gestation trophoblast cells and that while infection may alter gene expression and trigger an innate immune response, infection did not hinder cell differentiation. Based on these data, if the placenta is exposed to a low dose of ZIKV, there may

be damage and virus may disseminate to and infect the placenta. However, the infection will subside because it will trigger an adaptive immune response. On the other hand, if the placenta is exposed to a high dose of ZIKV, this will result in extensive cell death (as observed in other studies) partly due to the infection itself and partly due to the maternal immune response. This breakdown of the syncytial barrier will definitely result in virus disseminating to the fetus and may result in an adverse pregnancy outcome.

In conclusion, this thesis delves into the impact of ZIKV on early trophoblast cells, ranging from those present during the embryo stage through early pregnancy. In addition to increasing our understanding of which trophoblast cell types are permissive to ZIKV (trophectoderm, TSCs, and ST3Ds), we also analyzed EVs secreted by these cells to infer how infection could impact cell-cell communication. The tools used throughout this work (in vitro embryo culture, trophoblast stem cell culture, EV isolation and analysis by NTA, and next generation sequencing) were crucial to building on the present knowledge of how ZIKV impacts the placenta. Observations from these studies will lay the groundwork for future research into viral impact on the early placenta, trophoblast cell-cell communication, and potential identification of biomarkers of infection.

5.2 References

1. Nguyen SM, Antony KM, Dudley DM, Kohn S, Simmons HA, Wolfe B, Salamat MS, Teixeira LBC, Wiepz GJ, Thoong TH, Aliota MT, Weiler AM, et al. Highly efficient maternal-fetal Zika virus transmission in pregnant rhesus macaques. *PLoS Pathog* 2017; 13:e1006378.
2. Mohr EL, Block LN, Newman CM, Stewart LM, Koenig M, Semler M, Breitbach ME, Teixeira LBC, Zeng X, Weiler AM, Barry GL, Thoong TH, et al. Ocular and uteroplacental pathology in a macaque pregnancy with congenital Zika virus infection. *PLoS One* 2018; 13:e0190617.
3. Dudley DM, Van Rompay KK, Coffey LL, Ardeshir A, Keesler RI, Bliss-Moreau E, Grigsby PL, Steinbach RJ, Hirsch AJ, MacAllister RP, Pecoraro HL, Colgin LM, et al. Miscarriage and stillbirth following maternal Zika virus infection in nonhuman primates. *Nat Med* 2018; 24:1104-1107.
4. Ventura CV, Maia M, Travassos SB, Martins TT, Patriota F, Nunes ME, Agra C, Torres VL, van der Linden V, Ramos RC, Rocha MA, Silva PS, et al. Risk Factors Associated With the Ophthalmoscopic Findings Identified in Infants With Presumed Zika Virus Congenital Infection. *JAMA Ophthalmol* 2016; 134:912-918.
5. Tan L, Lacko LA, Zhou T, Tomoiaga D, Hurtado R, Zhang T, Sevilla A, Zhong A, Mason CE, Noggle S, Evans T, Stuhlmann H, et al. Pre- and peri-implantation Zika virus infection impairs fetal development by targeting trophoblast cells. *Nat Commun* 2019; 10:4155.
6. Rozner AE, Dambaeva SV, Drenzek JG, Durning M, Golos TG. Modulation of cytokine and chemokine secretions in rhesus monkey trophoblast co-culture with decidual but not peripheral blood monocyte-derived macrophages. *Am J Reprod Immunol* 2011; 66:115-127.
7. Rozner AE, Durning M, Kropp J, Wiepz GJ, Golos TG. Macrophages modulate the growth and differentiation of rhesus monkey embryonic trophoblasts. *Am J Reprod Immunol* 2016; 76:364-375.
8. Lai A, Elfeky O, Rice GE, Salomon C. Optimized Specific Isolation of Placenta-Derived Exosomes from Maternal Circulation. *Methods Mol Biol* 2018; 1710:131-138.
9. Sabapatha A, Gercel-Taylor C, Taylor DD. Specific isolation of placenta-derived exosomes from the circulation of pregnant women and their immunoregulatory consequences. *Am J Reprod Immunol* 2006; 56:345-355.
10. Block LN, Bowman BD, Schmidt JK, Keding LT, Stanic AK, Golos TG. The promise of placental extracellular vesicles: models and challenges for diagnosing placental dysfunction in uterodagger. *Biol Reprod* 2021; 104:27-57.

11. Nguyen SM, Wiepz GJ, Schotzko M, Simmons HA, Mejia A, Ludwig KD, Zhu A, Brunner K, Hernando D, Reeder SB, Wieben O, Johnson K, et al. Impact of ferumoxytol magnetic resonance imaging on the rhesus macaque maternal-fetal interface. *Biol Reprod* 2020; 102:434-444.
12. Bayer A, Lennemann NJ, Ouyang Y, Bramley JC, Morosky S, Marques ET, Jr., Cherry S, Sadovsky Y, Coyne CB. Type III Interferons Produced by Human Placental Trophoblasts Confer Protection against Zika Virus Infection. *Cell Host Microbe* 2016; 19:705-712.

Appendix A

The promise of placental extracellular vesicles: models and challenges for diagnosing placental dysfunction in utero

Publication:

Block LN, Bowman BD, Schmidt JK, Keding LT, Stanic AK, Golos TG. The promise of placental extracellular vesicles: models and challenges for diagnosing placental dysfunction in utero†. *Biol Reprod.* 2021 Jan 4;104(1):27-57. doi: 10.1093/biolre/ioaa152. PMID: 32856695; PMCID: PMC7786267.

A.1 Abstract

Monitoring the health of a pregnancy is of utmost importance to both the fetus and the mother. The diagnosis of pregnancy complications typically occurs after the manifestation of symptoms, and limited preventative measures or effective treatments are available. Traditionally, pregnancy health is evaluated by analyzing maternal serum hormone levels, genetic testing, ultrasonographic imaging, and monitoring maternal symptoms. However, researchers have reported a difference in extracellular vesicle (EV) quantity and cargo between healthy and at-risk pregnancies. Thus, placental EVs (PEVs) may help to understand normal and aberrant placental development, monitor pregnancy health in terms of developing placental pathologies, and assess the impact of environmental influences such as infection, on pregnancy. The diagnostic potential of PEVs could allow for earlier detection of pregnancy complications via noninvasive sampling and frequent monitoring. Understanding how PEVs serve as a means of communication with maternal cells and recognizing their potential utility as a readout of placental health has sparked a growing interest in basic and translational research. However, to date, PEV research with animal models lags behind human studies. The strength of animal pregnancy models is that they can be used to assess placental pathologies in conjunction with isolation of PEVs from fluid samples at different time points throughout gestation. Assessing PEV cargo in animals within normal and complicated pregnancies will accelerate the translation of PEV analysis into the clinic for potential use in prognostics. We propose that appropriate animal models of human pregnancy complications must be established in the PEV field.

A.2 Introduction

Placental complications arise in ~15% of pregnancies, and due to pregnancy and childbirth maternal deaths occur in ~275,000 cases worldwide annually [1]. In 2010, preterm birth (PTB) was the most common cause of infant mortality and morbidity affecting ~15 million babies; Southeastern Asia, South Asia, and sub-Saharan Africa had the highest rates [2]. PTB causes approximately one million neonatal deaths each year across the world [3], with surviving infants displaying elevated risks of cardiovascular and respiratory diseases, neurological deficits, and developmental disabilities [4]. Fetal growth restriction (FGR) is the second most common pregnancy complication (impacts ~8% of pregnancies) [5]. FGR increases the risks of intrauterine demise, neonatal morbidity, cognitive delay, and adult-onset disease later in life [6, 7]. Women with pre-gestational diabetes (pre-GD) (having type 1 or type 2 diabetes before becoming pregnant) also have a greater risk of exacerbated symptoms during pregnancy, such as diabetic ketoacidosis, myocardial infarctions, retinopathy, and nephropathy, as well as obstetric complications including preeclampsia (PE), uteroplacental insufficiency, preterm labor, shoulder dystocia, and stillbirth [8-11]. Pregnancy complications not only cause emotional stress and trauma on the parents, but they also create an extreme financial burden for the family and the health care system. The annual financial costs are estimated to be \$26.2 billion for PTB, \$2.18 billion for PE, and \$1.8 billion for pregnancy-acquired diabetes (gestational diabetes mellitus; GDM) in the United States [12-14]. Earlier detection of complications, preventative strategies or therapeutics, and placenta-targeted treatments are imperative to improving the in utero environment of the fetus to benefit the long-term health of both the mother and child.

Diagnosis of a pregnancy complication relies on close monitoring of maternal and fetal health. Obstetricians monitor maternal health by measuring blood pressure, checking vital organs (e.g., renal function), and monitoring fetal health by measuring uterine growth via fundal height and fetal growth directly with ultrasound. Clinicians can also complete a biophysical profile and use Doppler velocimetry to monitor fetal blood flow within the umbilical cord and fetal middle cerebral artery [15]. Although the placenta is essential in pregnancy no minimally invasive techniques to directly monitor placental health are available. If biomarkers of abnormal placentation could be identified before the pathophysiological complication manifests itself, they may reveal the underlying mechanism(s) that contributes to the insult and provide a targeted approach to develop therapies/treatments.

Pregnancy complications that arise due to a malfunctioning or maldeveloped placenta include PE, early/recurrent pregnancy loss (EPL/RPL), PTB, FGR/intrauterine growth restriction (IUGR), and pre-GD/GDM (Table 1, Supplemental Table 1) [16]. An overview of complications is provided in Table 1 and includes the frequency of the complication within the population, the diagnostic measure to identify the pregnancy complication, and the known pathophysiology for the condition. While GDM is not thought to be a placental disease per se, it may impact fetal well-being as structural and functional alterations can occur in the placenta [17-19]. In addition, maternal infection with vertically transmitted pathogens also gives rise to adverse pregnancy outcomes and may impact placental function or fetal development [20, 21]. Amongst the implicated pathogens, the **TORCHZ** group is of particular neonatal concern and

consists of the following: **T**oxoplasma gondii, **O**ther [*Listeria monocytogenes*, *Treponema pallidum*, varicella zoster virus (VZV), human immunodeficiency virus (HIV), enteroviruses and parvovirus B19], **R**ubella virus, **C**ytomegalovirus (CMV), **H**erpes simplex virus, and **Z**ika virus [20, 22]. Thus, it is necessary to monitor placental health during and after maternal infection to determine if vertical transmission has occurred and to assess the risk of developing an adverse pregnancy outcome following infection.

PEVs may provide an excellent tool with which to monitor placental health and function in human patients. Isolation from fluids is minimally invasive, repeated sampling is feasible, and the ability to monitor the same patient over time provides valuable information as to how the placenta matures, develops, and responds to insult. Most importantly, PEVs contain placenta-specific proteins which may be used to selectively isolate them from more complex samples, such as blood [23, 24]. However, the roles of PEVs in cellular communication and maternal physiology are not well understood. PEVs are present in maternal blood as early as six weeks of gestation [25], and their presence early on makes them attractive molecular packages that may contain a readout of placental health from the early stages of placental development through delivery of the newborn.

Table A.1. Human pregnancy complications

Pregnancy complication	Percent Impact	Current means of identification	Underlying pathology
PE	<ul style="list-style-type: none"> 3-5% of pregnancies [177] Accounts for 14% of pregnancy-associated maternal deaths [177, 178] 	<ul style="list-style-type: none"> High blood pressure Proteinuria Possible renal, liver, pulmonary, and neurological sequelae [177] PE is sometimes split into two categories with separate pathologies: early onset PE (EPE), <34 weeks gestation and late onset PE (LPE), ≥34 weeks gestation 	<ul style="list-style-type: none"> Abnormal trophoblast invasion of the maternal decidua and incomplete remodeling of maternal spiral arteries leads to placental ischemia and a pro-inflammatory environment [179] Often associated with IUGR [177] EPE: considered a fetal disease with associated placental dysfunction LPE: a maternal disorder; placenta usually functions properly and is associated with better maternal and fetal outcomes, at least in part based on later delivery (obviating prematurity as a contributor to pathology) [180]
EPL	<ul style="list-style-type: none"> 15-25% of all clinical pregnancies [181-183] 		<ul style="list-style-type: none"> Fetal chromosomal abnormalities are the major cause [184, 185]; however, in cases of normal fetal karyotype, the cause is typically unknown [186-189]
RPL	<ul style="list-style-type: none"> ~1% of all women [190] 	<ul style="list-style-type: none"> RPL is identified by 2 or more clinical EPLs (pregnancy diagnosis based on ultrasound or tissue/pathology, not chorionic gonadotropin detection alone) [191] [181] 	<ul style="list-style-type: none"> When uterine anatomical anomalies, genetic factors, antiphospholipid syndrome, or hormonal pathologies are ruled out, more than 50% of patients suffer from unexplained RPL [181, 182, 192]
FGR/IUGR	<ul style="list-style-type: none"> 10% of pregnancies [193] 	<ul style="list-style-type: none"> Ultrasound-estimated fetal weight less than the 10th percentile for that gestational age or a fetus at <10th percentile at birth [193] 	<ul style="list-style-type: none"> Origins stem from errors in early placental development [194] Caused by placental insufficiency, genetic syndromes, maternal malnutrition, multiple gestation, teratogens, and oxygen deprivation [134, 195] Maternal vascular malperfusion is considered the leading cause of pathology in FGR placentas and can be accompanied with placental hypoplasia, infarction, and hemorrhage [196] Often associated with PE [177]
Pre-GD	<ul style="list-style-type: none"> ~7% of all pregnancies [11] 	<ul style="list-style-type: none"> Having type 1 or type 2 diabetes prior to start of pregnancy 	<ul style="list-style-type: none"> Hyperglycemia can impair and disrupt fetal organ development [8]
GDM	<ul style="list-style-type: none"> High risk of maternal morbidity [197] Leading cause of fetal macrosomia [198] 	<ul style="list-style-type: none"> Glucose intolerance and insulin resistance development during pregnancy 	<ul style="list-style-type: none"> Placentas from women with diabetes generally have greater surface area, Hofbauer cells, vasculature, and diffusion distance [199] Placental pathologies include chorionic villus immaturity, high villus density, stromal edema, thicker than average collagen fibers, and diffuse villous stromal calcifications [17], potentially impacting function
PTB	<ul style="list-style-type: none"> ~11% of all pregnancies [170] 75% of perinatal mortality is due to PTB [200] 	<ul style="list-style-type: none"> Birth before 37 weeks gestation [170] 	<ul style="list-style-type: none"> Oxidative stress and inflammation leading to early rupture of membranes are known to be leading causes of PTB, in addition to retroplacental abruption, chronic villitis, and twin gestations [201] Other causes hypothesized to be involved include vertically transmitted infections, maternal environmental stress, and intra-amniotic inflammation [170, 200]

Supplemental Table A.1: Citations based on the pregnancy complication and animal model studied.

Pregnancy complication	Reviews on the human condition	Animal model	Research articles
PE	[177, 179, 180, 354]	NHP	[153, 154, 266, 269]
		Guinea pig	[131]
		Rabbit	[173, 267]
		Mouse/Rat	[268, 270-274]
		Pig	[275-278]
EPL & RPL	[182, 184-186, 189, 333]	NHP	[155]
		Sheep	[279]
		Pigs	[138, 139]
		Cattle	[135-137, 355]
FGR/IUGR	[193-195]	NHP	[121, 155, 156]
		Guinea pig	[280-282, 287]
		Rabbit	[5, 118, 119, 285]
		Mouse/Rat	[120, 272, 282, 283, 288]
		Sheep	[117, 134, 286, 289]
Pre-GD & GDM	[8, 9, 11, 17]	Pig	[5, 117, 122, 134, 290]
		NHP	[157, 158]
		Guinea pig	[249, 291, 300]
		Rabbit	[292]
		Mouse/Rat	[293-296, 301-303]
PTB	[3, 170, 200, 201]	Sheep	[249, 297, 298, 304]
		Pig	[299]
		NHP	[122, 169, 325]
		Guinea pig	[169, 326, 327]
		Rabbit	[169, 305, 306, 327]
		Sheep	[169, 316, 317, 319, 320, 326, 327]
		Cattle	[321]

The purposes of this review are to 1) introduce EVs, or more specifically PEVs, as a molecular readout of placental health, 2) provide an overview of current information known about human PEVs, 3) discuss animal models used to study pregnancy complications, and 4) discuss future expansion of animal model PEV research to address critical challenges in human PEV research. Although extensive information from human EVs has been obtained from cell cultures and maternal blood sampling, there is a limited understanding of in vivo PEV function in humans and animal pregnancy models. Implementing animal pregnancy models will extend our understanding of trophoblast physiology during pregnancy complications, define PEV cargo and function, and explore the diagnostic and therapeutic potential of PEVs. In vivo

studies in experimental pregnancy models are essential to make PEV research translational to a human clinical setting. Due to the breadth of topics this review covers, we apologize for any publications not discussed and refer to more specific reviews wherever possible.

A.3 What are extracellular vesicles (EVs)?

The three main subtypes of EVs are exosomes (small, 60-80 nm in diameter [26] and large 90-120 nm [26]), microvesicles ~100-1000 nm [27], and apoptotic bodies ~ <5 μ m [27]. These are distinguished not only by size, but also by their route of cellular release (Figure 1) [27-31]. Figure 1 also shows EV release and highlights some unique cargo among the different subtypes. These naming conventions have been greatly debated since it is now well-understood that there is overlap in the size and cargo across EV classes [32-34]. The size criteria do not consider the mechanism(s) by which the EV is derived or secreted from the cell. For instance, an EV population isolated based on EV size may encompass both large exosomes and microvesicles; however, these vesicles may differ in their cargo, composition, and biological role. The lipid content may be a more definitive criterion to classify vesicles, as Ouyang et al. [35] demonstrated that phospholipid composition varies between EV classes. Standardized nomenclature across studies regarding the vesicle of interest would greatly strengthen this field of research, as inconsistent nomenclature makes it difficult to compare data across studies. When referencing the work of others in this review, we have used the terminology stated in that publication.

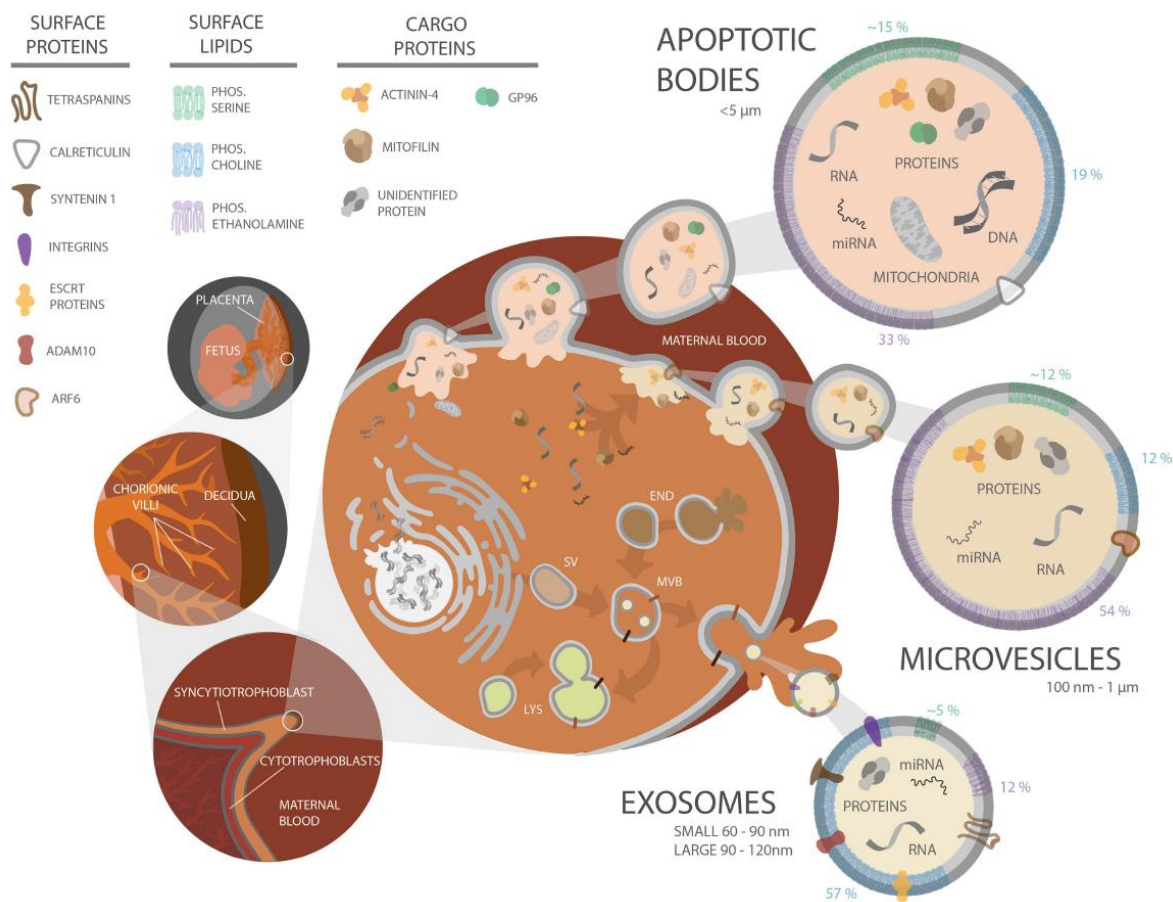


Figure A.1. Schematic diagram of human placental villous structure and PEV biogenesis. Placental structure with increasing magnification (organ level, tissue level, cellular level) is depicted at the left, along with apoptotic body, microvesicle, and exosome biogenesis in a trophoblast cell. A key for molecular elements is at the upper left. **Top right)** Apoptotic bodies form when a cell is undergoing apoptosis, as depicted by the breakdown of the nucleus and packaging of DNA and organelles. **Middle right)** Microvesicles are formed via pinching off of the plasma membrane, entrapping molecular cargo. **Bottom right)** Exosomes are assembled within the secretory pathway. Secretory vesicles (SV) are released by the golgi body and can fuse with endosomes (END). Endosomes also can fuse together or fuse with the lysosome (LYS) for cargo degradation. Late stage endosomes are also referred to as multivesicular bodies (MVBs) if they contain intraluminal vesicles (depicted as small light-yellow vesicles inside the MVB). All of these vesicles are then released into the maternal bloodstream. Some cargo and membrane proteins specific to the different EV classes are depicted. Lipid composition is depicted in a simplified, grouped manner on the border of the vesicles (green, phosphatidylserine; blue, phosphatidylcholine; purple, phosphatidylethanolamine), with the percent of each lipid content indicated adjacent to the membrane region. The gray membrane of the vesicles represents other lipids that have been identified including sphingomyelin,

phosphatidylglycerol, phosphatidylinositol, phosphatidic acid, bis-monoacylglycerophosphate, cardiolipin, lysophosphatidylcholine, and lysophosphatidylethanolamine [35].

A range of isolation techniques have been used to isolate exosomes, including differential ultracentrifugation, size exclusion chromatography, and polyethylene glycol precipitation [33, 36-42]. A major goal of these techniques is to obtain a homogenous population of EVs (i.e., only exosomes), but this remains a challenge given the overlap in size across EV sub-types. It is therefore difficult to compare data across studies, as sample types and isolation techniques vary greatly, especially if the EV populations being analyzed are not homogenous. While there is great scientific interest in exosomes due to their potentially bioactive cargo and ability to be taken up by target cells, recipient cells also can also take up microvesicles [43]. Moreover, both the quantity of exosomes and microvesicles present in maternal blood increases throughout gestation [44]. Given the current limitations in isolating a homogeneous population of an EV sub-type, it may be more appropriate to globally assess all PEVs to develop diagnostic tools for pregnancy complications. Once techniques are developed to isolate vesicles of a specific EV class, the approach to evaluating PEVs can be modified to assess specific EV sub-types.

A.4 EV formation, cargo packaging, and function

Exosomes form within an endosome that is also referred to as a multivesicular body (MVB). As depicted in Figure 1, MVBs can either fuse with the lysosome or the plasma membrane for cellular release. Exosomal surface proteins, such as the tetraspanins, are widely conserved across mammals, as shown in Table 2. Microvesicles form on the cell's surface where they

bleb off from the plasma membrane, and therefore, phosphatidylserine is commonly a component within their membranes [27]. Apoptotic bodies form when a cell undergoes apoptosis, where the cell's organelles organize into these non-inflammatory packages [27]. Microvesicles and apoptotic bodies commonly contain heat shock protein 96 (GP96), actinin-4, and mitofilin [34]. Although there is evidence for conservation of mammalian EV surface markers across EV sub-types, packaging of cargo still remains poorly understood. For more details on packaging of EV cargo and EV secretion pathways, the reader is directed to the following reviews [27, 29, 42, 45-47].

Biologically active nucleic acids, proteins, carbohydrates, and lipids can be packaged into EVs and secreted as a means of intercellular communication [28-30, 48-56]. Extensive research supports the concept that EVs have roles in diverse biological processes including the immune response [57, 58], inflammation [28-30, 59], and transmission of viral infection [28, 48-51, 60]. For example, researchers have shown that EV uptake by recipient cells induces cytokine release [61], inhibits protein translation [53, 62], influences cell proliferation and migration [63], and protects cells from oxidative stress [64]. Additional information on the impact of EVs on recipient cells and EV tropism and therapeutic potential can be found in the following papers [65-70].

Species	General EV markers	Placental markers	References
Human	CD9	PLAP	[27, 34, 202-208]
	CD63	PP13	
	CD81	Syncytin-1 and -2	
	syntenin-1	PAPP-A	
	EHD4	HLA-G	
	ADAM10	PSG-1	
	ESCRT proteins	C19MC	
NHP	CD63	PP13	[168, 209-214]
	CD81	Syncytin-1 and -2	
	Flotillin-2	PAPP-A	
		Mamu-AG	
		C19MC	
Guinea pig		PLAP	[215, 216]
		Env-cav1	
Rabbit	CD9	PLAP	[215, 217, 218]
	CD63	Syncytin-ory1	
	CD81		
	HSP101		
Mouse	CD9	Syncytin-A and -B	[89, 215, 219-222]
	Alix	PLAP	
	CD63		
	CD81		
Rat	CD63	PLAP*	[215, 223-226]
	TSG101		
Sheep	CD63	Syn-Rum1	[227-229]
	HSP70		
Cattle	CD9	PLAP	[103, 229-231]
	CD63	Syn-Rum1	
Pig	CD63		[232]

Table A.2.

Summary of known EV markers and placenta-specific markers across species.

Acronyms: cluster of differentiation (CD); placenta alkaline phosphatase (PLAP); placental protein 13 (PP13); chromosome 19 microRNA cluster (C19MC); pregnancy-specific glycoprotein 1 (PSG1); and pregnancy-associated plasma protein/pappalysin-1 (PAPP-A); EH domain containing protein 4 (EHD4); a disintegrin and metalloproteinase domain-containing protein 10 (ADAM10); endosomal-sorting complexes required for transport (ESCRT)

* indicates also expressed in other tissues

A.5 PEVs: sample sources, interactions with immune cells, and clinical potential

To highlight the potential information available from EV analysis, scientists have used the terms “circulating biopsy” [71], “fingerprint” [72], and “liquid biopsies” [72, 73]. EVs have received great attention as it has been shown that EV cargo may be altered under diseased and infection states [62, 64, 74], and they can be isolated from minimally invasive fluid samples. PEVs have been detected as early as six weeks of gestation [25](see Table 3 for an overview of the outcomes from human PEV research); however, trophoblasts secrete chorionic gonadotropin into maternal blood shortly after embryo implantation, suggesting that PEVs may encounter maternal cells just as soon.

The cellular and molecular bases of pregnancy complications are difficult to address within the complexities of an *in vivo* pregnancy setting, owing to variability in genetics, lifestyle influences, physiology, and differing environmental exposure. Researchers examining human PEVs have focused extensively on characterizing EVs isolated from placental cell cultures (e.g., primary cells and immortalized trophoblast cell lines), placental explants, the perfusate of intact placentas, and maternal peripheral blood. PEVs isolated from placental cell cultures and explants can interact with maternal immune cells [59, 75-77], suggesting that PEVs may modulate maternal immune responses during pregnancy.

Table A.3 PEV studies in humans, rodents, cows, pigs, and sheep.

Experimental model	Sources of EVs (experimental and control)	Pregnancy complication	Findings	References
Human	<ul style="list-style-type: none"> • Plasma from healthy first, second, and third trimester women • Plasma from women with PE • HUVEC-conditioned media • Plasma from women with PE • Plasma from women with EPE & LPE • PE placentas that underwent either mechanical disruption or perfusion • PE placental explant-conditioned media • PE placental explant-conditioned media • Sera from women with PE 	<p>—</p> <p>PE</p> <p>PE</p> <p>PE</p> <p>PE</p> <p>PE</p> <p>PE</p> <p>PE</p> <p>PE</p> <p>PE</p>	<ul style="list-style-type: none"> • Increased quantity of exosomes and PLAP+ exosomes with gestation • Exosomes had a positive impact on endothelial cell wound healing, with early gestation having the greatest impact • Higher quantities of EVs, ST-derived EVs, and phosphatidylserine/annexin-V-positive EVs in PE patients • Decreased expression of eNOS in HUVECs exposed to exosomes from PE patients • More miR-155 within EVs from PE patients • miR-155 downregulates eNOS expression • Elevated levels of exosomes and PLAP+ exosomes, throughout gestation in PE patients • Exosomal miRNA profiles differed significantly • Greater exosome quantity in EPE or LPE compared to control • Placental vesicle quantity was elevated in EPE and significantly decreased in LPE, which indicates that the etiology between them is different • Increased Flt-1 in PE ST-derived EVs • Decreased endoglin in PE ST-derived EVs • Decreased presence of integrins in ST microvesicles from PE placentas may be associated with reduced trophoblast invasion and defective placental vascularization • Isolated macro, micro, and nanovesicles with differential ultracentrifugation • Microvesicles from PE placentas were larger in size • PE placentas extruded more micro- and nanovesicles, which contained more Flt-1 than control vesicles • More VEGF was detected in EVs secreted by PE placentas • Syncytin-1 and -2 and PLAP are on the membrane of exosomes released by primary trophoblast cells • Less syncytin-2 in exosomes from women with PE compared to control • Decreased internalization of exosomes released by trophoblast cells deficient in syncytin-1 and -2 (via siRNA transfection) compared to controls 	<p>[102]</p> <p>[87, 91, 233, 234]</p> <p>[62]</p> <p>[92]</p> <p>[90]</p> <p>[74]</p> <p>[235]</p> <p>[93]</p> <p>[145]</p>

Experimental model	Sources of EVs (experimental and control)	Pregnancy complication	Findings	References
	<ul style="list-style-type: none"> Plasma from women throughout gestation that later developed LPE 	PE	<ul style="list-style-type: none"> Nonsignificant increase in total number of MP over gestation Over gestation in healthy samples, the quantity of HLA-G+ MPs that contained dsDNA decreased and minimal change in the quantity of PLAP+ MPs with dsDNA was observed LPE samples contained significantly more total MP than healthy; however, the quantity of HLA-G+ or PLAP+ MPs was not different. This suggests that the ontology of LPE is different than EPE 	[236]
	<ul style="list-style-type: none"> Placental explant-conditioned media from women with RPL or PE Plasma from women with either SGA or FGR fetuses 	RPL and PE	<ul style="list-style-type: none"> Altered lipid composition in ST microvesicles from RPL and PE compared to controls 	[237]
	<ul style="list-style-type: none"> Plasma from women with either EPE, LPE, or normotensive IUGR 	FGR	<ul style="list-style-type: none"> No difference in the total number of exosomes or PLAP+ exosomes in fetal plasma Lower percentage of placental exosomes in maternal and fetal plasma from FGR and SGA pregnancies compared to controls More placental exosomes in fetal than maternal plasma Significantly higher quantities of ST microparticles in EPE plasma, but not LPE or normotensive IUGR, compared to controls 	[238]
	<ul style="list-style-type: none"> Plasma from women with GDM 	PE and IUGR	<ul style="list-style-type: none"> Increase in total exosomes and PLAP+ exosomes from women with GDM compared to controls 	[56]
	<ul style="list-style-type: none"> Term perfused placenta from women with GDM 	GDM	<ul style="list-style-type: none"> Total number of exosomes detected in the plasma of GDM patients at later stages of gestation was negatively correlated with placental weight, while the amount of exosomal PLAP was positively correlated Increased cytokine release from HUVECs exposed to GDM exosomes than healthy exosomes or baseline 56% of medium/large EVs and 36% of small EVs were PLAP+ DPPiV, an enzyme that is inhibited in type 2 diabetes mellitus therapy, was co-expressed on PLAP+ EVs. DPPiV retained enzymatic activity on EVs EVs from GDM samples had greater quantities of DPPiV+ EVs and greater DPPiV activity than controls 	[239]
	<ul style="list-style-type: none"> Plasma from second trimester women with GDM 	GDM	<ul style="list-style-type: none"> 78 proteins were differentially expressed in exosomes from women with GDM compared to controls, including proteins involved in metabolic processes and biological regulation CAMK2beta was more abundant and PAPP-A was less abundant in exosomes from women with GDM compared to controls Selective enrichment of proteins from the placenta in GDM exosomes compared to controls 	[240]

Continued

Experimental Sources of EVs (experimental and control) model	Pregnancy complication	Findings	References
<ul style="list-style-type: none"> • Serum from first trimester women with GDM 	GDM	<ul style="list-style-type: none"> • PLAP+ EVs were not detected until the 8th week of pregnancy • 17 miRNAs were analyzed by qPCR in total serum EVs • Differential miRNA content between GDM and control EVs. Pathway analysis showed that increased quantities of miRNAs in EVs from GDM were involved in placental development, fetal growth, and insulin and glucose regulation 	[241]
<ul style="list-style-type: none"> • Placental explant-conditioned media from women with GDM 	GDM	<ul style="list-style-type: none"> • Explants from GDM placentas secreted more EVs • Exosomes from controls increased skeletal muscle cell proliferation and migration, in vitro, compared to GDM. Potentially due to differential miRNA expression in exosomes from GDM versus control 	[63]
<ul style="list-style-type: none"> • Plasma from women obese or overweight 	Obese/overweight	<ul style="list-style-type: none"> • miRNA content in exosomes differed from miRNAs in the cells of origin • There is an increase in exosome and PLAP+ exosome quantity over gestation, which is independent of BMI • There is a correlation between BMI and exosome quantity • No significant increase (12–20%) in PLAP+ exosomes throughout gestation • Exosomes were taken up by HUVECs and altered HUVEC cytokine release. Cytokine release changed based on the trimester and health status of the woman. Exosomes from obese plasma resulted in significantly more IL-6, TNF-alpha, and IL-8 release. No change in IL-10 was observed. 	[142]
<ul style="list-style-type: none"> • First trimester trophoblast cell-conditioned media incubated in high and low levels of glucose to mimic maternal hyperglycemia 	Hyperglycemia and hypoxia	<ul style="list-style-type: none"> • Exposure to hypoxia and high quantities of glucose resulted in increased exosome release • HUVECs released higher quantities of cytokines when exposed to exosomes isolated from cells grown under hypoxia and incubated in high quantities of glucose 	[242]
<ul style="list-style-type: none"> • HTR8/SVneo-conditioned media grown under normoxia and hypoxia 	PTB and PE	<ul style="list-style-type: none"> • Exosomes from cells grown under hypoxia negatively impacted endothelial cell wound healing • Unique miRNAs were identified in each condition and three miRNAs were only detected in exosomes from pathological conditions (hypoxic cells, PTB and PE) • Similar exosome miRNA cargo between cells grown under hypoxia and exosome miRNA cargo in early gestation maternal blood from PTB 	[115]
<ul style="list-style-type: none"> • Plasma collected throughout gestation from women who had a PTB 	PTB	<ul style="list-style-type: none"> • Altered exosomal miRNA cargo between term and PTB (throughout gestation) • Shows that alterations in miRNA expression are present early in gestation, which supports possible use of EVs as a screening tool for risk of PTB 	[243]
<ul style="list-style-type: none"> • Plasma from women who were undergoing preterm labor 	Preterm labor	<ul style="list-style-type: none"> • Small RNAseq was performed on whole plasma, EV-depleted plasma, and EVs • Pregnancy-associated miRNA cluster expression, including C14MC and C19MC miRNAs, were expressed at lower levels in preterm labor EV samples compared to healthy pregnancies 	[116]
<ul style="list-style-type: none"> • Plasma from women who experienced PTB or PPRM 	PTB	<ul style="list-style-type: none"> • No change in exosome quantity between the three groups • Significantly decreased levels of placental exosomes and different protein cargo in instances of PPRM compared to women with PTB or controls 	[244]

Experimental model	Sources of EVs (experimental and control)	Pregnancy complication	Findings	References
Rodent	<ul style="list-style-type: none"> • Mouse PEVs (syncytin-positive) obtained from freeze-thaw injured placentas • HTR8/SVneo cells grown under hypoxic oxygen • Human first trimester placenta explant conditioned media • Pregnant mouse plasma 	<p>PE</p> <p>—</p> <p>—</p> <p>PTB</p>	<ul style="list-style-type: none"> • Pregnant mice injected with PEVs had proteinuria and vascular leakage • Nonpregnant mice injected with PEVs resulted in hypertension and proteinuria • Enhancing EV clearance by treatment with the microvesicle-scavenging factor lactadherin prevented the development of this PE-like phenotype • Lactadherin ^{-/-} mice had elevated blood pressure, proteinuria, and fewer litters • Hypoxia induces increased secretion of small EVs • Protein cargo was different between small EVs from hypoxic and normoxic cells • Injection of the small EVs from cells grown under hypoxic conditions into rats resulted in elevated blood pressure, but had no impact on fetal survival or placental size • Nanovesicles (vesicles smaller than 100 nm) altered the sensitivity of mesenteric artery dilation in pregnant, but not nonpregnant, mice • Vesicles did not alter uterine artery dilation or constriction • Human vesicles preferentially end up in mouse maternal lungs, liver, and kidneys while the fetoplacental unit was negative • The uterus and cervix were not analyzed • Quantity of exosomes increased with gestation • Mouse plasma exosomes trafficked to the cervix, uterus, fetal membranes, and placenta, and no exosomes were detected in other maternal or fetal tissues • Late gestation exosomes had increased quantities of proinflammatory proteins compared to nonpregnant or early gestation exosomes • Injection of late gestation exosomes into early gestation mice resulted in PTB 	<p>[89]</p> <p>[226]</p> <p>[245]</p> <p>[221]</p>
Cow	<ul style="list-style-type: none"> • Pregnant cow plasma • Nonpregnant cow plasma 	—	<ul style="list-style-type: none"> • Pregnant plasma exosomes suppressed the expression of the inflammatory cytokines TNF-alpha and IL-6 in BEND cells • Preferential location of miR-499 is in exosomes • Inhibition of miR-499 expression in mice resulted in increased uterine inflammation, EPL, and FGR 	[231]
Pig	<ul style="list-style-type: none"> • Porcine trophectoderm cell line (PTr2) 	<ul style="list-style-type: none"> • Porcine aortic endothelial cells (PAOEC) 	<ul style="list-style-type: none"> • EVs from PTr2 influenced the proliferation of PAOECs • Uptake of heterologous EVs was more likely that autologous EV uptake 	[148]
Sheep	<ul style="list-style-type: none"> • Pregnant sheep sera • Nonpregnant sheep sera 	—	<ul style="list-style-type: none"> • Exosomal miRNA cargo changed throughout gestation • C14 miRNAs decreased in quantity as gestation continued 	[228]

MP, microparticle; eNOS, endothelial nitric oxide synthase; HUVEC, human umbilical vein endothelial cells; SGA, small for gestational age; PPRoM, preterm premature rupture of membranes; C14MC, chromosome 14 microRNA cluster; C19MC, chromosome 19 microRNA cluster; TNF-alpha, tumor necrosis factor-alpha; IL-6, interleukin-6; HTR8/SVneo, extravillous trophoblast cell line; BEND cells, bovine endometrial epithelial cells; ST, syncytiotrophoblast; DPPiV, dipeptidyl peptidase IV; qPCR, quantitative real time polymerase chain reaction; CAMK2beta, calcium/calmodulin-dependent protein kinase II beta.

A.6 Current in vivo and in vitro sources for isolating PEVs

In vitro placental cell cultures provide a means to isolate an enriched PEV population. Stable cell lines can be expanded quickly to generate a homogenous cell population, allowing investigators to define a cell type-specific readout or secretory profile in response to an experimental manipulation (e.g., genetic mutation, infection, hypoxia, drug treatment). However, because some trophoblast cell lines are derived from spontaneously arising tumors or have been immortalized by molecular tools, their gene and protein expression profiles differ from each other and with primary trophoblast cultures [78, 79].

Primary cells provide a more accurate representation of in vivo trophoblasts and can be isolated from gestationally age-matched healthy and maldeveloped placentas for direct comparison. The ability to obtain trophoblasts from first and second trimester placentas, however, may be limited due to constraints surrounding human samples. Until recently, primary term villous cytotrophoblast cells were used only for short-term experiments as they do not proliferate and spontaneously syncytialize [80]. Recent optimization of primate trophoblast cell culture conditions now supports long-term cell proliferation and culture of trophoblast stem (TS) cells derived from primary placental cells or embryos that can be directed toward cell-type specific differentiation [81-84].

Placental explant cultures contain all cell types within the placenta (placental macrophages, cytotrophoblasts, and syncytiotrophoblasts) and therefore provide a more complete system

compared to primary cell cultures. Limitations of this culture system include a limited duration of tissue viability [85, 86] and difficulty obtaining placentas from early pregnancies. It also is well accepted that pregnancy complications often stem from errors in early placentation. Therefore, it cannot be known if a complication would have arisen later in gestation when a placenta sample is obtained early in pregnancy. In addition, the large volume of medium used to culture explants can dilute the EV sample [86]. Alternative approaches include obtaining EVs by mechanical scraping the placental villi [61, 87] or perfusing fully intact term placentas [85]. Notably, vaginally-delivered term placentas may be confounded by the process of labor.

Overall, *in vitro* models are useful because they can allow for the rapid generation of PEV-enriched samples, be used to validate antibodies, and provide physiological readout in response to trophoblast insult (i.e., exposure to toxins, hypoxia, or pathogens). These *in vitro* models also predominantly contain EVs secreted by trophoblasts, whereas maternal blood contains the totality of EVs released by all maternal as well as placental cell types. It is likely that the changes in plasma-derived EVs in pregnancy reflect the maternal adaptation to pregnancy by all maternal organ systems, and not specifically placental development. While EVs from non-placental sources during pregnancy may provide novel biological information, they do not specifically provide direct feedback about placental health *per se*. Previous studies have demonstrated that the source (bodily fluids, culture media, tissue homogenization) and sample preparation method influence EV function [87, 88]. Therefore, when establishing a PEV model or interpreting study results it is important to consider the origin of the PEV population being analyzed.

A.7 PEVs isolated from adverse human pregnancies.

The analysis of human PEVs isolated from in vitro sources and maternal blood has revealed alterations in PEV cargo between healthy and unhealthy placentas. The isolation methods vary greatly across studies, thus limiting the ability to identify consensus biomarkers associated with an abnormal placental condition. A summary of the findings from studies that have evaluated EV cargo in human and animal pregnancy models in relation to a pregnancy complication is provided in Table 3, and here we focus on the highlights of quantity and cargo of EVs associated with human pregnancy complications.

Elevated PEV levels offer potential to distinguish complicated from healthy pregnancies. Increased quantities of EVs in maternal blood have been associated with various pregnancy complications as summarized in Table 3 [56, 89-93]. However, there are two concerns with these reports. First, it is unclear whether the research findings are specific to one complication or if they are applicable across pregnancy complications. If it is the latter, elevated EVs would be a general reflection of abnormal placental development and/or function. To determine the diagnostic value of EVs, a comprehensive analysis of EVs isolated from healthy pregnant women and women with a range of pregnancy complications is needed. Second, the techniques used to isolate and quantify (different instruments and/or different setting for the same instrument) EV samples vary widely, which dramatically hinders interstudy comparisons. Until standardized isolation and sample analysis techniques are implemented, variation in EV quantity will continue to be an uncertain indicator of a pregnancy's health status.

Although human PEV cargo is not well characterized, EVs may contain evidence of placental infection and may serve as means of modulating immune responses. For instance, EVs isolated from trophoblast conditioned media protected non-placental cells from viral infection [94-96]. Viral proteins and genomes also have been detected within exosomes and infection was found to alter exosome cargo [60, 97]. As such, clinicians could examine PEVs to learn if a pathogen has breached the maternal-fetal interface as they could directly monitor placental response and health status.

A.8 PEVs interact with immune cells during pregnancy.

Maternal immune systems inappropriately adapted to pregnancy are associated with pregnancy complications and pregnancy loss [98]. PEVs contain a range of immunoregulatory molecules [99, 100] and interact with maternal immune cells in vitro, which suggests PEVs may be involved in maternal immune adaptation in pregnancy. EVs are involved in the recruitment of monocytes and macrophages as well as in cytokine and chemokine regulation [76]. Syncytiotrophoblast-derived EVs from healthy placentas suppress and/or promote immunological pathways [77]. Thus, understanding the interaction between the maternal immune system, the feto-placental unit, and EVs is important. In addition, EVs from pregnant women impact immune cells differently than EVs from non-pregnant women [59, 75]. The dynamic complexities between PEVs and the immune system in a healthy and diseased state support the importance of in vivo models.

Differences in EV tropism for immune cells appears to depend on the source of the EV sample, i.e., peripheral blood versus placental tissue. Germain et al. observed strong binding of syncytiotrophoblast microvesicles from term placentas to monocytes in first trimester blood with decreased binding throughout gestation, as determined by ELISA [87]. However, microvesicles from third trimester human placentas bound preferentially to monocytes and B-cells versus T and NK cells as assessed by Image Stream technology [61]. In contrast, microvesicles isolated from third trimester blood bound to T cells and not B or NK-cells via FACS [59]. These studies co-incubated peripheral blood mononuclear cells (PBMCs) with EV samples in vitro. Since the methodologies used to isolate these EVs impacted tropism and downstream function, in vivo experiments will be important to study the interplay between PEVs and the immune system. EVs obtained from mechanical scraping of term placental villi did not stimulate PBMCs, whereas EV samples obtained from placental perfusate were more stimulatory [61, 87]. Notably, these EVs were obtained from term placentas and represent the end point of pregnancy. Pap et al. [59] found that 50% of microvesicles positive for Human leukocyte antigen G (HLA-G) were also positive for Fas ligand (FasL). The authors hypothesized that these two molecules present on the EV surface are involved in maternal immune tolerance [59].

A.9 Surveying PEV markers and cargo to identify pregnancy complications.

Classic EV markers, such as tetraspanins and ESCRT proteins [27], have been routinely identified in human and animal EVs, as listed in Table 2. As an adjunct to monitoring maternal systemic physiological changes (e.g., blood pressure or proteinuria), clinicians could directly

monitor placental health and development by surveying PEVs. The application of PEVs as a prognostic molecular tool, however, is hindered by the current lack of validated placental biomarkers associated with a pregnancy complication in humans or animals. Furthermore, there are few validated placenta-specific EV surface markers to isolate PEVs. The most widely used placenta-specific marker for PEV isolation is placenta alkaline phosphatase (PLAP) [23, 24, 87, 101]. A PLAP ELISA has been used to quantify PEVs from human [25, 90, 102] and bovine samples [103]; however, validation and information regarding cross-reactivity of this antibody is lacking. Despite its use by several labs, there are challenges with specificity as other alkaline phosphatases have been detected in various healthy tissues that can be recognized by PLAP antibodies [104-106]. Validating these PLAP antibodies and making other in-house antibodies, such as NDOG2 and ED822 [74, 87, 107], commercially available will increase reproducibility across studies. HLA-G, another placenta-specific protein, also has been used to isolate and detect PEVs [24, 59], recognizing that this would be an extravillous trophoblast marker. Other placenta-specific protein candidates include: syncytin-2, placental protein 13 (PP13), pregnancy-specific glycoprotein 1 (PSG1), and pappalysin-1 (PAPP-A) (Table 2).

Changes in PEV cargo highlight a difference between healthy and pathological placentas, as shown in Table 3. Cuffe et al. discussed the presence of two classes of molecules: “passive” and “bioactive” [108]. Passive molecules are hypothesized to have high predictive potential, whereas bioactive molecules are constitutively secreted by the placenta [108]. Further supporting the use of PEVs to monitor placental health. PE is perhaps one of the more well-

studied pregnancy complications in which PEV quantities and cargo have been evaluated [109]. Nair and Salomon's recent review on human GDM [110] discussed systemic and placental changes in EVs. Several studies have focused on RPL and procoagulant microparticles, EVs secreted by platelets and endothelial cells [111-114]; however, we were unable to find any reports regarding the association of PEVs and EPL/RPL. Researchers have observed alterations in PEV cargo between women experiencing PTB compared to controls; however, they have not identified a consistent biomarker [115, 116]. For instance, one study only detected miR-525-5p in EVs from a pathological condition (PTB, PE, or cells grown under hypoxia) [115]. Another study found miR-525-5p to be significantly lower in PTB EVs compared to controls [116]. To understand the changes in PEV cargo associated with the cell's physiological state, it is necessary to first understand whether EV cargo is selectively packaged. The survey of PEV cargo upon experimental knock out of lysosomal enzymes would provide insight to the critical question of cargo selection that spans all disciplines of the EV field.

The dearth of placenta-specific markers for PEV isolation and lack of agreement upon biomarkers of a pregnancy complication highlight the need for consistent methodologies and nomenclature in studies that isolate PEVs from these various pregnancy complications. Identification of biomarkers resulting from aberrant placental development may allow for earlier diagnosis and intervention or earlier application of a placental therapy. PEV analysis also could enable better categorization of adverse pregnancy outcomes via specific molecular changes in the placenta rather than by less specific maternal symptoms and fetal measurements.

A.10 Animal models of human pregnancy complications

Most PEV research has been performed using human fluid samples and in vitro trophoblast cultures, with relatively few studies in animal models. Due to the complexities of obtaining and working with human samples and the limitations of vitro systems discussed thus far, other systems are needed to advance the study of PEVs. Animal models can provide the rigor and reproducibility that are difficult to achieve with human samples, due to uncontrolled external factors and genetic diversity among clinical patients. Advantages of collecting PEV data from animal models include: access to large cohorts raised in controlled environments; rigorous sampling (i.e., the ability to collect samples early in pregnancy and at precise time points); control of the factor(s) causing the pregnancy complication (in some instances); the ability to utilize an animal as its own control during the same or subsequent pregnancy; the potential for longitudinal studies spanning pre-conception to the delivery of the offspring; and the opportunity for transgenerational studies.

Despite the differences in placentation across animal models, each animal model has strengths and shares similarities to humans that are useful when disentangling the mechanisms underlying pregnancy complications. When selecting an animal model to study a pregnancy complication, the following considerations should be addressed: placentation (i.e., depth of invasion, trophoblast cell organization, immune cell presence), animal husbandry for maintaining a study cohort (without/or without manipulation of an environmental factor), and the specific questions asked during the study (i.e., the importance of the fetus being born precocial; monotocous versus polytocous species). For example, the lack of endometrial

trophoblast invasion by the pig placenta and minimal invasion in sheep has limited their utility in modeling PE. Although the pig placenta may not ideally model PE, its similarities in fetal development with humans could be beneficial to study FGR [117]. Furthermore, FGR studies in sheep and rabbit models provide an opportunity for the animal to serve as its own control by evaluating the unmanipulated, opposite uterine horn [5, 118-120]. An overview of placentation is depicted in Figure 2 and details regarding pregnancy and translatability of each animal model discussed in this review are listed in Table 4 [121-125].

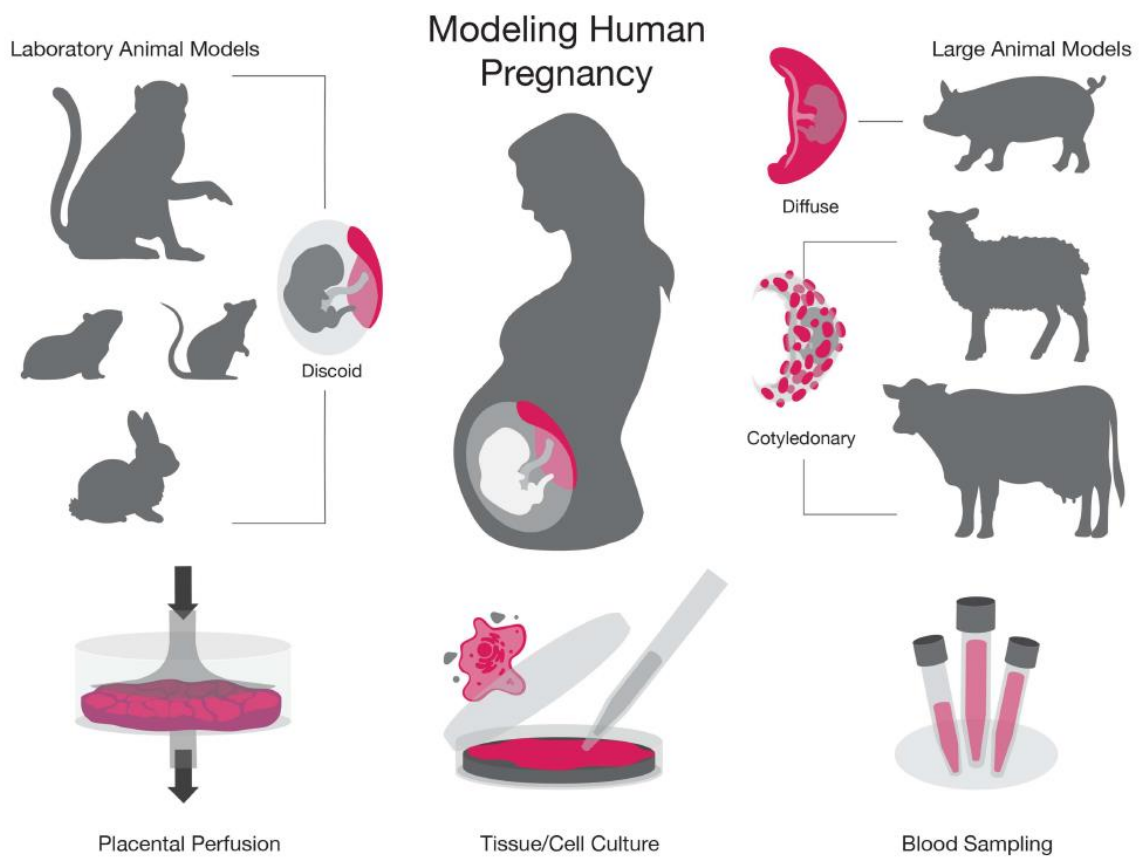


Figure A.2. Experimental models of human pregnancy. *Laboratory animal models (NHP, guinea pig, rodent, and rabbit), large animal models (pig, sheep, and cow), and in vitro systems (placental perfusion, tissue/cell culture, and blood) are depicted to represent experimental models of human pregnancy.*

Animal models allow for longitudinal study to identify early biomarkers prior to or at the onset of a complication, which is not possible in humans due to the delays in confirming pregnancy and the need to avoid perturbing early gestation. Identifying changes or biomarkers at the onset of a complication, even before placentation is complete, may be important for diagnosing or preventing a further adverse outcome. Once biomarkers have been identified in an animal model, they can then be validated for tissue-specificity and reproducibility within and across species for subsequent translation to humans. For example, miR-210 is more highly expressed in the placentas of mice with PE compared to healthy placentas. It is also expressed in human and ovine placentas [126, 127] with aberrant regulation in human PE and upregulation of the miRNA in hypoxic human placentas. Thus, animal models have led to the identification of a putative biomarker of PE, where upon further refinement of the timing of aberrant expression and identification of target mRNAs may reveal the biological processes contributing to the manifestation of the placental complication.

Table A.4. Comparison of placentation across different research models.

Model	Type of placentation	Gestation length (days)	Advantages	Limitations
Human	<ul style="list-style-type: none"> ▪ hemochorial ▪ discoid ▪ villous organization and extensive spiral artery remodeling ▪ interstitial extravillous trophoblast invasion 	280	<ul style="list-style-type: none"> ▪ maternal plasma readily accessible ▪ placenta samples available from a broad spectrum of adverse pregnancy outcomes ▪ diverse and extensive literature database ▪ well-established in vitro systems (e.g. cell culture, explants, placental perfusion) ▪ TS cells available[81-83] 	<ul style="list-style-type: none"> ▪ difficult to control environment factors ▪ highly variable genetics ▪ restrictions to testing treatments/therapeutics ▪ precise timing of start of pregnancy can be uncertain ▪ delays in pregnancy detection limits the ability to obtain samples within first few weeks of pregnancy
Macaque monkey	<ul style="list-style-type: none"> ▪ hemochorial ▪ bi-discoid placenta ▪ extensive endovascular extravillous trophoblast remodeling of decidual spiral arteries 	165	<ul style="list-style-type: none"> ▪ ability to test treatments/ therapeutics ▪ most appropriate model available for human placental physiology, immunology and endocrine function at the maternal-fetal interface[121, 246, 247] ▪ placental architecture is highly translational[121] ▪ offspring are born precocial ▪ placental transfer of passive immunity ▪ placental expression of C19MC[203] and nonclassical MHC class [247] 	<ul style="list-style-type: none"> ▪ trophoblast interstitial extravillous invasion is superficial in comparison to human ▪ limited transgenic models ▪ specialized veterinary expertise & housing required
Guinea Pig	<ul style="list-style-type: none"> ▪ hemomonochorial ▪ discoid ▪ labyrinthine, invasive [141, 169, 248, 249] 	67	<ul style="list-style-type: none"> ▪ offspring born precocial[141, 169, 249] ▪ blastocyst is completely encapsulated within the decidua, similar to human[248] ▪ passive immunity in late term[250] ▪ substantial trophoblast invasion[5] ▪ similar steroid production and metabolism in the decidua and fetal membranes as the human[169] 	<ul style="list-style-type: none"> ▪ dearth of available antibodies ▪ lack of transgenic models
Rabbit	<ul style="list-style-type: none"> ▪ hemodichorial ▪ discoid ▪ labyrinth organization[125, 169] 	32	<ul style="list-style-type: none"> ▪ fully sequenced genome[122] ▪ induced ovulator allowing for timed matings[122] ▪ offspring born precocial[172] ▪ passive immunity in late term[250] ▪ housing facilities are readily available 	<ul style="list-style-type: none"> ▪ placental endocrinology is different than human[169] ▪ dearth of available antibodies
Mouse	<ul style="list-style-type: none"> ▪ hemotrichorial ▪ discoid ▪ labyrinthine organization and some spiral artery remodeling[125] 	20	<ul style="list-style-type: none"> ▪ facile manipulation of genetics[122] ▪ ability to test treatments/ therapeutics ▪ timed mating ▪ NK cells present at MFI as with human[251] ▪ ability to perfuse mid and late gestation placentas[85] ▪ TS cells available[85, 252] 	<ul style="list-style-type: none"> ▪ offspring not born precocial ▪ placental organization, cell types, and endocrine profile differ compared to humans[253-255] ▪ PLAP is not expressed ▪ blood flow to the placenta is more limited than in human[121] ▪ lack non-classical MHC expression[251, 256] ▪ shallow implantation compared to rat or human[251] ▪ placental expression of C19MC miRNA is not conserved[203] ▪ TS cell isolation and propagation differ from primate[81-84, 257] ▪ murine cytotrophoblast cells are in direct contact with maternal blood, whereas syncytiotrophoblasts are in direct contact in the human[98]

Model	Type of placentation	Gestation length (days)	Advantages	Limitations
Rat	<ul style="list-style-type: none"> ▪ hemotrichorial ▪ discoid ▪ labyrinthine organization ▪ deep placental implantation[251, 258] 	22	<ul style="list-style-type: none"> ▪ non-classical MHC expression[251, 256] ▪ NK cells at MFI as human[251] ▪ larger size compared to mouse allows practical advantages (tissue availability, surgical procedures) ▪ TS cells available[85, 259] 	<ul style="list-style-type: none"> ▪ offspring not born precocial ▪ different placental organization & cell types compared to humans[258] ▪ placental expression of C19MC miRNA is not conserved[203] ▪ less extensive genetic technology and antibody development compared to the mouse[122] ▪ different endocrine profile than humans[255]
Sheep	<ul style="list-style-type: none"> ▪ epitheliochorial (synepitheliochorial) ▪ cotyledonary[250] 	150	<ul style="list-style-type: none"> ▪ relatively few offspring per liter[5, 260] ▪ offspring born precocial[122] ▪ large blood samples and surgical manipulations including chronic instrumentation of the fetus are feasible 	<ul style="list-style-type: none"> ▪ minimal trophoblast invasion[260] ▪ practical limitations on housing of research animals and length of gestation ▪ different placental cell types and endocrine profile than humans[255]
Cattle	<ul style="list-style-type: none"> ▪ epitheliochorial (synepitheliochorial) ▪ cotyledonary ▪ partially non-deciduate[103, 261, 262] 	280	<ul style="list-style-type: none"> ▪ sites of nutrient and waste exchange are villous[124] ▪ macrophages located at the maternal-fetal interface at low levels during the first two-thirds of pregnancy and increase substantially by term[261] ▪ nonclassical MHC expression towards the end of pregnancy[263] ▪ TS cells available[264] ▪ large blood samples and surgical manipulations are feasible 	<ul style="list-style-type: none"> ▪ minimal trophoblast invasion[260] ▪ practical limitations on housing of research animals and length of gestation ▪ different placental cell types and endocrine profile than humans[255]
Pig	<ul style="list-style-type: none"> ▪ epitheliochorial ▪ diffuse[262] 	114	<ul style="list-style-type: none"> ▪ fully sequenced genome[260] ▪ placental attachment is superficial and interdigitates with the highly folded maternal endometrium ▪ TS cells available[265] ▪ large blood samples and surgical manipulations are feasible 	<ul style="list-style-type: none"> ▪ fetal nutrition is predominantly acquired through uterine gland secretions ▪ passive immunity does not occur until after birth[250] ▪ unlike humans, there is no syncytiotrophoblast cell type[124] ▪ practical limitations on housing of research animals and length of gestation

Animal studies will have an essential role in showing proof of principle for the potential of a therapeutic intervention or diagnostic assay prior to translation into human clinical studies. For example, pregnant guinea pigs and sheep were used to test an experimental placental treatment, in which injection of an adenoviral vector overexpressing VEGF reduced FGR [128, 129]. Due to the positive outcomes in these animal models, this therapy subsequently was transitioned into a clinical trial in Europe (EVERREST project) [130]. Further use of animal models will not only enable the development of improved diagnostics, but they also can provide a platform for developing and evaluating the efficacy of placental therapies [120]. In these animal models a thorough understanding of the complication as well as the safety of a therapeutic can be appropriately evaluated prior to transition into a clinical trial; however, there must be a thorough understanding of the etiology of that pregnancy complication. The guinea pig and macaque, for example, are both ideal for placenta-targeted therapies as they similarly share a hemochorial type of placentation, bypassing additional maternal layers present in livestock species. Thus, a common workflow in placental research, and other fields, is to identify in rodents, verify in nonhuman primates (NHPs), and then translate to humans. This approach can be implemented in the PEV field by broadly utilizing various experimental animal pregnancy models.

A.11 Spontaneous versus induced animal models of adverse pregnancies

While pregnancy complications can develop spontaneously in animal models, they are frequently induced. Similar to the selection of the animal model, there are distinct advantages and limitations for choosing between a spontaneous or induced model to study adverse

pregnancy outcomes in animals. For the sake of brevity, we have collated the induction methods of a complication for the various species that are listed in Table 5.

Spontaneous development of a pregnancy complication in animals is valuable as it suggests there may be mechanistic overlap with humans. Although PE is observed primarily in humans, spontaneous cases have been documented in mice, rats, rabbits, guinea pigs, and monkeys [122, 131, 132]. Here we briefly describe a few examples that support the use of an animal model for various complications. In general, litter-bearing species can serve as natural models of FGR and IUGR [5, 117, 133]. For example, spontaneous IUGR occurs in 15-20% of swine [134]. Likewise, spontaneous pregnancy loss is common in cattle (~40%) [135-137], pigs (20-45%) [136, 138, 139], and marmoset monkeys (26%) [140]. In a cohort of guinea pigs, 20% of pregnancies spontaneously developed toxemia, and the observations from those animals validated their induced toxemia model [131]. Decreased reproductive efficiency has been observed in both humans and sheep at high altitudes; however, this environmental factor would limit the ability to study FGR in sheep to specific locations and might limit the relevance of such studies to the general human population. While spontaneous instances of these pregnancy complications can be used for experimental modeling, by definition, spontaneous complications are difficult to predict. Events preceding the adverse outcome cannot be efficiently studied and may require larger animal cohorts or specific conditions than is practical for many investigators.

Table A.5. Induced animal models of human pregnancy

Induction mechanism	NHP		Rabbit	Mouse/Rat	Guinea Pig	Pig
	NHP	Sheep	Pig	Cow		
PE	Artery ligation	<ul style="list-style-type: none"> Abdominal aortic constriction and uterine artery ligation led to hypertension and proteinuria with renal damage and/or impaired function [153, 154, 266] 	<ul style="list-style-type: none"> Constriction of the maternal aorta below the renal arteries led to proteinuria, kidney damage, and fetal demise [267] 	<ul style="list-style-type: none"> RUPP led to elevated TNF-α levels, hypertension, proteinuria, and FGR [268] 	<ul style="list-style-type: none"> Diet restriction led to ketosis, and minor PE symptoms and pathology [131] 	<ul style="list-style-type: none"> Fasting resulted in HELLP syndrome, hypertension, and proteinuria [275-277] <ul style="list-style-type: none"> Glucose restriction induced hemolysis and increased levels of free heme [278]
	Other	<ul style="list-style-type: none"> TNF-α injection resulted in proteinuria, hypertension, and elevated sFlt-1 levels [269] 	<ul style="list-style-type: none"> Fetal hemoglobin injection resulted in proteinuria, fetal demise, and increased apoptosis in the kidneys and placentas [173] 	<ul style="list-style-type: none"> sFlt-1 injection resulted in hypertension and proteinuria [270] <ul style="list-style-type: none"> TNF-α infusions resulted in hypertension [271] <ul style="list-style-type: none"> Injection of sEng and sFlt-1 [272] <ul style="list-style-type: none"> Modified nitric oxide production resulted in hypertension and FGR [273, 274] 		
EPL/RPL	Other	<ul style="list-style-type: none"> Low protein diet resulted in poor placental perfusion, miscarriage, and FGR [155] 	<ul style="list-style-type: none"> Lower insulin and progesterone levels were reported in pregnancy loss during days 18-40 of gestation [279] 	<ul style="list-style-type: none"> 20-45% implantation failure [136, 138, 139] <ul style="list-style-type: none"> Defects in vascular remodeling, inflammation, and altered miRNA expression have been associated with porcine embryonic death [138, 139] 	<ul style="list-style-type: none"> ~40% implantation failure [135-137] <ul style="list-style-type: none"> Genotyping of fetuses that died in utero, and genetic selection of sperm donors provided insight as to genes associated with EPL [135, 137] EPL is also associated with infection and uterine inflammation [136] Progesterone levels prior to implantation may contribute to the establishment and maintenance of pregnancy [135] 	
	Other					
FGR/IUGR	Uteroplacental vascular modification	<ul style="list-style-type: none"> Ligation of the vessels connecting the primary and secondary discs led to placental insufficiency, fetal death, and FGR [156] 	<ul style="list-style-type: none"> Uterine artery ligation negatively impacted kidney development in the fetuses [283], which is also seen in human cases of IUGR [284] <ul style="list-style-type: none"> Artery ligation resulted in a high prevalence of fetal mortality [118, 119] and negatively impacted renal development [119] A limitation of uteroplacental vessel ligation is the necessity of a short study duration due to high fetal mortality [285] 	<ul style="list-style-type: none"> Bilateral uterine artery ligation resulted in asymmetrical IUGR and negatively impacted kidney development in the fetuses [283] <ul style="list-style-type: none"> Has been shown to result in altered insulin levels, IGF and IGF binding protein levels, decreased placental weight, hypertension, and delayed growth [120] A limitation of uteroplacental vessel ligation is the necessity of a short study duration due to high fetal mortality [285] 	<ul style="list-style-type: none"> Utero-placental embolization [134, 286] <ul style="list-style-type: none"> Single umbilical artery ligation [134, 286] 	<ul style="list-style-type: none"> Duration of nutrient restriction is correlated to the severity of IUGR [117] <ul style="list-style-type: none"> A limitation of nutrient restriction is lack of hyperproteinemia, as is observed in humans and rats [290] See review [117]
	Other	<ul style="list-style-type: none"> Experience placental insufficiency and IUGR similar to humans [121, 155] 	<ul style="list-style-type: none"> Natural model due to the large litter size (embryo crowding within the uterus can impact growth) [5] <ul style="list-style-type: none"> See review [285] 	<ul style="list-style-type: none"> Injection of sEng and sFlt-1 resulted in FGR [272] <ul style="list-style-type: none"> See reviews [120, 288] 	<ul style="list-style-type: none"> Heat stress decreased placental blood flow and led to IUGR [134, 286] <ul style="list-style-type: none"> Sheep living at high elevations develop IUGR [134] See reviews [117, 289] 	

	NHP		Guinea Pig		Rabbit		Mouse/Rat		Sheep		Pig	
Pre-GD / GDM	Induction mechanism											
	Chemical induced	Alloxan and STZ [157, 158]	STZ [291]	Alloxan and STZ [171, 292]	Alloxan and STZ [293-296]					STZ [297, 298]		STZ [299] did not significantly alter fetal size at birth
	Other		Useful to model GDM: as the humans, the placenta and fetus are reliant on maternal supply of glucose until late in gestation, which is also the case in humans [249]		Stress, nutritional, and drug manipulations accurately recapitulate insulin resistance, hyperlipidemia, increased inflammation, fetal death, and macrosomia [301]					Useful to model GDM, as the placenta and fetus are reliant on maternal supply of glucose until late in gestation, which is also the case in humans [249]		
			Low preconception vitamin D status increases the risk of developing GDM [300]		Rats fed a high fat, high sugar diet instigated increased glucose and insulin levels but decreased insulin sensitivity. Offspring were not born macrosomic, potentially due to the immature state of rats at birth [303]					A high fat diet resulted in increased levels of insulin, glucose, and cortisol in the ewe and fetus compared to controls [304]		
PTB	Induction mechanism	NHP	Guinea Pig	Rabbit	Mouse/Rat	Sheep	Cow					
	Infection/inflammation	Intra-amniotic injection of bacterial proteins, IL-1beta, and TNF-alpha resulted in PTB [169]		Intrauterine administration of bacterial agents and inflammatory cytokines resulted in PTB [305, 306]	Inoculation of rodents with inflammatory cytokines and alarmins present during human PTB resulted in PTB [307-310]					The ability for intra-amniotic modeling of infection as opposed to intraperitoneal is of great utility, as this administration route is most closely in line with the pregnancy infection clinical literature [316, 317]		Candida infection resulted in severe placental pathology and is associated with abortion in cows [321] and PTB in women [322-324]
	Parturition	Progesterone withdrawal is not a prerequisite for labor, similar to humans [122, 169, 325]	Increasing progesterone levels in late pregnancy similar to humans [169, 326, 327]	labor is dependent on progesterone withdrawal [169, 327]	labor is dependent on progesterone withdrawal [169, 326, 327]					labor is dependent on progesterone withdrawal [169, 326, 327]		
	Other		Naturally experience preterm birth (~7% compared to 5% -11% in human) [169, 170]		Genetic contributions to PTB in humans have been elucidated through mutant mouse models, such as Calmus et al., 2011's work on Ehlers-Danlos syndrome [328]					Glucocorticoids have been shown to induce preterm labor [318-320]. However, in humans glucocorticoids are actually used as a treatment in PTB pregnancies to accelerate fetal lung development [332]		

Acronyms: nonhuman primate (NHP), soluble Endoglin (sEng), soluble fms-like tyrosine kinase-1 (sFlt-1), hemolysis, elevated liver enzymes, and low platelets (HELLP), insulin growth factor (IGF), streptozotocin (STZ), Reduced uterine perfusion pressure (RUPP)

In contrast to the uncertainty in occurrence and timing of a spontaneous complication, researchers can administer precise insults or experimental treatments to control the induction of a pregnancy complication (Table 5). Pregnancy complications may be induced by drug treatment, diet, surgery, or genetic manipulation. Genetic manipulation is commonly used in rodent models to induce a pregnancy complication, where a gene knock-in or knock-out can aid in further investigating causative genes underlying the development of a complication. Information derived from these genetic mutations then can be translated to other animal models, such as nonhuman primates (NHPs), that more closely model human pregnancy. The biological relevance of the induced complication must be determined on a species and approach basis. As with any laboratory study, there are limitations to the comparisons that can be made to natural cases of disease. Data gleaned from induced models should be compared to data obtained from spontaneous cases of pregnancy complications whenever possible.

Etiology is important when selecting an approach to induce a pregnancy complication, as the mechanisms impacted may not be translatable to humans. For example, diet-restricted guinea pigs displayed similar symptoms and pathology as those with spontaneous PE [141]; however, the etiologies appear different. Spontaneous PE resulted from uteroplacental ischemia induced by aortic compression caudal to the renal arteries. In contrast, induced PE from fasting led to ketosis and resulted in less severe symptoms and pathology [131]. Notably, similar symptoms of varying severity were observed in this study, and it is important to consider the mechanistic differences underlying the PE symptoms observed as they may relate or differ from the human pathogenesis of the complication.

A.12 Animal models of experimental infections during pregnancy

Pathogens can be host restricted, so ensuring that a pathogen can induce similar pathophysiology in an animal model of human pregnancy is essential to better understanding the downstream implications. Other important considerations for congenital infection models include the route of infection, maternal symptoms, fetal/congenital symptoms, and the role the maternal immune system plays in fighting the infection. Researchers have used in vitro animal and human placental cell culture systems to identify the cell types most susceptible to vertically transmitted pathogens and to unravel the mechanisms behind infection [20]. While in vitro systems have aided in understanding the cellular mechanisms of vertical transmission (e.g., receptors that mediate pathogen trophoblast entry), these mechanisms largely remain elusive. The various animal models that have been used to model TORCHZ infections during pregnancy are broadly summarized in Table 6.

Table A.6. Pathogens in animal models that cause adverse pregnancy outcomes (APOs)

Pathogen	Animal model	Observed APO
Brucella	<ul style="list-style-type: none"> ▪ Cattle [333] ▪ Sheep [333] 	Pregnancy loss
Chlamydia	<ul style="list-style-type: none"> ▪ Sheep [334] ▪ Mice [334, 335] ▪ Guinea pigs [336] ▪ Pigs [337] 	Pregnancy loss
Cytomegalovirus	<ul style="list-style-type: none"> ▪ Mice [338] ▪ Guinea pigs [338, 339] ▪ NHP [159, 160] 	Neurological sequelae, pregnancy loss
Hepatitis E virus	<ul style="list-style-type: none"> ▪ Rabbit [340, 341] 	Pregnancy loss
Group B Streptococcus	<ul style="list-style-type: none"> ▪ Mice [342] ▪ NHP [343] 	Pregnancy loss, meningitis, pneumonia, neurological developmental disabilities
Listeria monocytogenes	<ul style="list-style-type: none"> ▪ NHP [161-163] ▪ Guinea pigs [254, 344] 	Pregnancy loss
Rubella	<ul style="list-style-type: none"> ▪ Rats [345, 346] 	Pregnancy loss, neonatal demise, ocular abnormalities
Toxoplasma gondii	<ul style="list-style-type: none"> ▪ Sheep [347, 348] ▪ Mice [349] ▪ NHP [350] 	Pregnancy loss
Zika virus	<ul style="list-style-type: none"> ▪ NHP [164-166] ▪ Mice [351] ▪ Guinea pigs [352] ▪ Pigs [353] 	Pregnancy loss, fetal malformations

A.13 Current knowledge of PEVs in animal pregnancy models

This section provides a brief overview of PEV studies that have been performed using mouse and livestock pregnancy models, with more details presented in Table 3. Similar to humans [102, 142], the total number of exosomes and PLAP-positive vesicles isolated from blood increased throughout bovine gestation (Table 3) [103]. Sequencing of miRNAs from bovine exosomes revealed unique expression profiles across trimesters [103]. The placental miRNA profile also changes throughout gestation in humans [143] and rhesus macaques [144]. These data suggest that despite minimal placental invasion in the cow, placental exosomes similarly circulate in the maternal bloodstream as observed in humans. Thus, there may be conservation

in marker expression and function of cargo given the similarities in EV miRNA profiles during gestation.

Data collected from mouse and human studies support that EV clearance may impact pregnancy health status. Excess vesicles in lactadherin $-/-$ pregnant mice resulted in elevated blood pressure, proteinuria, and fewer litters, suggesting that EV clearance opposes development of PE-like symptoms (Table 3) [89]. Moreover, elevated levels of PEVs or PEVs from injured murine placentas can induce PE symptoms when injected into pregnant mice [89]. This impact supports and expands upon human data. An *in vitro* human trophoblast culture study found that less syncytin-1 and -2 cellular expression resulted in decreased exosome uptake and thus, an excess of released EVs [145]. Interestingly, placentas from women with PE expressed less syncytin-1 and -2 than controls [145]. Germain et al. [87] also reported elevated levels of circulating free and fewer bound syncytiotrophoblast microvesicles in patients with PE than healthy subjects. The overlap in findings is an excellent example of the insight rodent models offer into unraveling the impact of EVs.

Observations from rodent pregnancy models have revealed that PEVs may serve as a means of communication at the maternal fetal interface. In mice, fetal and maternal exosomes trafficked across the maternal-fetal interface and fetal exosomes impacted maternal cell function [146]. Similarly, PEV trafficking to maternal cells also has been shown in large animal pregnancy models. A recent study showed that the binucleate trophoblast cells of the ruminant placenta also secrete exosome-like vesicles to the maternal uterine epithelium and connective tissue

[147]. Similarly, in vitro study showed that porcine trophectoderm cell lines secreted EVs that influenced the proliferation of porcine aortic endothelial cells (Table 3). This supports fetomaternal cross-talk in the pig [148], a phenomenon similarly observed in sheep [149]. In addition, EVs isolated from ovine uterine fluid are taken up by embryos/trophectodermal cells and vice versa [149, 150]. EV uptake by these cells suggests maternal-fetal communication occurs very early in pregnancy and shows the potential to assess embryo-derived PEVs as early as the pre/peri implantation stages. Investigation of the earliest stages of development could reveal how these EVs may be altered in EPL.

While the results of in vitro PEV studies are intriguing, the prevalence of PEVs in ovine and porcine maternal blood remains unclear. PEVs are expected to be present in ovine maternal circulation as they have been detected in bovine maternal blood, and these species share similar placental architecture. Further isolation of PEVs from all stages of pregnancy, including embryo-derived EVs, across livestock species will help to understand complications that arise from errors in the establishment of pregnancy as well as maldeveloped placentation. Although there are few published animal PEV studies, the similarities in findings between animal models and human in vitro data further supports the need for additional in vivo animal studies.

A.14 Future perspectives: expansion of PEV research in animal pregnancy models

The studies discussed in the previous section represent all current, but limited, publications on PEVs in animal pregnancy models. Studies with animal models provide an opportunity to improve our understanding of the consequences of placental complications through comprehensive study of PEVs and their cargo. Additional studies in the animal models discussed above, especially in those with a hemochorial placenta, are needed to identify biomarkers and expand our knowledge of PEV cargo and function. The development of PEV animal models is especially important to elucidate the impact EVs have on the maternal immune system and maternal physiology in healthy and complicated pregnancies, as this cannot be studied *in vitro*.

The use of NHPs in PEV research would be particularly valuable as there are extensive similarities between humans and NHPs as listed in Table 4. Macaques share a similar hemochorial type of placentation with extensive remodeling of decidual spiral arteries by endovascular trophoblasts [121, 123]. Unlike rodent models but similar to humans, NHPs express miRNAs from the primate-specific chromosome 19 microRNA cluster (C19MC) (Table 4). miRNAs of the C19MC are almost exclusively expressed in the placenta, and have been detected within human EVs [35]. The C19MC miRNAs have roles in placental function, and are aberrantly expressed in pregnancy complications [151, 152]. Several pregnancy complication paradigms are already in place with NHPs [121, 153-167]. Applying the study of PEVs to these established models will enable advances not feasible in human pregnancy

research -- for example, monitoring vertical pathogen transmission by PEV analysis with timed infection studies. Investigators have recently characterized and validated rhesus and cynomolgus macaque TS cell lines that can be differentiated into syncytiotrophoblasts and extravillous trophoblasts [84, 168]. These cell lines may have tremendous value in terms of identifying PEV biomarkers of infection and disease.

Guinea pigs may also offer utility in PEV research as they have a discoid, hemomonochorial, labyrinthine placenta, and are relatively low cost compared to NHPs. Their longer gestation (~68 days) compared to the mouse and rat (~20 and ~22 days, respectively) allows for enhanced longitudinal sampling. They also naturally experience PTB at ~7% rate (the human rate is 5-11%) [169, 170]. Hence, guinea pigs may be a useful model for biomarker identification as well as drug development as an intermediate model between rodents and NHPs.

The use of rabbits could be beneficial as they are induced ovulators [122, 171], which allows for early and precisely timed pregnancy sample collection. Rabbits, like humans, have a syncytial trophoblast layer [122], and their genome has been fully sequenced. Their relatively short gestation (~32 days) allows for short studies that can assess the impact of pregnancy on the fetus as the offspring are born precocial [172], a feature more similar to humans than rodents. A representative example of the rabbit model being used to understand a pregnancy complication is a study in which injection of fetal hemoglobin resulted in proteinuria, fetal demise, and increased apoptosis in the kidneys and placentas [173]. This study helped elucidate

the impact fetal hemoglobin may have on PE in humans and showed the efficacy of alpha1-microglobulin (A1M) as a therapy to alleviate PE-like symptoms [173].

There are additional advantages and limitations of a model that are particularly relevant to PEV biomarker identification. Animal models with smaller litter sizes, such as the macaque or the sheep, allow for more focused biomarker detection for singleton pregnancies as in humans. In animals with large litters, some fetuses may normally develop, while others are resorbed. If healthy fetuses are present, it may be difficult to parse out and identify a biomarker of the pregnancy complication. Animals that mature more quickly typically have shorter gestations and allow for transgenerational study design. Moreover, animal pregnancy models are advantageous as they provide the ability to survey PEVs in relation to fetal growth and development over time, as well as in association with offspring physiology throughout their lifespan in a manageable time frame.

A.15 Next steps in establishing animal pregnancy models for PEV research.

A major limitation in the use of PEVs to diagnose pregnancy complications is the lack of information regarding early, predictive markers [108], which makes identification of longitudinal markers difficult. As illustrated in Table 2, there is overlap between general human EV markers and those of the animal models; however, only a few studies have specifically looked at PEVs in animal models despite similarity in some placental markers. For PEV research to be translational, we propose the following goals:

1. Rigorous **assessment** of placenta-specific markers in longitudinal in vivo studies, in additional cohorts for repeatability, and across species to ensure translatability
2. **Validation** of antibodies that are subsequently made commercially available for use across labs and species (when applicable).
3. Thorough **assessment** of the prognostic potential of a biomarker associated with a pregnancy complication in various animal models
4. **Development** of a database for placenta-specific markers and biomarkers of pregnancy complications using high-throughput techniques (i.e. next-generation RNA sequencing, mass spectrometry for proteomics, and lipidomics)
5. Pre-clinical **evaluation** of a biomarker associated with a human pregnancy condition in human samples (retrospective and prospective studies)

Animal models will enable the development of datasets with predictive markers because researchers will have control over sample collection and the timing of the insult. Researchers also can use established animal models to determine the predictive power of potential biomarkers that were identified in humans [108]. The harrows of identifying a single biomarker in humans also supports the need for induced pregnancy complication studies because a marker consistently identified across species with varied disease severity has translational potential. Overall, animal models can greatly strengthen the PEV field in terms of studying and prospectively identifying pregnancy complications.

A.16 Current questions and future opportunities in the PEV field

Having discussed the opportunities in pregnancy complication research with a range of animal models, there remain questions in PEV research that are cross-cutting, regardless of the species used, including research with human clinical samples.

- Is PEV cargo selectively packaged? – If so, how?

- How are the presence of PEV membrane proteins and cargos altered when EVs are derived from a diseased placenta?
- Do the embryo and the placenta use PEVs to communicate to maternal cells before and during implantation?
- What role(s) do PEVs have in regulating maternal immune adaptation to pregnancy? Are PEVs essential for the successful establishment of pregnancy?
- Do PEVs from a maldeveloped placenta cause or contribute to a pregnancy complication by triggering a maternal physiological or immune response, or is their presence a manifestation of the impact of the pregnancy complication on placental function?

PEVs hold the promise of future prognostic and diagnostic development as they can provide high “clinical predictive power” [101] for pregnancy complications. Unraveling the mechanisms of cargo packaging is crucial to understand how EV cargo of a malfunctioning placenta may be altered in comparison to those derived from a healthy placenta. There is currently a debate in the EV literature as to what “exosomes” are, and whether these truly can be isolated from a complex EV population [32]. Consistent nomenclature and standard techniques to isolate EVs would allow comparison among studies. There are currently three EV databases, EVpedia [174], ExoCarta [175], and Vesiclepedia [176]; however, a database specifically for PEV research would enable meta-analysis of results, allow for marker identification reported across pregnancy complication research, and enable the field to quickly advance. Since placental development is continuous and gene expression changes throughout pregnancy, it is important that investigators develop a database of EV cargo from all stages of pregnancy. The NIH Human Placenta Project would be an excellent platform to support such a database.

In conclusion, representative in vitro and in vivo animal models are necessary to identify biomarkers of pregnancy complications. A better understanding of PEV biology will allow deeper insights into placental function and development throughout gestation, help to identify maldeveloped and/or infected placentas, and potentially underpin development of placental therapeutics. We propose that to achieve these advances, appropriate animal models of human pregnancy complications must be established.

A.17 References

1. Koblinsky M, Chowdhury ME, Moran A, Ronsmans C. Maternal morbidity and disability and their consequences: neglected agenda in maternal health. *J Health Popul Nutr* 2012; 30:124-130.
2. Blencowe H, Cousens S, Oestergaard MZ, Chou D, Moller AB, Narwal R, Adler A, Vera Garcia C, Rohde S, Say L, Lawn JE. National, regional, and worldwide estimates of preterm birth rates in the year 2010 with time trends since 1990 for selected countries: a systematic analysis and implications. *Lancet* 2012; 379:2162-2172.
3. Lawn JE, Kerber K, Enweronu-Laryea C, Cousens S. 3.6 million neonatal deaths--what is progressing and what is not? *Semin Perinatol* 2010; 34:371-386.
4. Harrison MS, Goldenberg RL. Global burden of prematurity. *Semin Fetal Neonatal Med* 2016; 21:74-79.
5. Swanson AM, David AL. Animal models of fetal growth restriction: Considerations for translational medicine. *Placenta* 2015; 36:623-630.
6. ACOG Practice Bulletin No. 204: Fetal Growth Restriction. *Obstet Gynecol* 2019; 133:e97-e109.
7. Nardoza LM, Caetano AC, Zamarian AC, Mazzola JB, Silva CP, Marcal VM, Lobo TF, Peixoto AB, Araujo Junior E. Fetal growth restriction: current knowledge. *Arch Gynecol Obstet* 2017; 295:1061-1077.
8. ACOG Practice Bulletin No. 201 Summary: Pregestational Diabetes Mellitus. *Obstet Gynecol* 2018; 132:1514-1516.

9. Mackin ST, Nelson SM, Kerssens JJ, Wood R, Wild S, Colhoun HM, Leese GP, Philip S, Lindsay RS, Group SE. Diabetes and pregnancy: national trends over a 15 year period. *Diabetologia* 2018; 61:1081-1088.
10. Rackham O, Paize F, Weindling AM. Cause of death in infants of women with pregestational diabetes mellitus and the relationship with glycemic control. *Postgrad Med* 2009; 121:26-32.
11. Committee on Practice B-O. ACOG Practice Bulletin No. 190: Gestational Diabetes Mellitus. *Obstet Gynecol* 2018; 131:e49-e64.
12. Stevens W, Shih T, Incerti D, Ton TGN, Lee HC, Peneva D, Macones GA, Sibai BM, Jena AB. Short-term costs of preeclampsia to the United States health care system. *Am J Obstet Gynecol* 2017; 217:237-248 e216.
13. In: Behrman RE, Butler AS (eds.), *Preterm Birth: Causes, Consequences, and Prevention*. Washington (DC); 2007.
14. Lenoir-Wijnkoop I, van der Beek EM, Garssen J, Nuijten MJ, Uauy RD. Health economic modeling to assess short-term costs of maternal overweight, gestational diabetes, and related macrosomia - a pilot evaluation. *Front Pharmacol* 2015; 6:103.
15. Signore C, Spong C. Overview of antepartum fetal surveillance. In. *UpToDate: Wolters Kluwer*; 2020.
16. Brosens I, Pijnenborg R, Vercruyse L, Romero R. The "Great Obstetrical Syndromes" are associated with disorders of deep placentation. *Am J Obstet Gynecol* 2011; 204:193-201.
17. Edu A, Teodorescu C, Dobjanschi CG, Socol ZZ, Teodorescu V, Matei A, Albu DF, Radulian G. Placenta changes in pregnancy with gestational diabetes. *Rom J Morphol Embryol* 2016; 57:507-512.
18. Nguyen-Ngo C, Jayabalan N, Salomon C, Lappas M. Molecular pathways disrupted by gestational diabetes mellitus. *J Mol Endocrinol* 2019; 63:R51-R72.
19. Whittington JR, Cummings KF, Ounpraseuth ST, Aughenbaugh AL, Quick CM, Dajani NK. Placental changes in diabetic pregnancies and the contribution of hypertension. *J Matern Fetal Neonatal Med* 2020:1-9.
20. Delorme-Axford E, Sadovsky Y, Coyne CB. The Placenta as a Barrier to Viral Infections. *Annu Rev Virol* 2014; 1:133-146.
21. Leeper C, Lutzkanin A, 3rd. Infections During Pregnancy. *Prim Care* 2018; 45:567-586.
22. Coyne CB, Lazear HM. Zika virus - reigniting the TORCH. *Nat Rev Microbiol* 2016; 14:707-715.

23. Sabapatha A, Gercel-Taylor C, Taylor DD. Specific isolation of placenta-derived exosomes from the circulation of pregnant women and their immunoregulatory consequences. *Am J Reprod Immunol* 2006; 56:345-355.
24. Lai A, Elfeky O, Rice GE, Salomon C. Optimized Specific Isolation of Placenta-Derived Exosomes from Maternal Circulation. *Methods Mol Biol* 2018; 1710:131-138.
25. Sarker S, Scholz-Romero K, Perez A, Illanes SE, Mitchell MD, Rice GE, Salomon C. Placenta-derived exosomes continuously increase in maternal circulation over the first trimester of pregnancy. *J Transl Med* 2014; 12:204.
26. Zhang H, Freitas D, Kim HS, Fabijanic K, Li Z, Chen H, Mark MT, Molina H, Martin AB, Bojmar L, Fang J, Rampersaud S, et al. Identification of distinct nanoparticles and subsets of extracellular vesicles by asymmetric flow field-flow fractionation. *Nat Cell Biol* 2018; 20:332-343.
27. Pocsfalvi G, Stanly C, Vilasi A, Fiume I, Capasso G, Turiak L, Buzas EI, Vekey K. Mass spectrometry of extracellular vesicles. *Mass Spectrom Rev* 2016; 35:3-21.
28. Schorey JS, Cheng Y, Singh PP, Smith VL. Exosomes and other extracellular vesicles in host-pathogen interactions. *EMBO Rep* 2015; 16:24-43.
29. Yuana Y, Sturk A, Nieuwland R. Extracellular vesicles in physiological and pathological conditions. *Blood Rev* 2013; 27:31-39.
30. Gyorgy B, Szabo TG, Pasztoi M, Pal Z, Misjak P, Aradi B, Laszlo V, Pallinger E, Pap E, Kittel A, Nagy G, Falus A, et al. Membrane vesicles, current state-of-the-art: emerging role of extracellular vesicles. *Cell Mol Life Sci* 2011; 68:2667-2688.
31. Kalra H, Drummen GP, Mathivanan S. Focus on Extracellular Vesicles: Introducing the Next Small Big Thing. *Int J Mol Sci* 2016; 17:170.
32. They C, Witwer KW, Aikawa E, Alcaraz MJ, Anderson JD, Andriantsitohaina R, Antoniou A, Arab T, Archer F, Atkin-Smith GK, Ayre DC, Bach JM, et al. Minimal information for studies of extracellular vesicles 2018 (MISEV2018): a position statement of the International Society for Extracellular Vesicles and update of the MISEV2014 guidelines. *J Extracell Vesicles* 2018; 7:1535750.
33. Coumans FAW, Brisson AR, Buzas EI, Dignat-George F, Drees EEE, El-Andaloussi S, Emanuelli C, Gasecka A, Hendrix A, Hill AF, Lacroix R, Lee Y, et al. Methodological Guidelines to Study Extracellular Vesicles. *Circ Res* 2017; 120:1632-1648.
34. Kowal J, Arras G, Colombo M, Jouve M, Morath JP, Primdal-Bengtson B, Dingli F, Loew D, Tkach M, They C. Proteomic comparison defines novel markers to characterize heterogeneous populations of extracellular vesicle subtypes. *Proc Natl Acad Sci U S A* 2016; 113:E968-977.

35. Ouyang Y, Bayer A, Chu T, Tyurin VA, Kagan VE, Morelli AE, Coyne CB, Sadovsky Y. Isolation of human trophoblastic extracellular vesicles and characterization of their cargo and antiviral activity. *Placenta* 2016; 47:86-95.
36. Wang W, Luo J, Wang S. Recent Progress in Isolation and Detection of Extracellular Vesicles for Cancer Diagnostics. *Adv Healthc Mater* 2018; 7:e1800484.
37. Lobb RJ, Becker M, Wen SW, Wong CS, Wiegman AP, Leimgruber A, Moller A. Optimized exosome isolation protocol for cell culture supernatant and human plasma. *J Extracell Vesicles* 2015; 4:27031.
38. Li P, Kaslan M, Lee SH, Yao J, Gao Z. Progress in Exosome Isolation Techniques. *Theranostics* 2017; 7:789-804.
39. Kalra H, Adda CG, Liem M, Ang CS, Mechler A, Simpson RJ, Hulett MD, Mathivanan S. Comparative proteomics evaluation of plasma exosome isolation techniques and assessment of the stability of exosomes in normal human blood plasma. *Proteomics* 2013; 13:3354-3364.
40. Van Deun J, Mestdagh P, Sormunen R, Cocquyt V, Vermaelen K, Vandesompele J, Bracke M, De Wever O, Hendrix A. The impact of disparate isolation methods for extracellular vesicles on downstream RNA profiling. *J Extracell Vesicles* 2014; 3.
41. Gardiner C, Di Vizio D, Sahoo S, Thery C, Witwer KW, Wauben M, Hill AF. Techniques used for the isolation and characterization of extracellular vesicles: results of a worldwide survey. *J Extracell Vesicles* 2016; 5:32945.
42. Simon C, Greening DW, Bolumar D, Balaguer N, Salamonsen LA, Vilella F. Extracellular Vesicles in Human Reproduction in Health and Disease. *Endocr Rev* 2018; 39:292-332.
43. Tong M, Kleffmann T, Pradhan S, Johansson CL, DeSousa J, Stone PR, James JL, Chen Q, Chamley LW. Proteomic characterization of macro-, micro- and nano-extracellular vesicles derived from the same first trimester placenta: relevance for fetomaternal communication. *Hum Reprod* 2016; 31:687-699.
44. Lok CA, Van Der Post JA, Sargent IL, Hau CM, Sturk A, Boer K, Nieuwland R. Changes in microparticle numbers and cellular origin during pregnancy and preeclampsia. *Hypertens Pregnancy* 2008; 27:344-360.
45. Gruenberg J, Stenmark H. The biogenesis of multivesicular endosomes. *Nat Rev Mol Cell Biol* 2004; 5:317-323.
46. Villarroya-Beltri C, Baixauli F, Gutierrez-Vazquez C, Sanchez-Madrid F, Mittelbrunn M. Sorting it out: regulation of exosome loading. *Semin Cancer Biol* 2014; 28:3-13.
47. Mincheva-Nilsson L, Baranov V. Placenta-derived exosomes and syncytiotrophoblast microparticles and their role in human reproduction: immune modulation for pregnancy success. *Am J Reprod Immunol* 2014; 72:440-457.

48. Ahsan NA, Sampey GC, Lepene B, Akpamagbo Y, Barclay RA, Iordanskiy S, Hakami RM, Kashanchi F. Presence of Viral RNA and Proteins in Exosomes from Cellular Clones Resistant to Rift Valley Fever Virus Infection. *Front Microbiol* 2016; 7:139.
49. Longatti A, Boyd B, Chisari FV. Virion-independent transfer of replication-competent hepatitis C virus RNA between permissive cells. *J Virol* 2015; 89:2956-2961.
50. Saadeldin IM, Oh HJ, Lee BC. Embryonic-maternal cross-talk via exosomes: potential implications. *Stem Cells Cloning* 2015; 8:103-107.
51. Chahar HS, Bao X, Casola A. Exosomes and Their Role in the Life Cycle and Pathogenesis of RNA Viruses. *Viruses* 2015; 7:3204-3225.
52. Valadi H, Ekstrom K, Bossios A, Sjostrand M, Lee JJ, Lotvall JO. Exosome-mediated transfer of mRNAs and microRNAs is a novel mechanism of genetic exchange between cells. *Nat Cell Biol* 2007; 9:654-659.
53. Kambe S, Yoshitake H, Yuge K, Ishida Y, Ali MM, Takizawa T, Kuwata T, Ohkuchi A, Matsubara S, Suzuki M, Takeshita T, Saito S, et al. Human exosomal placenta-associated miR-517a-3p modulates the expression of PRKG1 mRNA in Jurkat cells. *Biol Reprod* 2014; 91:129.
54. Kahlert C, Melo SA, Protopopov A, Tang J, Seth S, Koch M, Zhang J, Weitz J, Chin L, Futreal A, Kalluri R. Identification of double-stranded genomic DNA spanning all chromosomes with mutated KRAS and p53 DNA in the serum exosomes of patients with pancreatic cancer. *J Biol Chem* 2014; 289:3869-3875.
55. Sansone P, Savini C, Kurelac I, Chang Q, Amato LB, Strillacci A, Stepanova A, Iommarini L, Mastroleo C, Daly L, Galkin A, Thakur BK, et al. Packaging and transfer of mitochondrial DNA via exosomes regulate escape from dormancy in hormonal therapy-resistant breast cancer. *Proc Natl Acad Sci U S A* 2017; 114:E9066-E9075.
56. Salomon C, Scholz-Romero K, Sarker S, Sweeney E, Kobayashi M, Correa P, Longo S, Duncombe G, Mitchell MD, Rice GE, Illanes SE. Gestational Diabetes Mellitus Is Associated With Changes in the Concentration and Bioactivity of Placenta-Derived Exosomes in Maternal Circulation Across Gestation. *Diabetes* 2016; 65:598-609.
57. Gohner C, Plosch T, Faas MM. Immune-modulatory effects of syncytiotrophoblast extracellular vesicles in pregnancy and preeclampsia. *Placenta* 2017; 60 Suppl 1:S41-S51.
58. Robbins PD, Morelli AE. Regulation of immune responses by extracellular vesicles. *Nat Rev Immunol* 2014; 14:195-208.
59. Pap E, Pallinger E, Falus A, Kiss AA, Kittel A, Kovacs P, Buzas EI. T lymphocytes are targets for platelet- and trophoblast-derived microvesicles during pregnancy. *Placenta* 2008; 29:826-832.

60. Altan-Bonnet N. Extracellular vesicles are the Trojan horses of viral infection. *Curr Opin Microbiol* 2016; 32:77-81.
61. Southcombe J, Tannetta D, Redman C, Sargent I. The immunomodulatory role of syncytiotrophoblast microvesicles. *PLoS One* 2011; 6:e20245.
62. Shen L, Li Y, Li R, Diao Z, Yany M, Wu M, Sun H, Yan G, Hu Y. Placenta-associated serum exosomal miR155 derived from patients with preeclampsia inhibits eNOS expression in human umbilical vein endothelial cells. *Int J Mol Med* 2018; 41:1731-1739.
63. Nair S, Jayabalan N, Guanzon D, Palma C, Scholz-Romero K, Elfeky O, Zuniga F, Ormazabal V, Diaz E, Rice GE, Duncombe G, Jansson T, et al. Human placental exosomes in gestational diabetes mellitus carry a specific set of miRNAs associated with skeletal muscle insulin sensitivity. *Clin Sci (Lond)* 2018; 132:2451-2467.
64. Eldh M, Ekstrom K, Valadi H, Sjostrand M, Olsson B, Jernas M, Lotvall J. Exosomes communicate protective messages during oxidative stress; possible role of exosomal shuttle RNA. *PLoS One* 2010; 5:e15353.
65. Smyth T, Kullberg M, Malik N, Smith-Jones P, Graner MW, Anchordoquy TJ. Biodistribution and delivery efficiency of unmodified tumor-derived exosomes. *J Control Release* 2015; 199:145-155.
66. Ohno S, Takanashi M, Sudo K, Ueda S, Ishikawa A, Matsuyama N, Fujita K, Mizutani T, Ohgi T, Ochiya T, Gotoh N, Kuroda M. Systemically injected exosomes targeted to EGFR deliver antitumor microRNA to breast cancer cells. *Mol Ther* 2013; 21:185-191.
67. Wu AY-T, Sung Y-C, Chou ST-Y, Guo V, Chien JC-Y, Ko JJ-S, Yang AL, Chuang J-C, Huang H-C, Wu Y, Ho M-R, Ericsson M, et al. Redirected tropisms of extracellular vesicles and exomeres yield distinct biodistribution profiles. *bioRxiv* 2020:2020.2003.2027.012625.
68. Wiklander OP, Nordin JZ, O'Loughlin A, Gustafsson Y, Corso G, Mager I, Vader P, Lee Y, Sork H, Seow Y, Heldring N, Alvarez-Erviti L, et al. Extracellular vesicle in vivo biodistribution is determined by cell source, route of administration and targeting. *J Extracell Vesicles* 2015; 4:26316.
69. Kooijmans SAA, Schiffelers RM, Zarovni N, Vago R. Modulation of tissue tropism and biological activity of exosomes and other extracellular vesicles: New nanotools for cancer treatment. *Pharmacol Res* 2016; 111:487-500.
70. Di Rocco G, Baldari S, Toietta G. Towards Therapeutic Delivery of Extracellular Vesicles: Strategies for In Vivo Tracking and Biodistribution Analysis. *Stem Cells Int* 2016; 2016:5029619.
71. Tannetta D, Collett G, Vatish M, Redman C, Sargent I. Syncytiotrophoblast extracellular vesicles - Circulating biopsies reflecting placental health. *Placenta* 2017; 52:134-138.

72. Salomon C, Nuzhat Z, Dixon CL, Menon R. Placental Exosomes During Gestation: Liquid Biopsies Carrying Signals for the Regulation of Human Parturition. *Curr Pharm Des* 2018; 24:974-982.
73. Homer H, Rice GE, Salomon C. Review: Embryo- and endometrium-derived exosomes and their potential role in assisted reproductive treatments-liquid biopsies for endometrial receptivity. *Placenta* 2017; 54:89-94.
74. Tannetta DS, Dragovic RA, Gardiner C, Redman CW, Sargent IL. Characterisation of syncytiotrophoblast vesicles in normal pregnancy and pre-eclampsia: expression of Flt-1 and endoglin. *PLoS One* 2013; 8:e56754.
75. Nardi Fda S, Michelon TF, Neumann J, Manvailer LF, Wagner B, Horn PA, Bicalho Mda G, Rebmann V. High levels of circulating extracellular vesicles with altered expression and function during pregnancy. *Immunobiology* 2016; 221:753-760.
76. Atay S, Gercel-Taylor C, Suttles J, Mor G, Taylor DD. Trophoblast-derived exosomes mediate monocyte recruitment and differentiation. *Am J Reprod Immunol* 2011; 65:65-77.
77. Mincheva-Nilsson L, Baranov V. The role of placental exosomes in reproduction. *Am J Reprod Immunol* 2010; 63:520-533.
78. Hannan NJ, Paiva P, Dimitriadis E, Salamonsen LA. Models for study of human embryo implantation: choice of cell lines? *Biol Reprod* 2010; 82:235-245.
79. Gierman LM, Stodle GS, Tangeras LH, Austdal M, Olsen GD, Follestad T, Skei B, Rian K, Gundersen AS, Austgulen R, Iversen AC. Toll-like receptor profiling of seven trophoblast cell lines warrants caution for translation to primary trophoblasts. *Placenta* 2015; 36:1246-1253.
80. Orendi K, Kivity V, Sammar M, Grimpel Y, Gonen R, Meiri H, Lubzens E, Huppertz B. Placental and trophoblastic in vitro models to study preventive and therapeutic agents for preeclampsia. *Placenta* 2011; 32 Suppl:S49-54.
81. Okae H, Toh H, Sato T, Hiura H, Takahashi S, Shirane K, Kabayama Y, Suyama M, Sasaki H, Arima T. Derivation of Human Trophoblast Stem Cells. *Cell Stem Cell* 2018; 22:50-63 e56.
82. Haider S, Meinhardt G, Saleh L, Kunihs V, Gamperl M, Kaindl U, Ellinger A, Burkard TR, Fiala C, Pollheimer J, Mendjan S, Latos PA, et al. Self-Renewing Trophoblast Organoids Recapitulate the Developmental Program of the Early Human Placenta. *Stem Cell Reports* 2018; 11:537-551.
83. Turco MY, Gardner L, Kay RG, Hamilton RS, Prater M, Hollinshead MS, McWhinnie A, Esposito L, Fernando R, Skelton H, Reimann F, Gribble FM, et al. Trophoblast organoids as a model for maternal-fetal interactions during human placentation. *Nature* 2018; 564:263-267.

84. Kropp Schmidt J, Meyer MG, Wiepz GJ, Block LN, Dusek BM, Kroner KM, Bertogliat MJ, Keding LT, Koenig MR, Mean KD, Golos TG. Derivation of macaque trophoblast stem cells. *bioRxiv* 2020.
85. Renaud SJ. *Strategies for Investigating hemochorial placentation*. Elsevier Inc. ; 2017: 1259.
86. Di Santo S, Malek A, Sager R, Andres AC, Schneider H. Trophoblast viability in perfused term placental tissue and explant cultures limited to 7-24 hours. *Placenta* 2003; 24:882-894.
87. Germain SJ, Sacks GP, Sooranna SR, Sargent IL, Redman CW. Systemic inflammatory priming in normal pregnancy and preeclampsia: the role of circulating syncytiotrophoblast microparticles. *J Immunol* 2007; 178:5949-5956.
88. Rice TF, Donaldson B, Bouqueau M, Kampmann B, Holder B. Macrophage- but not monocyte-derived extracellular vesicles induce placental pro-inflammatory responses. *Placenta* 2018; 69:92-95.
89. Han C, Wang C, Chen Y, Wang J, Xu X, Hilton T, Cai W, Zhao Z, Wu Y, Li K, Houck K, Liu L, et al. Placenta-derived extracellular vesicles induce preeclampsia in mouse models. *Haematologica* 2019.
90. Pillay P, Maharaj N, Moodley J, Mackraj I. Placental exosomes and pre-eclampsia: Maternal circulating levels in normal pregnancies and, early and late onset pre-eclamptic pregnancies. *Placenta* 2016; 46:18-25.
91. Goswami D, Tannetta DS, Magee LA, Fuchisawa A, Redman CW, Sargent IL, von Dadelszen P. Excess syncytiotrophoblast microparticle shedding is a feature of early-onset pre-eclampsia, but not normotensive intrauterine growth restriction. *Placenta* 2006; 27:56-61.
92. Salomon C, Guanzon D, Scholz-Romero K, Longo S, Correa P, Illanes SE, Rice GE. Placental Exosomes as Early Biomarker of Preeclampsia: Potential Role of Exosomal MicroRNAs Across Gestation. *J Clin Endocrinol Metab* 2017; 102:3182-3194.
93. Tong M, Chen Q, James JL, Stone PR, Chamley LW. Micro- and Nano-vesicles from First Trimester Human Placentae Carry Flt-1 and Levels Are Increased in Severe Preeclampsia. *Front Endocrinol (Lausanne)* 2017; 8:174.
94. Delorme-Axford E, Donker RB, Mouillet JF, Chu T, Bayer A, Ouyang Y, Wang T, Stolz DB, Sarkar SN, Morelli AE, Sadovsky Y, Coyne CB. Human placental trophoblasts confer viral resistance to recipient cells. *Proc Natl Acad Sci U S A* 2013; 110:12048-12053.
95. Bayer A, Delorme-Axford E, Sleighter C, Frey TK, Trobaugh DW, Klimstra WB, Emert-Sedlak LA, Smithgall TE, Kinchington PR, Vadia S, Seveau S, Boyle JP, et al. Human

- trophoblasts confer resistance to viruses implicated in perinatal infection. *Am J Obstet Gynecol* 2015; 212:71 e71-71 e78.
96. Bayer A, Lennemann NJ, Ouyang Y, Bramley JC, Morosky S, Marques ET, Jr., Cherry S, Sadovsky Y, Coyne CB. Type III Interferons Produced by Human Placental Trophoblasts Confer Protection against Zika Virus Infection. *Cell Host Microbe* 2016; 19:705-712.
 97. Kaminski VL, Ellwanger JH, Chies JAB. Extracellular vesicles in host-pathogen interactions and immune regulation - exosomes as emerging actors in the immunological theater of pregnancy. *Heliyon* 2019; 5:e02355.
 98. Ander SE, Diamond MS, Coyne CB. Immune responses at the maternal-fetal interface. *Sci Immunol* 2019; 4.
 99. Kshirsagar SK, Alam SM, Jasti S, Hodes H, Nauser T, Gilliam M, Billstrand C, Hunt JS, Petroff MG. Immunomodulatory molecules are released from the first trimester and term placenta via exosomes. *Placenta* 2012; 33:982-990.
 100. Alam SMK, Jasti S, Kshirsagar SK, Tannetta DS, Dragovic RA, Redman CW, Sargent IL, Hodes HC, Nauser TL, Fortes T, Filler AM, Behan K, et al. Trophoblast Glycoprotein (TPGB/5T4) in Human Placenta: Expression, Regulation, and Presence in Extracellular Microvesicles and Exosomes. *Reprod Sci* 2018; 25:185-197.
 101. Morgan TK. Cell- and size-specific analysis of placental extracellular vesicles in maternal plasma and pre-eclampsia. *Transl Res* 2018; 201:40-48.
 102. Salomon C, Torres MJ, Kobayashi M, Scholz-Romero K, Sobrevia L, Dobierzewska A, Illanes SE, Mitchell MD, Rice GE. A gestational profile of placental exosomes in maternal plasma and their effects on endothelial cell migration. *PLoS One* 2014; 9:e98667.
 103. Zhao G, Guo S, Jiang K, Zhang T, Wu H, Qiu C, Deng G. MiRNA profiling of plasma-derived exosomes from dairy cows during gestation. *Theriogenology* 2019; 130:89-98.
 104. Hamilton-Dutoit SJ, Lou H, Pallesen G. The expression of placental alkaline phosphatase (PLAP) and PLAP-like enzymes in normal and neoplastic human tissues. An immunohistological survey using monoclonal antibodies. *APMIS* 1990; 98:797-811.
 105. Garattini E, Margolis J, Heimer E, Felix A, Udenfriend S. Human placental alkaline phosphatase in liver and intestine. *Proc Natl Acad Sci U S A* 1985; 82:6080-6084.
 106. Galski H, Weinstein D, Abraham K, de Groot N, Segal S, Folman R, Hochberg AA. The in vitro synthesis and secretion of alkaline phosphatase from first trimester human decidua. *Eur J Obstet Gynecol Reprod Biol* 1982; 14:1-11.
 107. Alijotas-Reig J, Palacio-Garcia C, Llurba E, Vilardell-Tarres M. Cell-derived microparticles and vascular pregnancy complications: a systematic and comprehensive review. *Fertil Steril* 2013; 99:441-449.

108. Cuffe JSM, Holland O, Salomon C, Rice GE, Perkins AV. Review: Placental derived biomarkers of pregnancy disorders. *Placenta* 2017; 54:104-110.
109. Dutta S, Kumar S, Hyett J, Salomon C. Molecular Targets of Aspirin and Prevention of Preeclampsia and Their Potential Association with Circulating Extracellular Vesicles during Pregnancy. *Int J Mol Sci* 2019; 20.
110. Nair S, Salomon C. Extracellular vesicles as critical mediators of maternal-fetal communication during pregnancy and their potential role in maternal metabolism. *Placenta* 2020.
111. Carp H, Dardik R, Lubetsky A, Salomon O, Eskaraev R, Rosenthal E, Inbal A. Prevalence of circulating procoagulant microparticles in women with recurrent miscarriage: a case-controlled study. *Hum Reprod* 2004; 19:191-195.
112. Kaptan K, Beyan C, Ifran A, Pekel A. Platelet-derived microparticle levels in women with recurrent spontaneous abortion. *Int J Gynaecol Obstet* 2008; 102:271-274.
113. Alijotas-Reig J, Palacio-Garcia C, Farran-Codina I, Zarzoso C, Cabero-Roura L, Vilardell-Tarres M. Circulating cell-derived microparticles in women with pregnancy loss. *Am J Reprod Immunol* 2011; 66:199-208.
114. Toth B, Nieuwland R, Kern M, Rogenhofer N, Berkman R, Rank A, Lohse P, Friese K, Thaler CJ. Systemic changes in haemostatic balance are not associated with increased levels of circulating microparticles in women with recurrent spontaneous abortion. *Am J Reprod Immunol* 2008; 59:159-166.
115. Truong G, Guanzon D, Kinhal V, Elfeky O, Lai A, Longo S, Nuzhat Z, Palma C, Scholz-Romero K, Menon R, Mol BW, Rice GE, et al. Oxygen tension regulates the miRNA profile and bioactivity of exosomes released from extravillous trophoblast cells - Liquid biopsies for monitoring complications of pregnancy. *PLoS One* 2017; 12:e0174514.
116. Fallen S, Baxter D, Wu X, Kim TK, Shynlova O, Lee MY, Scherler K, Lye S, Hood L, Wang K. Extracellular vesicle RNAs reflect placenta dysfunction and are a biomarker source for preterm labour. *J Cell Mol Med* 2018; 22:2760-2773.
117. Wu G, Bazer FW, Wallace JM, Spencer TE. Board-invited review: intrauterine growth retardation: implications for the animal sciences. *J Anim Sci* 2006; 84:2316-2337.
118. Eixarch E, Hernandez-Andrade E, Crispi F, Illa M, Torre I, Figueras F, Gratacos E. Impact on fetal mortality and cardiovascular Doppler of selective ligation of uteroplacental vessels compared with undernutrition in a rabbit model of intrauterine growth restriction. *Placenta* 2011; 32:304-309.
119. Bassan H, Trejo LL, Kariv N, Bassan M, Berger E, Fattal A, Gozes I, Harel S. Experimental intrauterine growth retardation alters renal development. *Pediatr Nephrol* 2000; 15:192-195.

120. Haugaard C, Bauer M. Rodent models of intrauterine growth restriction. *Scandinavian Journal of Laboratory Animal Science* 2001; 28.
121. Grigsby PL. Animal Models to Study Placental Development and Function throughout Normal and Dysfunctional Human Pregnancy. *Semin Reprod Med* 2016; 34:11-16.
122. Bonney EA. Demystifying animal models of adverse pregnancy outcomes: touching bench and bedside. *Am J Reprod Immunol* 2013; 69:567-584.
123. Carter AM, Pijnenborg R. Evolution of invasive placentation with special reference to non-human primates. *Best Pract Res Clin Obstet Gynaecol* 2011; 25:249-257.
124. Leiser R, Kaufmann P. Placental structure: in a comparative aspect. *Exp Clin Endocrinol* 1994; 102:122-134.
125. Furukawa S, Kuroda Y, Sugiyama A. A comparison of the histological structure of the placenta in experimental animals. *J Toxicol Pathol* 2014; 27:11-18.
126. Frazier S, McBride MW, Mulvana H, Graham D. From animal models to patients: the role of placental microRNAs, miR-210, miR-126, and miR-148a/152 in preeclampsia. *Clin Sci (Lond)* 2020; 134:1001-1025.
127. Hu XQ, Dasgupta C, Xiao D, Huang X, Yang S, Zhang L. MicroRNA-210 Targets Ten-Eleven Translocation Methylcytosine Dioxygenase 1 and Suppresses Pregnancy-Mediated Adaptation of Large Conductance Ca(2+)-Activated K(+) Channel Expression and Function in Ovine Uterine Arteries. *Hypertension* 2017.
128. Swanson AM, Rossi CA, Ofir K, Mehta V, Boyd M, Barker H, Ledwozyw A, Vaughan O, Martin J, Zachary I, Sebire N, Peebles DM, et al. Maternal Therapy with Ad.VEGF-A165 Increases Fetal Weight at Term in a Guinea-Pig Model of Fetal Growth Restriction. *Hum Gene Ther* 2016; 27:997-1007.
129. Carr DJ, Wallace JM, Aitken RP, Milne JS, Mehta V, Martin JF, Zachary IC, Peebles DM, David AL. Uteroplacental adenovirus vascular endothelial growth factor gene therapy increases fetal growth velocity in growth-restricted sheep pregnancies. *Hum Gene Ther* 2014; 25:375-384.
130. Spencer R, Ambler G, Brodzki J, Diemert A, Figueras F, Gratacos E, Hansson SR, Hecher K, Huertas-Ceballos A, Marlow N, Marsal K, Morsing E, et al. EVERREST prospective study: a 6-year prospective study to define the clinical and biological characteristics of pregnancies affected by severe early onset fetal growth restriction. *BMC Pregnancy Childbirth* 2017; 17:43.
131. Seidl DC, Hughes HC, Bertolet R, Lang CM. True pregnancy toxemia (preeclampsia) in the guinea pig (*Cavia porcellus*). *Lab Anim Sci* 1979; 29:472-478.
132. Krugner-Higby L, Luck M, Hartley D, Crispen HM, Lubach GR, Coe CL. High-risk pregnancy in rhesus monkeys (*Macaca mulatta*): a case of ectopic, abdominal pregnancy

- with birth of a live, term infant, and a case of gestational diabetes complicated by pre-eclampsia. *J Med Primatol* 2009; 38:252-256.
133. Wang J, Feng C, Liu T, Shi M, Wu G, Bazer FW. Physiological alterations associated with intrauterine growth restriction in fetal pigs: Causes and insights for nutritional optimization. *Mol Reprod Dev* 2017; 84:897-904.
 134. Gonzalez-Bulnes A, Astiz S, Parraguez VH, Garcia-Contreras C, Vazquez-Gomez M. Empowering Translational Research in Fetal Growth Restriction: Sheep and Swine Animal Models. *Curr Pharm Biotechnol* 2016; 17:848-855.
 135. Diskin MG, Waters SM, Parr MH, Kenny DA. Pregnancy losses in cattle: potential for improvement. *Reprod Fertil Dev* 2016; 28:83-93.
 136. Spencer TE. Early pregnancy: Concepts, challenges, and potential solutions. *Animal Frontiers* 2013; 3:48-55.
 137. Kropp J, Penagaricano F, Salih SM, Khatib H. Invited review: Genetic contributions underlying the development of preimplantation bovine embryos. *J Dairy Sci* 2014; 97:1187-1201.
 138. Bidarimath M, Tayade C. Pregnancy and spontaneous fetal loss: A pig perspective. *Mol Reprod Dev* 2017; 84:856-869.
 139. Kridli RT, Khalaj K, Bidarimath M, Tayade C. Placentation, maternal-fetal interface, and conceptus loss in swine. *Theriogenology* 2016; 85:135-144.
 140. Rutherford JN, deMartelly VA, Layne Colon DG, Ross CN, Tardif SD. Developmental origins of pregnancy loss in the adult female common marmoset monkey (*Callithrix jacchus*). *PLoS One* 2014; 9:e96845.
 141. Manning PJ, Wagner, J.P., Harkness, J.E. *Laboratory Animal Medicine*. Associated Press: Academic Press; 1984: 149-181.
 142. Elfeky O, Longo S, Lai A, Rice GE, Salomon C. Influence of maternal BMI on the exosomal profile during gestation and their role on maternal systemic inflammation. *Placenta* 2017; 50:60-69.
 143. Morales-Prieto DM, Chaiwangyen W, Ospina-Prieto S, Schneider U, Herrmann J, Gruhn B, Markert UR. MicroRNA expression profiles of trophoblastic cells. *Placenta* 2012; 33:725-734.
 144. Schmidt JK, Block LN, Golos TG. Defining the rhesus macaque placental miRNAome: Conservation of expression of placental miRNA clusters between the macaque and human. *Placenta* 2018; 65:55-64.
 145. Vargas A, Zhou S, Ethier-Chiasson M, Flipo D, Lafond J, Gilbert C, Barbeau B. Syncytin proteins incorporated in placenta exosomes are important for cell uptake and show

- variation in abundance in serum exosomes from patients with preeclampsia. *FASEB J* 2014; 28:3703-3719.
146. Sheller-Miller S, Choi K, Choi C, Menon R. Cyclic-recombinase-reporter mouse model to determine exosome communication and function during pregnancy. *Am J Obstet Gynecol* 2019; 221:502 e501-502 e512.
 147. Klisch K, Schraner EM. Intraluminal vesicles of binucleate trophoblast cell granules are a possible source of placental exosomes in ruminants. *Placenta* 2020; 90:58-61.
 148. Bidarimath M, Khalaj K, Kridli RT, Kan FW, Koti M, Tayade C. Extracellular vesicle mediated intercellular communication at the porcine maternal-fetal interface: A new paradigm for conceptus-endometrial cross-talk. *Sci Rep* 2017; 7:40476.
 149. Burns GW, Brooks KE, Spencer TE. Extracellular Vesicles Originate from the Conceptus and Uterus During Early Pregnancy in Sheep. *Biol Reprod* 2016; 94:56.
 150. Ruiz-Gonzalez I, Xu J, Wang X, Burghardt RC, Dunlap KA, Bazer FW. Exosomes, endogenous retroviruses and toll-like receptors: pregnancy recognition in ewes. *Reproduction* 2015; 149:281-291.
 151. Anton L, Olarerin-George AO, Hogenesch JB, Elovitz MA. Placental expression of miR-517a/b and miR-517c contributes to trophoblast dysfunction and preeclampsia. *PLoS One* 2015; 10:e0122707.
 152. Hromadnikova I, Kotlabova K, Ondrackova M, Pirkova P, Kestlerova A, Novotna V, Hymanova L, Krofta L. Expression profile of C19MC microRNAs in placental tissue in pregnancy-related complications. *DNA Cell Biol* 2015; 34:437-457.
 153. Abitbol MM, Ober MB, Gallo GR, Driscoll SG, Pirani CL. Experimental toxemia of pregnancy in the monkey, with a preliminary report on renin and aldosterone. *Am J Pathol* 1977; 86:573-590.
 154. Makris A, Thornton C, Thompson J, Thomson S, Martin R, Ogle R, Waugh R, McKenzie P, Kirwan P, Hennessy A. Uteroplacental ischemia results in proteinuric hypertension and elevated sFLT-1. *Kidney Int* 2007; 71:977-984.
 155. Roberts VHJ, Lo JO, Lewandowski KS, Blundell P, Grove KL, Kroenke CD, Sullivan EL, Roberts CT, Jr., Frias AE. Adverse Placental Perfusion and Pregnancy Outcomes in a New Nonhuman Primate Model of Gestational Protein Restriction. *Reprod Sci* 2018; 25:110-119.
 156. Myers RE, Hill DE, Holt AB, Scott RE, Mellits ED, Cheek DB. Fetal growth retardation produced by experimental placental insufficiency in the rhesus monkey. I. Body weight, organ size. *Biol Neonate* 1971; 18:379-394.
 157. Kemnitz JW, Eisele SG, Lindsay KA, Engle MJ, Perelman RH, Farrell PM. Changes in food intake during menstrual cycles and pregnancy of normal and diabetic rhesus monkeys. *Diabetologia* 1984; 26:60-64.

158. Reynolds WA, Chez RA, Bhuyan BK, Neil GL. Placental transfer of streptozotocin in the rhesus monkey. *Diabetes* 1974; 23:777-782.
159. Barry PA, Lockridge KM, Salamat S, Tinling SP, Yue Y, Zhou SS, Gospe SM, Jr., Britt WJ, Tarantal AF. Nonhuman primate models of intrauterine cytomegalovirus infection. *ILAR J* 2006; 47:49-64.
160. Itell HL, Kaur A, Deere JD, Barry PA, Permar SR. Rhesus monkeys for a nonhuman primate model of cytomegalovirus infections. *Curr Opin Virol* 2017; 25:126-133.
161. Smith MA, Takeuchi K, Brackett RE, McClure HM, Raybourne RB, Williams KM, Babu US, Ware GO, Broderon JR, Doyle MP. Nonhuman primate model for *Listeria monocytogenes*-induced stillbirths. *Infect Immun* 2003; 71:1574-1579.
162. Wolfe B, Kerr AR, Mejia A, Simmons HA, Czuprynski CJ, Golos TG. Sequelae of Fetal Infection in a Non-human Primate Model of Listeriosis. *Front Microbiol* 2019; 10:2021.
163. Wolfe B, Wiepz GJ, Schotzko M, Bondarenko GI, Durning M, Simmons HA, Mejia A, Faith NG, Sampene E, Suresh M, Kathariou S, Czuprynski CJ, et al. Acute Fetal Demise with First Trimester Maternal Infection Resulting from *Listeria monocytogenes* in a Nonhuman Primate Model. *mBio* 2017; 8.
164. Mohr EL, Block LN, Newman CM, Stewart LM, Koenig M, Semler M, Breitbach ME, Teixeira LBC, Zeng X, Weiler AM, Barry GL, Thoong TH, et al. Ocular and uteroplacental pathology in a macaque pregnancy with congenital Zika virus infection. *PLoS One* 2018; 13:e0190617.
165. Nguyen SM, Antony KM, Dudley DM, Kohn S, Simmons HA, Wolfe B, Salamat MS, Teixeira LBC, Wiepz GJ, Thoong TH, Aliota MT, Weiler AM, et al. Highly efficient maternal-fetal Zika virus transmission in pregnant rhesus macaques. *PLoS Pathog* 2017; 13:e1006378.
166. Hirsch AJ, Roberts VHJ, Grigsby PL, Haese N, Schabel MC, Wang X, Lo JO, Liu Z, Kroenke CD, Smith JL, Kelleher M, Broeckel R, et al. Zika virus infection in pregnant rhesus macaques causes placental dysfunction and immunopathology. *Nat Commun* 2018; 9:263.
167. Sever JL, Meier GW, Windle WF, Schiff GM, Monif GR, Fabiyi A. Experimental rubella in pregnant rhesus monkeys. *J Infect Dis* 1966; 116:21-26.
168. Matsumoto S, Porter CJ, Ogasawara N, Iwatani C, Tsuchiya H, Seita Y, Chang YW, Okamoto I, Saitou M, Ema M, Perkins TJ, Stanford WL, et al. Establishment of macaque trophoblast stem cell lines derived from cynomolgus monkey blastocysts. *Sci Rep* 2020; 10:6827.
169. Mitchell BF, Taggart MJ. Are animal models relevant to key aspects of human parturition? *Am J Physiol Regul Integr Comp Physiol* 2009; 297:R525-545.

170. Vogel JP, Chawanpaiboon S, Moller AB, Watananirun K, Bonet M, Lumbiganon P. The global epidemiology of preterm birth. *Best Pract Res Clin Obstet Gynaecol* 2018; 52:3-12.
171. Fischer B, Chavatte-Palmer P, Viebahn C, Navarrete Santos A, Duranthon V. Rabbit as a reproductive model for human health. *Reproduction* 2012; 144:1-10.
172. Carter AM. Animal models of human placentation--a review. *Placenta* 2007; 28 Suppl A:S41-47.
173. Naav A, Erlandsson L, Axelsson J, Larsson I, Johansson M, Wester-Rosenlof L, Morgelin M, Casslen V, Gram M, Akerstrom B, Hansson SR. A1M Ameliorates Preeclampsia-Like Symptoms in Placenta and Kidney Induced by Cell-Free Fetal Hemoglobin in Rabbit. *PLoS One* 2015; 10:e0125499.
174. Kim DK, Lee J, Kim SR, Choi DS, Yoon YJ, Kim JH, Go G, Nhung D, Hong K, Jang SC, Kim SH, Park KS, et al. EVpedia: a community web portal for extracellular vesicles research. *Bioinformatics* 2015; 31:933-939.
175. Keerthikumar S, Chisanga D, Ariyaratne D, Al Saffar H, Anand S, Zhao K, Samuel M, Pathan M, Jois M, Chilamkurti N, Gangoda L, Mathivanan S. ExoCarta: A Web-Based Compendium of Exosomal Cargo. *J Mol Biol* 2016; 428:688-692.
176. Pathan M, Fonseka P, Chitti SV, Kang T, Sanwlan R, Van Deun J, Hendrix A, Mathivanan S. Vesiclepedia 2019: a compendium of RNA, proteins, lipids and metabolites in extracellular vesicles. *Nucleic Acids Res* 2019; 47:D516-D519.
177. Ramos JGL, Sass N, Costa SHM. Preeclampsia. *Rev Bras Ginecol Obstet* 2017; 39:496-512.
178. Possomato-Vieira JS, Khalil RA. Mechanisms of Endothelial Dysfunction in Hypertensive Pregnancy and Preeclampsia. *Adv Pharmacol* 2016; 77:361-431.
179. Rana S, Lemoine E, Granger JP, Karumanchi SA. Preeclampsia: Pathophysiology, Challenges, and Perspectives. *Circ Res* 2019; 124:1094-1112.
180. Raymond D, Peterson E. A critical review of early-onset and late-onset preeclampsia. *Obstet Gynecol Surv* 2011; 66:497-506.
181. Practice Committee of the American Society for Reproductive M. Evaluation and treatment of recurrent pregnancy loss: a committee opinion. *Fertil Steril* 2012; 98:1103-1111.
182. ACOG Practice Bulletin No. 200: Early Pregnancy Loss. *Obstet Gynecol* 2018; 132:e197-e207.
183. Hosseini MK, Gunel T, Gumusoglu E, Benian A, Aydinli K. MicroRNA expression profiling in placenta and maternal plasma in early pregnancy loss. *Mol Med Rep* 2018; 17:4941-4952.

184. Menasha J, Levy B, Hirschhorn K, Kardon NB. Incidence and spectrum of chromosome abnormalities in spontaneous abortions: new insights from a 12-year study. *Genet Med* 2005; 7:251-263.
185. Pylyp LY, Spynenko LO, Verhoglyad NV, Mishenko AO, Mykytenko DO, Zukin VD. Chromosomal abnormalities in products of conception of first-trimester miscarriages detected by conventional cytogenetic analysis: a review of 1000 cases. *J Assist Reprod Genet* 2018; 35:265-271.
186. Goddijn M, Leschot NJ. Genetic aspects of miscarriage. *Baillieres Best Pract Res Clin Obstet Gynaecol* 2000; 14:855-865.
187. Jia CW, Wang L, Lan YL, Song R, Zhou LY, Yu L, Yang Y, Liang Y, Li Y, Ma YM, Wang SY. Aneuploidy in Early Miscarriage and its Related Factors. *Chin Med J (Engl)* 2015; 128:2772-2776.
188. Petracchi F, Colaci DS, Igarzabal L, Gadow E. Cytogenetic analysis of first trimester pregnancy loss. *Int J Gynaecol Obstet* 2009; 104:243-244.
189. Massalska D, Zimowski JG, Bijok J, Pawelec M, Czubak-Barlik M, Jakiel G, Roszkowski T. First trimester pregnancy loss: Clinical implications of genetic testing. *J Obstet Gynaecol Res* 2017; 43:23-29.
190. Shahine L, Lathi R. Recurrent pregnancy loss: evaluation and treatment. *Obstet Gynecol Clin North Am* 2015; 42:117-134.
191. Practice Committee of the American Society for Reproductive Medicine. Electronic address aao. Definitions of infertility and recurrent pregnancy loss: a committee opinion. *Fertil Steril* 2020; 113:533-535.
192. Hong Li Y, Marren A. Recurrent pregnancy loss: A summary of international evidence-based guidelines and practice. *Aust J Gen Pract* 2018; 47:432-436.
193. Gagnon R. Placental insufficiency and its consequences. *Eur J Obstet Gynecol Reprod Biol* 2003; 110 Suppl 1:S99-107.
194. Burton GJ, Jauniaux E. Pathophysiology of placental-derived fetal growth restriction. *Am J Obstet Gynecol* 2018; 218:S745-S761.
195. Darby JRT, Varcoe TJ, Orgeig S, Morrison JL. Cardiorespiratory consequences of intrauterine growth restriction: Influence of timing, severity and duration of hypoxaemia. *Theriogenology* 2020.
196. Zur RL, Kingdom JC, Parks WT, Hobson SR. The Placental Basis of Fetal Growth Restriction. *Obstet Gynecol Clin North Am* 2020; 47:81-98.
197. Langer O, Yogev Y, Most O, Xenakis EM. Gestational diabetes: the consequences of not treating. *Am J Obstet Gynecol* 2005; 192:989-997.

198. Plows JF, Stanley JL, Baker PN, Reynolds CM, Vickers MH. The Pathophysiology of Gestational Diabetes Mellitus. *Int J Mol Sci* 2018; 19.
199. Vambergue A, Fajardy I. Consequences of gestational and pregestational diabetes on placental function and birth weight. *World J Diabetes* 2011; 2:196-203.
200. Goldenberg RL, Culhane JF, Iams JD, Romero R. Epidemiology and causes of preterm birth. *Lancet* 2008; 371:75-84.
201. Morgan TK. Role of the Placenta in Preterm Birth: A Review. *Am J Perinatol* 2016; 33:258-266.
202. Luo SS, Ishibashi O, Ishikawa G, Ishikawa T, Katayama A, Mishima T, Takizawa T, Shigihara T, Goto T, Izumi A, Ohkuchi A, Matsubara S, et al. Human villous trophoblasts express and secrete placenta-specific microRNAs into maternal circulation via exosomes. *Biol Reprod* 2009; 81:717-729.
203. Morales-Prieto DM, Ospina-Prieto S, Chaiwangyen W, Schoenleben M, Markert UR. Pregnancy-associated miRNA-clusters. *J Reprod Immunol* 2013; 97:51-61.
204. Holder BS, Tower CL, Abrahams VM, Aplin JD. Syncytin 1 in the human placenta. *Placenta* 2012; 33:460-466.
205. Soygur B, Sati L, Demir R. Altered expression of human endogenous retroviruses syncytin-1, syncytin-2 and their receptors in human normal and gestational diabetic placenta. *Histol Histopathol* 2016; 31:1037-1047.
206. Masoura S, Kalogiannidis IA, Gitas G, Goutsioulis A, Koiou E, Athanasiadis A, Vavatsi N. Biomarkers in pre-eclampsia: a novel approach to early detection of the disease. *J Obstet Gynaecol* 2012; 32:609-616.
207. Raposo G, Stoorvogel W. Extracellular vesicles: exosomes, microvesicles, and friends. *J Cell Biol* 2013; 200:373-383.
208. Jin J, Menon R. Placental exosomes: A proxy to understand pregnancy complications. *Am J Reprod Immunol* 2018; 79:e12788.
209. Hong X, Schouest B, Xu H. Effects of exosome on the activation of CD4+ T cells in rhesus macaques: a potential application for HIV latency reactivation. *Sci Rep* 2017; 7:15611.
210. McNamara RP, Costantini LM, Myers TA, Schouest B, Maness NJ, Griffith JD, Damania BA, MacLean AG, Dittmer DP. Nef Secretion into Extracellular Vesicles or Exosomes Is Conserved across Human and Simian Immunodeficiency Viruses. *mBio* 2018; 9.
211. Dupressoir A, Lavalie C, Heidmann T. From ancestral infectious retroviruses to bona fide cellular genes: role of the captured syncytins in placentation. *Placenta* 2012; 33:663-671.

212. Lin TM, Halbert SP. Immunological relationships of human and subhuman primate pregnancy-associated plasma proteins. *Int Arch Allergy Appl Immunol* 1978; 56:207-223.
213. Sammar M, Drobnjak T, Mandala M, Gizurarson S, Huppertz B, Meiri H. Galectin 13 (PP13) Facilitates Remodeling and Structural Stabilization of Maternal Vessels during Pregnancy. *Int J Mol Sci* 2019; 20.
214. Boyson JE, Iwanaga KK, Golos TG, Watkins DI. Identification of a novel MHC class I gene, Mamu-AG, expressed in the placenta of a primate with an inactivated G locus. *J Immunol* 1997; 159:3311-3321.
215. Manning JP, Inglis NR, Green S, Fishman WH. Characterization of placental alkaline phosphatase from the rabbit, guinea pig, mouse and hamster. *Enzymologia* 1970; 39:307-318.
216. Vernochet C, Heidmann O, Dupressoir A, Cornelis G, Dessen P, Catzeflis F, Heidmann T. A syncytin-like endogenous retrovirus envelope gene of the guinea pig specifically expressed in the placenta junctional zone and conserved in Caviomorpha. *Placenta* 2011; 32:885-892.
217. Liu X, Wang L, Ma C, Wang G, Zhang Y, Sun S. Exosomes derived from platelet-rich plasma present a novel potential in alleviating knee osteoarthritis by promoting proliferation and inhibiting apoptosis of chondrocyte via Wnt/beta-catenin signaling pathway. *J Orthop Surg Res* 2019; 14:470.
218. Black SG, Arnaud F, Palmarini M, Spencer TE. Endogenous retroviruses in trophoblast differentiation and placental development. *Am J Reprod Immunol* 2010; 64:255-264.
219. Bobrie A, Colombo M, Krumeich S, Raposo G, Thery C. Diverse subpopulations of vesicles secreted by different intracellular mechanisms are present in exosome preparations obtained by differential ultracentrifugation. *J Extracell Vesicles* 2012; 1.
220. Luga V, Zhang L, Vitoria-Petit AM, Ogunjimi AA, Inanlou MR, Chiu E, Buchanan M, Hosein AN, Basik M, Wrana JL. Exosomes mediate stromal mobilization of autocrine Wnt-PCP signaling in breast cancer cell migration. *Cell* 2012; 151:1542-1556.
221. Sheller-Miller S, Trivedi J, Yellon SM, Menon R. Exosomes Cause Preterm Birth in Mice: Evidence for Paracrine Signaling in Pregnancy. *Sci Rep* 2019; 9:608.
222. Gong R, Huang L, Shi J, Luo K, Qiu G, Feng H, Tien P, Xiao G. Syncytin-A mediates the formation of syncytiotrophoblast involved in mouse placental development. *Cell Physiol Biochem* 2007; 20:517-526.
223. Otero-Ortega L, Gomez de Frutos MC, Laso-Garcia F, Rodriguez-Frutos B, Medina-Gutierrez E, Lopez JA, Vazquez J, Diez-Tejedor E, Gutierrez-Fernandez M. Exosomes promote restoration after an experimental animal model of intracerebral hemorrhage. *J Cereb Blood Flow Metab* 2018; 38:767-779.

224. Campbell WJ, Larsen D, Deb S, Kwok SC, Soares MJ. Expression of alkaline phosphatase in differentiated rat labyrinthine trophoblast tissue. *Placenta* 1991; 12:227-237.
225. Hunt JS, Soares MJ. Expression of histocompatibility antigens, transferrin receptors, intermediate filaments, and alkaline phosphatase by in vitro cultured rat placental cells and rat placental cells in situ. *Placenta* 1988; 9:159-171.
226. Dutta S, Lai A, Scholz-Romero K, Shiddiky MJA, Yamauchi Y, Mishra JS, Rice GE, Hyett J, Kumar S, Salomon C. Hypoxia-induced small extracellular vesicle proteins regulate proinflammatory cytokines and systemic blood pressure in pregnant rats. *Clin Sci (Lond)* 2020; 134:593-607.
227. Burns G, Brooks K, Wildung M, Navakanitworakul R, Christenson LK, Spencer TE. Extracellular vesicles in luminal fluid of the ovine uterus. *PLoS One* 2014; 9:e90913.
228. Cleys ER, Halleran JL, McWhorter E, Hergenreder J, Enriquez VA, da Silveira JC, Bruemmer JE, Winger QA, Bouma GJ. Identification of microRNAs in exosomes isolated from serum and umbilical cord blood, as well as placentomes of gestational day 90 pregnant sheep. *Mol Reprod Dev* 2014; 81:983-993.
229. Cornelis G, Heidmann O, Degrelle SA, Vernochet C, Lavialle C, Letzelter C, Bernard-Stoecklin S, Hassanin A, Mulot B, Guillomot M, Hue I, Heidmann T, et al. Captured retroviral envelope syncytin gene associated with the unique placental structure of higher ruminants. *Proc Natl Acad Sci U S A* 2013; 110:E828-837.
230. Caballero JN, Frenette G, Belleanne C, Sullivan R. CD9-positive microvesicles mediate the transfer of molecules to Bovine Spermatozoa during epididymal maturation. *PLoS One* 2013; 8:e65364.
231. Zhao G, Yang C, Yang J, Liu P, Jiang K, Shaukat A, Wu H, Deng G. Placental exosome-mediated Bta-miR-499-Lin28B/let-7 axis regulates inflammatory bias during early pregnancy. *Cell Death Dis* 2018; 9:704.
232. Eirin A, Zhu XY, Puranik AS, Tang H, McGurren KA, van Wijnen AJ, Lerman A, Lerman LO. Mesenchymal stem cell-derived extracellular vesicles attenuate kidney inflammation. *Kidney Int* 2017; 92:114-124.
233. Guller S, Tang Z, Ma YY, Di Santo S, Sager R, Schneider H. Protein composition of microparticles shed from human placenta during placental perfusion: Potential role in angiogenesis and fibrinolysis in preeclampsia. *Placenta* 2011; 32:63-69.
234. Gilani SI, Anderson UD, Jayachandran M, Weissgerber TL, Zand L, White WM, Milic N, Suarez MLG, Vallapureddy RR, Naav A, Erlandsson L, Lieske JC, et al. Urinary Extracellular Vesicles of Podocyte Origin and Renal Injury in Preeclampsia. *J Am Soc Nephrol* 2017; 28:3363-3372.

235. Baig S, Kothandaraman N, Manikandan J, Rong L, Ee KH, Hill J, Lai CW, Tan WY, Yeoh F, Kale A, Su LL, Biswas A, et al. Proteomic analysis of human placental syncytiotrophoblast microvesicles in preeclampsia. *Clin Proteomics* 2014; 11:40.
236. Orozco AF, Jorgez CJ, Ramos-Perez WD, Popek EJ, Yu X, Kozinetz CA, Bischoff FZ, Lewis DE. Placental release of distinct DNA-associated micro-particles into maternal circulation: reflective of gestation time and preeclampsia. *Placenta* 2009; 30:891-897.
237. Baig S, Lim JY, Fernandis AZ, Wenk MR, Kale A, Su LL, Biswas A, Vasoo S, Shui G, Choolani M. Lipidomic analysis of human placental syncytiotrophoblast microvesicles in adverse pregnancy outcomes. *Placenta* 2013; 34:436-442.
238. Miranda J, Paules C, Nair S, Lai A, Palma C, Scholz-Romero K, Rice GE, Gratacos E, Crispi F, Salomon C. Placental exosomes profile in maternal and fetal circulation in intrauterine growth restriction - Liquid biopsies to monitoring fetal growth. *Placenta* 2018; 64:34-43.
239. Kandzija N, Zhang W, Motta-Mejia C, Mhlomi V, McGowan-Downey J, James T, Cerdeira AS, Tannetta D, Sargent I, Redman CW, Bastie CC, Vatish M. Placental extracellular vesicles express active dipeptidyl peptidase IV; levels are increased in gestational diabetes mellitus. *J Extracell Vesicles* 2019; 8:1617000.
240. Jayabalan N, Lai A, Nair S, Guanzon D, Scholz-Romero K, Palma C, McIntyre HD, Lappas M, Salomon C. Quantitative Proteomics by SWATH-MS Suggest an Association Between Circulating Exosomes and Maternal Metabolic Changes in Gestational Diabetes Mellitus. *Proteomics* 2019; 19:e1800164.
241. Gillet V, Ouellet A, Stepanov Y, Rodosthenous RS, Croft EK, Brennan K, Abdelouahab N, Baccarelli A, Takser L. miRNA Profiles in Extracellular Vesicles From Serum Early in Pregnancies Complicated by Gestational Diabetes Mellitus. *J Clin Endocrinol Metab* 2019; 104:5157-5169.
242. Rice GE, Scholz-Romero K, Sweeney E, Peiris H, Kobayashi M, Duncombe G, Mitchell MD, Salomon C. The Effect of Glucose on the Release and Bioactivity of Exosomes From First Trimester Trophoblast Cells. *J Clin Endocrinol Metab* 2015; 100:E1280-1288.
243. Menon R, Debnath C, Lai A, Guanzon D, Bhatnagar S, Kshetrapal PK, Sheller-Miller S, Salomon C, Garbhini Study T. Circulating Exosomal miRNA Profile During Term and Preterm Birth Pregnancies: A Longitudinal Study. *Endocrinology* 2019; 160:249-275.
244. Menon R, Dixon CL, Sheller-Miller S, Fortunato SJ, Saade GR, Palma C, Lai A, Guanzon D, Salomon C. Quantitative Proteomics by SWATH-MS of Maternal Plasma Exosomes Determine Pathways Associated With Term and Preterm Birth. *Endocrinology* 2019; 160:639-650.
245. Tong M, Stanley JL, Chen Q, James JL, Stone PR, Chamley LW. Placental Nano-vesicles Target to Specific Organs and Modulate Vascular Tone In Vivo. *Hum Reprod* 2017; 32:2188-2198.

246. Terasawa E, Keen KL, Grendell RL, Golos TG. Possible role of 5'-adenosine triphosphate in synchronization of Ca²⁺ oscillations in primate luteinizing hormone-releasing hormone neurons. *Mol Endocrinol* 2005; 19:2736-2747.
247. Golos TG, Bondarenko GI, Dambaeva SV, Breburda EE, Durning M. On the role of placental Major Histocompatibility Complex and decidual leukocytes in implantation and pregnancy success using non-human primate models. *Int J Dev Biol* 2010; 54:431-443.
248. Telugu BP, Greening JA. Comparative Placentation. In: *Comparative Reproductive Biology*: 271-319.
249. Morrison JL, Botting KJ, Darby JRT, David AL, Dyson RM, Gatford KL, Gray C, Herrera EA, Hirst JJ, Kim B, Kind KL, Krause BJ, et al. Guinea pig models for translation of the developmental origins of health and disease hypothesis into the clinic. *J Physiol* 2018; 596:5535-5569.
250. Enders AC, Blankenship TN. Comparative placental structure. *Adv Drug Deliv Rev* 1999; 38:3-15.
251. Clark DA. The use and misuse of animal analog models of human pregnancy disorders. *J Reprod Immunol* 2014; 103:1-8.
252. Tanaka S, Kunath T, Hadjantonakis AK, Nagy A, Rossant J. Promotion of trophoblast stem cell proliferation by FGF4. *Science* 1998; 282:2072-2075.
253. Soares MJ, Varberg KM, Iqbal K. Hemochorial placentation: development, function, and adaptations. *Biol Reprod* 2018; 99:196-211.
254. Lowe DE, Robbins JR, Bakardjiev AI. Animal and Human Tissue Models of Vertical *Listeria monocytogenes* Transmission and Implications for Other Pregnancy-Associated Infections. *Infect Immun* 2018; 86.
255. Soares MJ. The prolactin and growth hormone families: pregnancy-specific hormones/cytokines at the maternal-fetal interface. *Reprod Biol Endocrinol* 2004; 2:51.
256. Bainbridge DR. Evolution of mammalian pregnancy in the presence of the maternal immune system. *Rev Reprod* 2000; 5:67-74.
257. Niakan KK, Eggan K. Analysis of human embryos from zygote to blastocyst reveals distinct gene expression patterns relative to the mouse. *Dev Biol* 2013; 375:54-64.
258. Soares MJ, Chakraborty D, Karim Rumi MA, Konno T, Renaud SJ. Rat placentation: an experimental model for investigating the hemochorial maternal-fetal interface. *Placenta* 2012; 33:233-243.
259. Verstuyf A, Sobis H, Goebels J, Fonteyn E, Cassiman JJ, Vandeputte M. Establishment and characterization of a continuous in vitro line from a rat choriocarcinoma. *Int J Cancer* 1990; 45:752-756.

260. Andersen MD, Alstrup A.K.O., Duvald, C. S., Mikkelsen E.F.R., Vendelbo, M.H., Ovesen, P. G., Pedersen, M. *Animal Models of Fetal Medicine and Obstetrics*. 2018.
261. Peter AT. Bovine placenta: a review on morphology, components, and defects from terminology and clinical perspectives. *Theriogenology* 2013; 80:693-705.
262. Introduction to Comparative Placentation. In: *Comparative Reproductive Biology*: 263-270.
263. Rapacz-Leonard A, Dabrowska M, Janowski T. Major histocompatibility complex I mediates immunological tolerance of the trophoblast during pregnancy and may mediate rejection during parturition. *Mediators Inflamm* 2014; 2014:579279.
264. Hashizume K, Shimada A, Nakano H, Takahashi T. Bovine trophoblast cell culture systems: a technique to culture bovine trophoblast cells without feeder cells. *Methods Mol Med* 2006; 121:179-188.
265. Flechon JE, Laurie S, Notarianni E. Isolation and characterization of a feeder-dependent, porcine trophoblast cell line obtained from a 9-day blastocyst. *Placenta* 1995; 16:643-658.
266. Cavanagh D, Rao PS, Tsai CC, O'Connor TC. Experimental toxemia in the pregnant primate. *Am J Obstet Gynecol* 1977; 128:75-85.
267. Abitbol MM, Gallo GR, Pirani CL, Ober WB. Production of experimental toxemia in the pregnant rabbit. *Am J Obstet Gynecol* 1976; 124:460-470.
268. Fushima T, Sekimoto A, Minato T, Ito T, Oe Y, Kisu K, Sato E, Funamoto K, Hayase T, Kimura Y, Ito S, Sato H, et al. Reduced Uterine Perfusion Pressure (RUPP) Model of Preeclampsia in Mice. *PLoS One* 2016; 11:e0155426.
269. Sunderland NS, Thomson SE, Heffernan SJ, Lim S, Thompson J, Ogle R, McKenzie P, Kirwan PJ, Makris A, Hennessy A. Tumor necrosis factor alpha induces a model of preeclampsia in pregnant baboons (*Papio hamadryas*). *Cytokine* 2011; 56:192-199.
270. Maynard SE, Min JY, Merchan J, Lim KH, Li J, Mondal S, Libermann TA, Morgan JP, Sellke FW, Stillman IE, Epstein FH, Sukhatme VP, et al. Excess placental soluble fms-like tyrosine kinase 1 (sFlt1) may contribute to endothelial dysfunction, hypertension, and proteinuria in preeclampsia. *J Clin Invest* 2003; 111:649-658.
271. LaMarca BB, Bennett WA, Alexander BT, Cockrell K, Granger JP. Hypertension produced by reductions in uterine perfusion in the pregnant rat: role of tumor necrosis factor-alpha. *Hypertension* 2005; 46:1022-1025.
272. Venkatesha S, Toporsian M, Lam C, Hanai J, Mammoto T, Kim YM, Bdolah Y, Lim KH, Yuan HT, Libermann TA, Stillman IE, Roberts D, et al. Soluble endoglin contributes to the pathogenesis of preeclampsia. *Nat Med* 2006; 12:642-649.

273. Huang PL, Huang Z, Mashimo H, Bloch KD, Moskowitz MA, Bevan JA, Fishman MC. Hypertension in mice lacking the gene for endothelial nitric oxide synthase. *Nature* 1995; 377:239-242.
274. Salas SP, Altermatt F, Campos M, Giacaman A, Rosso P. Effects of long-term nitric oxide synthesis inhibition on plasma volume expansion and fetal growth in the pregnant rat. *Hypertension* 1995; 26:1019-1023.
275. Talosi G, Nemeth I, Nagy E, Pinter S. The pathogenetic role of heme in pregnancy-induced hypertension-like disease in ewes. *Biochem Mol Med* 1997; 62:58-64.
276. Wester-Rosenlof L, Casslen V, Axelsson J, Edstrom-Hagerwall A, Gram M, Holmqvist M, Johansson ME, Larsson I, Ley D, Marsal K, Morgelin M, Rippe B, et al. A1M/alpha1-microglobulin protects from heme-induced placental and renal damage in a pregnant sheep model of preeclampsia. *PLoS One* 2014; 9:e86353.
277. Thatcher CD, Keith JC, Jr. Pregnancy-induced hypertension: development of a model in the pregnant sheep. *Am J Obstet Gynecol* 1986; 155:201-207.
278. Buehler PW, D'Agnillo F. Toxicological consequences of extracellular hemoglobin: biochemical and physiological perspectives. *Antioxid Redox Signal* 2010; 12:275-291.
279. de Brun V, Meikle A, Fernandez-Foren A, Forcada F, Palacin I, Menchaca A, Sosa C, Abecia JA. Failure to establish and maintain a pregnancy in undernourished recipient ewes is associated with a poor endocrine milieu in the early luteal phase. *Anim Reprod Sci* 2016; 173:80-86.
280. Briscoe TA, Rehn AE, Dieni S, Duncan JR, Wlodek ME, Owens JA, Rees SM. Cardiovascular and renal disease in the adolescent guinea pig after chronic placental insufficiency. *Am J Obstet Gynecol* 2004; 191:847-855.
281. Turner AJ, Trudinger BJ. A modification of the uterine artery restriction technique in the guinea pig fetus produces asymmetrical ultrasound growth. *Placenta* 2009; 30:236-240.
282. Lopez-Tello J, Jimenez-Martinez MA, Herrera EA, Krause BJ, Sferruzzi-Perri AN. Progressive uterine artery occlusion in the Guinea pig leads to defects in placental structure that relate to fetal growth. *Placenta* 2018; 72-73:36-40.
283. Pham TD, MacLennan NK, Chiu CT, Laksana GS, Hsu JL, Lane RH. Uteroplacental insufficiency increases apoptosis and alters p53 gene methylation in the full-term IUGR rat kidney. *Am J Physiol Regul Integr Comp Physiol* 2003; 285:R962-970.
284. Wang YP, Chen X, Zhang ZK, Cui HY, Wang P, Wang Y. Increased renal apoptosis and reduced renin-angiotensin system in fetal growth restriction. *J Renin Angiotensin Aldosterone Syst* 2016; 17.
285. Lopez-Tello J, Arias-Alvarez M, Gonzalez-Bulnes A, Sferuzzi-Perri AN. Models of Intrauterine growth restriction and fetal programming in rabbits. *Mol Reprod Dev* 2019; 86:1781-1809.

286. Vuguin PM. Animal models for small for gestational age and fetal programming of adult disease. *Horm Res* 2007; 68:113-123.
287. Thompson LP, Pence L, Pinkas G, Song H, Telugu BP. Placental Hypoxia During Early Pregnancy Causes Maternal Hypertension and Placental Insufficiency in the Hypoxic Guinea Pig Model. *Biol Reprod* 2016; 95:128.
288. Sunderland N, Hennessy A, Makris A. Animal models of pre-eclampsia. *Am J Reprod Immunol* 2011; 65:533-541.
289. Morrison JL. Sheep models of intrauterine growth restriction: fetal adaptations and consequences. *Clin Exp Pharmacol Physiol* 2008; 35:730-743.
290. Metges CC, Lang IS, Hennig U, Brussow KP, Kanitz E, Tuchscherer M, Schneider F, Weitzel JM, Steinhoff-Ooster A, Sauerwein H, Bellmann O, Nurnberg G, et al. Intrauterine growth retarded progeny of pregnant sows fed high protein:low carbohydrate diet is related to metabolic energy deficit. *PLoS One* 2012; 7:e31390.
291. Saintonge J, Cote R. Fetal brain development in diabetic guinea pigs. *Pediatr Res* 1984; 18:650-653.
292. Merritt TA, Curbelo V, Gluck L, Clements RS, Jr. Alterations in fetal lung phosphatidylinositol metabolism associated with maternal glucose intolerance. *Biol Neonate* 1981; 39:217-224.
293. Caluwaerts S, Holemans K, van Bree R, Verhaeghe J, Van Assche FA. Is low-dose streptozotocin in rats an adequate model for gestational diabetes mellitus? *J Soc Gynecol Investig* 2003; 10:216-221.
294. Hellerstrom C, Swenne I, Eriksson UJ. Is there an animal model for gestational diabetes? *Diabetes* 1985; 34 Suppl 2:28-31.
295. Giachini FR, Carriel V, Capelo LP, Tostes RC, Carvalho MH, Fortes ZB, Zorn TM, San Martin S. Maternal diabetes affects specific extracellular matrix components during placentation. *J Anat* 2008; 212:31-41.
296. Vajnerova O, Kafka P, Kratzerova T, Chalupsky K, Hampl V. Pregestational diabetes increases fetoplacental vascular resistance in rats. *Placenta* 2018; 63:32-38.
297. Dickinson JE, Meyer BA, Brath PC, Chmielowiec S, Walsh SW, Parisi VM, Palmer SM. Placental thromboxane and prostacyclin production in an ovine diabetic model. *Am J Obstet Gynecol* 1990; 163:1831-1835.
298. Dickinson JE, Meyer BA, Chmielowiec S, Palmer SM. Streptozocin-induced diabetes mellitus in the pregnant ewe. *Am J Obstet Gynecol* 1991; 165:1673-1677.
299. Ezekwe MO, Ezekwe EI, Sen DK, Ogolla F. Effects of maternal streptozotocin-diabetes on fetal growth, energy reserves and body composition of newborn pigs. *J Anim Sci* 1984; 59:974-980.

300. Tabatabaei N, Rodd CJ, Kremer R, Weiler HA. High vitamin D status before conception, but not during pregnancy, is inversely associated with maternal gestational diabetes mellitus in guinea pigs. *J Nutr* 2014; 144:1994-2001.
301. Abdul Aziz SH, John CM, Mohamed Yusof NI, Nordin M, Ramasamy R, Adam A, Mohd Fauzi F. Animal Model of Gestational Diabetes Mellitus with Pathophysiological Resemblance to the Human Condition Induced by Multiple Factors (Nutritional, Pharmacological, and Stress) in Rats. *Biomed Res Int* 2016; 2016:9704607.
302. Szlapinski SK, King RT, Retta G, Yeo E, Strutt BJ, Hill DJ. A mouse model of gestational glucose intolerance through exposure to a low protein diet during fetal and neonatal development. *J Physiol* 2019; 597:4237-4250.
303. Holemans K, Caluwaerts S, Poston L, Van Assche FA. Diet-induced obesity in the rat: a model for gestational diabetes mellitus. *Am J Obstet Gynecol* 2004; 190:858-865.
304. Pasek RC, Gannon M. Advancements and challenges in generating accurate animal models of gestational diabetes mellitus. *Am J Physiol Endocrinol Metab* 2013; 305:E1327-1338.
305. Dombroski RA, Woodard DS, Harper MJ, Gibbs RS. A rabbit model for bacteria-induced preterm pregnancy loss. *Am J Obstet Gynecol* 1990; 163:1938-1943.
306. Bry K, Hallman M. Transforming growth factor-beta 2 prevents preterm delivery induced by interleukin-1 alpha and tumor necrosis factor-alpha in the rabbit. *Am J Obstet Gynecol* 1993; 168:1318-1322.
307. Heng YJ, Liong S, Permezel M, Rice GE, Di Quinzio MK, Georgiou HM. The interplay of the interleukin 1 system in pregnancy and labor. *Reprod Sci* 2014; 21:122-130.
308. Romero R, Chaiworapongsa T, Alpay Savasan Z, Xu Y, Hussein Y, Dong Z, Kusanovic JP, Kim CJ, Hassan SS. Damage-associated molecular patterns (DAMPs) in preterm labor with intact membranes and preterm PROM: a study of the alarmin HMGB1. *J Matern Fetal Neonatal Med* 2011; 24:1444-1455.
309. Romero R, Mazor M, Tartakovsky B. Systemic administration of interleukin-1 induces preterm parturition in mice. *Am J Obstet Gynecol* 1991; 165:969-971.
310. Gomez-Lopez N, Romero R, Plazyo O, Panaitescu B, Furcron AE, Miller D, Roumayah T, Flom E, Hassan SS. Intra-Amniotic Administration of HMGB1 Induces Spontaneous Preterm Labor and Birth. *Am J Reprod Immunol* 2016; 75:3-7.
311. Hirsch E, Saotome I, Hirsh D. A model of intrauterine infection and preterm delivery in mice. *Am J Obstet Gynecol* 1995; 172:1598-1603.
312. Kaga N, Katsuki Y, Obata M, Shibutani Y. Repeated administration of low-dose lipopolysaccharide induces preterm delivery in mice: a model for human preterm parturition and for assessment of the therapeutic ability of drugs against preterm delivery. *Am J Obstet Gynecol* 1996; 174:754-759.

313. Fidel PL, Jr., Romero R, Wolf N, Cutright J, Ramirez M, Araneda H, Cotton DB. Systemic and local cytokine profiles in endotoxin-induced preterm parturition in mice. *Am J Obstet Gynecol* 1994; 170:1467-1475.
314. Romero R, Brody DT, Oyarzun E, Mazor M, Wu YK, Hobbins JC, Durum SK. Infection and labor. III. Interleukin-1: a signal for the onset of parturition. *Am J Obstet Gynecol* 1989; 160:1117-1123.
315. Okawa T, Suzuki H, Yaanagida K, Sato A, Vedernikov Y, Saade G, Garfield R. Effect of lipopolysaccharide on uterine contractions and prostaglandin production in pregnant rats. *Am J Obstet Gynecol* 2001; 184:84-89.
316. Gibbs RS, Blanco JD, St Clair PJ, Castaneda YS. Quantitative bacteriology of amniotic fluid from women with clinical intraamniotic infection at term. *J Infect Dis* 1982; 145:1-8.
317. Kemp MW. *Infection-Associated Preterm Birth: Advances From the Use of Animal Models*. Academic Press; 2017: 769-804.
318. Liggins GC. Premature delivery of foetal lambs infused with glucocorticoids. *J Endocrinol* 1969; 45:515-523.
319. Liggins GC. Premature parturition after infusion of corticotrophin or cortisol into foetal lambs. *J Endocrinol* 1968; 42:323-329.
320. Schlafer DH, Yuh B, Foley GL, Elssasser TH, Sadowsky D, Nathanielsz PW. Effect of Salmonella endotoxin administered to the pregnant sheep at 133-142 days gestation on fetal oxygenation, maternal and fetal adrenocorticotrophic hormone and cortisol, and maternal plasma tumor necrosis factor alpha concentrations. *Biol Reprod* 1994; 50:1297-1302.
321. Foley GL, Schlafer DH. Candida abortion in cattle. *Vet Pathol* 1987; 24:532-536.
322. Rasti S, Asadi MA, Taghriri A, Behrashi M, Mousavie G. Vaginal candidiasis complications on pregnant women. *Jundishapur J Microbiol* 2014; 7:e10078.
323. Holzer I, Farr A, Kiss H, Hagmann M, Petricevic L. The colonization with Candida species is more harmful in the second trimester of pregnancy. *Arch Gynecol Obstet* 2017; 295:891-895.
324. Maki Y, Fujisaki M, Sato Y, Sameshima H. Candida Chorioamnionitis Leads to Preterm Birth and Adverse Fetal-Neonatal Outcome. *Infect Dis Obstet Gynecol* 2017; 2017:9060138.
325. *The Physiology of Reproduction*. Raven Press; 1988: 2183-2186.
326. Hirst JJ, Palliser HK, Shaw JC, Crombie G, Walker DW, Zakar T. Birth and Neonatal Transition in the Guinea Pig: Experimental Approaches to Prevent Preterm Birth and Protect the Premature Fetus. *Front Physiol* 2018; 9:1802.

327. Csapo AI, Puri CP, Tarro S. Relationship between timing of ovariectomy and maintenance of pregnancy in the guinea-pig. *Prostaglandins* 1981; 22:131-140.
328. Calmus ML, Macksoud EE, Tucker R, Iozzo RV, Lechner BE. A mouse model of spontaneous preterm birth based on the genetic ablation of biglycan and decorin. *Reproduction* 2011; 142:183-194.
329. Akgul Y, Holt R, Mummert M, Word A, Mahendroo M. Dynamic changes in cervical glycosaminoglycan composition during normal pregnancy and preterm birth. *Endocrinology* 2012; 153:3493-3503.
330. Elovitz MA, Wang Z, Chien EK, Rychlik DF, Phillippe M. A new model for inflammation-induced preterm birth: the role of platelet-activating factor and Toll-like receptor-4. *Am J Pathol* 2003; 163:2103-2111.
331. Osmers R, Rath W, Pflanz MA, Kuhn W, Stuhlsatz HW, Szeverenyi M. Glycosaminoglycans in cervical connective tissue during pregnancy and parturition. *Obstet Gynecol* 1993; 81:88-92.
332. Brownfoot FC, Gagliardi DI, Bain E, Middleton P, Crowther CA. Different corticosteroids and regimens for accelerating fetal lung maturation for women at risk of preterm birth. *Cochrane Database Syst Rev* 2013:CD006764.
333. Giakoumelou S, Wheelhouse N, Cuschieri K, Entrican G, Howie SE, Horne AW. The role of infection in miscarriage. *Hum Reprod Update* 2016; 22:116-133.
334. Rodolakis A, Salinas J, Papp J. Recent advances on ovine chlamydial abortion. *Vet Res* 1998; 29:275-288.
335. De Clercq E, Kalmar I, Vanrompay D. Animal models for studying female genital tract infection with *Chlamydia trachomatis*. *Infect Immun* 2013; 81:3060-3067.
336. Poonia A, Purohit VD. Abortion in guinea pigs by *Chlamydia psittaci* isolates from natural sheep abortion. *Indian J Exp Biol* 1998; 36:411-413.
337. Thoma R, Guscelli F, Schiller I, Schmeer N, Corboz L, Pospischil A. *Chlamydiae* in porcine abortion. *Vet Pathol* 1997; 34:467-469.
338. Weisblum Y, Panet A, Haimov-Kochman R, Wolf DG. Models of vertical cytomegalovirus (CMV) transmission and pathogenesis. *Semin Immunopathol* 2014; 36:615-625.
339. Harrison CJ, Caruso N. Correlation of maternal and pup NK-like activity and TNF responses against cytomegalovirus to pregnancy outcome in inbred guinea pigs. *J Med Virol* 2000; 60:230-236.
340. Ahn HS, Han SH, Kim YH, Park BJ, Kim DH, Lee JB, Park SY, Song CS, Lee SW, Choi C, Myoung J, Choi IS. Adverse fetal outcomes in pregnant rabbits experimentally infected with rabbit hepatitis E virus. *Virology* 2017; 512:187-193.

341. Xia J, Liu L, Wang L, Zhang Y, Zeng H, Liu P, Zou Q, Wang L, Zhuang H. Experimental infection of pregnant rabbits with hepatitis E virus demonstrating high mortality and vertical transmission. *J Viral Hepat* 2015; 22:850-857.
342. Andrade EB, Magalhaes A, Puga A, Costa M, Bravo J, Portugal CC, Ribeiro A, Correia-Neves M, Faustino A, Firon A, Trieu-Cuot P, Summavielle T, et al. A mouse model reproducing the pathophysiology of neonatal group B streptococcal infection. *Nat Commun* 2018; 9:3138.
343. Rubens CE, Raff HV, Jackson JC, Chi EY, Bielitzki JT, Hillier SL. Pathophysiology and histopathology of group B streptococcal sepsis in *Macaca nemestrina* primates induced after intraamniotic inoculation: evidence for bacterial cellular invasion. *J Infect Dis* 1991; 164:320-330.
344. Bakardjiev AI, Stacy BA, Fisher SJ, Portnoy DA. Listeriosis in the pregnant guinea pig: a model of vertical transmission. *Infect Immun* 2004; 72:489-497.
345. Avila L, Rawls WE, Dent PB. Experimental infection with rubella virus. I. Acquired and congenital infection in rats. *J Infect Dis* 1972; 126:585-592.
346. Cotlier E, Fox J, Bohigian G, Beaty C, Du Pree A. Pathogenic effects of rubella virus on embryos and newborn rats. *Nature* 1968; 217:38-40.
347. Owen MR, Clarkson MJ, Trees AJ. Acute phase toxoplasma abortions in sheep. *Vet Rec* 1998; 142:480-482.
348. Buxton D. Protozoan infections (*Toxoplasma gondii*, *Neospora caninum* and *Sarcocystis* spp.) in sheep and goats: recent advances. *Vet Res* 1998; 29:289-310.
349. Menzies FM, Henriquez FL, Roberts CW. Immunological control of congenital toxoplasmosis in the murine model. *Immunol Lett* 2008; 115:83-89.
350. Schoondermark-Van de Ven E, Melchers W, Galama J, Camps W, Eskes T, Meuwissen J. Congenital toxoplasmosis: an experimental study in rhesus monkeys for transmission and prenatal diagnosis. *Exp Parasitol* 1993; 77:200-211.
351. Morrison TE, Diamond MS. Animal Models of Zika Virus Infection, Pathogenesis, and Immunity. *J Virol* 2017; 91.
352. Bierle CJ, Fernandez-Alarcon C, Hernandez-Alvarado N, Zabeli JC, Janus BC, Putri DS, Schleiss MR. Assessing Zika virus replication and the development of Zika-specific antibodies after a mid-gestation viral challenge in guinea pigs. *PLoS One* 2017; 12:e0187720.
353. Udenze D, Trus I, Berube N, Gerdtz V, Karniychuk U. The African strain of Zika virus causes more severe in utero infection than Asian strain in a porcine fetal transmission model. *Emerg Microbes Infect* 2019; 8:1098-1107.

354. Burton GJ, Redman CW, Roberts JM, Moffett A. Pre-eclampsia: pathophysiology and clinical implications. *BMJ* 2019; 366:12381.
355. De Bem THC, da Silveira JC, Sampaio RV, Sangalli JR, Oliveira MLF, Ferreira RM, Silva LA, Perecin F, King WA, Meirelles FV, Ramos ES. Low levels of exosomal-miRNAs in maternal blood are associated with early pregnancy loss in cloned cattle. *Sci Rep* 2017; 7:14319.